Newcastle University

Institute for Cell and Molecular Biosciences

Molecular Characterization of the Cell Division Protein SepF

ILKAY NAZLI CELIK

A thesis submitted for the degree of Doctor of Philosophy

October 2013

Babama….

Abstract

SepF is identified as a late cell division protein which is conserved among Gram-positive bacteria. It was shown that SepF also has a positive role in formation of FtsZ filaments. Moreover, SepF forms rings by itself and tubules with FtsZ *in vitro*. Here, it is shown that ring formation is conserved. Several SepF orthologs was purified and studied with electron microscopy. Most of these SepF orthologs polymerized and some of them formed clear rings that are similar to SepF rings of *Bacillus subtilis*. Furthermore, the C-terminal domain of SepF is sufficient to form SepF rings. The crystal structure of this domain revealed that it forms tight dimers which polymerize through interactions between α-helices. Yeast-two-hybrid studies of SepF mutants showed that the C-terminal domain of SepF is also required for FtsZ interaction. The analysis of the N-terminus of SepF both *in vitro* and *in vivo* revealed an amphipathic helix which is crucial for the function of SepF. This study showed that similar to FtsA, SepF anchors FtsZ to the cell membrane. A second project, called *Bacillus* Minimal Divisome, revealed the core division proteins which are sufficient to initiate the cell division.

Acknowledgements

I would like to thank Leendert Hamoen for accepting me as a part of his group and giving me the chance to work in a wonderful environment. I also would like to thank you, Leendert, for the support you gave me with your expertise to overcome obstacles in my project. Furthermore, I acknowledge Newcastle University and Overseas Research Studentship Award for funding this study.

I would like to thank Henrik Strahl for his help with everything I struggled, and also for the SepF mutants he constructed. I must acknowledge our collaborators Ramona Duman for her work in crystallography of SepF (Chapter 3.3) and Shu Ishikawa for the two hybrid experiments (Chapter 4.1) and both for sending me strains and proteins required for completing my study. I would also like to acknowledge Graham Scholefield, Nada Pavlendova and David Adams for their help with protein purifications, Simon Syvertsson for his preliminary work on *Bacillus* Minimal Divisome project, Tracey Davey and Vivian Thompson for the electron microscopy work and Ian Selmes for making sure that laboratory runs smoothly. Pamela Gamba, Yoshikazu Kawai, Patricia Dominguez-Cuevas, Katarina Surdova and all the members of the CBCB thank you all for your help and support in my research.

Finally, I would like to thank my family for believing me and supporting me through my education.

Table of Contents

List of Figures

List of Tables

Chapter 1. Introduction

Bacillus subtilis, a rod-shaped, Gram-positive bacterium, either divides symmetrically into two equal-sized daughter cells, or asymmetrically to form spores that survive under stress conditions, such as nutrient deficiency and extreme temperatures. It is a well-studied microorganism to define the cellular activities in Gram-positive bacteria. On the other hand, *Escherichia coli*, also a widely used model organism, is a Gram-negative bacterium. Similar to *B. subtilis*, *E. coli* is rod shaped and divides at the middle of the cell. However, it does not sporulate. The structure of the cell wall differs between Gram-positive and Gram-negative bacteria (Egan and Vollmer, 2013). This difference affects how these bacteria divide and eventually affects the proteins that function in the cell division. These proteins might be divided into three groups. The first group of proteins are conserved in both *B. subtilis* and *E. coli*, such as FtsZ and FtsA. Second, proteins like ZipA are only conserved in Gram-negative. Finally, there are proteins conserved in only Gram-positive bacteria such as SepF and EzrA. These proteins will be explained in detail in the following sections.

Cell division in bacteria is a well-orchestrated event, involving at least 15 known proteins, called the divisome proteins, which localize at the division site. These proteins are categorized in three different groups. The first group is responsible for the precise localization of the cell division site at the middle of the cell. These proteins regulate the polymerization of FtsZ, a bacterial homolog of the eukaryotic protein tubulin, which forms a ring-like structure, that is called the Z-ring, at midcell (Adams and Errington, 2009). The second group, the early divisome proteins, function in the assembly of the Z-ring at midcell. Finally, the late divisome proteins have roles in the production of the new cell wall (Gamba et al., 2009).

1.1. FtsZ and the Z-ring

FtsZ is the first protein known to localize at the division site and forms a structure called the Z-ring. It is highly conserved among bacteria and also found in mitochondria and chloroplasts of several eukaryotes (Margolin, 2005). The Z-ring acts as a scaffold for the recruitment of the other division proteins (Addinall and Lutkenhaus, 1996b). The tertiary structures of FtsZ monomer and polymer are very similar to that of the eukaryotic protein tubulin (Löwe, 1998). Also, both

FtsZ and tubulin uses similar mechanisms to hydrolyse GTP (de Boer et al., 1992a, RayChaudhuri and Park, 1992, Mukherjee et al., 1993). Moreover, an FtsZ inhibiting molecule called PG190723 binds to a region on FtsZ monomer which was identified as equivalent to the binding site of tumor inhibiting molecule taxol on tubulin (Andreu et al., 2010, Haydon et al., 2008). Therefore, despite the lack of clear sequence similarities, FtsZ is described as homologous to tubulin. FtsZ monomers bind to GTP through their GTP-binding domain located at the N-terminus, then polymerize in head-to-tail conformation to create tubulin-like loop 7 (T7-loop) that functions in GTP hydrolysis (Mukherjee and Lutkenhaus, 1994, Scheffers et al., 2001, Löwe, 1998).

The N-terminus of FtsZ is highly conserved. However, the C-terminal domain is not, except for 10 residues at the extreme C-terminus. This conserved region is the binding domain for many proteins that interact with FtsZ (Ma and Margolin, 1999, Erickson, 2001). Moreover, a recent study by Buske and Levin (2012) identified a small region adjacent to this conserved residues, called the C-terminal variable (CTV). The CTV affects the polymerization of FtsZ and differs between *B. subtilis* ($FtsZ_{BS}$) and *E. coli* ($FtsZ_{EC}$). The same study showed that the CTV of *B. subtilis* is positively charged while the CTV of *E. coli* is neutral. Furthermore, these regions were not interchangeable between $FtsZ_{BS}$ and $FtsZ_{EC}$, suggesting that the charge of the CTV is important for its function (Buske and Levin, 2012).

It is possible to observe polymerization of FtsZ both *in vivo* and *in vitro*. Electron microscopy, immunofluorescence microscopy, and later fluorescence microscopy using GFP tagged FtsZ have shown that FtsZ polymerizes into a ring-like structure at the periphery of the cell (Ma et al., 1996, Bi and Lutkenhaus, 1991, Addinall et al., 1996). The Z-ring becomes smaller in diameter as cell division progresses, and finally disappears when cells separate (Den Blaauwen et al., 1999). The Z-ring is preceded by the accumulation of FtsZ into a helical pattern in *E. coli* and *B. subtilis* (Thanedar and Margolin, 2004, Peters et al., 2007). Srinivasan et al. (2008) studied the behaviour of FtsZ when expressed in fission yeast and found that FtsZ behaves similar in both bacteria and fission yeast, forming a ring-like structure at the division site (Srinivasan et al., 2008). The amount of FtsZ in the Z-ring was measured as 30-35% of total FtsZ in *E. coli* and *B. subtilis* using quantitative fluorescence measurements (Anderson et al., 2004). This amount is enough to encircle the

division site 2-3 times which is contradictory to the results of cryoelectron microscopy of *Caulobacter crescentus* (Li et al., 2007). In this study, Li et al. (2007) proposed that FtsZ forms short overlapping filaments that circumvent the septum. The reason for this difference might be that some FtsZ filaments were not observed with cryoelectron microscopy.

Electron microscopy is often used to image FtsZ polymerization *in vitro*. FtsZ polymers might form filaments, sheets, bundles and ribbons (Popp et al., 2009, Mukherjee and Lutkenhaus, 1994, Bramhill and Thompson, 1994, Erickson et al., 1996). Presence of GTP in the medium induces the polymerization of FtsZ. Addition of crowding agents such as DEAE-dextran results in increase in the number of denser structures formed such as FtsZ sheets, bundles and ribbons. Ions like Ca^{2+} and Rb^{+} also stimulate the polymerization of FtsZ (Yu and Margolin, 1997, Tadros et al., 2006). Electron microscopy studies showed that FtsZ filaments become curved when they hydrolyse the bound GTP (Lu et al., 2000). Furthermore, an atomic force microscopy study showed slightly curved FtsZ filaments when it is bound to GMPCPP, a non-hydrolysable GTP analog (Mingorance et al., 2005). This conformational change of FtsZ filaments is assumed to provide the energy for the constriction of the division septum (Li et al., 2007, Oliva et al., 2007). Recently, this was nicely demonstrated by Osawa et al. (2008). This group constructed a variant of FtsZ that contained a membrane targeting sequence at the C-terminus. Mixing this FtsZ mutant with tubular liposomes resulted in the constriction of these liposomes when GTP was added (Osawa et al., 2008). This provides the evidence that FtsZ has a direct role in the constriction force of septa.

There are two models for the assembly mechanism of FtsZ. In the first model, FtsZ polymers assemble in a cooperative way starting with a lag phase followed by a rapid increase in polymerization (Caplan and Erickson, 2003, Chen et al., 2005). This model explains the reported critical concentration for FtsZ polymerization (Wang and Lutkenhaus, 1993, Oliva et al., 2003, Mukherjee and Lutkenhaus, 1998, Romberg and Mitchison, 2003). The second model, called isodesmic assembly, assumes that single-stranded FtsZ polymers are formed by the addition of each monomer from both sides of the filament. Therefore, the length of the filament increases in both directions (González et al., 2005, Romberg et al., 2001). This model is supported by the fact that the

initial assembly of FtsZ protofilaments does not require GTP hydrolysis. It is still undecided which mechanism is correct.

It is very important that its activity in the cell is controlled until the cell is ready to divide. This control might be in two main steps; first, control of the expression of *ftsZ* gene, and second, the control of the polymerization of FtsZ. Weart and Levin (2003) showed that FtsZ concentration in *B. subtilis* and *E. coli* cells is constant throughout the cell cycle (Weart and Levin, 2003). Therefore, its polymerization should be tightly controlled by both negative and positive regulators. The Min system and nucleoid occlusion prevent FtsZ polymerization at the cell poles and on the nucleoids, respectively, but there are also proteins, like FtsA and ZapA, that promote polymerization of FtsZ.

1.2. Regulating the Site of Cell Division

The precise localization of the divisome complex is orchestrated by two known mechanisms; the Min system and nucleoid occlusion (Bramkamp and van Baarle, 2009, Wu and Errington, 2012).

1.2.1. Min system

Adler et al. (1967) discovered small, anucleate cells of *E. coli* while searching for mutants resistant to UV radiation (Adler et al., 1967). These cells, called minicells, were the result of mutations in the *minB* locus, containing the *minC*, *minD* and *minE* genes (de Boer et al., 1989). These genes inhibit cell division close to the cell poles in *E. coli*. MinE acts as a topological protein for the localization of MinC and MinD (de Boer et al., 1989). Later, it has been shown that MinE, which forms a ring-like structure, oscillates from pole to pole moving the components of Min system away from midcell (Fu et al., 2001, Hale et al., 2001). MinD is a peripheral membrane protein that hydrolyses ATP (de Boer et al., 1991, Szeto et al., 2003). The ATPase activity was shown to be necessary for the function of MinD. MinE stimulates the ATPase activity of MinD, resulting in the dissociation of the MinD from the cell membrane. As a result, MinD diffuses to the other cell pole (Hu and Lutkenhaus, 2001). This oscillation of MinE and MinD was also shown *in vitro* using single-molecule and confocal microscopy (Loose et al., 2011). Moreover, Park et al. (2011) showed that interaction between MinD and MinE results in conformational change in MinE (Park et al., 2011). MinD tethers MinC to the cell membrane and

enhances its activity (de Boer et al., 1992b). MinC is the key inhibitor and directly interacts with FtsZ (Hu et al., 1999). The MinC structure can be divided into two domains. The N-terminus is required for FtsZ interaction, while the C-terminal domain interacts with MinD (Shen and Lutkenhaus, 2009, Shiomi and Margolin, 2007a, Hu and Lutkenhaus, 2003, Hu and Lutkenhaus, 2000). The mechanism by which MinC inhibits FtsZ polymerization is not entirely known. However, it has been suggested that MinC affects the flexibility of FtsZ filaments without affecting its GTPase activity (Dajkovic et al., 2008).

The *B. subtilis* Min system also contains MinC and MinD, but instead of MinE, this bacterium contains the proteins MinJ and DivIVA that function as topological proteins (Varley and Stewart, 1992, Levin P. A. et al., 1992, Patrick and Kearns, 2008, Bramkamp et al., 2008). MinC and MinD of *B. subtilis* function as the MinCD proteins in *E. coli* except that the proteins do not oscillate from pole to pole. Instead, DivIVA and MinJ, which are located at cell poles, recruit MinD to the cell poles (Bramkamp et al., 2008, Patrick and Kearns, 2008, Cha and Stewart, 1997, Edwards and Errington, 1997). DivIVA is a membrane bound protein that has a preference for negatively curved membranes (Lenarcic et al., 2009). MinJ is a trans-membrane protein that forms a molecular bridge between DivIVA and MinD (Patrick and Kearns, 2008, Bramkamp et al., 2008). MinJ also interacts with the cell division proteins FtsA, FtsL, EzrA and PBP2B (Bramkamp et al., 2008), and it was suggested that MinJ might stimulate the disassembly of the divisome complex after cell division is completed (van Baarle and Bramkamp, 2010).

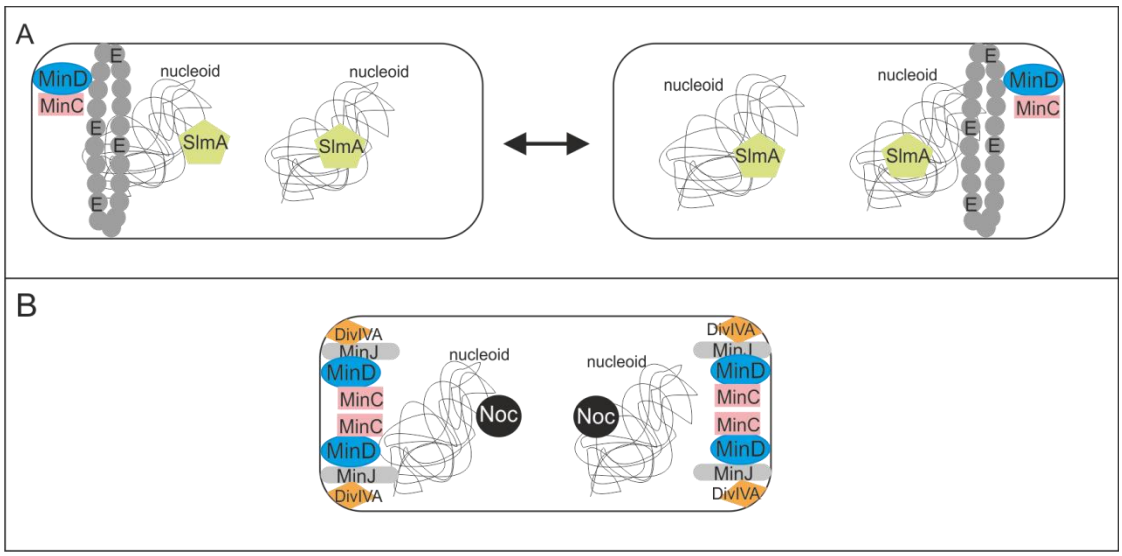

Figure 1.1 Summary of the division site selection. (A) In *E. coli*, MinE (shown as E), which form a ring-like structure, oscillates from one pole to the other pole. MinE dissociates MinD from the cell membrane which then travels to the other cell pole with MinC. Later, MinE oscillates to towards MinD resulting in re-dissociation of it. This pattern of MinE and MinCD proteins prevent FtsZ polymerization at the cell poles. SlmA binds to DNA and prevents FtsZ polymerization over the nucleoid. (B) In *B. subtilis*, DivIVA and MinJ tether MinCD to the cell poles. Unlike MinE, MinJ and DivIVA do not oscillate. Noc acts as the nucleoid occlusion protein.

1.2.2. Nucleoid occlusion system

The Min system and nucleoid occlusion work together to ensure the right positioning of the divisome complex. The nucleoid occlusion proteins SlmA and Noc in *E. coli* and *B. subtilis*, respectively, were discovered by searching for synthetic lethal mutants in *min* mutants (Bernhardt and de Boer, 2005, Wu and Errington, 2004). Bernhardt and de Boer (2005) reported that in *E. coli,* the protein SlmA interacts with the nucleoid and directly binds to FtsZ. Later, it was shown that SlmA binds to specific DNA sequences on the chromosome and that the binding of SlmA to DNA enhances its activity (Cho et al., 2011, Tonthat et al., 2011). Moreover, Tonthat et al. (2011) showed that the SlmA binding sites are found over the entire chromosome except for the Ter region, which contains several DNA replication termination sites. The crystal structure of the protein suggests that anti-parallel FtsZ protofilaments bind to both sides of the SlmA dimers, which result in trapped FtsZ molecules that prevent the formation of functional FtsZ filaments. However, in another study, it was shown that SlmA inhibits the formation of FtsZ filaments and disassembles ready-formed FtsZ protofilaments (Cho et al., 2011), and that anti-parallel binding of FtsZ to the

dimers is very likely not the mechanism by which SlmA inhibits FtsZ polymerization (Cho and Bernhardt, 2013).

In *B. subtilis*, nucleoid occlusion is controlled by Noc. SlmA and Noc do not share any sequence similarities. However, they both have the same role in cell division which is to protect the nucleoid from guillotining by the nascent septum. Noc also binds to specific DNA sequences on the chromosome that are absent from the replication termination region (Wu et al., 2009). Unlike SlmA, Noc does not interact with FtsZ *in vitro*, and therefore the mechanism by which Noc prevents the Z-ring formation *in vivo* is not yet known.

The Min system and nucleoid occlusion have been accepted as two mechanisms to determine the cell division site. However, recent studies demonstrated that in the absence of these systems, cell division still occurs at midcell, even when FtsZ is overproduced (Rodrigues and Harry, 2012). Rodrigues and Harry (2012) suggested that the Min system and nucleoid occlusion are primarily required for the efficient formation of the divisome complex. However, there is at least another, yet unknown, mechanism that has a role in the division site determination.

1.3. Division Proteins that Regulate FtsZ Polymerization

1.3.1. FtsA

FtsA is located at the *dcw* cluster, which contains a group of genes for peptidoglycan synthesis and cell division including *ftsZ*, and is conserved among Gram-positive and Gram-negative bacteria (Pichoff and Lutkenhaus, 2005, Rothfield et al., 1999). However, unlike FtsZ, FtsA is not essential in all organisms. For instance, in *B. subtilis* deletion of *ftsA* results in filamentous and non-sporulating cells, but the mutant is able to grow (Beall and Lutkenhaus, 1992). Several studies have demonstrated that FtsA interacts with itself and with FtsZ (Addinall and Lutkenhaus, 1996a, Ma et al., 1996, Feucht et al., 2001). Moreover, the protein helps to recruit the late divisome proteins to the Z-ring in *E. coli* (Rico et al., 2004).

FtsA is a member of the actin/HSP70 protein family (Bork et al., 1992). The crystal structure revealed 4 subdomains called 1A, 2A, 2B and 1C (van den Ent and Lowe, 2000).These subdomains form two domains which connect in the centre, resulting in the formation of an interdomain cleft. The cleft functions

as the ATP-binding site. The structure of FtsA is similar to the structure of eukaryotic actin with the main difference being subdomain 1C which has a different direction in the FtsA crystal (Figure 1.2A) (Szwedziak et al., 2012). Initially, it was assumed that the presence of the 1C subdomain prevents FtsA to polymerize like actin (Shiomi and Margolin, 2007b, Yim et al., 2000, Rico et al., 2004). However, in a recent study of the crystal structure it was shown that FtsA is indeed able to form actin-like polymers. This finding required crystallization in the presence of the non-hydrolysable ATP analog ATPγS (Figure 1.2B) (Szwedziak et al., 2012).

FtsA localizes at the division site after FtsZ, and its localization depends on FtsZ (Jensen et al., 2005, Ma et al., 1996, Addinall and Lutkenhaus, 1996a, Shiomi and Margolin, 2008). The last 16 residues at the C-terminal end of FtsZ are required and sufficient for the interaction with FtsA (Yan et al., 2000, Pichoff and Lutkenhaus, 2002, Din et al., 1998). These residues interact with a region in 2B subdomain of FtsA (Figure 1.2A) (Pichoff and Lutkenhaus, 2007, Szwedziak et al., 2012). FtsA and FtsZ are continuously produced during the cell cycle and are kept in a constant ratio of approximately 1:5 (FtsA:FtsZ) in *B. subtilis* (Trip et al., 2013, Feucht et al., 2001). Phenotypic effects of FtsA overexpression are compensated by overexpression of FtsZ, or vice versa (Rueda et al., 2003, Feucht et al., 2001, Dai and Lutkenhaus, 1992). In *E. coli*, FtsA is required for recruitment of divisome proteins such as FtsN and FtsI through the interaction with the 1C subdomain and mutations in this region results in inactive protein (Rico et al., 2004, Corbin et al., 2004, Shiomi and Margolin, 2007b).

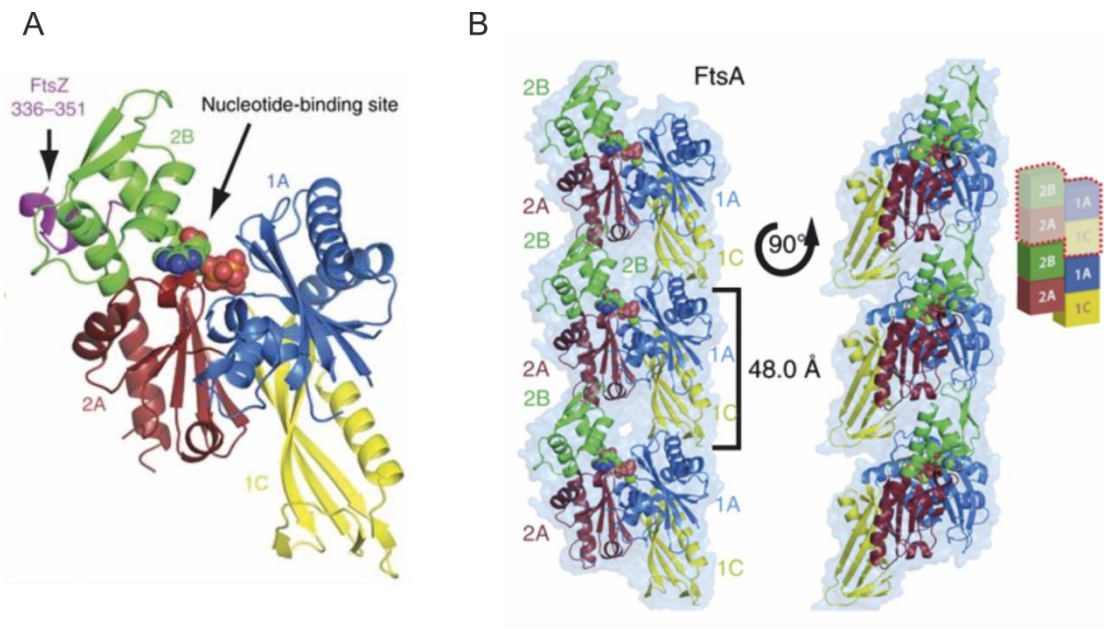

Figure 1.2 Crystal structure of FtsA (A) Monomeric FtsA has four subdomains 2A, 2B, 1A and 1C. The C-terminal end of FtsZ (shown in purple) was crystalized with FtsA. (B) FtsA polymerizes through interaction between subdomains 2B-2A and 1A-1C (Panels A and B were reproduced by permission from Macmillan Publishers Ltd: The EMBO Journal, (Szwedziak et al., 2012), copyright (2012)).

It has been shown that FtsA binds ATP. However, there has been only one reported ATPase activity assay with purified FtsA until this date (Feucht et al., 2001). It has been hypothesized that the ATPase activity is not required for the function of FtsA (Sanchez et al., 1994). On the other hand, abolishing ATP binding affects self-interaction of FtsA and FtsA-FtsZ interaction (Pichoff and Lutkenhaus, 2007).

The C-terminus of FtsA is unstructured and could not be solved in crystal structure studies (van den Ent et al., 2001). Several studies showed that truncations and point mutations in this region results in curved cells in *E. coli* (Gayda et al., 1992, Yim et al., 2000) and in *Staphylococcus aureus* (Yan et al., 2000). Moreover, rod-shaped aggregates of FtsA are observed in the cytoplasm of the cells containing the C-terminally truncated FtsA mutants (Pichoff and Lutkenhaus, 2005). Eventually, Pichoff and Lutkenhaus (2005) showed that the C-terminus of FtsA contains an amphipathic helix which interacts with the cell membrane (Pichoff and Lutkenhaus, 2005). This shows that FtsA tethers FtsZ to the cell membrane. Another protein that tethers FtsZ to the cell membrane is an essential protein, called ZipA in *E. coli*. However, studies showed that some mutations in FtsA, for instance R286W (known as FtsA*), overcome the

necessity of ZipA and several other division proteins in *E. coli* (Geissler et al., 2003, Geissler and Margolin, 2005, Geissler et al., 2007, Goehring et al., 2007a, Bernard et al., 2007). The R286W mutant was also shown to decrease the inhibitory effect of MinC on FtsZ polymerization and overproduction of ZipA on cell division (Geissler et al., 2003, Bernard et al., 2007). Recently, Pichoff et al. (2012) studied the self-interaction of FtsA using the aggregation phenotype of the C-terminal truncation of FtsA. In their study, several mutants including R286W were identified with decreased self-interaction compared to wild type FtsA (Pichoff et al., 2012). Furthermore, these self-interaction mutants were able to compensate for the loss of *zipA*. It was suggested that in *E. coli*, these self-interaction mutants contained free 1C domain which is required for polymerization of FtsA, so they could easily interact with the other division proteins (Pichoff et al., 2012). On the other hand, the mutations that prevent self-interaction in *B. subtilis* result in elongated cells, suggesting that polymerization of FtsA is important in *B. subtilis* (Szwedziak et al., 2012).

A study by Osawa and Erickson (2011) showed that an FtsZ chimera with a YFP protein and an amphipathic helix (MTS) was able to constrict tubular liposomes (Osawa and Erickson, 2011). Recently, the same group repeated this experiment with FtsA and FtsZ-YFP that were incorporated into unilamellar liposomes. The most striking observation of this experiment was the complete constriction liposomes by a Z-ring like structure (Osawa and Erickson, 2013). This result supported the constriction force of FtsZ and suggested that the FtsA may function in completion of the septum, since complete constriction was not observed in experiments that uses only FtsZ-YFP-MTS.

In summary, FtsA tethers FtsZ to the cell membrane in *B. subtilis* and in *E. coli* and connects it to other divisome proteins in *E. coli*. Moreover, the interaction between FtsA and FtsZ stabilizes the Z-ring (Adams and Errington, 2009). Although the role of FtsA in cell division is mostly understood, a possible function for ATP hydrolysis remains to be established.

1.3.2. ZipA

ZipA, a membrane-bound division protein, is conserved in Gram-negative gammaproteobacteria (Hale and de Boer, 1997). It is shown that FtsZ directly recruits ZipA, which is spread along the cell membrane during cell growth, to the septa and this recruitment does not depend on the presence of FtsA (Hale and de Boer, 1997, Liu et al., 1999, Hale and de Boer, 1999). The N-terminal

transmembrane domain and the C-terminal globular domain of ZipA are separated by a linker that mainly consists of proline and glutamine residues (Hale and de Boer, 1997, Moy et al., 2000, Mosyak et al., 2000). The crystal structure of ZipA reveals a hydrophobic cleft at the C-terminal domain which is also shown to be binding pocket for the C-terminal tail of FtsZ (Mosyak et al., 2000, Liu et al., 1999, Ma and Margolin, 1999, Haney et al., 2001). Although the C-terminal tail of FtsZ interacts with both FtsA and ZipA, the crystal structure of this region together with either FtsA or ZipA showed that it does not keep the same conformation for binding to both proteins (Mosyak et al., 2000, Moy et al., 2000, Szwedziak et al., 2012).

As mentioned above, ZipA has a role in tethering FtsZ to the cell membrane. Besides, it also increases polymerization of FtsZ both *in vitro* and *in vivo* (RayChaudhuri, 1999, Hale et al., 2000, Hale and de Boer, 1999). Moreover, overexpression of ZipA overcomes the division defects of the temperature sensitive FtsZ mutant, FtsZ84, at high temperatures (RayChaudhuri, 1999). In addition to its roles in FtsZ polymerization and tethering, ZipA recruits other divisome proteins, such as FtsK and FtsQ, to the septa (Pichoff and Lutkenhaus, 2002, Hale and de Boer, 2002).

Recently, a study using giant unilamellar vesicles (GUVs) and purified proteins ZipA and FtsZ once more showed that FtsZ is tethered to the membrane by ZipA (López-Montero et al., 2013). Later, it was also shown that in the presence of GTP, FtsZ, tethered to membrane by ZipA, shrinks the GUVs, an event similar to constriction of cell (Cabré et al., 2013). This experiment supports the findings of Osawa and Erickson (Osawa and Erickson, 2011, Osawa and Erickson, 2013).

1.3.3. ZapA

FtsZ polymerization is regulated both negatively and positively to ensure the correct timing and the localization of the septum. One of the positive regulators is ZapA. Guerios-Filho and Losick (2002) discovered ZapA which is widely conserved among Eubacteria, while searching for proteins that increase the polymerization of FtsZ (Gueiros-Filho and Losick, 2002). ZapA is a non-essential division protein, and its absence does not result in a clear phenotype. However, deletion of both *zapA* and *divIVA* causes a reduction in cell division resulting in filamentous cells. Moreover, reduced levels of FtsZ become lethal in a *zapA* null mutant (Gueiros-Filho and Losick, 2002). Furthermore, in *B. subtilis*,

overproduction of ZapA reverses the effect of temperature sensitive FtsZ mutants (Monahan et al., 2009). Furthermore, overproduction of ZapA overcomes a cell division block caused by overexpression of MinCD (Gueiros-Filho and Losick, 2002, Scheffers, 2008, Dajkovic et al., 2008). These genetic results indicate that ZapA stimulates the activity of FtsZ.

The crystal structure of ZapA from *Pseudomonas aeruginosa* shows that the protein forms both dimers and tetramers (Low et al., 2004). The protein consists of two domains; the N-terminal globular domain and a C-terminus coiled-coil protrusion (Low et al., 2004). The structure reveals that the coiled-coil region interacts with the coiled-coil region of the next protein, forming a symmetrical dimer. Moreover, mutations in this region revealed that the C-terminus also functions in tetramer formation (Pacheco‐Gómez et al., 2013).

In *E. coli* cells, the number of ZapA monomers is close to the number of FtsZ monomers (Mohammadi et al., 2009), which would allow each ZapA molecule to interact with an FtsZ monomer on the Z-ring (Low et al., 2004). Presumably, ZapA tetramers interact with FtsZ protofilaments in a way that it increases the lateral interactions of FtsZ. This interaction between FtsZ and ZapA stabilize FtsZ filaments, in other words, ZapA molecules crosslink the FtsZ protofilaments (Gueiros-Filho and Losick, 2002, Mohammadi et al., 2009). Mohammadi et al. (2009) suggested that the increase in lateral interactions between FtsZ filaments decreases the GTPase activity, as a result of which the Z-ring is stabilized.

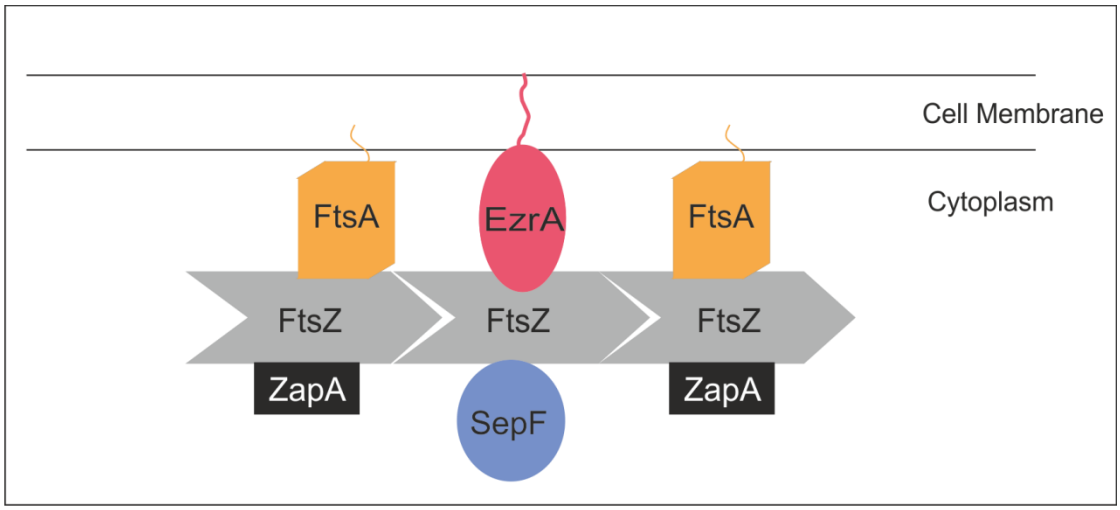

Figure 1.3 Assembly of the Z-ring in *B. subtilis*. FtsZ is tethered to the cell membrane by FtsA and EzrA. FtsA is attached to the membrane with an amphipathic helix while EzrA is a transmembrane protein. ZapA and SepF increase the stability of the Z-ring.

1.3.4. ZapB, ZapC and ZapD

Besides ZapA, several FtsZ-ring associated proteins (Zaps) were identified in *E.coli*. Among these, ZapB, ZapC and ZapD are conserved among gammaproteobacteria. These proteins have overlapping functions and they are not essential (Ebersbach et al., 2008, Hale et al., 2011, Durand-Heredia et al., 2011, Durand-Heredia et al., 2012). Like ZapA, ZapB is a small protein that consists of 81 amino acids. The deletion of *zapB* results in elongated cells and less frequent Z-rings. These Z-rings have abnormal shapes such as spirals and short helices (Ebersbach et al., 2008, Buss et al., 2013). The deletion of *zapB* becomes lethal in the presence of a temperature sensitive FtsZ mutant, but not with deletion of *min* or *zapA* (Ebersbach et al., 2008). Overproduction of ZapB resulted in condensed nucleoids (Ebersbach et al., 2008).

ZapB localizes to the division site in a ring like pattern inside the Z-ring, and its localization depends on the FtsZ and ZapA, but not other division proteins (Ebersbach et al., 2008, Galli and Gerdes, 2010). Moreover, overproduction of ZapA displaces the ZapB localization (Galli and Gerdes, 2012). The crystal structure of ZapB revealed a homodimer that is formed of coiled-coils (Ebersbach et al., 2008). Moreover, bacterial two hybrid assay and electron microscopy showed that ZapB polymerizes and forms long filaments (Ebersbach et al., 2008). ZapB interacts directly with ZapA through the N-terminus of ZapB and it is proposed that ZapB increases stability of the Z-ring by crosslinking the ZapA molecules (Galli and Gerdes, 2010, Galli and Gerdes, 2012). However, ZapB is able to support cell division in the absence of ZapA, suggesting that ZapB may directly increase the Z-ring stability (Galli and Gerdes, 2010). Moreover, Galli and Gerdes (2012) showed that ZapA-ZapB interaction is more favourable than ZapA-FtsZ interaction which might be a control mechanism for the polymerization of FtsZ, since ZapA and ZapB molecules are highly abundant in the cell (Ebersbach et al., 2008, Mohammadi et al., 2009). Recently, it was shown that ZapB interacts with MatP which interacts with and condenses the Ter region of chromosomes to guarantee proper segregation of chromosomes in *E. coli* (Espeli et al., 2012). Same study also showed that deletion of *matP* with either *zapA* or *zapB* results in chromosomal segregation defects. This result points to the possibility that the interaction between ZapB and MatP forms a link between chromosome segregation and cell division.

ZapC was identified as part of the divisome machinery in *E. coli* only a few years ago (Durand-Heredia et al., 2011, Hale et al., 2011). ZapC localizes at the Z-ring and directly interacts with FtsZ (Durand-Heredia et al., 2011). The localization of ZapC to the Z-ring requires only FtsZ (Hale et al., 2011). Both overproduction and underproduction of ZapC result in elongated cells and abnormal FtsZ ring structures (Durand-Heredia et al., 2011, Hale et al., 2011). Furthermore, Hale et al. (2011) showed that the deletion of *zapC* increases the cell division defects in cells that overexpress MinC. The electron microscopy and co-sedimentation studies with ZapC and FtsZ showed that ZapC interacts with FtsZ and increases the bundling of FtsZ protofilaments (Durand-Heredia et al., 2011, Hale et al., 2011). Also, ZapC has been shown to decrease the GTPase activity of FtsZ (Hale et al., 2011). Moreover, FtsZ and ZapC interact with each other in yeast (Durand-Heredia et al., 2011).

ZapD is the last identified member of Zaps (Durand-Heredia et al., 2012). Its localization on the Z-ring depends on only FtsZ through interaction with the conserved C-terminal tail of FtsZ (Durand-Heredia et al., 2012). The same study also showed that overproduction of ZapD increases cell length while the deletion of *zapD* decreases the cell division frequency in cells with a temperature sensitive FtsZ mutant at permissive temperature (Durand-Heredia et al., 2012). ZapD forms dimers in solution and increases the bundling of FtsZ filaments probably through decreasing GTPase activity (Durand-Heredia et al., 2012).

Despite having slight differences in their roles in the cell, the main function of Zaps is to stabilize the Z-ring. While it is not known why there are several proteins with redundant functions in the cell, it is possible that the differences, such as ZapB-MatP interaction, make all of these proteins necessary for the cell division.

1.3.5. SepF

The *ylm* locus, which is located upstream of *divIVA*, is conserved among Gram-positive bacteria and cyanobacteria (Miyagishima et al., 2005, Marbouty et al., 2009, Fadda et al., 2003). The *ylmF* gene codes for a protein called SepF. SepF was discovered by two independent groups (Hamoen et al., 2006, Ishikawa et al., 2006). Ishikawa et al. (2006) showed that a *sepF ftsA* double mutant is lethal, and that overexpression of *sepF* compensates for the filamentous cell phenotype of an *ftsA* mutant. Yeast-two-hybrid experiments and

in vitro data showed that SepF interacts with itself and with FtsZ (Ishikawa et al., 2006, Hamoen et al., 2006). Using electron microscopy, Hamoen et al. (2006) demonstrated that a deletion of *sepF* results in abnormal septa formation, and it was suggested that SepF has a function in septal synthesis rather than a function in formation or stabilization of the Z-ring (Hamoen et al., 2006).

The interaction of SepF with FtsZ has been studied extensively. It was shown that SepF interacts with the last 16 residues of the C-terminus of FtsZ (Singh et al., 2008, Król et al., 2012). This interaction increases bundling of FtsZ polymers (Singh et al., 2008). Recent studies using purified SepF and FtsZ show that under physiological conditions, SepF polymerizes into large, ring-like structures called SepF rings (Figure 3.3A) (Gundogdu et al., 2011). Interestingly, when the SepF rings were mixed together with FtsZ, the FtsZ protofilaments were wrapped around the SepF rings, forming large tubules with the same diameter as the SepF rings. Furthermore, Gundogdu et al. (2011) identified two mutants, A98V and F124S that are deficient in FtsZ binding. These mutants polymerize into rings, but these rings are unable to bundle FtsZ. Deletion of the last 17 residues prevents polymerization of SepF into rings. FtsZ binding mutants, non-polymerizing mutants and non-ring forming mutants are unable to prevent filamentation of an *ftsA* mutant.

1.3.6. EzrA

In *B. subtilis*, there is another protein, EzrA, which functions as a negative regulator of FtsZ. EzrA is conserved among Gram-positive bacteria (Considine et al., 2011, Jorge et al., 2011, Steele et al., 2011). Levin et al. (1999) discovered EzrA during a study of the temperature sensitive GFP-FtsZ fusion. They discovered that EzrA prevents the Z-ring formation at cell poles, and the absence of EzrA lowers the critical concentration of FtsZ polymerization. EzrA contains an N-terminal transmembrane helix and the protein is distributed along the cell membrane during growth and later it localizes at the cell division site in an FtsZ-dependent manner (Levin et al., 1999). EzrA is not an essential protein, however, it is required for efficient cell division (Kawai and Ogasawara, 2006, Chung et al., 2004, Levin et al., 1999). In the absence of EzrA, cells become slightly elongated and occasionally minicells are observed (Dempwolff et al., 2012, Levin et al., 1999).

EzrA has two domains; the C-terminal domain with 4 conserved coiled-coils and the N-terminus transmembrane anchor (Levin et al., 1999, Haeusser et al., 2004). EzrA interacts directly with FtsZ (Singh et al., 2007, Chung et al., 2007, Haeusser et al., 2004). It is constitutively expressed by two promoters (Chung et al., 2004). It has been postulated that the cytoplasmic domain of EzrA interacts with FtsZ through a conserved seven amino acids residue in its C-terminus, called the QNR patch (Haeusser et al., 2007). Deletion of this patch diminishes the localization of EzrA to the Z-ring. However, it does not affect inhibition of FtsZ polymerization, and cells are significantly longer but do not contain extra Z-rings, which is typical for *ezrA* null mutants. This suggests that EzrA interacts with divisome proteins other than FtsZ. Like FtsA and SepF, EzrA also binds to the conserved C-terminal tail of FtsZ (Singh et al., 2007).

As mentioned above, deletion of *ezrA* by itself is not lethal. However, combining an *ezrA* deletion with deletions of other cell division genes results in a synthetic sick or synthetic lethal phenotype. For instance, a *sepF ezrA* double mutant is not viable (Hamoen et al., 2006). Deletion of *ezrA* also suppresses filamentous growth due to artificial overexpression of MinCD (Levin et al., 2001).

It has been proposed that EzrA controls polymer stability of FtsZ to ensure that the Z-rings are only formed at division sites (Levin et al., 2001). However, the function of EzrA is more complex and it has been shown that this protein also plays a role in the recruitment of the penicillin binding protein PBP1 from the lateral wall to the site of cell division (Claessen et al., 2008). Thus EzrA appears to play both a negative as well as positive role in cell division.

1.3.7. FtsE and FtsX

The genes *ftsE* and *ftsX* in *ftsE* locus were first identified in *E. coli* (Gill et al., 1986). An ATP binding protein, FtsE, and a membrane binding protein, FtsX, which are broadly conserved among bacteria, are the components of an ATP binding cassette (ABC) transporter (Gill et al., 1986, Schmidt et al., 2004). The fact that FtsE is required for cell viability only under low salt and low-osmolarity conditions suggested that FtsEX might not have a role in cell division (De Leeuw et al., 1999, Reddy, 2007). However, a study of Schmidt et al. (2004) showed that FtsEX functions in the cell division. It is shown that the *ftsE* mutants grew poorly even in the presence of salt, and double mutant of *ftsE ftsX* prevented the cell division (Schmidt et al., 2004). The same study also

showed that FtsEX localizes at the division site after FtsZ, FtsA and ZipA in *E. coli* (Schmidt et al., 2004). It is later shown that overproduction of divisome proteins FtsZ, FtsA, FtsQ or FtsN in *E. coli* rescued the division defects of an *ftsE ftsX* double mutant in low-osmolarity medium (Reddy, 2007). A recent study showed that FtsEX recruit EnvC, an activator of cell wall amidases that function in cell separation, to the septum through an interaction between periplasmic loop of FtsX and EnvC (Yang et al., 2011). They also suggested that the ATPase activity of FtsEX complex is required for the interaction with the EnvC, so that FtsEX forms a bridge between cell separation and the Z-ring formation (Yang et al., 2011).

In *B. subtilis*, the ABC transporter FtsEX was shown to have a role in sporulation initiation (Garti-Levi et al., 2008). It is shown that the absence of this ABC transporter results in a delay in sporulation and formation of a septum in midcell instead of the cell poles (Garti-Levi et al., 2008). This phenotype could be compensated by activation of Spo0A, which is a primary sporulation regulator, suggesting that FtsEX function in this pathway before this activation (Garti-Levi et al., 2008). Besides their role in sporulation, FtsEX also functions in cell elongation in *B. subtilis*. Similar to its role in *E. coli*, FtsEX activates an endopeptidase called CwlO, which hydrolyses peptide crosslinks in lateral cell wall (Meisner et al., 2013, Domínguez-Cuevas et al., 2013). Absence of the FtsEX complex results in different phenotypes in *E. coli* and in *B. subtilis*; either it affects the cell division or it inhibits the sporulation without any known effect on vegetative growth. This difference suggests that FtsEX has different roles in these organisms. However, the fact that FtsEX activates the cell wall hydrolysis proteins in both organisms suggests that the different phenotypes in *ftsE ftsX* mutants might be a result of differences in cell division between Gram-negative and Gram-positive bacteria.

1.3.8. FtsK

FtsK was identified in a study searching for temperature sensitive mutants with filamentous cell phenotype (Begg et al., 1995). FtsK contains two domains; the N-terminal membrane domain and the C-terminal nucleotide binding domain that are separated by a linker (Begg et al., 1995). It localizes to the midcell only after the constriction starts and this localization is mediated through the N-terminal membrane binding domain of FtsK (Yu et al., 1998a, Dorazi and Dewar, 2000). However, it is shown that the deletion of *ftsK* gene

resulted in smooth filamentous cells, suggesting that FtsK stops the cell division before constriction starts (Wang and Lutkenhaus, 1998). The absence of functional FtsK protein causes a block in cell division in late stage, and is compensated by deletion of *dacB*, which codes for a penicillin-binding protein PBP5, FtsN overproduction or the expression of only a small part of N-terminal domain of FtsK (Begg et al., 1995, Draper et al., 1998). Wang and Lutkenhaus (1998) showed that the expression of *ftsK* increases with the DNA damage and activation of the SOS system (Wang and Lutkenhaus, 1998). Later, it was shown that the C-terminal domain of FtsK is required for chromosome segregation and is suggested to present a link between cell division and separation of chromosomes (Liu et al., 1998, Steiner et al., 1999, Yu et al., 1998b).

Homologs of FtsK exist in other organisms, for instance SpoIIIE and SftA in *B. subtilis* (Begg et al., 1995, Biller and Burkholder, 2009, Kaimer et al., 2009). These proteins are known as DNA translocases. However, SpoIIIE and SftA are not multifunctional like FtsK. The *spoIIIE* gene was identified in 1987 (Errington and Jones, 1987). Later, it was shown that SpoIIIE is essential for sporulation in *B. subtilis* (Wu and Errington, 1994). The function of SpoIIIE is to segregate chromosome after the closure of polar septa, in other words SpoIIIE ensures that the chromosome is not left on the mother cell by pulling it through the membrane into the forespore (Wu et al., 1995, Wu and Errington, 1997, Bath et al., 2000). SftA has a role in vegetative growth in *B. subtilis*. Its localization at the Z-ring depends on PBP2B and it is proposed that SftA has a similar function as FtsK in separation of chromosome dimers (Biller and Burkholder, 2009, Kaimer et al., 2009). The deletion of *sftA* resulted in guillotining of unsegregated chromosome (Biller and Burkholder, 2009). Kaimer et al. (2009) showed that StfA form dimers and has DNA-dependent ATPase activity *in vitro* (Kaimer et al., 2009). The ATPase activity is required for the function of SftA (Kaimer et al., 2009). Although both SpoIIIE and SftA function in chromosome segregation, SftA localizes at septa and SpoIIIE at the polar division site (Biller and Burkholder, 2009, Kaimer et al., 2009). Moreover, deletion of *sftA* did not affect the sporulation, suggesting that SftA and SpoIIIE have different roles in the cell cycle (Biller and Burkholder, 2009). It is also shown that presence of two distinct DNA translocases such as SftA and SpoIIIE

is conserved among soil-growing bacteria, but not in endospore forming ones (Biller and Burkholder, 2009).

1.4. Late Division Proteins

Another set of proteins are recruited to the division site after the formation and stabilization of the Z-ring. These proteins, grouped as the late division proteins, are mainly responsible for the synthesis of new cell wall (Gamba et al., 2009).

1.4.1. DivIB, DivIC and FtsL

Harry and Wake (1989) identified *divIB* as a temperature sensitive mutant with cell division defects at high temperatures (Harry and Wake, 1989). Later, it was shown that DivIB in *B. subtilis* is a homolog of FtsQ in *E. coli* (Harry et al., 1994). DivIB localizes at the division site before constriction occurs (Harry and Wake, 1997). It is essential only at temperatures above 37°C (Rowland et al., 1997). Another cell division protein DivIC, homologous to FtsB in *E. coli*, was identified as an essential protein whose absence blocks the septum formation (Levin and Losick, 1994). Localization of both DivIB and DivIC to the division site depends on the presence of FtsZ (Katis et al., 2000). Another protein required for the localization of DivIC and DivIB is the conserved protein FtsL, also known as FtsL in *E. coli* (Daniel et al., 1998). Studies with GFP-FtsL showed that it localizes at midcell and remains there until septation ends (Sievers and Errington, 2000b).

DivIB, DivIC and FtsL share the same topological structure; a small cytoplasmic N-terminal domain linked to a larger extra-cytoplasmic C-terminal domain by a single membrane spanning region (Katis et al., 1997, Harry and Wake, 1989, Sievers and Errington, 2000a, Daniel and Errington, 2000). FtsL is a highly unstable protein, which is quickly degraded at high temperatures in the absence of DivIB, explaining why DivIB is required for growth of *B. subtilis* above 37°C (Daniel and Errington, 2000). It was also shown that in the absence of FtsL, DivIC becomes unstable (Daniel et al., 1998). DivIC and FtsL appear to form a heterodimer which is stabilized by DivIB interaction (Daniel et al., 2006, Noirclerc-Savoye et al., 2005, Masson et al., 2009). The stability of this ternary complex is an important checkpoint for cell division in *B. subtilis*. The cytoplasmic N-terminal end of FtsL is recognized by a regulatory protease

called RasP (YluC), which cleaves the protein resulting in degradation of FtsL (Bramkamp et al., 2006, Wadenpohl and Bramkamp, 2010).

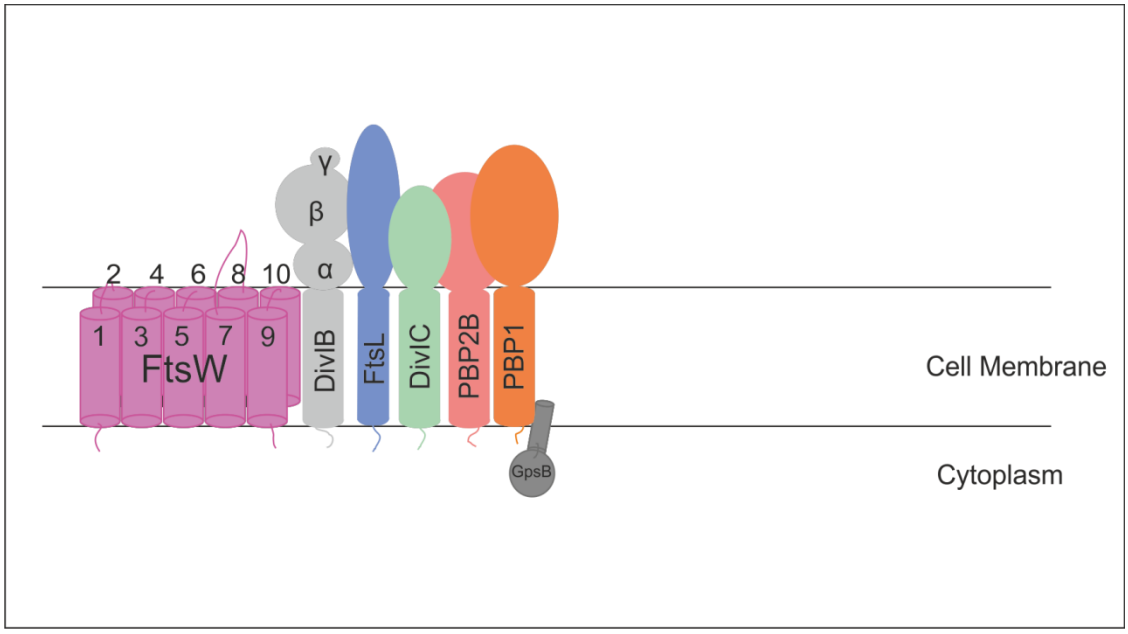

Figure 1.4 Assembly of the late divisome proteins in *B. subtilis*. FtsL, DivIB, DivIC, PBP2B, PBP1 and FtsW are transmembrane proteins. FtsL, DivIB and DivIC form a complex to stabilize themselves. DivIB has three subdomains, α, β, and γ, at the C-terminus. PBP2B is a transpeptidase, and PBP1 is a transglycosylase/transpeptidase. Both PBP2B and PBP1 have a role in synthesis of new cell wall. FtsW is involved in translocation of the lipid-linked peptidoglycan precursor. The transmembrane segments of FtsW are numbered. GpsB is responsible for the disassociation of PBP1 from septa.

Study of chimeric $DivIB_C$ (the C-terminus of DivIB) and $DivIC_C$ (the C-terminus of DivIC) proteins that contain only the C-terminal domains of DivIB and DivIC showed that the C-termini of DivIB and DivIC are sufficient for the interaction between these proteins. Moreover, the extracytoplasmic region of DivIB is shown to be functional by itself while the extracytoplasmic region of DivIC is sensitive to high temperatures suggesting a role for the N-terminus and the transmembrane domain of DivIC (Katis and Wake, 1999). The transmembrane domain and the C-terminus of DivIB contain division targeting signals which are also required for FtsL and DivIC interactions (Wadsworth et al., 2008). The C-terminal region consists of three subdomains; α, β, and γ (Robson et al., 2005, Robson and King, 2005). It has been suggested that the β subdomain changes its conformation in order to make the protein available for interactions with the other divisome proteins (Robson and King, 2006). Both DivIC and FtsL contain a leucine zipper at their C-terminal domains. These

zipper domains are believed to interact with each other (Daniel et al., 1998, Sievers and Errington, 2000a, Daniel et al., 2006, Robichon et al., 2008). All the experiments performed *in vivo* and *in vitro* suggest that FtsL and DivIC interact with each other through their C-terminal domains. However, Robson et al. (2002) reported that they could not detect such interactions in *in vitro* (Robson et al., 2002).

In *E. coli*, the proteins FtsQ, FtsB and FtsL form a complex similar to DivIB, DivIC and FtsL (Buddelmeijer and Beckwith, 2004). The localization of this complex to the division site depends on the interaction between FtsQ and FtsK (Chen and Beckwith, 2001). However, unlike DivIB, FtsQ is essential for the cell division in *E. coli* (Storts et al., 1989). FtsL and FtsB are also essential proteins in *E. coli* (Guzman LM et al., 1992, Buddelmeijer et al., 2002).

1.4.2. Penicillin binding proteins (PBPs)

Penicillin binding proteins (PBPs) function in the synthesis of either the lateral or the septal cell wall. They are separated in three groups: class A high-molecular weight (MW), class B high-molecular weight, and low-molecular weight PBPs. The primary functions of PBPs are the polymerization of the peptidoglycan backbone via either, transpeptidase activity to crosslink the peptidoglycan, transglycosylase activity for addition of glycosides to the peptidoglycan or carboxypeptidation to control the degree of crosslinking (Goffin and Ghuysen, 1998). There are two known PBPs involved in septal cell wall synthesis; PBP2B and PBP1.

PBP2B, encoded by the *pbpB* gene which codes for PBP3 (FtsI) in *E. coli*, is an essential, class B high-MW PBP with a transpeptidase domain (Yanouri et al., 1993). The penicillin binding domain of PBP2B separates the N-terminal domain, which is homologous to the other class B PBPs, from the C-terminal domain (Yanouri et al., 1993). Depletion of PBP2B results in filamentous cells that will eventually lyse (Daniel and Errington, 2000). The septal localization of PBP2B depends on the presence of FtsZ (Scheffers et al., 2004). Recently, Daniel et al. (2006) showed that PBP2B stabilizes DivIC and FtsL, and a single amino acid change in the N-terminus of PBP2B overcomes the necessity of DivIB at high temperatures (Daniel et al., 2006). These data show that PBP2B is also necessary to assemble the late division proteins to the cell division site.

The gene *ponA* codes for a conserved, class A high-MW PBP, called PBP1. PBP1 has transglycosylase and transpeptidase activities in *B. subtilis* (Popham and Setlow, 1995). Deletion of this gene only mildly decreases the growth rate, and does not have a significant effect on cell division (Popham and Setlow, 1995). Later studies showed that PBP1 becomes important in divalent-cation deficient environments (Murray et al., 1998). Deletion of *ponA* under this condition results in bended and filamentous cells that can be prevented by the addition of Mg^{2+} or Ca^{2+} (Murray et al., 1998). PBP1 localizes at the division site, and depends on the presence of the late division proteins PBP2B, DivIC and DivIB (Scheffers and Errington, 2004). Recently, Kawai et al. (2009) demonstrated that PBP1 localization also depends on the cytoskeletal protein MreB (Kawai et al., 2009).

1.4.3. FtsN

One of the last proteins that localize at the division site in *E. coli* is an essential protein, called FtsN. This protein was identified as a suppressor of temperature sensitive FtsA mutant (Dai et al., 1993). The membrane spanning region of FtsN separates a short N-terminal cytoplasmic domain and larger extracytoplasmic region with unusual amount of glutamine residues (Dai et al., 1993, Dai et al., 1996). The C-terminal domain of FtsN binds to the long peptidoglycan strands of the cell wall. However, this binding does not affect the cell division (Ursinus et al., 2004). Furthermore, the C-terminal domain contains a short region called SPOR (sporulation-related domain) which was binding region for the peptidoglycan chains (Yang et al., 2004, Ursinus et al., 2004). The presence of SPOR region also increases the localization efficiency of FtsN to the division site (Gerding et al., 2009). Moreover, Gerding et al. (2009) identified several other proteins that have SPOR domains. Two of these proteins, DamX and DedD, are shown to localize at the division site probably through interaction between the SPOR domains (Gerding et al., 2009). On the other hand, the N-terminal cytoplasmic region of FtsN was shown to be important for the suppression of the *ftsK* null mutant (Goehring et al., 2007b).

FtsN localizes to the division site in later stages of cell division and requires localization of FtsQ and FtsI (Addinall et al., 1997). Rico et al. (2010) showed that the already formed divisome complex disassembles when FtsN is depleted (Rico et al., 2010). The fact that FtsN might have a role in recruitment of proteins that involve in metabolizing the peptidoglycan chains suggests that

FtsN might be a control mechanism which signals the completion of divisome complex, so that the separation of the daughter cells starts (Gerding et al., 2009, Lutkenhaus, 2009). The disassembly of the whole divisome complex in the absence of FtsN supports that FtsN recruitment might be a checkpoint for the cell division.

1.4.4. FtsW

FtsW is a membrane-bound protein with 10 membrane spanning domains. There is a large extracytoplamic region between transmembrane domains 7 and 8 (Gérard et al., 2002, Lara and Ayala, 2002). The protein was first identified in *E. coli,* but homologs exist in many other bacteria (Ikeda et al., 1989). In *B. subtilis*, SpoVE and YlaO, also called FtsW, are homologs of FtsW (Errington et al., 2003, Henriques et al., 1992).

In *E. coli*, FtsW is an essential protein. Its absence results in a division block and cells eventually lyse (Boyle et al., 1997). Wang et al. (1998) showed that FtsW localizes at the division site in *E. coli* (Wang et al., 1998). It has been speculated that FtsW is involved in the translocation of the lipid-linked precursors of peptidoglycan (Höltje, 1998, Matsuhashi, 1994). Indeed, a recent study showed that FtsW flips the lipid-linked peptidoglycan precursors (Lipid-II) across the cytoplasmic membrane (Mohammadi et al., 2011). Another role of FtsW in cell division is the localization of its cognate PBP to the division site (Errington et al., 2003). In *E. coli*, FtsW recruits PBP3 to septa through its transmembrane domains 9 and 10 while transmembrane domains 7 and 8 are required for septal peptidoglycan synthesis (Pastoret et al., 2004).

1.4.5. GpsB (= YpsB)

GpsB (YpsB) has been identified as being part of the divisome only a few years ago (Tavares et al., 2008, Claessen et al., 2008). The N-terminal region of GpsB shows homology to the cell division protein DivIVA and GpsB is conserved amongst Gram-positive bacteria (Tavares et al., 2008, Claessen et al., 2008). Although a deletion of *gpsB* does not have an effect on cell division, double mutants of *ezrA gpsB* and *ftsA gpsB* are synthetic sick. Moreover, the presence of GpsB becomes important when cells are grown at high salt concentrations (Claessen et al., 2008). Claessen et al. (2008) showed that together with EzrA, GpsB is required to shuttle PBP1 between the septal and the lateral cell wall. While GpsB is responsible for the removal of PBP1 from

newly formed cell poles after division, EzrA has a role in recruitment of PBP1 to the new division sites (Claessen et al., 2008). The secondary structure prediction of GpsB shows that it forms an extended coiled-coil domain. The N-terminus together with the coiled-coil region is required for septal localization, while the C-terminus with the coiled-coil region is important for self-interaction (Tavares et al., 2008). Bacterial two-hybrid experiments have shown that GpsB interacts with EzrA and PBP1 (Claessen et al., 2008). Moreover, similar to DivIVA, GpsB localizes at the division site as a late division protein. However, unlike DivIVA, it does not stay at the cell poles after completion of the cell division (Tavares et al., 2008).

1.5. Proteins that Affect Cell Division

1.5.1. UgtP

UgtP is a glucosyltransferase which takes part in the synthesis of glycolipids. It uses UDP-glucose for the synthesis of the diglucosyl diacylglycerol anchor of lipoteichoic acids (LTA) (Jorasch et al., 1998). Price et al. (1997) showed that deletion of *ugtP* causes formation of shorter and rounder cells (Price et al., 1997). Later, it was shown that UgtP-GFP localizes at the septal region and at cell poles (Nishibori et al., 2005).

Recently, UgtP was identified as the link between cell division and nutrient availability. Weart et al. (2007) showed that UgtP directly inhibits FtsZ assembly in a concentration-dependent manner *in vitro*. They calculated the amount of UgtP as 2400 molecules per cell in LB, which decreases as UDP-glucose levels are reduced (Weart et al., 2007). This results in self-interaction of UgtP. On the other hand, UDP-glucose decreases the affinity of UgtP for itself, resulting in increased FtsZ-UgtP interaction. Chien et al. (2012) showed that UgtP inhibits the single-filament formation of FtsZ (Chien et al., 2012). It was shown that UgtP expression and localization is nutrient dependent. When nutrients are available UgtP localizes mainly at the cell poles and division sites, thereby inhibiting FtsZ, resulting in longer cells. Under poor growth conditions, UgtP localizes as distinct foci in the cytoplasm (Weart et al., 2007). They also showed that the cell division defect caused by MinCD overproduction is suppressed by a deletion of *ugtP.* These data show a clear link between cell division and nutrient availability.

1.5.2. ClpX

ClpXP is a chaperone complex in which ClpP functions as a protease while the role of ClpX is substrate recognition. ClpX directly inhibits FtsZ assembly independent of its chaperone activity and ATP hydrolysis (Haeusser et al., 2009, Weart et al., 2005). This inhibition of FtsZ by ClpX is concentration dependent (Weart et al., 2005, Haeusser et al., 2009). Sugimoto et al. (2010) suggested that FtsZ is found in equilibrium between monomers and polymers, and the role of ClpX is to block reassembly of FtsZ polymers, hence, keeping the equilibrium in favour of FtsZ monomers (Sugimoto et al., 2010).

Interaction between ClpX and FtsZ depends on the N-terminal recognition site of ClpX and the C-terminus of FtsZ, which shows similarity to the normal peptide recognition signal of ClpX (Camberg et al., 2009, Sugimoto et al., 2010). It has been suggested that in *E. coli*, the division protein ZipA and ClpX compete for the same binding site on FtsZ, which results in either protection of FtsZ polymers by ZipA or disassembly by ClpX (Pazos et al., 2013).

Overproduction of ClpX results in a complete block in cell division and the cell length increase (Weart et al., 2005). Moreover, deletion of *clpX* suppresses the division defect when MinCD are overproduced (Weart et al., 2005, Haeusser et al., 2009). In addition, the absence of *clpX* compensates for the certain temperature sensitive mutants of FtsZ (Weart et al., 2005).

1.6. Aim of the Thesis

SepF is an important part of the divisome complex in *B. subtilis* and many other Gram-positive bacteria. Together with FtsA, it stabilizes the Z-ring (Ishikawa et al., 2006) and the absence of SepF results in cell division with abnormal septa (Hamoen et al., 2006). Analysis of SepF *in vitro* shows that SepF and FtsZ form large tubular structures while SepF itself polymerizes into a ring called the SepF ring (Gundogdu et al., 2011). The significance of the SepF rings or the FtsZ-SepF tubules *in vivo* is not known yet. However, a study that shows conservation of the SepF rings in other organisms might support that these structures are formed in the cell. One of the aims of this thesis is to demonstrate that SepF homologs form the SepF rings *in vitro* by visualizing purified proteins with transmission electron microscopy.

Deletion of SepF in *ezrA* null mutants or *ftsA* null mutants is lethal (Ishikawa et al., 2006, Hamoen et al., 2006). Although both EzrA and FtsA localize at the septum, EzrA negatively regulates the Z-ring assembly while FtsA stabilizes the divisome complex (Adams and Errington, 2009). Their ability to interact with the cell membrane is one thing they have in common. Hence, it is possible that SepF also shares this characteristic with FtsA and EzrA. The second aim of this thesis is to test whether SepF is able to interact with the cell membrane using *in vitro* and *in vivo* approaches. Finally, we aimed to construct a *B. subtilis* strain which does not contain the nonessential cell division proteins. This strain would show the minimal divisome that is required for formation of two daughter cells.

In summary, this work focuses on understanding the characteristics of SepF and its role in cell division.

Chapter 2. Methods and Materials

2.1. Construction of Strains and Plasmids

Strains constructed in this study are listed in Table 2.1 for *Bacillus subtilis* and in Table 2.2 for *Escherichia coli*. *B. subtilis* strains were constructed by transformation of either chromosomal DNA or PCR products, while *E. coli* strains were transformed with plasmids. Genotypes of the plasmids used in this study are found in Table 2.3. The list of primers used in this study is found in Table 2.4.

2.2. Construction of pMALC2 Plasmids for MBP-SepF Fusions

SepF orthologs were amplified from chromosomal DNA of the organism of interest using forward and reverse primers (Eurogentec, Belgium) with *Sma*I or *Eco*RI and *Xba*I (Roche) restriction sites, respectively. PCR products were digested with *Sma*I or *Eco*RI and *Xba*I (Roche) while pMALC2 was digested with *Xmn*I (NEB) or *Eco*RI (Roche) and *Xba*I (Roche). Ligation of digested products was carried out overnight at 4°C with T4 ligase (Roche). The ligation mixture was then transformed to competent DH5α cells. Clones were isolated and sequenced.

Gundogdu et al. (2011) used purified SepF protein in their experiments. Re-sequencing of *B. subtilis* genome showed that the start codon of SepF is slightly different than SepF used in those experiments. Therefore, the sequence of pMalC2-SepF used by Gundogdu et al. (Gundogdu et al., 2011) was modified using the Quickchange method with primers inc26/inc27 and inc28/inc29 (Table 2.4).

2.3. Polymerase Chain Reaction (PCR)

The region of interest was amplified from either chromosomal DNA or plasmids using custom oligonucleotide primers and a TECHNE TC312 thermocycler (Techgene). Different DNA polymerases were used depending on the purpose of the amplification. *Pfu* Turbo and *Pfu* Ultra (Stratagene) were used for sited-directed mutagenesis using the Quickchange method. Phusion polymerase (NEB) and Expand High Fidelity system (Roche) were used for amplification of large regions of DNA with high precision. GoTaq polymerase (Promega) was generally used for control PCRs.

Screening of a high number of colonies was first performed by colony PCR in which colonies were used as template instead of isolated DNAs. The colony was picked by a sterile pipette tip and mixed with dH_2O. Cell lysis was achieved by vigorous mixing of the colony and water with a vortex machine. Lysed cells were used as template DNA in the PCR reaction. Using GoTaq polymerase (Promega), PCR was performed.

Strain	Relevant Genotype	Construction, source or reference
168	*trpC2*	(Kunst et al., 1997)
BFA2863	*ylmF:pMUTIN4, ery*	Leendert Hamoen
MD120	Δ*ezrA::spec*	Shu Ishikawa
MD136	Δ*ftsA::erm*, *(*P_{spac}*-ftsZ)*	Shu Ishikawa
MD137	Δ*ezrA::spec,* Δ*ftsA::erm*, *(*P_{spac}*-ftsZ)*	Shu Ishikawa
NC19	*amy::*P_{xyl}*-sepF*(G109K)*-gfp, spec*	pNC14 > 168
NC20	*amy::*P_{xyl}*-sepF*(G109N)*-gfp, spec*	pNC15 > 168
NC21	*ylmF::pMUTIN4, ery, amy::*P_{xyl}*-sepF*(G109K)*-gfp, spec*	pNC14> BFA2863
NC22	*ylmF::pMUTIN4, ery, amy::*P_{xyl}*-sepF*(G109N)*-gfp, spec*	pNC15 > BFA2863
NC23	*amy::*P_{xyl}*-sepF*(Y112A)*-gfp, spec*	pNC16 > 168
NC24	*ylmF::pMUTIN4, ery, amy::*P_{xyl}*-sepF*(Y112A)*-gfp, spec*	pNC16 > BFA2863
4181	*amy::*P_{xyl}*-sepF-gfp, spec*	Leendert Hamoen
LH3	*ylmF::pMUTIN4, ery, amy::* P_{xyl}*-sepF-gfp, spec*	Leendert Hamoen
2020	*amyE::spec* P_{xyl} *-gfp-pmut1-ftsZ*	Laboratory stock
YK80	Δ*noc::cm*	Yoshi Kawai
noc::tet	Δ*noc::tet*	Ling J. Wu
noc::spec	Δ*noc::spec*	Ling J. Wu
1801	*ftsZ::(ble,* P_{spac}*-ftsZ)*	(Marston et al., 1998)
NC28	*amy::*P_{xyl}*-sepF-gfp, spec, ftsZ::*P_{spac}*-ftsZ, ble*	4181 > 1801
YK204	CRK6000 Δ*sepF::spec*	(Ishikawa et al., 2006)
NC40	Δ*sepF::neo*	ECE140 > YK204
LH75	*lacA::tet* (SG82), Δ*ftsA::ery* (YK206)	Leendert Hamoen
LH69	Δ*ezrA::tet*, *amyE::*P_{xyl}*-gfp-ftsZ*, *spec*	Leendert Hamoen
PG160	Δ*ezrA::tet, amyE::*P_{xyl}-Δ30*ftsL, cat*	Pamela Gamba
minC-spec	Δ*minC::spec,* P_{spac}*-mazF*	Takuya Morimoto
zapA-spec	Δ*zapA::spec,* P_{spac}*-mazF*	Takuya Morimoto
gpsB-spec	Δ*gpsB::spec,* P_{spac}*-mazF*	Takuya Morimoto
noc-spec	Δ*noc::spec,* P_{spac}*-mazF*	Takuya Morimoto
divIB-spec	Δ*divIB::spec,* P_{spac}*-mazF*	Takuya Morimoto
ugtP-spec	Δ*ugtP::spec,* P_{spac}*-mazF*	Takuya Morimoto

ezrA-spec	Δ*ezrA::spec,* P_{spac}*-mazF*	Takuya Morimoto
minJ-spec	Δ*minJ::spec,* P_{spac}*-mazF*	Takuya Morimoto
clpX-spec	Δ*clpX::spec,* P_{spac}*-mazF*	Takuya Morimoto
ftsA-spec	Δ*ftsA::spec,* P_{spac}*-mazF*	Takuya Morimoto
spxA-spec	Δ*spxA::spec,* P_{spac}*-mazF*	Takuya Morimoto
BMD1	*ΔzapA*	Simon Syvertsson
BMD2	*ΔzapA ΔminC*	Simon Syvertsson
BMD3	*ΔzapA ΔminC ΔugtP*	Simon Syvertsson
BMD4	*ΔzapA ΔminC ΔugtP ΔclpX*	Simon Syvertsson
BMD5	*ΔzapA ΔminC ΔugtP ΔminJ*	Simon Syvertsson
BMD6	*ΔzapA ΔminC ΔugtP ΔminJ ΔezrA*	Simon Syvertsson
BMD7	*ΔzapA ΔminC ΔugtP ΔminJ ΔezrA ΔspxA*	spxA-spec > BMD6
BMD8	*ΔzapA ΔminC ΔugtP ΔminJ ΔezrA ΔspxA ΔdivIB*	divIB-spec > BMD7
BMD9	*ΔzapA ΔminC ΔugtP ΔminJ ΔezrA ΔspxA ΔclpX*	clpX-spec > BMD7
BMD10	*ΔftsA*	ftsA-spec > 168
BMD11	*ΔminC ΔugtP ΔminJ ΔezrA ΔspxA ΔdivIB*	noc-spec > BMD8
BMD12	*ΔzapA ΔminC ΔugtP ΔminJ ΔspxA ΔclpX Δnoc*	noc-spec > BMD9
BMD13	*ΔzapA ΔminC ΔminJ ΔezrA ΔspxA ΔclpX ΔgpsB*	gpsB-spec > BMD9
BMD14	*ΔzapA ΔminC ΔugtP ΔminJ ΔspxA ΔclpX Δnoc ΔezrA::tet*	LH69 > BMD12
BMD15	*ΔzapA ΔminC ΔugtP ΔminJ ΔspxA ΔclpX Δnoc ΔezrA::tet*	LH69 > BMD12
BMD16	*ΔminC ΔugtP ΔminJ ΔspxA ΔclpX ylmF::pMUTIN4, ery*	BFA2863 > BMD9
BMD17	*ΔzapA ΔminC ΔugtP ΔminJ ΔezrA ΔspxA ΔclpX ylmF::pMUTIN4, ery*	BFA2863 > BMD9
BMD18	*ΔzapA ΔminC ΔugtP ΔminJ ΔspxA ΔclpX Δnoc::tet ylmF::pMUTIN4, ery*	noc::tet > BMD17
BMD19	*ΔzapA ΔminC ΔugtP ΔminJ ΔspxA ΔclpX Δnoc::spec ylmF::pMUTIN4, ery*	noc::spec > BMD17
BMD20	*ΔzapA ΔminC ΔugtP ΔminJ ΔspxA ΔclpX Δnoc::tet ylmF::pMUTIN4, ery, amyE::*P_{xyl} *Δ30ftsL-cat*	PG160 > BMD18
BMD21	*ΔzapA ΔminC ΔugtP ΔminJ ΔspxA ΔclpX Δnoc ylmF::pMUTIN4, ery, ΔezrA::tet*	BMD17 > BMD14
BMD22	*ΔzapA ΔminC ΔugtP ΔminJ ΔezrA ΔspxA ΔclpX ylmF::pMUTIN4, ery, Δnoc::cm*	YK80 > BMD17
BMD23	*ΔzapA ΔminC ΔugtP ΔclpX Δnoc ΔezrA::tet ΔftsA::ery*	LH75 > BMD14

BMD24	*ΔzapA ΔminC ΔclpX* Δ*ezrA::tet* Δ*ftsA::ery*	LH75 > BMD14
BMD25	*ΔzapA ΔminC ΔugtP ΔminJ ΔspxA ΔclpX Δnoc* Δ*ezrA::tet* Δ*ftsA::ery*	LH75 > BMD14
BMD26	*ΔzapA ΔminC ΔugtP ΔminJ ΔspxA ΔclpX Δnoc* Δ*ezrA::tet* Δ*ftsA::ery*	LH75 > BMD14
BMD27	*ΔzapA ΔminC ΔugtP ΔminJ ΔspxA ΔclpX Δnoc* Δ*ezrA::tet* Δ*ftsA::ery*	LH75 > BMD14
BMD28	*ΔzapA ΔminC ΔugtP ΔminJ ΔspxA ΔclpX Δnoc* Δ*sepF::spec*	YK204 > BMD14
BMD29	*ΔzapA ΔminC ΔugtP ΔminJ ΔspxA ΔclpX Δnoc* Δ*sepF::spec*	YK204 > BMD14
BMD30	*ΔzapA ΔminC ΔugtP ΔminJ ΔspxA ΔclpX Δnoc* Δ*ezrA::tet amyE::*P_{xyl} *gfp-ftsZ, spec*	2020 > BMD14
BMD31	*ΔzapA ΔminC ΔugtP ΔminJ ΔspxA ΔclpX Δnoc* Δ*ezrA::tet amyE::*P_{xyl} *gfp-ftsZ, spec*	2020 > BMD14
BMD32	*ΔzapA ΔminC ΔugtP ΔminJ ΔspxA ΔclpX Δnoc* Δ*ezrA::tet amyE::*P_{xyl} *gfp-ftsZ, spec*	BMD26 > BMD30
BMD33	*amyE::*P_{xyl} *gfp-ftsZ, spec*	2020 > 168
BMD34	*ΔzapA ΔminC ΔugtP ΔminJ ΔspxA ΔclpX Δnoc* Δ*sepF::kan*	ECE140 > BMD28
BMD35	*ΔzapA ΔminC ΔugtP ΔminJ ΔspxA ΔclpX Δnoc* Δ*sepF::kan amyE::*P_{xyl} *gfp-ftsZ, spec*	2020 > BMD34
BMD36	*ΔzapA ΔminC ΔugtP ΔminJ ΔspxA ΔclpX Δnoc* Δ*sepF::kan amyE::*P_{xyl} *gfp-ftsZ, spec*	2020 > BMD34
BMD37	*ΔzapA ΔminC ΔugtP ΔminJ ΔspxA ΔclpX Δnoc* Δ*ezrA::tet* Δ*ftsA::ery amyE::*P_{xyl} *gfp-ftsZ, spec*	BMD25 > BMD31
BMD38	*ΔzapA ΔminC ΔugtP ΔminJ ΔspxA ΔclpX Δnoc* Δ*ezrA::tet* Δ*ftsA::ery amyE::*P_{xyl} *gfp-ftsZ, spec*	2020 > BMD27
BMD39	*ΔzapA ΔminC ΔugtP ΔminJ ΔspxA ΔclpX Δnoc* Δ*ezrA::tet pLOSS*ezrA*	pLOSS*ezrA > BMD14
HS206	*trpC2 amyE::spec,* P_{xyl}*-sepF1-39* (SepF1-13)*-gfp*	Henrik Strahl
HS207	*trpC2 amyE::spec,* P_{xyl}*-sepF1-75* (SepF1-25)*-gfp*	Henrik Strahl
HS208	*trpC2 amyE::spec,* P_{xyl}*-sepF1-75* (SepF1-25)*-junLZ-gfp*	Henrik Strahl
HS223	*trpC2 amyE::spec* P_{xyl}*-sepF1-39* (SepF1-13, L7D)*-gfp*	Henrik Strahl
HS226	*trpC2 amyE::spec* P_{xyl}*-sepF1-39* (SepF1-13)*-gfp sepF::ery*	Henrik Strahl
HS227	*trpC2 amyE::spec* P_{xyl}*-sepF1-75* (SepF1-25)*-gfp sepF::ery*	Henrik Strahl

HS228	*trpC2 amyE::spec* P_{xyl}*-sepF1-75* (SepF1-25)*-junLZ-gfp sepF::ery*	Henrik Strahl
HS229	*trpC2 amyE::spec* P_{xyl}*-sepF1-39* (SepF1-13, L7D)*-gfp sepF::ery*	Henrik Strahl
HS230	*trpC2 aprE::spec* P_{xyl}*-sepF*$_{\Delta AH}$ (SepFΔ2-13)	Henrik Strahl
HS232	*trpC2 aprE::spec* P_{xyl}*-AH*$_{minD}$*-sepF* (MinD$_{248-268}$-SepF$_{14-151}$)	Henrik Strahl
HS233	*trpC2* Δ*ftsA::ery aprE::spec* P_{xyl}*-sepF*$_{\Delta AH}$ (SepFΔ2-13)	Henrik Strahl
HS235	*trpC2* Δ*ftsA::ery aprE::spec* P_{xyl}*-AH*$_{minD}$*-sepF* (MinD$_{248-268}$-SepF$_{14-151}$)	Henrik Strahl
HS236	*trpC2* Δ*sepF::neo aprE::spec* P_{xyl}*-sepF*$_{\Delta AH}$ (SepFΔ2-13)	Henrik Strahl
HS238	*trpC2* Δ*sepF::neo aprE::spec* P_{xyl}*-AH*$_{minD}$*-sepF* (MinD$_{248-268}$-SepF$_{14-151}$)	Henrik Strahl
HS239	*trpC2 amyE::cat* P_{xyl}*-sepF*	Henrik Strahl
HS240	*trpC2* Δ*sepF::neo amyE::cat* P_{xyl}*-sepF*	Henrik Strahl
HS241	*trpC2* Δ*ftsA::ery amyE::cat* P_{xyl}*-sepF*	Henrik Strahl
HS242	*trpC2* Δ*ftsA::ery* Δ*sepF::neo aprE::spec* P_{xyl}*-AH*$_{minD}$*-sepF* (MinD$_{248-268}$-SepF$_{14-151}$)	Henrik Strahl

Table 2.1 List of *Bacillus subtilis* strains used in this study. For the construction of strains, DNA used in transformation was given first, followed by the recipient strain. The symbol Δ was used to indicate marker-free deletions of the genes.

Strain	Genotype	Source
DH5α	F^- Φ80*lac*ZΔM15 Δ(*lac*ZYA-*arg*F) U169 *rec*A1 endA1 *hsd*R17 (rK^-, mK^+) *pho*A *sup*E44 λ^- *thi*-1 *gyr*A96 *rel*A1	Invitrogen
BL21 (DE3)	F^- *omp*T *gal dcm lon hsd*S_B(r_B^- m_B^-) λ(DE3 [*lac*I *lac*UV5-T7 *gene* 1 *ind*1 *sam*7 *nin*5])	Invitrogen
SepF	BL21 (DE3) pMAL-SepF	(Gundogdu et al., 2011)
NC1	BL21 (DE3) pNC1	This work
NC2	BL21 (DE3) pNC2	This work
NC4	BL21 (DE3) pNC4	This work
NC5	BL21 (DE3) pNC5	This work
NC6	BL21 (DE3) pNC6	This work
NC7	BL21 (DE3) pNC7	This work
NC8	BL21 (DE3) pNC8	This work
NC9	BL21 (DE3) pNC9	This work
NC29	BL21 (DE3) pNC12	This work
HS214	BL21 (DE3) pHJS106	Henrik Strahl
HS224	BL21 (DE3) pMBP-SepF(25-151)	Henrik Strahl
HS225	BL21 (DE3) pHJS107	Henrik Strahl
G137N	BL21 (DE3) pMAL-SepF(G137N)	(Gundogdu et al., 2011)
ΔC (1-136)	BL21 (DE3) pMAL-SepF(ΔC (1-136))	(Gundogdu et al., 2011)

Table 2.2 List of *E. coli* strains used in this work.

Name	Genotype	Source
pMALC2	P_{tac}, *ApR, ori ColE1, malE, lacZα, lacI*^{q}	NEB
pNC1	P_{tac}-*malE-sepF*$_{SC3}$	This work
pNC2	P_{tac}-*malE-sepF*$_{BC}$	This work
pNC4	P_{tac}-*malE-sepF*$_{MT}$	This work
pNC5	P_{tac}-*malE-sepF*$_{SC2}$	This work
pNC6	P_{tac}-*malE-sepF*$_{SC1}$	This work
pNC7	P_{tac}-*malE-sepF*$_{CP}$	This work
pNC8	P_{tac}-*malE-sepF*$_{BM}$	This work
pNC9	P_{tac}-*malE-sepF*$_{SP}$	This work
pNC12	P_{tac}-*malE-sepF*$_{new}$	This work
pNC13	P_{tac}-*malE-sepF* (G109K)	This work
pHJS106	P_{tac}-*malE-sepF*ΔN13 (SepF14-151)	Henrik Strahl
pHJS107	P_{tac}-*malE-sepF* (SepF L7D)	Henrik Strahl
pMBP-SepF(25-151)	P_{tac}-*malE-sepF*ΔN24 (SepF25-151)	This work
pFG1	*bla, spec, amyE3'* P_{xyl}-*ylmF-gfp amyE5'*	Leendert Hamoen
pNC14	*bla, spec, amyE3'* P_{xyl}-*sepF*(G109K)-*gfp amyE5'*	This work
pNC15	*bla, spec, amyE3'* P_{xyl}-*sepF*(G109N)-*gfp amyE5'*	This work
pNC16	*bla, spec, amyE3'* P_{xyl}-*sepF*(Y112A)-*gfp amyE5'*	This work
pHJS108	*bla, spec, amyE3'* P_{xyl}-*sepF1-39-gfp amyE5'*	Henrik Strahl
pHJS109	*bla, spec, amyE3'* P_{xyl}-*sepF1-75-gfp amyE5'*	Henrik Strahl
pHJS110	*bla, spec, amyE3'* P_{xyl}-*sepF1-75-junLZ-gfp amyE5'*	Henrik Strahl
pHJS111	*bla, spec, amyE3'* P_{xyl}-*sepF1-39*(L7D)-*gfp amyE5'*	Henrik Strahl
pLOSS*	*bla spec* P_{spac}-*MCS* P_{divIA}-*lacZ lacI rep pIS20(GA-CC)*	(Claessen et al. 2008)
pLOSS* ezrA	*bla spec* P_{spac}-*MCS* P_{divIA}-*lacZ ezrA lacI rep pIS20(GA-CC)*	(Claessen et al. 2008)
pCXZ	*bla* P_{tac}-*ftsZBS*	(Wang & Lutkenhaus, 1993)
pBS58	*spec ftsQAZEC*	(Wang & Lutkenhaus, 1993)

Table 2.3 List of plasmids used in this work

Primer	Sequence (5'-3')	Usage
MD1	TATCTGCCGGAGGGGCATAG	*zapA* outF1
MD2	CGTTCACATATGTTTCCATC	*zapA* outR1
bmd33	TCGGTCGTCCTGTTCCAGAG	*zapA* outF2
bmd34	CGCCTGATTGTGCAGCAAAG	*zapA* outR2
bmd1	TTGACATTTACGGCCAGCAC	*zapA* inF1
bmd2	TCGTGCACCACATTTACCG	*zapA* inR1
bmd41	CGGTGAAGAAAGCAGAG	*zapA* inF2
bmd42	TTTACCGCTGTCAGCAC	*zapA* inR2
MD7	ACGAGCCGCGGCGGTTCAAT	*minC* outF
MD8	TCTATTAGGCGTTTACATGT	*minC* outR
bmd3	CATCTGGATGATGCGTGTTC	*minC* inF
bmd4	CCTCCCTCAAGCCTTGTTAG	*minC* inR
oSS42	GGGCACCCTGAATATGATAC	*ugtP* outF
oSS43	CCGCCTTCAACTTCAATG	*ugtP* outR
bmd7	ATGTGTACGGCTCGGCTTTC	*ugtP* inF
bmd8	CATCTGCAAGAAGGGAAGTG	*ugtP* inR
oSS52	GGTTAATGGCAGCTGAACG	*minJ* outF
oSS53	ACATCTAACAGCGGGATGG	*minj* outR
bmd5	AAAGCGCGGGCTTGTTCTTC	*minJ* inF
bmd6	GAAGCGACTGCTTCGTCTTC	*minJ* inR
oSS61	CAAAGAAGCTTGCGCCATCG	*ezrA* outF
oSS7	CGGTTCATTGGGCAACATCG	*ezrA*

4		outR
bmd9	TGTACTGCTTGCGCTGTTTG	*ezrA* inF
bmd10	ACAGCGGCAGCGGCAATTTC	*ezrA* inR
bmd11	CTTGAAGCCATGAAACAGAC	*spxA* outF
bmd12	CTTCTGATTTACGCGGGAAG	*spxA* outR
bmd13	TCATGCAGAAAGGCGAGAGC	*spxA* inF
bmd14	TGCCAAACGCTGTGCTTCTC	*spxA* inR
bmd35	CCGGTGGCCCATAGACAATC	*clpX* outF
bmd36	GGGGCAATATAGTTAATGCAGGGC	*clpX* outR
bmd15	CACGAGAAGGCAGCTCAAAC	*clpX* inF1
bmd16	AGAGGAAGAACTCGGAACAG	*clpX* inR1
bmd43	GCAATAACCGGAAGACG	*clpX* inF2
bmd44	CGTGGGTGAAGATGTAG	*clpX* inR2
bmd29	TTTCGTCTGATCGGCTCTCG	*noc* outF
bmd30	AAAGCAATCACGACGCTTGG	*noc* outR
bmd31	TTTACACCGCTGTCTTCCAC	*noc* inF
bmd32	TCTCGTTTCTTCGGGCTTGG	*noc* inR
bmd17	TTTATCGCTTGCGGTGCTTG	*ftsA* outF
bmd18	TCCTCCTAATCTGCCGAATG	*ftsA* *out*R
bmd19	GATCGTCGGAGAAATGACAG	*ftsA* inF
bmd20	TGGTGATGATGCTGCTCTTG	*ftsA* inR
bmd39	GTCTCATCATCTGAGGAACAAGAGC	*ftsZ* outF
bmd40	GGGTCTAATTATCTGTTTTGTTAC	*ftsZ* outR

bmd45	TGCGGGCAAACAGAATG	*sepF* inF
bmd46	CCTGGTCATGCTGTATC	*sepF* inR
inc11	GCTGTCTCCCGGGATGAGTATGAAAAATCG	$SepF_{BM}$ F
inc12	ACGATGTCTCTAGACTACCACCTCTTTACG	$SepF_{BM}$ R
inc7	GGTTACGGAATTCGTGAATAGTCACTGTAG	$SepF_{MT}$ F (*Eco*RI)
inc8	GGCGACCGTCTAGACTATTGGTAGGCGTAG	$SepF_{MT}$ R
inc9	GATTAGCCCGGGATGTGTATGTCAAAAG	$SepF_{CP}$ F
inc10	GACTATCTAGATTATTTTGAAGCCCAGTTG	$SepF_{CP}$ R
inc15	GTAGGAGCCCGGGATGTCTTTAAAAGATAG	$SepF_{SP}$ F
inc16	GCTAGACTCTAGATTATCGTACTCTATTTC	$SepF_{SP}$ R
inc17	GTGAGAGGAGGAATTCATGGGATCGGTAC	$SepF_{SC1}$ F (*Eco*RI)
inc18	TGTGCGGCTCTAGATCAGCTCTGGTTGAAG	$SepF_{SC1}$ R
inc19	GAGGACTCCCGGGATGGCCGGCGCGATG	$SepF_{SC2}$ F
inc20	ACCGGTAGTCTAGATCAGCTCTGGTTGAAG	$SepF_{SC2}$ R
eg139	GACGAATTCGTGAAATCGGGGGAGC	$SepF_{SC3}$ F (*Eco*RI)
eg140	GACTCTAGATCACACTCCCGGCAC	$SepF_{SC3}$ R
eg122	GACGAATTCATGAGTTGGTCAAAAG	$SepF_{BC}$ F (*Eco*RI)
eg123	GACTCTAGATTACCACCTCTTTAT	$SepF_{BC}$ R
inc26	GATCGAGGGAAGGATGAGTATGAAAAATAAACTGAAAAA	$SepF_{B}$

	CTTTTTC	$_S$ (new) F1
inc27	GAAAAAGTTTTTCAGTTTATTTTTCATACTCATCCTTCCCTCGATC	$SepF_B$ $_S$ (new) R1
inc28	CTTTTTCTCAATGGAAGATGAAG	$SepF_B$ $_S$ (new) F2
inc29	CTTCATCTTCCATTGAGAAAAAG	$SepF_B$ $_S$ (new) R2
inc6	GACTCTAGATTACCACCTCTGATGTTC	SepF R
inc21	GAAACCCGGGAAAGTGGTGTTGAGTG	ΔN (60-151) F
inc22	GTTGCCCGGGGAAGATGAAGAATAC	ΔN (14-151) F
inc30	CCCGGGATGGAGCGGGAATCTCATGAG	ΔN (25-151) F
inc40	GACTTTTTAAGCAACACCGTTTATG	G109N F
inc41	CATAAACGGTGTTGCTTAAAAAGTC	G109N R
inc42	CTTTTTAAGCAAAACCGTTTATG	G109K F
inc43	CATAAACGGTTTTGCTTAAAAAG	G109K R
inc57	TTAAGCGGAACCGTTGCGGCCATTGGCGGCGAT	Y112A F
inc58	ATCGCCGCCAATGGCCGCAACGGTTCCGCTTAA	Y112A R
inc63	CCTGACAACGTAGATGTATCAAACACAATTTCTGAGCTCATATC	G137N F
inc64	GATATGAGCTCAGAAATTGTGTTTGATACATCTACGTTGTCAGG	G137N R
inc31	TGCCCATTAACGTCACCATC	pFG1 seq R
inc32	TCAAAGCCTGTCGGAATTGG	pFG1 seq F
inc46	CCGTTGCTGTCGTCACTAAG	FtsZ seq F
inc47	CTTTCGGGCTTTGTTAGCAG	FtsZ

		seq R1
inc48	TGCGTACGTCTGCAAAGTCC	FtsZ seq R2

Table 2.4 List of primers used in this study. F means forward primer while R is used for reverse primer. When the primers are inside the gene it was shown as 'in'. If the primers are outside the gene, 'out' was used. Primers designed for sequencing was shown as 'seq'. Unless it was stated otherwise the primers were designed for $SepF_{BS}$.

2.4. Purification of PCR Products, Isolation of Plasmids and Gel Extraction

Removing dNTPs and enzymes after a PCR reaction or changing buffers between different processes such as restriction digestions were performed using the QIAquick PCR Purification Kit. First, reaction was mixed with Buffer PB that contains guanidine hydrochloride and isopropanol to allow efficient binding of DNA to the spin column which uses silica-gel-membrane technology. The binding was followed by washing the column-bound DNA with Buffer PE that contained ethanol. Finally, DNA was eluted using MilliQ water.

Plasmids were isolated using the QIAprep Spin Miniprep Kit. Cells were resuspended in Buffer P1 (50 mM Tris·Cl pH 8.0, 10 mM EDTA, 100 µg/ml RNase A), followed by lysis in Buffer P2 (200 mM NaOH, 1% SDS (w/v)). After neutralization of solution with Buffer N3, cell debris was pelleted. The supernatant was transferred to a spin column so that the plasmids would bind to the column. Plasmids then washed with Buffer PB and Buffer PE. Finally, they were eluted using MilliQ water.

Where necessary, DNA was extracted from agarose gels using the QIAquick Gel Extraction Kit (QIAGEN). DNA separated by agarose gel electrophoresis was removed from rest of the gel by excision with a clean, sharp scalpel. Agarose was then dissolved in Buffer QG, which is the solubilisation and binding buffer, at 50°C. After addition of isopropanol to increase the yield, the mixture was transferred to a spin column. An extra washing with Buffer QG was done to ensure that agarose was completely removed. DNA was washed with Buffer PE, followed by elution in MilliQ water.

2.5. Restriction Endonuclease Digestion

Enzymes were purchased from either Roche or New England Biolabs (NEB) and stored at -20°C. DNA to be digested was incubated with 10 units of enzyme with the recommended reaction buffer at 37°C for 2 hours. The incubation temperature was changed if the optimum temperature differed for a particular enzyme. Digested products were purified with a PCR purification kit or by extraction from an agarose gel.

2.6. Ligation of DNA Fragments

T4 DNA ligase (Roche) was used to ligate DNA fragments. Usually, about 100 ng of vector DNA was incubated with about 3-4 fold molar excess of

the insert DNA, which was determined using an agarose gel and the NanoDrop 1000 measurements, with 10 units of T4 DNA ligase in the supplied buffer. Ligation was performed at 4°C for a length of ten hours to overnight.

2.7. Agarose Gel Electrophoresis

Generally, 1% (w/v) agarose dissolved in TAE buffer (40mM Tris, 20mM acetic acid, 1mM EDTA pH 8.0) was used to separate DNA fragments. Gels were run at 120V for about 30-40 min at room temperature. Ethidium bromide was used to visualize DNA with a UV trans-illuminator (Syngene). A 1 kb DNA ladder (NEB) was used for size comparison.

2.8. Sequencing of DNA

DNA Sequencing & Services (University of Dundee) was used for sequencing purposes. The advised amount of DNA was used.

2.9. Growth Media and Supplements

Bacterial strains were grown at 37°C unless it was stated otherwise. Solid media used for growing *B. subtilis* and *E. coli* were either nutrient agar (Oxoid) or Luria-Bertani (LB) with agar bacteriological No.1 (Oxoid) (10 g Tryptone, 5 g Yeast extract, 10 g NaCl, 15 g Agar in 1 litre dH_2O). LB broth (10 g Tryptone, 5 g Yeast extract, 10 g NaCl in 1 litre dH_2O) was used as the liquid medium. Transformation of *B. subtilis* strains were performed in SMM (Ammonium sulphate (0.2% w/v), Dipotassium phosphate (1.4%), Potassium dihydrogen phosphate (0.6%), Sodium citrate dihydrate (0.1%), Magnesium sulphate (0.02%)) competence medium (Anagnostopoulos and Spizizen, 1961, Young and Spizizen, 1961).

Several antibiotics were used for growth and selection of *B. subtilis* in following concentrations: chloramphenicol (5 µg/ml), erythromycin (1 µg/ml), kanamycin (5 µg/ml), phleomycin (0.5 µg/ml), spectinomycin (100 µg/ml), and tetracycline (10 µg/ml). Selection of *E. coli* was done with ampicillin (100 µg/ml).

2.10. Competent Cell Preparation of *E. coli* Cells

A single colony was inoculated in overnight culture at 37°C. It was then diluted 1:100 in fresh 100 ml LB, grown for 2 hours. Cells were collected (3300

g, 10 min, 4°C), and then resuspended in 30 ml ice cold 0.1 M $CaCl_2$. After incubation on ice for 30 min, cells were again centrifuged for 10 min at 3300 g at 4°C. The pellet was resuspended in 6 ml ice-cold 0.1 M $CaCl_2$ with 15% v/v glycerol. Competent cells were aliquoted and stored at -80°C.

2.11. Transformation of Chemically Competent *E. coli* Cells

Cells were thawed and incubated with DNA (100 µl cells/5-10 µl DNA, total of 20-30 ng) for 30 min on ice. A heat shock was applied at 42°C for 90 sec and cells were immediately put on ice for 2 min. 900 µl of fresh LB was added. Cells were shaken at 37°C for 1 hour and plated on nutrient agar plates with 100 µg/ml ampicillin, and then incubated at 37°C overnight.

2.12. Isolation of Bacterial Chromosomal DNA of *B. subtilis*

Overnight cultures of *B. subtilis* grown in LB were harvested by centrifugation. Cells were washed and resuspended in TES buffer (0.1 M Tris-HCl pH 8.0, 0.01 M EDTA, 0.1 M NaCl). Then, cells were lysed by incubating with lysozyme (0.33 mg/ml) at 37°C for 15 minutes, followed by pronase (0.6 mg/ml) and Sarkosyl (30%) treatment for 10 minutes. Using a phenol/chloroform mixture, DNA was separated from proteins and lipids. It was precipitated and washed with ethanol (100%, then 70%). DNA was then air dried and was solubilized in dH_2O.

2.13. Transformation of Competent *B. subtilis* Cells

Cells were made competent as described by Hamoen et al. (Hamoen et al., 2002). A single colony of cells was inoculated in 10 ml competence medium (MM = 10 ml SMM, Glucose (0.5% w/v), Tryptophan (10 mM), Mg_2SO_4 (6 mM), CAA (Casamino acid, 0.02% w/v), Ferric Ammonium Citrate (0.0001% w/v)) and culture was grown overnight at 37°C. The next day, 1 ml of the culture was inoculated in 10 ml fresh MM and vigorously shaken for 3 hours at 37°C. 10 ml of prewarmed starvation medium (10 ml SMM, Glucose (0.5% w/v), Mg_2SO_4 (6 mM)) was added and the culture was kept shaking for additional 2 hours. 400 µl of competent cells were mixed with 10 µl of DNA (0.1-1 µg), and then shaken for 45 min-1h at 37°C. Cells were plated on nutrient agar or LB agar plates with appropriate antibiotics. Plates were incubated at 37°C overnight.

2.14. Marker-free Deletion of *B. subtilis* Genes

Genes of *B. subtilis* were deleted using the protocol described by Morimoto et al. (Morimoto et al., 2011). The constructs which were designed and made by Morimoto were transformed into *B. subtilis* using spectinomycin for selection. The clones later were streaked on plates with 0.5 mM IPTG for removal of marker via intramolecular double crossover. As a result, colonies that grew on IPTG plates would not grow on spectinomycin plates any longer (Figure 2.1). Final control of the deletions was performed using PCR with two sets of primers (Table 2.4) that bind both inside and outside region of the gene of interest.

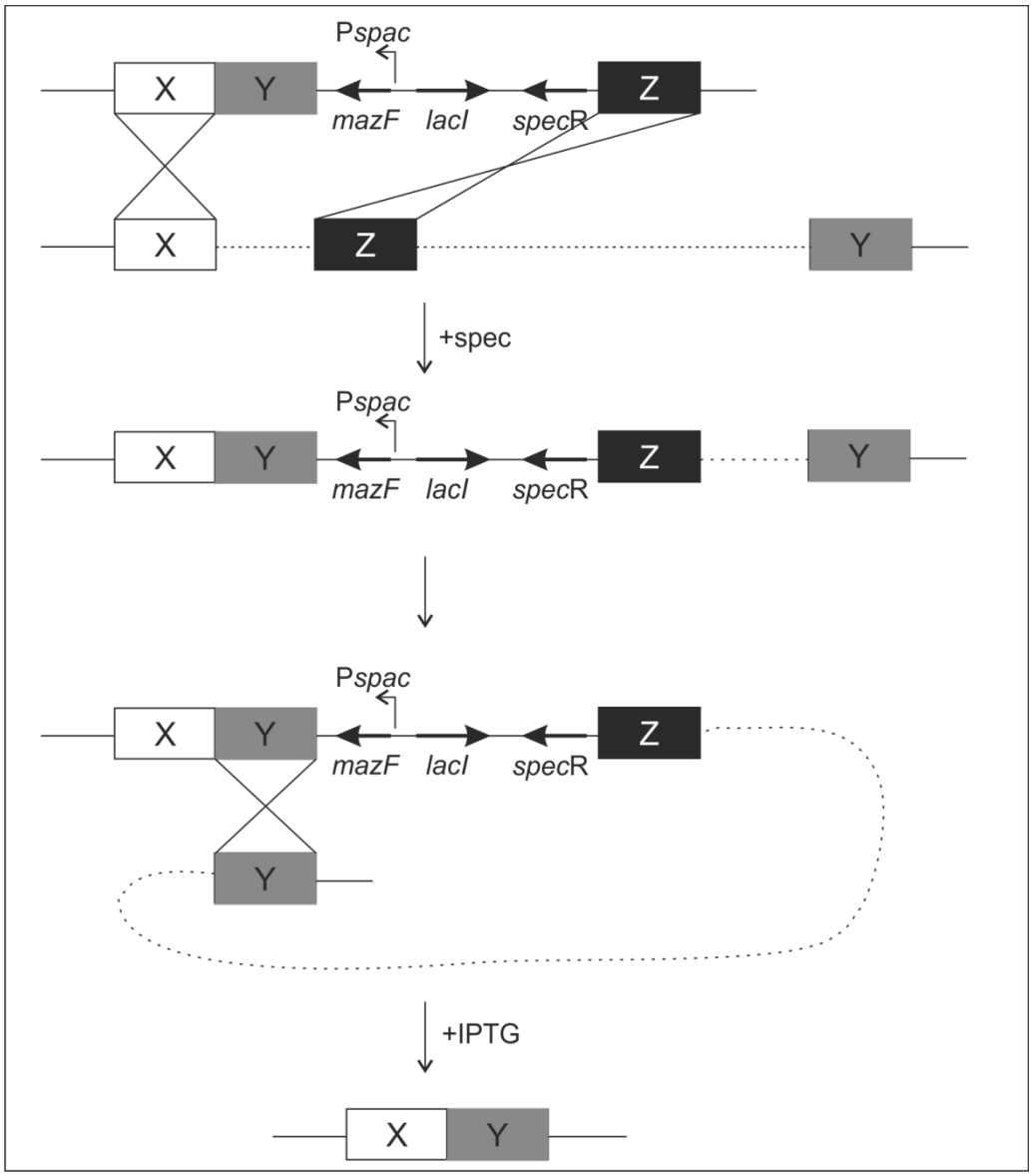

Figure 2.1 A schematic for the marker-free deletion of a gene. First spectinomycin media, then IPTG media were used to select for transformants. X shows the upstream sequence, while Y indicates the downstream sequence. Z fragment is required for integration of the *mazF* cassette. The scheme is adapted from Morimoto et al. (2011).

2.15. Southern Blotting

Digestion of the chromosomal DNAs was performed by restriction enzymes *Not*I-*Sal*I (Buffer H) and *Nar*I-*Bam*HI (Buffer A) (Roche). Equal amounts of digested DNAs were run on agarose gel (0.7%) at 40 V for 5 h. Transfer of DNA from agarose gel to the membrane was performed as described in the manual of Hybond N+. DNA was crosslinked to the membrane by UV exposure (302 nm, 100% intensity) for 20 seconds (UV trans-illuminator (Syngene)). The AlkPhos Direct Hybridization system was used to label the probe and detect the specific sequence (GE Healthcare). The exactly same protocol described in the manual was used.

2.16. Calculation of Doubling Time of *B. subtilis* and Growth Curves

To calculate the doubling time of absorbance of BMD strains, overnight cultures grown in LB were diluted to absorbance at 600 nm (A_{600}) 0.01 in 10 ml pre-warmed LB with glucose (1%) and $MgSO_4$ (10 mM). Cultures were then grown at 37 °C on a shaker. The absorbance at 600 nm (A_{600}) was measured for 7 hours at 30 minute intervals. Each measurement was used to draw the growth curve of the strain. The slope of exponential phase was used to calculate the doubling times of absorbance for each BMD strain.

For the growth curves of BMD strains, strains were grown in LB to mid-exponential phase (A_{600} 0.4-0.6). Cultures then were diluted in LB supplemented with 1% glucose and 10 mM $MgSO_4$ to the A_{600} of 0.05. 200 µl of the diluted cultures were transferred to a 96-well microtitre plate (Falcon 96 3072). The plate was incubated at 37°C in a microtitre plate reader (Fluostar Galaxy, BMG Lab Technologies) and growth was followed for 20 hours while A_{600} readings were taken every 5 minutes (orbital shake width 7 mm; 87 r.p.m). Growth until the mid-stationary phase was plotted as the mean of six independent wells.

2.17. Protein Purifications

Chromatography was performed with an AKTA purifier FPLC (GE Healthcare). Data was analysed with UNICORN software. All purification steps were done at 4°C unless stated otherwise. Purified proteins were concentrated using Amicon Ultra-4 Centrifugal Filter Units (Millipore) where necessary. The protocol described by Millipore was followed. Purified FtsZ was desalted using

PD-10 desalting columns (GE Healthcare) by gravity flow as described by GE Healthcare. Protein concentrations were determined with either NanoDrop 1000 which uses Beer-Lambert law by measuring absorbance at 280 nm or by Bradford method using Bio-Rad protein assay (Bio-rad).

2.17.1. Purification of untagged, full-length FtsZ

E. coli BL21 (DE3) cells were freshly transformed with pCXZ and pBS58, and grown on ampicillin (100 µg/ml) + spectinomycin (50 µg/ml) + glucose (0.4%) plates at 30°C. The next morning, colonies on the plate were inoculated in 1L LB and grown at 37°C until OD_{600} was 0.3-0.4. FtsZ production was induced with 0.5 mM IPTG for 4 h. Cells were collected, washed with ice-cold PBS (1 PBS tablet (Oxoid) per 100 ml dH_2O) and stored at -80°C. The following morning the pellet was resuspended in solubilisation buffer (50 mM Tric-HCl pH 8.0, 50 mM KCl, 10 mM $MgCl_2$, 1 mM EDTA) (4 ml/g of cell pellet) and sonicated (13W, pulse 3) twice for 10 minutes with a Vibra-Cell Ultrasonic Processor (Sonics&Materials, Inc) and incubated on ice for 10 minutes between each sonication. After centrifugation at 31000g for 1h at 4°C (JA25.50), the supernatant was collected. FtsZ was precipitated by adding 80% ammonium sulphate in solubilisation buffer drop-by-drop to the final concentration of 40%. The solution was stirred for 30 min at 4°C until the precipitation was equilibrated. The precipitate was recovered by centrifugation for 30 min at 12000g at 4°C (JA25.50). The protein pellet was resuspended in 100 ml Buffer A_Z (10 mM Tris-HCl pH 8.0), briefly centrifuged (10 min, 12000g, 4°C), and filtered through a 0.45 µm filter. Protein suspension was loaded to a 5 ml HiTrap Q column (GE Healthcare) (1ml/min) pre-equilibrated with Buffer A_Z. Column was washed with 5 column volumes (CV) of Buffer A_Z (2ml/min), followed by elution of FtsZ with a linear gradient of 0-50% Buffer B_Z (10 mM Tris-HCl pH 8.0, 1 M KCl) in Buffer A_Z over 5 CV (1 ml/min). The fractions were analysed with SDS-PAGE, and appropriate fractions were pooled, desalted in 50 mM Tris-HCl pH 7.5, 1 mM EDTA and concentrated. Small aliquots were frozen with liquid nitrogen and stored at -80°C.

2.17.2. Purification of SepF

SepF was purified in two steps. First, MBP fused SepF was purified then MBP and SepF were cleaved using Factor Xa and separated by anion exchange chromatography. *E. coli* cells containing the pMAL-SepF plasmid

were grown in LB + ampicillin (100 µg/ml) overnight at 37°C. The next morning, culture was diluted to 1:100 in 1L fresh pre-warmed LB + ampicillin (100 µg/ml). Cells were grown until OD_{600} was 0.4. Production of fusion protein was induced with 0.5 mM IPTG for 3h. Cells were collected and washed with ice-cold PBS (1 PBS tablet (Oxoid) per 100 ml dH_2O) with 1 mM PMSF. The pellet was stored at -80°C. The following day, cells were resuspended in 40 ml Buffer A_F (50 mM Tris-HCl pH 7.4, 200 mM KCl, 5 mM EDTA, 0.5 mM DTT), and disrupted with a French Press (20 kpsi). Cell debris was removed by centrifugation (1h, 31000g, 4°C). The supernatant was filtered through a 0.2 µm filter and loaded onto a 3 ml amylose column equilibrated with Buffer A_F (0.5 ml/min). The column was washed with 3 CV of Buffer A_F, followed by 3 CV of Buffer B_F (50 mM Tris-HCl pH 7.4) (1 ml/min). Fusion protein was eluted with 100% Buffer B_F + 10 mM Maltose (0.5 ml/min). Fusion protein was treated with Factor Xa (1 µg for 100 µg of fusion protein, NEB) with 2 mM $CaCl_2$ overnight at 4°C.

Separation of MBP and SepF was done with anion exchange chromatography. Proteins were loaded into a 1 ml HiTrapQ (GE Healthcare) columns pre-equilibrated with Buffer B_F (0.5 ml/min). The column was then washed with Buffer B_F, 15% Buffer C_F (50 mM Tris-HCl pH 7.4, 1 M KCl), 35% Buffer C_F for 5 CV each in this order. Elution of SepF was performed at 0.5 ml/min with 100% Buffer C_F. The location of protein was visualized with SDS-PAGE. Appropriate samples were collected, concentrated and stored at -80°C as small aliquots.

2.18. SDS-PAGE (Sodium Dodecyl Sulphate-Polyacrylamide Gel Electrophoresis)

The Novex Midi Gel System (Invitrogen) was used to separate proteins. Samples were prepared in NuPAGE LDS sample buffer and NuPAGE sample reducing agent, heated at 95°C for 5 min prior to loading the gel. NuPAGE Novex Bis-Tris Midi Gels (4-12 % w/v) were run in NuPAGE MOPS SDS Running Buffer using an XCell4 SureLock Midi-Cell (Invitrogen) at 200V for 50 min. Either Benchmark or Benchmark Pre-stained Protein Ladders (Invitrogen) were used to estimate protein sizes.

For staining, Coomassie blue staining was used. After washing gels briefly with dH_2O, gels were placed in the fixative solution (50% methanol, 10% acetic acid) for 10 min, shaking. The gel was then transferred to 20 ml methanol

with 75 ml solution A (8% w/v $(NH_4)_2SO_4$, 1.6% v/v Phosphoric acid). After shaking for 10 min, 5 ml of solution B (1.6% w/v Brilliant Blue G – Sigma) was added and left for staining at least for 3 hours. The gels were destained with distilled water. They were scanned with an Epson Perfection V700 flat-bed scanner (Epson).

2.19. Western Blotting

Proteins were transferred to Hybond-P PVDF membrane (GE Healthcare) using a semi-dry apparatus (Semi-Phor, Hoefer Scientific Instruments). Membranes were activated in pure methanol before equilibration in transfer buffer. Proteins were transferred to the membrane from SDS-PAGE at 100 mA for 1 h. The membrane was blocked overnight in milk buffer (PBS (1 PBS tablet (Oxoid) per 100 ml dH_2O), 1% Tween 20, 5% skimmed milk powder). The membrane was probed with primary antibodies (diluted depending on the concentration of antibody) in milk buffer (PBS, 1% Tween 20, 1% skimmed milk powder) for 2-3 hours. Then, the membrane was washed with PBST (PBS, 1% Tween 20) three times for 10 min. The secondary antibody (Anti-Rabbit IgG Peroxidase, Sigma) was diluted 1:10000 in PBST and incubated with the membrane for 30 min. The membrane was washed 2x15 min with PBST, 1x10 min with PBST and 5 min with PBS. Detection was done with Amersham ECL Plus Western Blotting Detection Kit (GE Healthcare). Membranes were then visualized with an ImageQuant LAS4000 mini (GE Healthcare). Exposure time depended on the strength of the signal.

2.20. Fluorescence Microscopy

2.20.1. Slide preparation

Cells were immobilized on a thin layer of 1.2 % w/v agarose in dH_2O, and covered with No.1 glass coverslips (0.15 nm) (VWR).

For imaging liposomes, clean slides were framed with vacuum grease using a pipette tip to avoid the evaporation of liquid during the microscopy. After putting the liposome mixture within the grease frame, it was covered with No. 1 glass coverslips (0.15 nm) (VWR).

For SIM imaging, coverslips were coated with dopamine as follows: 2 mg/ml dopamine in 10 mM Tris-HCl pH 8.0 was freshly prepared. After waiting

for 10 min at RT, clean coverslips were covered with the dopamine solution and incubated at RT for 30 min. The coverslips were then washed with dH_2O and left to air dry.

2.20.2. Visualization of proteins, DNA, and cell membrane

Production of SepF-GFP and GFP-FtsZ were induced with 0.5% and 0.25% xylose, respectively in cultures grown in LB until A_{600} 0.3-0.4 at 30°C. Excitation of GFP signals is 460-500 nm while emission of GFP signals is 510-560 nm.

DNA was stained with DAPI (Sigma) by mixing 100 µl of cells with 0.5 µl DAPI (5 µg/ml of final concentration). DAPI signal has an excitation of 340-380 nm and an emission of 435-485 nm.

The cell membrane was visualized with FM5-95 (1 µg/ml of final concentration, Invitrogen) or Nile Red (0.5 µg/ml of final concentration). 100 µl cells were mixed with 0.5 µl dye. RED signal has an excitation of HQ550-600 nm and an emission of HQ615-665 nm.

2.20.3. Microscopes used

Nikon Ti-E microscope images were acquired with a QImaging Camera using the software called Metamorph 6 (Molecular Devices, Inc.). Nikon Ti-E was equipped with a Nikon Intensilight C-HGFIE Precentered Fiber Illuminator and a Nikon Plain fluor 100x/1.30 Oil OFN25 Ph3 DLI objective.

Axiovert 200 M microscope (Zeiss) was equipped with a 100 W mercury lamp and a 100x / 1.30 numerical aperture Plan-neofluar oil immersion objective lens. Digital images were taken with Sony Cool-Snap HQ cooled CCD camera (Roper Scientific) and analysed with Metamorph 6 software (Molecular Devices, Inc.).

Nikon Ti equipped with a spinning disk confocal module, a 488 nm solid state Calypso 491 nm DPSS laser, 50 mW (Cobolt) light source, and Apo VC 100x/1.40 Oil (Nikon) objective was used to visualize the fluorescently labelled liposomes. Images were acquired with Frap-AI 7.7.5.0 (MAG Biosystems) using a QImaging Camera and analysed with ImageJ 1.46 (NIH).

2D Structured Illumination Microscopy (SIM) images were obtained with a Nikon N-SIM microscope equipped with a Sapphire HP 488 nm, 500 mW (Coherent) light source and a CFI APO TIRF 100x/1.49 Oil (Nikon) objective using an IXON X3 (Andor) camera and NIS-Elements 4.1 (Nikon) software.

2.21. Electron Microscopy

2.21.1. Thin-section electron microscopy of B. subtilis cells

Samples were prepared by Electron Microscopy Research Services, Newcastle University as follows:

Cells were harvested by centrifugation during mid-exponential phase. After washing with PBS, they were resuspended in 2% gluteraldehyde (w/v) in Sorensons Phosphate Buffer (TAAB Laboratory Equipment). Cells were fixed overnight at 4°C followed by washing with several changes of Sorensons Phosphate Buffer. Fixed and washed cells were subjected to a secondary fixation step in 1% w/v osmium tetroxide (Agar Scientific) for 1h.

Samples were dehydrated in an acetone graded series, followed by impregnation in graded series of epoxy resin (TAAB Laboratory Equipment) in acetone. Finally, 100% w/v resin embedding was done at 60°C for 24h. Ultrathin sections (80 nm) were cut using a diamond knife on a RMC MT-XL ultramicrotome (Boeckeler Instruments). The sections were stretched with chloroform, to eliminate compression, and mounted on Pioloform filmed copper grids (Agar Scientific). Cells were then counter-stained with 2% w/v uranyl acetate and lead citrate (Leica) before imaging with a Philips CM100 compustage transmission electron microscope (FEI) with an AMT CCD camera (Deben).

2.21.2. TEM of SepF, FtsZ, and liposomes

To image SepF with liposomes, preformed liposomes were diluted to 5 mg/ml in 10 mM Tris-HCl pH 7.4, 50 mM KCl, 2 mM $MgCl_2$, and sonicated for 15 min in a bath sonicator. SepF (0.3 mg/ml) was incubated with the sonicated liposome suspension (25 µl final volume) for 10 min at room temperature. In cases where FtsZ was included (0.1 mg/ml) the buffer also contained 4 mM GTP. After incubation, 20 µl of sample was applied to glow-discharged 200 mesh carbon coated grids, which were negatively stained with 100 µl of uranyl-acetate (2%). Grids were then imaged using a Philips CM100 electron microscope.

2.22. Lipid Interaction Assays

Lipid binding experiments were carried out with unilamellar vesicles prepared from *E. coli* polar lipid extract (Avanti, Alabaster, USA), as described

by Heitkamp et al. (Heitkamp et al., 2008). Lipid extract was solubilized in chloroform and was subjected to evaporation of chloroform under an argon stream. Dry lipids were resolubilized in 50 mM Tris-HCl pH 7.5, 2 mM β-mercaptoethanol, 1.5% octylglycoside (20 mg/ml lipids) under an argon stream and dialyzed against 50 mM Tris-HCl pH 7.5, 2 mM β-mercaptoethanol. Liposomes were aliqouted and stored at -80°C. In one case, the dye DiIC18 (0.1% w/w lipids) (Invitrogen) was added to resolubilization buffer (50 mM Tris-HCl pH 7.5, 2 mM β-mercaptoethanol, 1.5% octylglycoside) to obtain fluorescently labelled liposomes.

2.22.1. Sedimentation of SepF with liposomes and FtsZ

For pelleting experiments, preformed liposomes (20 mg/ml) were diluted to 5 mg/ml and extruded through a 0.4 µm diameter membrane (Avanti Polar Lipids) in SepF binding buffer (20 mM Tris-HCl pH 8.0, 2 mM $MgCl_2$, 200 mM KCl, 0.5 mM DTT, 1 mg/ml BSA). Purified SepF (0.25-0.5 mg/ml) and liposomes (5 mg/ml) were mixed in a total volume of 110 µl, and incubated for 10 min at room temperature. In cases where FtsZ (0.15 mg/ml) was included, the test was performed with and without 2 mM GTP in 10 mM Tris-HCl pH 7.4, 50 mM KCl, 2 mM $MgCl_2$, 1 mg/ml BSA. The mixtures were centrifuged in 0.8 ml ultra-clear centrifuge tubes (Beckman) at 40,000 rpm for 10 min at 20°C, in a Beckman TLA100 Rotor. Pellets and supernatants were analysed by SDS-PAGE stained with Coomassie Brilliant Blue G.

2.22.2. Sucrose gradient centrifugation

For sucrose gradient density (flotation) experiments, preformed liposomes (20 mg/ml) were diluted to 1 mg/ml in SepF binding buffer (20 mM Tris-HCl pH 8.0, 2 mM $MgCl_2$, 200 mM KCl, 0.5 mM DTT, 1 mg/ml BSA) containing a final concentration of 45 % sucrose. After extrusion through a 0.1 µm pore filter, liposomes (80 µl) were mixed with SepF (0.25-0.5 mg/ml), resulting in a final volume of 120 µl and 30 % sucrose, and then the mixture was incubated at room temperature for 10 min. A sucrose gradient was prepared using SepF binding buffer containing 10 % (100 µl), 15 % (100 µl), 20 % (200 µl), or 25 % (200 µl) sucrose, loaded on top of the SepF-liposome mixture. Centrifugation was carried out for 2 h (25 krpm, 25ºC) in a Beckman Rotor MLS50 using 0.8 ml tubes (5 x 41mm) (Beckman) and suitable adapters (Beckman), followed by collection of 100 µl samples from top to bottom.

Samples were analyzed by SDS-PAGE and Coomassie Brilliant Blue G staining. Interaction of FtsZ (3 µg/ml) with SepF (0.25-0.5 mg/ml) and liposomes (1 mg/ml, 0.1 µm diameter) was tested with and without GTP (2 mM) in 10 mM Tris-HCl pH 7.4, 50 mM KCl, 2 mM $MgCl_2$, 1 mg/ml BSA. The reactions were performed at room temperature for 10 min. Gradient samples were analysed by western blotting using FtsZ primary antibody and goat anti-rabbit HRP (Sigma).

2.22.3. Microscope analysis of liposomes with SepF

For the microscopic liposome binding assay, 5 µl of liposomes (5 mg/ml) were sonicated for 10 min in a bath sonicator (Decon, Ultrasonic Ltd), followed by incubation with SepF (0.25-0.5 mg/ml) in SepF binding buffer for 10 min at room temperature (completed to 10 µl with SepF binding buffer). Liposomes were stained with 0.1 mg/ml Bodipy FL C16 (Invitrogen). A Nikon Ti microscope equipped with a spinning disk confocal module, and a 488 nm solid state laser light source, was used to visualize the fluorescently labeled liposomes. Images were acquired with Frap-AI 7.7.5.0 and analyzed with ImageJ 1.46 (NIH).

2.22.4. Interaction of SepF and FtsZ with biotinylated liposomes

0.4% N-Cap-Biotin PE (Avanti - 10 mg/ml) was mixed with *E.coli* Polar Lipids (Avanti - 25 mg/ml) and subjected to detergent dialysis to form biotinylated unilamellar vesicles (20 mg/ml) (Heitkamp et al., 2008). Biotinylated liposomes were diluted to 1 mg/ml in 10 mM Tris-HCl pH 7.4, 50 mM KCl, 2 mM $MgCl_2$, then extruded through 0.1 µm filters. Extruded liposomes were incubated with 1 mg/ml BSA and buffer-equilibrated streptavidin beads (0.4 mg/ml of final concentration) (Dynabeads M-280, Invitrogen), and gently rotated for 10 min at room temperature. Next, excess free biotin (1 M) (Sigma) was added to solution to completely cover the streptavidin beads while rotation continued for 5 min. After the beads were covered with biotinylated liposomes and free biotin, SepF (0.5 mg/ml), and FtsZ (0.05 mg/ml) were added together or separately with or without 2 mM GTP. Rotation continued for another 10 min and the beads were separated from the supernatant using a magnetic stand. The supernatant and the beads were run on SDS-PAGE gel and stained with Coomassie Brilliant Blue G.

2.23. Sedimentation Assay of FtsZ

To control the activity of purified FtsZ, it (~8 mg/ml) was diluted in 50 µl of 50 mM HEPES-KOH pH 6.8, 50 mM KCl, 10 mM $MgCl_2$. After incubation at room temperature for 3 min, 2 mM GTP was added and mixture was incubated at 30°C for 10 min. Polymerized FtsZ was pelleted by centrifugation in 0.8 ml ultra-clear centrifuge tubes (Beckman) at 80000 rpm for 10 min with TLA100 rotor. Pellet and supernatant were separated and analysed with SDS-PAGE, followed by Coomassie Brilliant Blue G staining.

Chapter 3. Evolutionary Conservation of the SepF ring

SepF is a cell division protein which is widely conserved among Gram-positive bacteria and cyanobacteria. No homologs have been identified in Gram-negative bacteria (Hamoen et al., 2006, Ishikawa et al., 2006, Miyagishima et al., 2005). *In vitro* studies show that *Bacillus subtilis* SepF ($SepF_{BS}$) forms large, regular ring-like structures (Gundogdu et al., 2011). In the same study, Gundogdu et al. (2011) also demonstrated that these ring structures assemble into large tubules when mixed with FtsZ. It was further shown that, unlike wild type SepF, SepF mutants that abolish the ring formation are not able to compensate for an *ftsA* deletion, thereby indicating that the ability to form ring structures *in vitro* correlates with the activity of SepF *in vivo*. To examine whether the ring structure is a conserved property of SepF, we analysed six different Gram-positive organisms that are closely related to *B. subtilis* or that are important pathogens (Table 3.1). Similar to *B. subtilis*, *Bacillus cereus*, *Bacillus megaterium* and *Clostridium perfringens* are rod-shaped, endospore forming bacteria. In contrast, *Mycobacterium tuberculosis* is an important intracellular pathogen which has a complex cell wall and much slower generation time as compared to *B. subtilis*. While *Streptococcus pneumoniae* is a coccus shaped bacterium, *Streptomyces coelicolor* forms rod-shaped hyphae that undergoes two different types of cell division during its life cycle. The vegetative hyphae of *S. coelicolor* replicate and segregate their chromosomes but this process is not coupled to cell division and although cross-walls are made, cell separation does not occur until the aerial hyphae are formed. The final step of the life cycle of *S. coelicolor* is sporulation which occurs at the tips of the aerial hyphae. Interestingly, *S. coelicolor* has three SepF orthologs unlike *B. subtilis* and the other organisms examined in this study.

Organism	Abbreviation	Match (%)	Protein Size (Da)
Bacillus subtilis	$SepF_{BS}$	-	17386
Bacillus cereus	$SepF_{BC}$	30	17743
Bacillus megaterium	$SepF_{BM}$	27	17714
Clostridium perfringens	$SepF_{CP}$	37	16621
Streptococcus pneumoniae	$SepF_{SP}$	58	20627
Streptomyces coelicolor 1	$SepF_{SC1}$	61	15889
Streptomyces coelicolor 2	$SepF_{SC2}$	43	23723
Streptomyces coelicolor 3	$SepF_{SC3}$	37	14665
Mycobacterium tuberculosis	$SepF_{MT}$	34	25028

Table 3.1 List of organisms from which SepF was cloned and purified. The match (%) data shows percentage of matching residues calculated by CloneManager. Protein size data is taken from UniProt database.

A multiple sequence alignment (ClustalOmega (Goujon et al., 2010, Sievers et al., 2011)) of these proteins shows that the C-terminal domain of SepF (57-140 aa), which is later shown to be the ring forming domain (Chapter 3.3), is highly conserved (Figure 3.1). We purified these SepF orthologs and examined them with transmission electron microscopy.

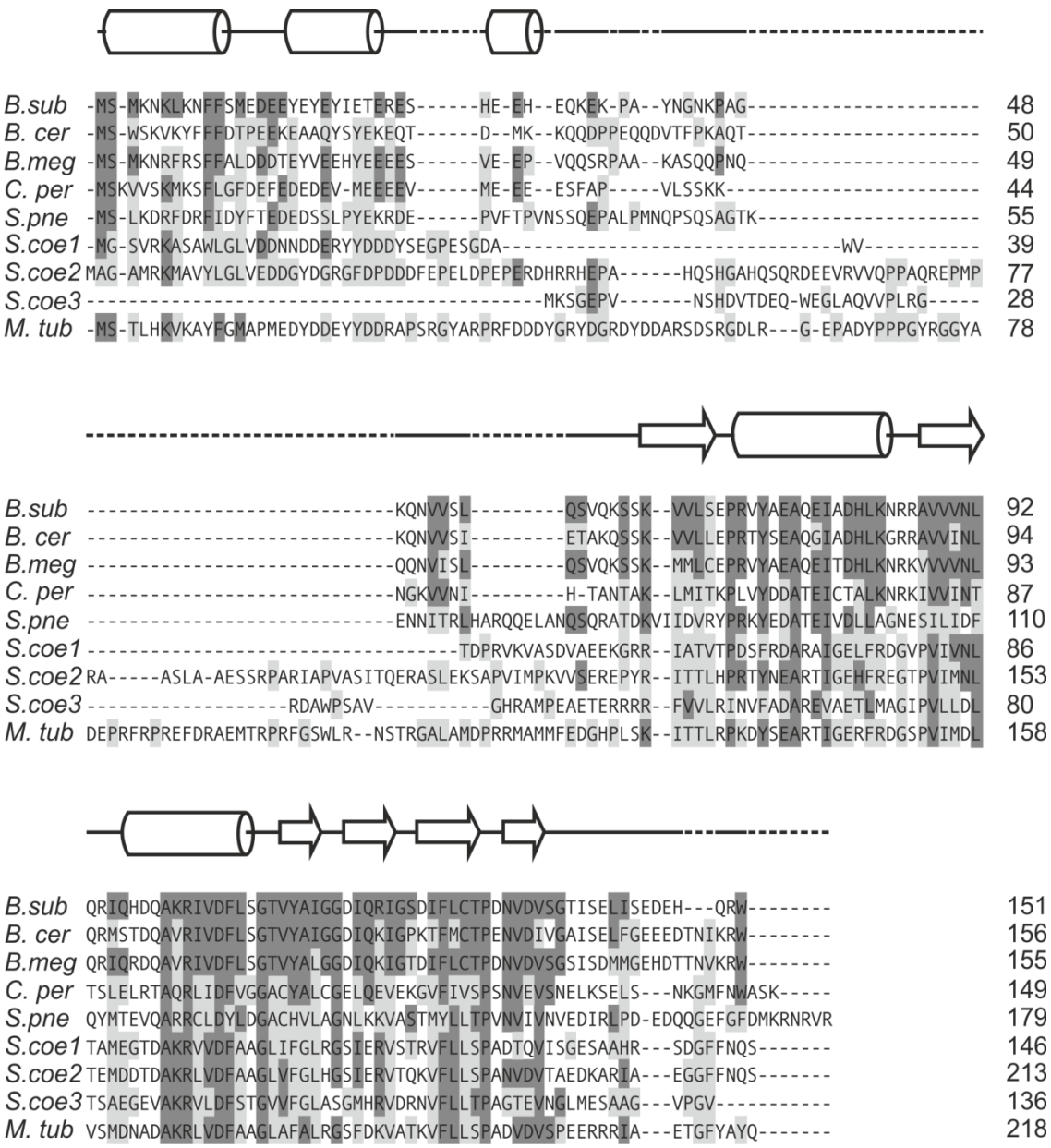

Figure 3.1 The ClustalOmega alignment of SepF of nine proteins from different organisms which were used in this study. The dark grey areas show the exact matches while the light grey areas indicate similar amino acids. The secondary structure was predicted by PSIPRED (Jones, 1999).

3.1. Purification of SepF Orthologs

Each protein was purified as an MBP (Maltose binding protein) fusion protein using *E. coli* BL21 (DE3) cells containing pMAL-SepF. After cloning of SepF in pMALC2, expression of the MBP-SepF fusion proteins was analysed (Figure 3.2A).

Initial purification attempts were carried out as described by Gundogdu et al. (2011). In brief, purification of the fusion protein was performed using affinity chromatography on amylose resin columns (Figure 3.2B). The purified fusion protein was digested with Factor Xa in order to separate MBP and SepF, followed by separation using anion exchange chromatography. However, the MBP fusions with SepF orthologs behaved differently compared to the fusion protein with $SepF_{BS}$. Despite increasing the amount of Factor Xa, in several cases digestion of the whole fusion protein was not successful. Separation of un-cleaved fusion protein from cleaved products using anion exchange chromatography was unsuccessful (Figure 3.2D, E). It was possible that the difference in digestion efficiency would be caused by difference in folding of the fusion protein. The Factor Xa digestion site may not be readily available to the enzyme unlike with the $SepF_{BS}$ fusion. To overcome this obstacle, an attempt to optimize the buffer in which the digestion occurs was performed. Therefore, buffers with different pH, salt concentrations and with mild detergent were tested (Table 3.2). However, in most cases a complete digestion was not achieved (Figure 3.2C). In some cases, the protein would be obtained in a reasonably pure state. In others, samples before anion exchange chromatography, which contain a mixture of MBP, MBP-SepF, and SepF, were used. The final protein samples which are used in TEM were shown in Figure 3.2E.

Name	Recipe
A	50 mM Tris-HCl pH 7.4, 200 mM KCl
B	50 mM Tris-HCl pH 8.5, 200 mM KCl
C	50 mM Tris-HCl pH 8.0, 200 mM KCl
D	50 mM Tris-HCl pH 8.0
E	50 mM Tris-HCl pH 8.5
F	50 mM Tris-HCl pH 7.4
G	50 mM Tris-HCl pH 8.0, 200 mM KCl, 1% Tween20
H	50 mM Tris-HCl pH 8.0, 1% Tween20

Table 3.2 Buffers that were used to improve Factor Xa cleavage of MBP-SepF fusion proteins.

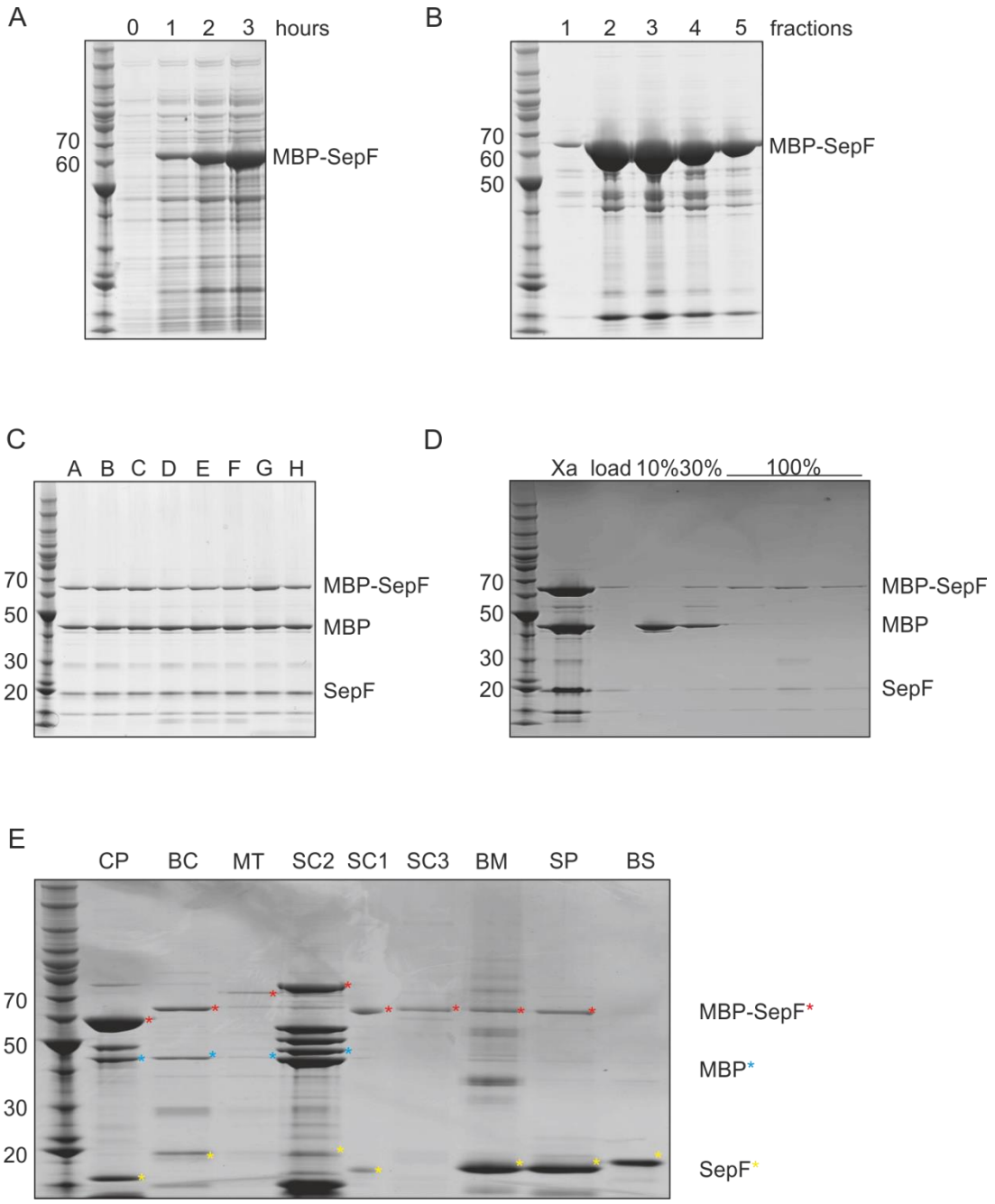

Figure 3.2 Step by step purification of SepF from *Bacillus cereus* using N-terminal MBP fusion protein. (A) Induction test of fusion protein, induction started with 0.5 mM IPTG at time 0 and followed for 3 hours with samples taken every hour (0, 1, 2, and 3). (B) Purification of MBP-SepF using an amylose column. (C) Factor Xa cleavage test with different buffers that are shown in Table 3.2. (D) Anion exchange chromatography, SepF is eluted with 100% Buffer C_F. (E) Purified SepF orthologs that were used for TEM analyses. The red stars indicate MBP-SepF fusion protein while blue stars show MBP and yellow stars mark SepF. The size of markers was given on the left-hand side of the gels in kDa.

3.2. Transmission Electron Microscopy of SepF Orthologs

Purified protein samples were stored at -80°C in small aliquots which were thawed on ice immediately before each experiment. For transmission electron microscopy, 200-mesh carbon coated, glow-discharged, hydrophilic grids were used. 20 µl of the purified protein in 50 mM Tris-HCl pH 7.5, 1 M KCl was applied onto the grids, followed by staining with 2% uranyl acetate. The grids were visualized using a Phillips CM100 Compustage transmission electron microscope and images were acquired with an ADT camera.

As has been shown before, $SepF_{BS}$ forms ring-like structures *in vitro* (Gundogdu et al., 2011). When analysed with TEM, it turned out that beside $SepF_{BS}$ (A), also $SepF_{BC}$ (D), $SepF_{SC1}$ (G), $SepF_{SC2}$ (E), and $SepF_{SC3}$ (I) are able to form ring-like structures (Figure 3.3). Moreover, as pointed out with arrows in Figure 3.3, curved filaments, which might be an intermediate phase, were visible with $SepF_{BM}$ (C) and $SepF_{SP}$ (B) (Figure 3.3). $SepF_{MT}$ (H) and $SepF_{CP}$ (F) also showed filament-like structures as marked with arrows (Figure 3.3). However, these structures are not as clear as the other ring structures observed so far. It is possible that the purification problem mentioned above is the main reason for this, assuming that these samples were contaminated with MBP and MBP-SepF fusion (Figure 3.2E). In addition, the amount of $SepF_{MT}$ was very little compared to $SepF_{BS}$, which makes it difficult to evaluate the ability to form rings. Nevertheless, the electron microscopy study of the SepF orthologs shows that the SepF ring is conserved.

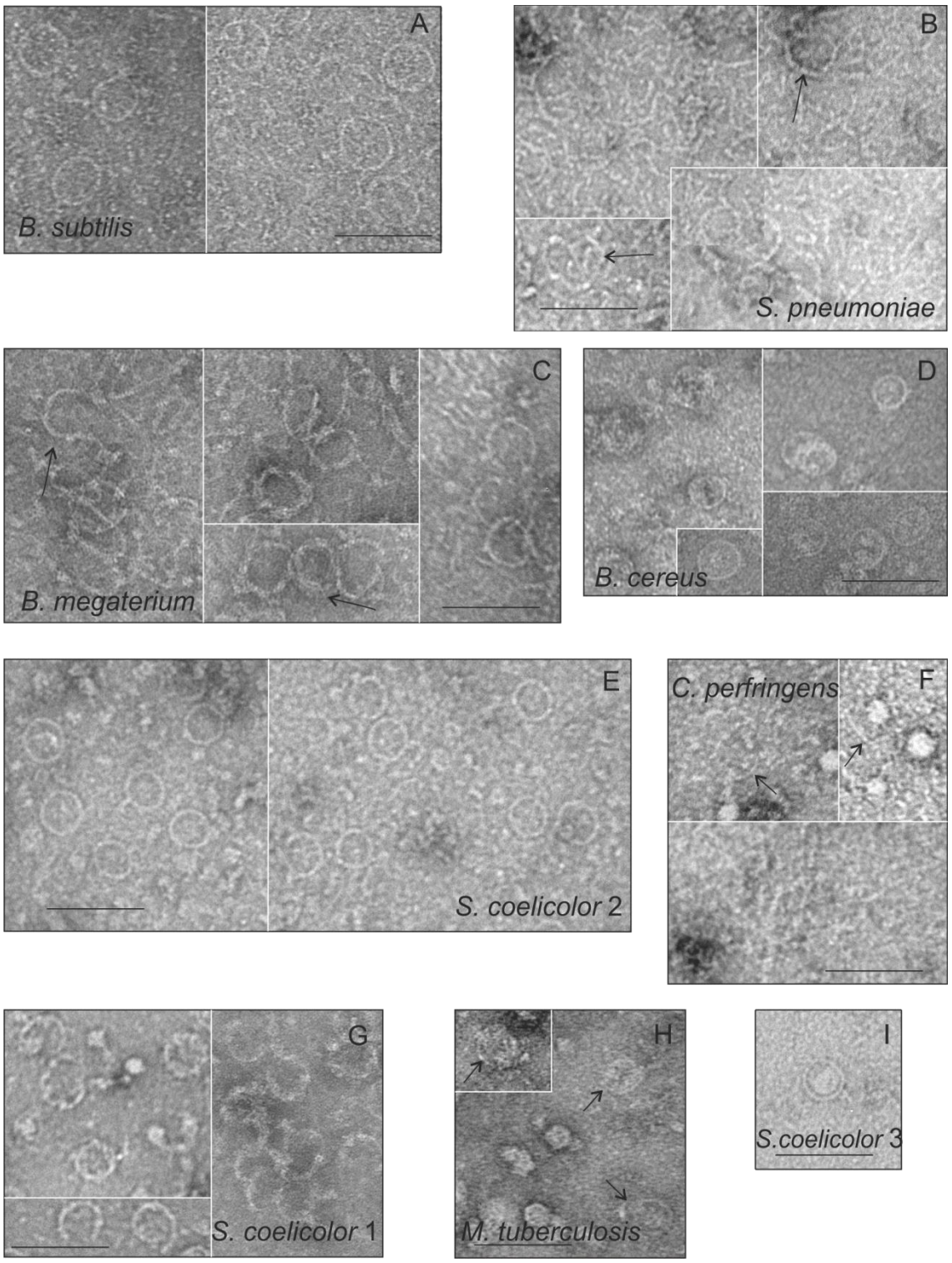

Figure 3.3 Transmission electron microscopy images of SepF orthologs. The bars show 100 nm (A) *Bacillus subtilis* (B) *Streptococcus pneumoniae* (C) *Bacillus megaterium* (D) *Bacillus cereus* (E) *Streptomyces coelicolor* 2 (F) *Clostridium perfringens* (G) *Streptomyces coelicolor* 1 (H) *Mycobacterium tuberculosis* (I) *Streptomyces coelicolor* 3

3.3. Crystal Structure of the Ring-Forming Domain (by Ramona Duman)

There were several attempts to crystallize full-length SepF of *Bacillus subtilis*. However, obtaining diffraction-quality crystals of full-length $SepF_{BS}$ was not successful, possibly due to the presence of unstructured regions within the protein. Therefore, mild proteolytic treatment with α-chymotrypsin was used to remove such regions. As a result of this treatment, truncated SepF (ΔN (57-151)), which consisted of residues 57 to 151, was purified. TEM images of ΔN (57-151) showed that it was able to form rings at high pH and stacks of rings at neutral pH (Figure 3.4A).

The crystal structure of $SepF_{BS}$ was solved along with two additional SepF-like proteins from *Archaeoglobus fulgidus* and *Pyrococcus furiosus* which were chosen solely for their sequence similarity to $SepF_{BS}$ (Figure 3.4B). The structure consists of two alpha-helices and five stranded beta-sheets which form an alpha/beta sandwich spanning residues Ser 61 to Ser 140. This suggested that first four and last eleven amino acids of ΔN (57-151) remained disordered. ΔN (57-151) existed as a tight dimer with the last beta strand of one monomer parallel to the first beta strand of adjacent monomer (Figure 3.4B).

The crystal structure also gave insight into polymerization of SepF. The structure showed that tight dimers interact with each other through alpha-helices that faced away from the dimer (Figure 3.4C). Analysis of these helices showed that the residue G109 located within the longest helix formed a point where helices from neighbouring dimers interact and assemble into polymers. The lack of a side chain in glycine residues forms a pocket for the close interaction of the adjacent helices (Figure 3.5A). It was possible to substitute the glycine residue with a bulky lysine (G109K) residue without affecting SepF dimerization. However, the crystal lattice of G109K showed an unstructured organization (Figure 3.5C) unlike the crystal lattice of ΔN (57-151) (Figure 3.5B). The dimerization of G109K was observed with gel filtration chromatography (data not shown). Moreover, SepF (G109K)-GFP did not localize at the division site when expressed in *B. subtilis* (Figure 3.5D). Behaviour of this mutant supports the idea that the dimers assemble into polymers through interaction between the alpha-helices.

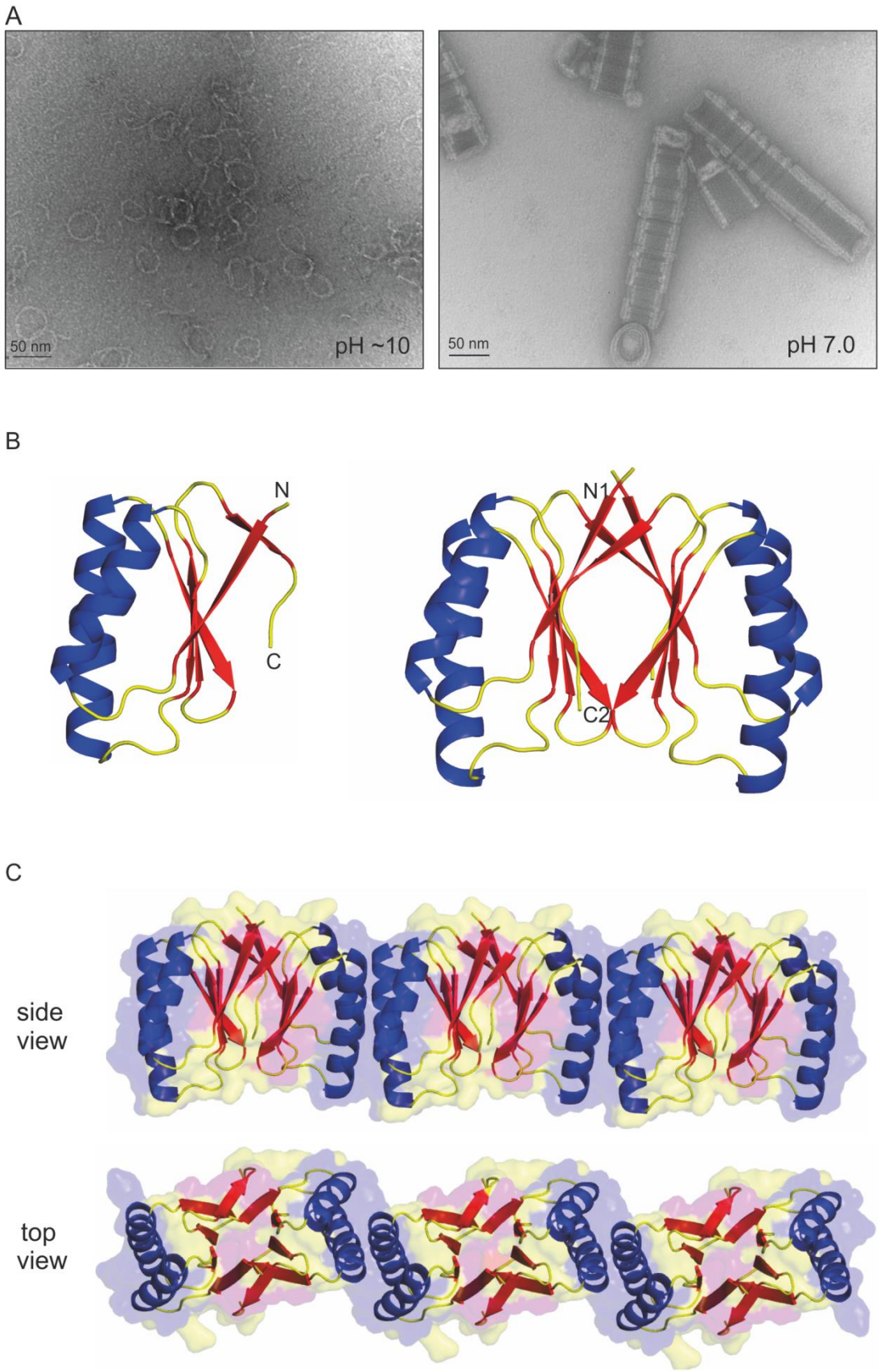

Figure 3.4 Crystal structure of the C-terminus of SepF. (A) TEM image of ΔN (57-151) at pH 10 (left panel) and pH 7.0 (right panel) (B) The structure of monomer (left panel) and dimer (right dimer) (C) Dimers polymerize into polymers through interaction between adjacent alpha-helices (The data was obtained by Ramona Duman).

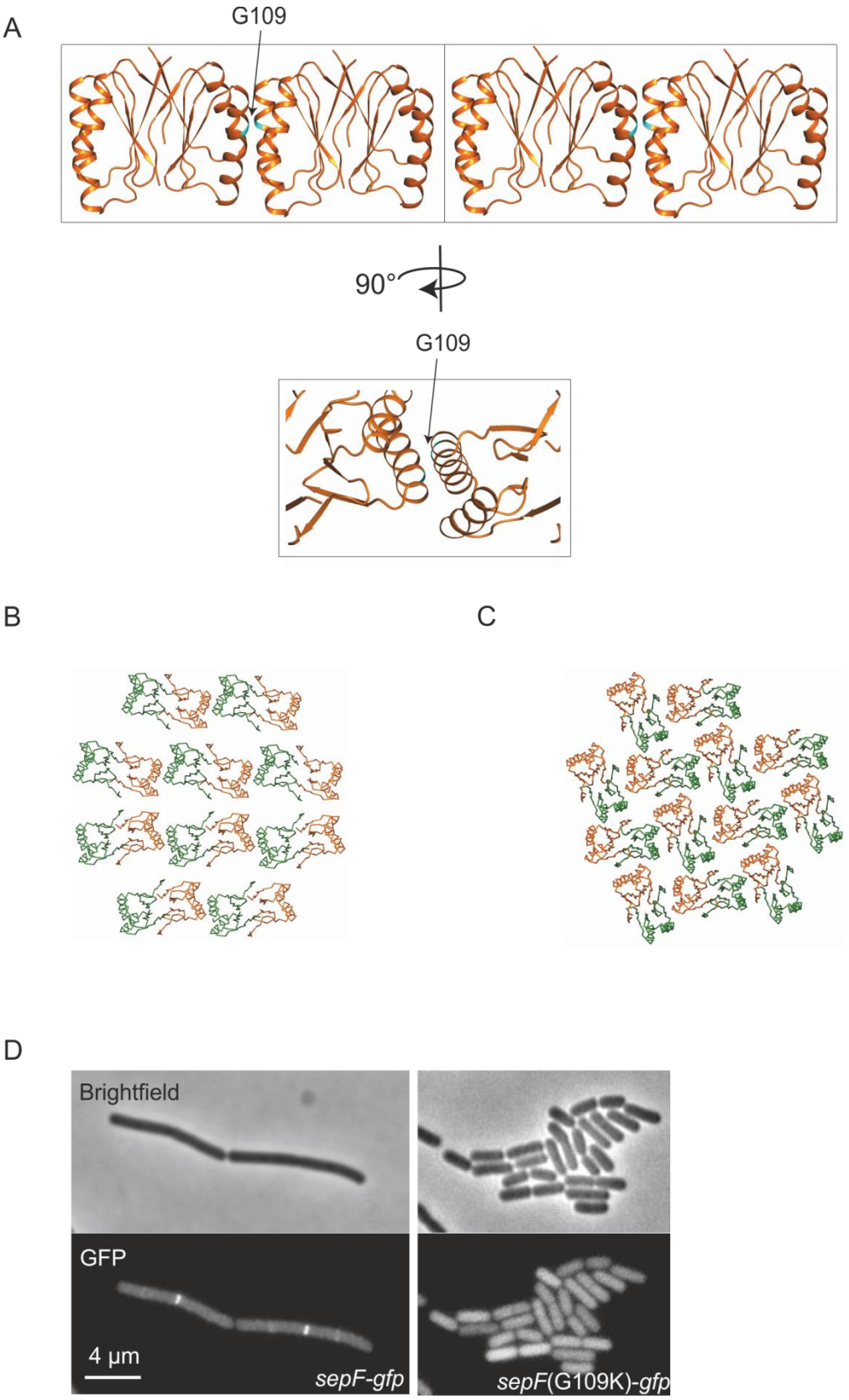

Figure 3.5 SepF (G109K) is not able to polymerize. (A) G109 is located on the longest helix that faces outward of the dimers (B) The crystal lattice of wild type ΔN (57-151) shows a structured organization while (C) the crystal lattice of G109K ΔN (57-151) remains unstructured. (D) SepF (G109K)-GFP does not localize at the division site (The crystallography data was obtained Ramona Duman).

Discussion

In this study, we aimed to show that the ring-like structure formed by SepF *in vitro* was conserved among Gram-positive bacteria which have SepF orthologs. For this purpose, eight purified SepF orthologs were analysed with TEM. Electron microscopy images showed that these proteins were indeed able to polymerize. Moreover, six of them were able to form rings with $SepF_{BM}$ and $SepF_{SP}$ being mostly curved filaments. It was anticipated that the curved filaments of $SepF_{BM}$ and $SepF_{SP}$ were an intermediate state between filaments and rings, considering that the diameter of curvature appears to be in the same range as SepF rings. Alignment of these proteins with $SepF_{BS}$ showed that there were seven amino acids in the ring forming region (ΔN (57-151)) that differed in both $SepF_{BM}$ and $SepF_{SP}$ (Figure 3.6A). Localization of these residues on the crystal structure (PyMOL (System)) showed that out of the seven residues only three of them are located at the alpha-helices, and could therefore affect polymerization of SepF. One important residue was T138. Previous studies have shown that mutations in residues G137 and I139 caused disruption of the ring structure, but did not interfere with polymerization which was observed with TEM ((Gundogdu et al., 2011), personal communication with Leendert Hamoen). Haeusser and Margolin (2011) suggested that the exchange of the small glycine within the larger protein might change the polymerization of the protein (Haeusser and Margolin, 2011). Clearly, it will be interesting to make more point mutations in these residues (G137, T138 and I139) to better understand ring formation and its effects on cell division.

It was difficult to reach any conclusion about $SepF_{MT}$ and $SepF_{CP}$ since their purification was not successful, and impure samples of these two proteins gave no clear filaments or rings. Future improved purification of these proteins will hopefully help to draw a conclusion. In order to have better purification, the second step of the purification might be replaced with size exclusion chromatography. In addition, Factor Xa digestion, while the fusion protein is bound to the amylose resin column, might also improve the digestion and purification. Also, using the amylose resin column after Factor Xa digestion may separate SepF from MBP and MBP-SepF.

A

```
B.sub  MSMKNKLKNFFSMEDEEYEYEYIETERE-SHEEHEQKEK-PAYNGNKPAGK--------------QNVVSLQS 57
B.meg  MSMKNRFRSFFALDDDTEYVEEHYEEEE-SVEEPVQQSRPAAKASQQPNQQ--------------QNVISLQS 58
S.pne  MSLKDRFDRFIDYFTEDEDSSLPYEKRDEPVFTSVNSSQEPALPMNQPSQSAGTKENNITRLHARQQELANQS 73

B.sub  VQKSS--KVVLSEPRVYAEAQEIADHLKNRRAVVVNLQRIQHDQAKRIVDFLSGTVYAIGGDIQRIGSDIFLC 128
B.meg  VQKSS--KMMLCEPRVYAEAQEITDHLKNRKVVVVNLQRIQRDQAVRIVDFLSGTVYALGGDIQKIGTDIFLC 129
S.pne  QRATDKVIIDVRYPRKYEDATEIVDLLAGNESILIDFQYMTEVQARRCLDYLDGACHVLAGNLKKVASTMYLL 146

B.sub  TPDNVDVSGTISELISEDEH-------QRW---                                         151
B.meg  TPDNVDVSGSISDMMGEHDTTNV----KRW---                                         155
S.pne  TPVNVIVNVEDIRLPDEDQQGEFGFDMKRNRVR                                         179
```

B

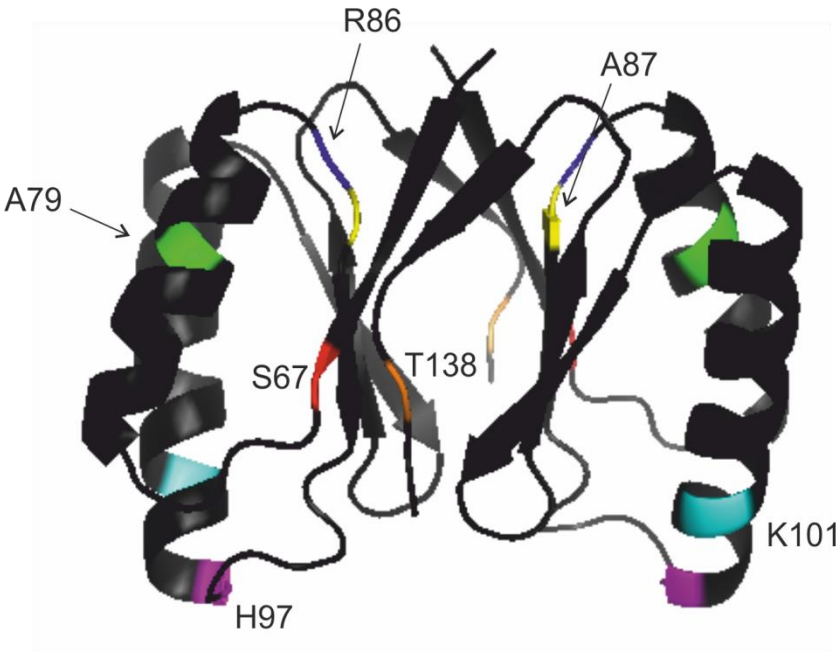

Figure 3.6 SepF orthologs that form curved filaments and their sequence differences with *Bacillus subtilis* SepF. (A) The ClustalOmega alignment of $SepF_{BS}$, $SepF_{BM}$ and $SepF_{SP}$. The dark grey areas show exact matches while the light grey areas show similar residues. (B) The tight dimer of $SepF_{BS}$. Residues that are different in $SepF_{BM}$ and $SepF_{SP}$ are shown. The structure is drawn using PyMol.

The SepF rings are highly regular and large structures that are easily observed with electron microscope. When they were first discovered by Gundogdu et al. (2011), it was believed that SepF would not form similar structures *in vivo*, since they would be visible with electron microscopy of *B. subtilis* cells, for instance, due to their large diameters. This work shows that the SepF rings are conserved in several other Gram-positive organisms, and supports the hypothesis that these rings are functional *in vivo*.

The crystal structure of ΔN (57-151) showed that SepF monomers formed tight dimers which polymerize laterally. It has been shown that one residue, G109, located on the longest helix is highly important for polymerization of SepF. However, the assembly of dimers in the crystal lattice (Figure 3.5B) did not indicate a curvature that could explain how the polymers form rings, and this question remains unanswered. Along with the C-terminus of $SepF_{BS}$, those of *A. fulgidus* and *P. furiosus* were also crystallized. These organisms were chosen for their sequence similarity to *B. subtilis* SepF. However, the experiments so far did not reveal a ring-like structure for SepF from *A. fulgidus* and *P. furiosus* (personal communication with Ramona Duman). It is possible that the conditions used to detect the ring structures were not optimal for the SepF protein from these archaeal bacteria. Moreover, they might have proteins with overlapping functions to SepF.

The crystal structure of the C-terminal domain of SepF also allowed us to make a comparison with the predicted secondary structure of the same region. As Figure 3.7 shows the number and the order of α-helices and β-sheets are predicted correctly by the program we used (PSIPRED). However, the exact amino acids in those helices and sheets were quite different than the actual structure. For instance, the G109 residue is shown to be on the coiled region in the predicted structure. However, it is now known that this residue is a part of the α-helix and has an important role in polymerization of SepF. This comparison showed that although the predicted structure programs give considerable information on the protein, they are not very accurate.

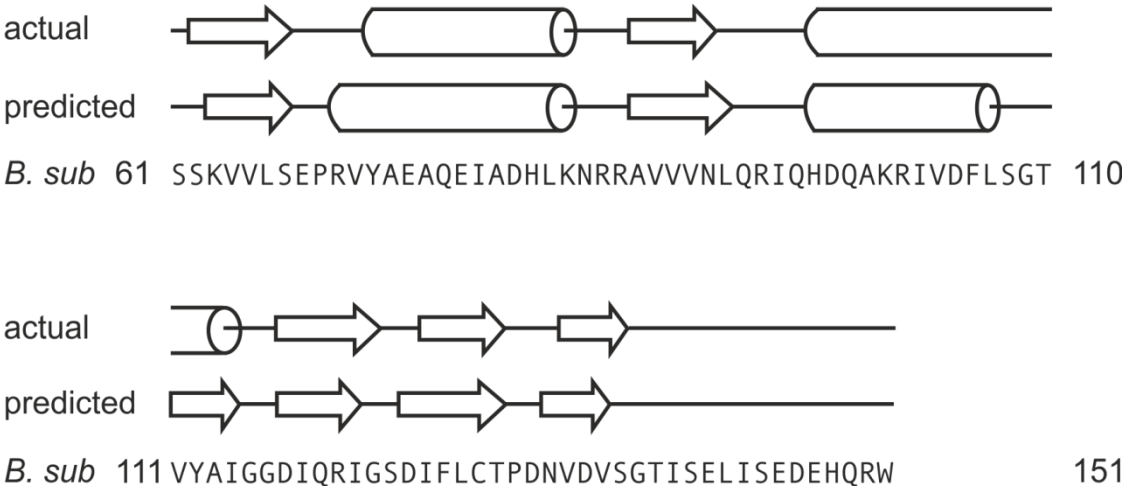

Figure 3.7 Comparison of predicted secondary structure and secondary structure from crystal structure of the C-terminal domain of SepF

Future Work

For further studies, it would be important to make point mutations in the residues mentioned above to learn more about the mechanism behind the ring formation. Also, it is important to use other assays to show that the SepF orthologs studied here polymerizes. Gel filtration chromatography might be used for this purpose. It was shown that the C-terminal end of FtsZ is required for its interaction with SepF (Król et al., 2012, Singh et al., 2008). However, there have been no studies to investigate where FtsZ binds onto SepF. Complementation studies on *sepF ftsA* background in *B. subtilis* would give information of the activity of SepF mutants mentioned above. Studying these mutants and their interaction with FtsZ might also point out the FtsZ binding region on SepF. In addition, the N-terminal domain of SepF could be crystallized to learn more about the structure and function of SepF. Finally, it would be useful to improve purification of SepF for future studies.

Chapter 4. SepF Tethers FtsZ to the Cell Membrane

SepF is known to interact only with FtsZ and itself (Hamoen et al., 2006, Ishikawa et al., 2006). It was shown that the last 17 amino acids of FtsZ are required for the interaction with SepF (Król et al., 2012, Singh et al., 2008). However, there are no studies which investigate the FtsZ binding site on SepF. This work examines mutations in the *sepF* gene to find out the FtsZ binding region using a yeast-two hybrid experiment.

4.1. The C-terminus of SepF is Required for its Function and its Interaction to FtsZ (by Shu Ishikawa)

Ishikawa et al. (2006) and Hamoen et al. (2006) demonstrated SepF-FtsZ and SepF-SepF interactions using yeast two-hybrid (Y2H) assays. To learn more about the binding site of FtsZ, several SepF mutants generated with error prone PCR were tested against FtsZ, wild-type SepF and themselves using Y2H. Fifteen of these mutants were identified as FtsZ-binding deficient (Figure 4.1A). Analysis of these mutants showed 10 amino acid substitutions and 3 nonsense mutations which resulted in the C-terminal truncations of SepF after 16, 60 and 120 amino acids (Figure 4.1C). Truncation mutants also lacked self-interaction similar to G109R. All FtsZ-binding mutants were located at the C-terminal domain of SepF. To show that the N-terminus of SepF does not involve in FtsZ interaction a set of N-terminal truncations were constructed and tested with Y2H (Figure 4.1A). This data supported the model that the absence of the first 63 residues does not affect FtsZ binding and self-interaction of SepF. It was also important to show that these mutants are not functional *in vivo*, since FtsZ binding is an essential characteristic of SepF (Gundogdu et al., 2011), so the mutants found in this study should not compensate for a *ftsA* deletion (Ishikawa et al., 2006). Indeed, when expressed from the native locus, these mutants were not able to survive in the absence of FtsA (Figure 4.1B). Although, it does not give a clear location for FtsZ binding region, this study shows that the C-terminus of SepF is important for FtsZ interaction.

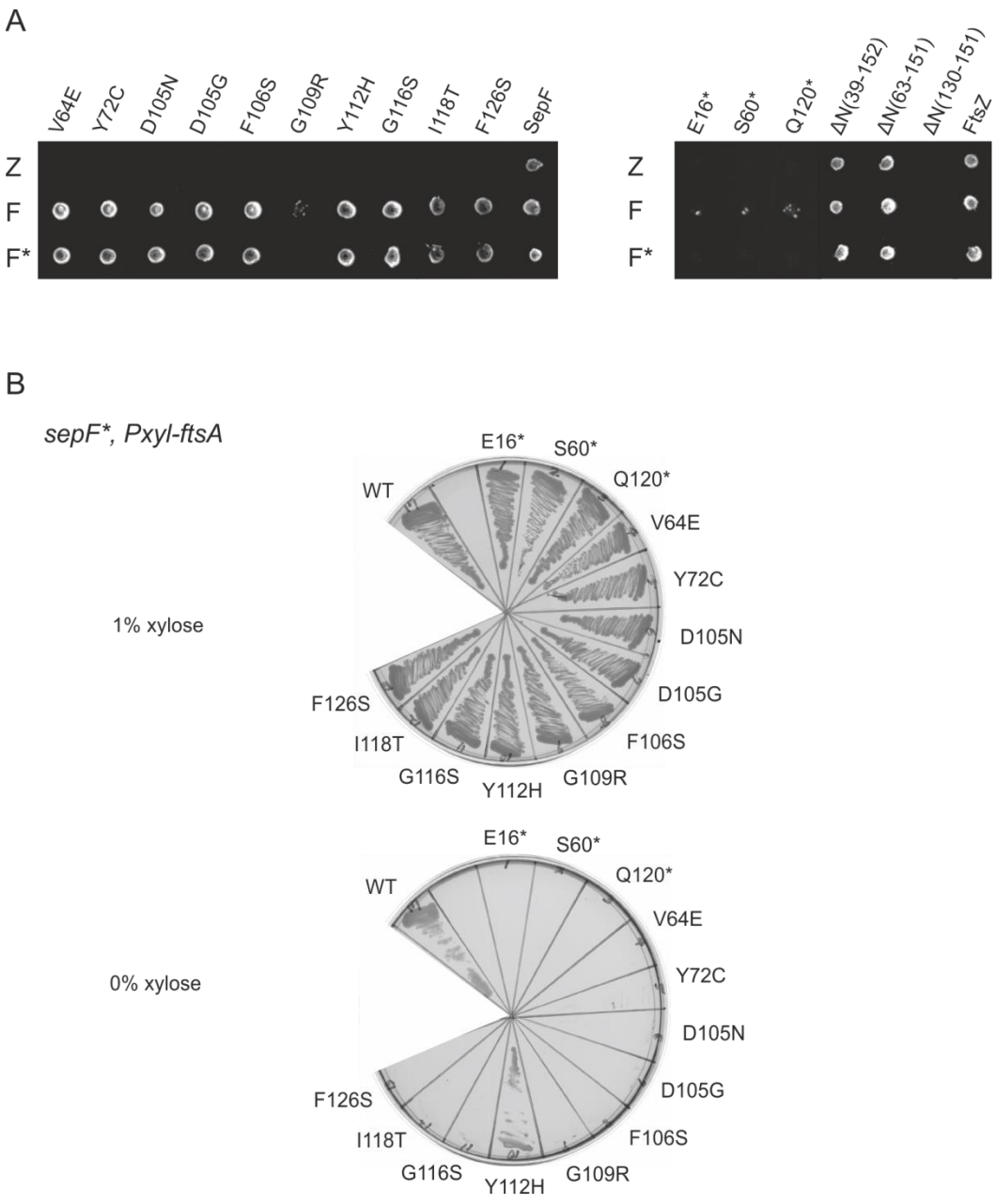

Figure 4.1 FtsZ binding region on SepF. (A) Interactions between FtsZ (Z), wild type SepF (F) and mutants (F*) were investigated with yeast two-hybrid experiment. (B) These mutants do not compensate for *ftsA* deletion when expressed from native SepF locus. (C) FtsZ binding deficient mutants are shown on SepF sequence. Filled arrows indicate the truncations while others indicate the amino acid substitutions (The data was obtained by Shu Ishikawa).

4.2. *Bacillus subtilis* Cells Divide in the Absence of Cell Division Proteins, FtsA and EzrA

FtsZ is the first protein to localize at the septum and all other divisome proteins are recruited to the division site depending on FtsZ (Adams and Errington, 2009). An essential property of FtsZ is that it needs to be tethered to the cell membrane. In *E. coli*, FtsA and ZipA are two proteins responsible for this (Adams and Errington, 2009). *B. subtilis* contains a homolog of FtsA, but not ZipA (Adams and Errington, 2009). Moreover, FtsA is not essential in *B. subtilis* (Beall and Lutkenhaus, 1992) suggesting that there is at least one more protein that would tether FtsZ to the cell membrane. EzrA is another cell division protein in *B. subtilis*. It has been identified as a negative regulator of FtsZ (Levin et al., 1999). However, it was later shown that it is required for recruitment of PBP1 (Claessen et al., 2008). Like ZipA, it has a transmembrane domain, and therefore it might tether FtsZ to the cell membrane (Levin et al., 1999). However, EzrA is also not essential in *B. subtilis* (Levin et al., 1999). In our study, a double mutant of *ezrA ftsA* strain was constructed (Figure 4.2A). Deletion of these proteins did not have a dramatic effect on the cell division which brought up the possibility of a third membrane tether of FtsZ.

The C-terminal domain of SepF is shown to function in polymerization and FtsZ binding. However, the role of the first 60 amino acids is not known. Previous studies have shown that *sepF ftsA* double knockout (Ishikawa et al., 2006) and *sepF ezrA* deletions (Hamoen et al., 2006) are synthetic lethal. This raised the possibility that SepF might be the third membrane tether for FtsZ. To test this, a strain in which the *ftsZ* gene is under the control of the P_{spac} promoter with P_{xyl} *sepF-gfp* located at the *amyE* locus was constructed. In this strain, SepF-GFP was recruited to the division site when *ftsZ* was induced with IPTG (Figure 4.2B). However, when IPTG was removed and FtsZ levels were depleted, SepF localized at the cell periphery (Figure 4.2B, - IPTG). These images are obtained with Structure Illumination Microscopy (SIM) in which sample is illuminated with a light that has a grid pattern. Using this light pattern, the images of a sample are taken in several shifted phases. These images, then, are computationally superimposed to obtain an image with a higher resolution than the conventional wide-field images. The SIM we used in these experiments sometimes produces an artefact which might sometimes resemble a helically localized protein (Figure 4.2B, - IPTG). Therefore, only the strongest

signals are accepted as SepF-GFP signal which localizes at the cell membrane. This experiment showed that SepF was able to interact with the cell membrane and might indeed be a membrane tether for FtsZ.

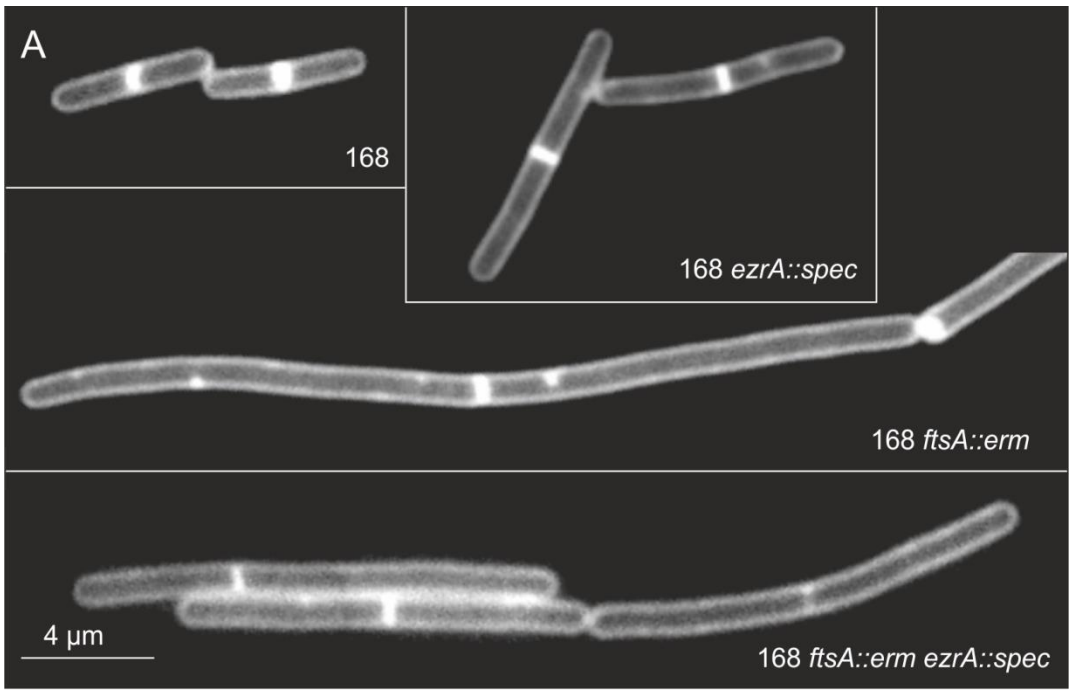

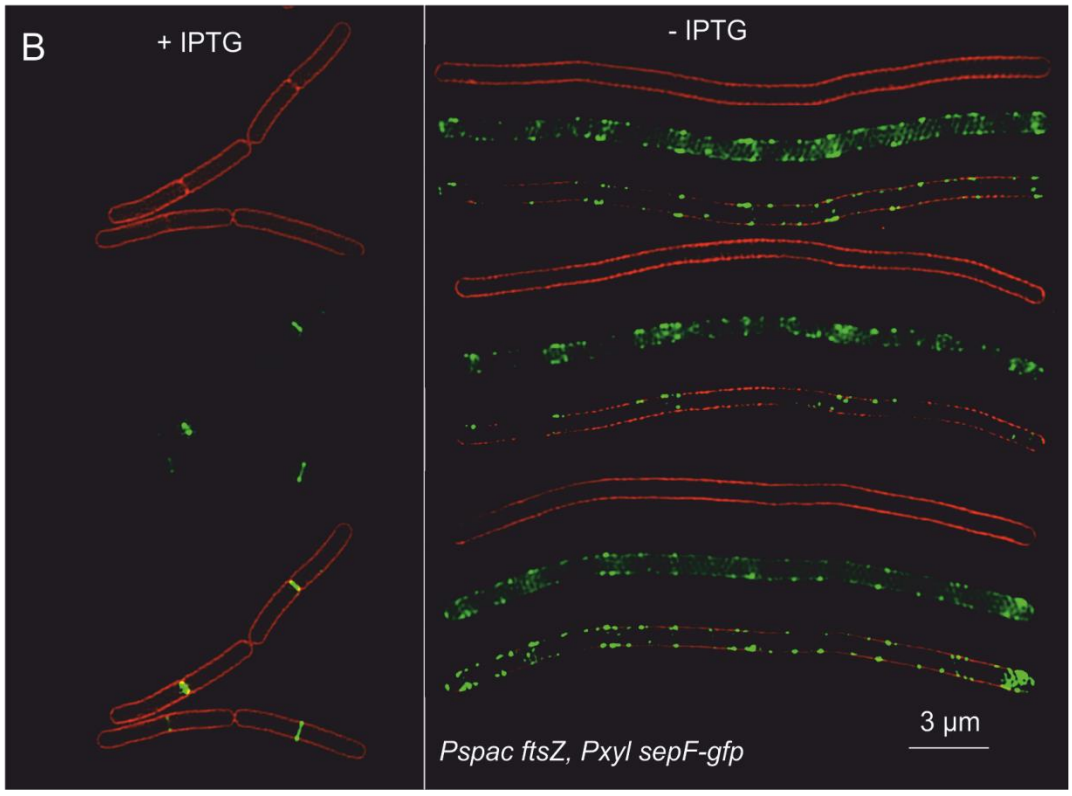

Figure 4.2 SepF interacts with the cell membrane (A) Cells are able to divide without FtsA and EzrA. Figures show wide-field images (Nikon Ti) of FM95-5 stained membranes. (B) SepF is recruited to the septa in the presence of FtsZ (+ IPTG). In the absence of FtsZ (- IPTG), SepF localizes at the cell membrane. Images are acquired with SIM (Structured Illumination Microscopy). Cells were stained with Nile Red membrane dye.

4.3. SepF Binds to Liposomes and Deforms them

In our *in vivo* study, SepF-GFP localized at the cell periphery, suggesting that SepF interacts with the cell membrane. To further analyse the interaction between SepF and the cell membrane, an *in vitro* system was constructed with liposomes which consist of *E. coli* polar lipids (Avanti). Excess BSA and 200 mM KCl were used in all experiments to avoid unspecific interactions. The first test applied was high speed centrifugation. When SepF was centrifuged by itself, it did not precipitate efficiently. However, in the presence of liposomes, the fraction of SepF in the pellet increased about 5-fold (Figure 4.3A). Since part of the SepF fraction precipitated when centrifuged, a more specific test was applied, namely sucrose gradient centrifugation. SepF was loaded at the bottom of the gradient with or without liposomes. In this experiment, SepF alone stayed at the bottom of the gradient, but when mixed with liposomes it moved to an upper sucrose concentration (Figure 4.3B). In the sucrose gradient, the flotation of liposomes also changed in the presence of SepF which could be observed with a naked eye and using fluorescently labelled liposomes (Figure 4.3C). In the absence of SepF, it was not possible to see liposomes. However, in the presence of SepF, liposomes formed clumps which are easily observed. The specificity of the sucrose gradient assay was shown with BSA and GFP (Figure 4.4A). These two proteins do not show any affinity to liposomes, and they show no change in the presence of the liposomes (Figure 4.4A-B). This experiment supported the notion that SepF interacts directly with the cell membrane. To further investigate this interaction, fluorescence microscopy was used. Fluorescently stained liposomes were mixed with SepF. Surprisingly, liposomes were deformed and clumped together in the presence of SepF (Figure 4.3D). The mechanism behind this deformation is not understood. However, this microscopy assay visually verified that SepF interacts with liposomes.

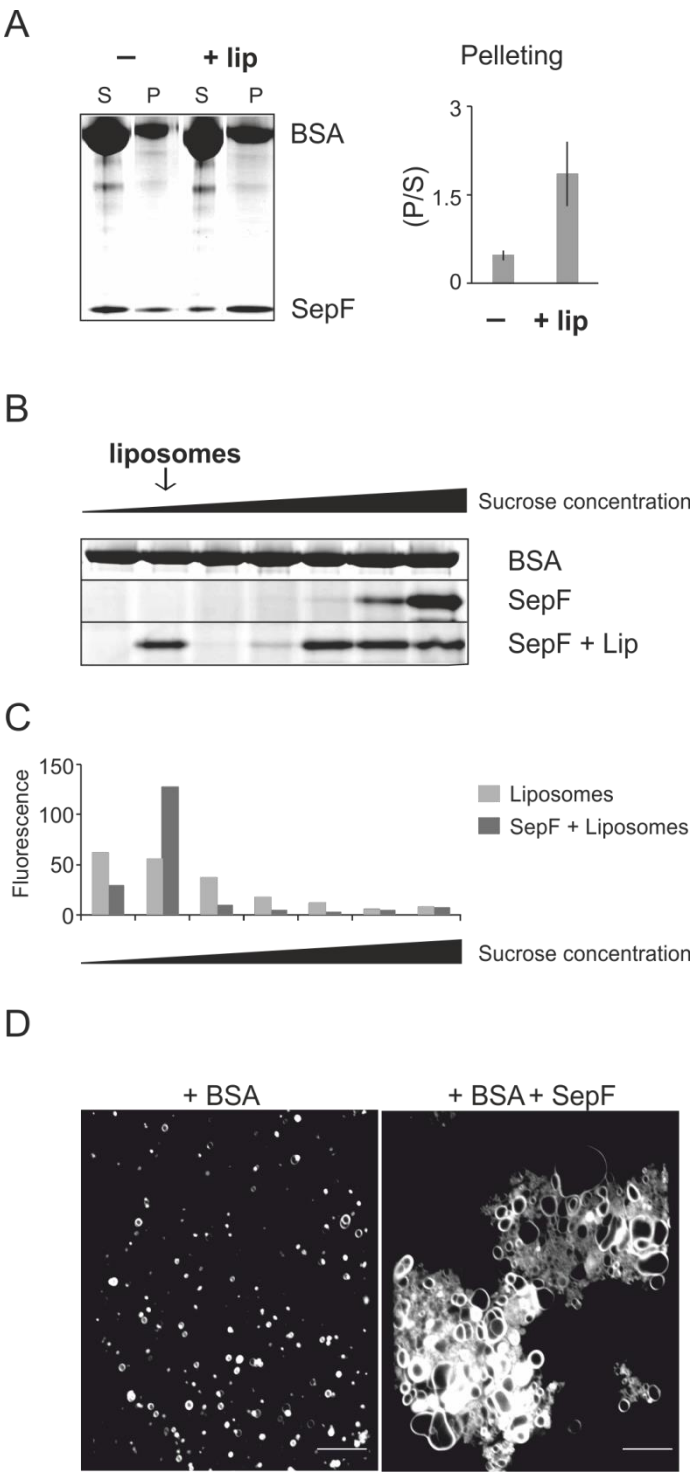

Figure 4.3 SepF interacts with liposomes. (A) High speed centrifugation of SepF with or without liposomes (Although the experiment was performed at the same time, '- liposomes' and '+ liposomes' were run at different gels. Later they were combined together for comparison purposes). Graph shows the ratio of amount of SepF in the pellet over amount of SepF in the supernatant. (B) Sucrose gradient centrifugation of SepF with and without liposomes. BSA did not show any interactions with liposomes. (C) The location of liposomes in the sucrose gradient after centrifugation. Liposomes were fluorescently labelled with DiI-C18. (D) Bodipy FL C16 stained liposomes were deformed in the presence of SepF. The scale bars show 10 μm.

4.4. Polymerization is Required but FtsZ Binding is not Necessary for Liposome Interaction

The question was whether other properties of SepF affect liposome interaction or not. Therefore, several known mutants were tested in the sucrose gradient centrifugation assay.

Gundogdu et al. (2011) characterized two SepF mutants that are not able to interact with FtsZ, A100V and F126S. In our assay, these mutants were used to test whether FtsZ binding affects membrane interaction. Figure 4.4A shows that these mutants maintain the interaction with liposomes. In the same study, several non-polymerizing mutants were also identified (Gundogdu et al., 2011). MBP-SepF and the ΔC (1-136) mutant were deficient in polymerization. Also, the G109K mutant that was discovered during crystallization work is unable to polymerize. These SepF mutants stayed at the bottom of the gradient even with liposomes (Figure 4.4A). These results suggest that polymerization is required for efficient membrane interaction under the reaction conditions used in this assay. Another SepF mutant that was described by Gundogdu et al. (2011) was G137N which was able to polymerize but could not form rings. This mutant was used to test the importance of ring formation, which turned out not to be required for membrane interaction (Figure 4.4A). Figure 4.4B shows these mutants in the sucrose gradient without liposomes. Binding efficiency of wild type and mutants were also calculated using the band intensities of the SDS-PAGE gel by measuring each band separately (Figure 4.4C).

The sucrose gradient assay data was supported by fluorescent microscopy assay. Figure 4.5 show that the mutants that interacted with liposomes in the gradient also clustered and deformed liposomes.

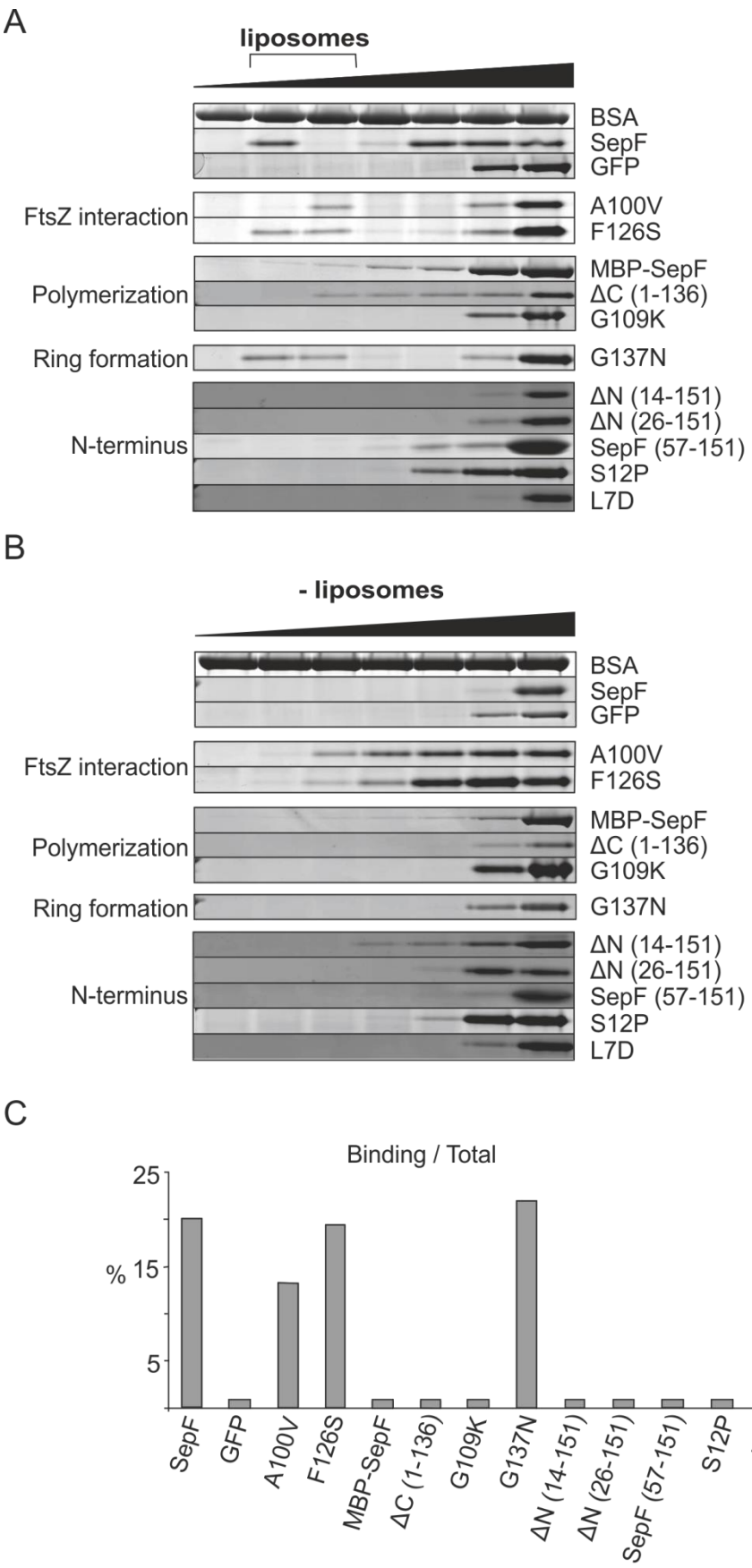

Figure 4.4 Liposome interactions of SepF mutants. (A) Sucrose gradient with liposomes and mutants. (B) Mutants were subjected to sucrose gradient in the absence of liposomes. (C) Binding efficiencies of all proteins that were calculated using band intensities of SDS-PAGE gel.

4.5. The N-terminus of SepF is Required for Membrane Interaction

In the previous sections, it was shown that the C-terminal domain of SepF is required for polymerization and FtsZ binding. On the other hand, the N-terminus was not required for any of these functions. According to the secondary structure prediction results, the N-terminus of SepF contains two large α-helices and one smaller α-helix (Figure 3.1). It was possible that one of these helices was a membrane interaction domain for SepF. Therefore, first the N-terminal truncation mutant, which was used in crystallization studies, was tested for membrane interaction. ΔN (57-151) did not interact with liposomes in the sucrose gradient (Figure 4.4A) and did not deform liposomes (Figure 4.5). This result supported the notion that the N-terminus is required for membrane interaction. Indeed, the AmphipaSeek predictions and helical wheel projection (Figure 4.10A) suggest that the first 12 residues of SepF form an amphipathic helix (Sapay et al., 2006). To investigate this possibility, two more truncations were constructed; ΔN (14-151) and ΔN (26-151) which lack the putative amphipathic helix and the first two predicted α-helices respectively. As expected, both these mutants were unable to bind to liposomes in the gradient (Figure 4.4A). Furthermore, they did not deform liposomes (Figure 4.5). This suggests that the first 12 residues of SepF are required for the membrane interaction and deformation of liposomes.

S12P is a SepF mutant that was discovered during studies to determine the dominant negative mutants of SepF (personal communication Leendert Hamoen). This mutant presented an excellent opportunity to test the importance of the N-terminus for the membrane interaction. Replacing any amino acid with proline which has a bulky structure would result in disruption in the helix (Alias et al., 2010). Indeed, the S12P mutant does not show any interaction with liposomes (Figure 4.4A). This was confirmed with the fluorescent microscopy assay (Figure 4.5). Furthermore, a mutant, L7D in which a hydrophobic amino acid replaced with a negatively charged amino acid, was designed to abolish membrane interaction by interfering with the amphipathic helix. Indeed, L7D did not react to the presence of liposomes in the sucrose gradient (Figure 4.4 A) and did not deform them (Figure 4.5).

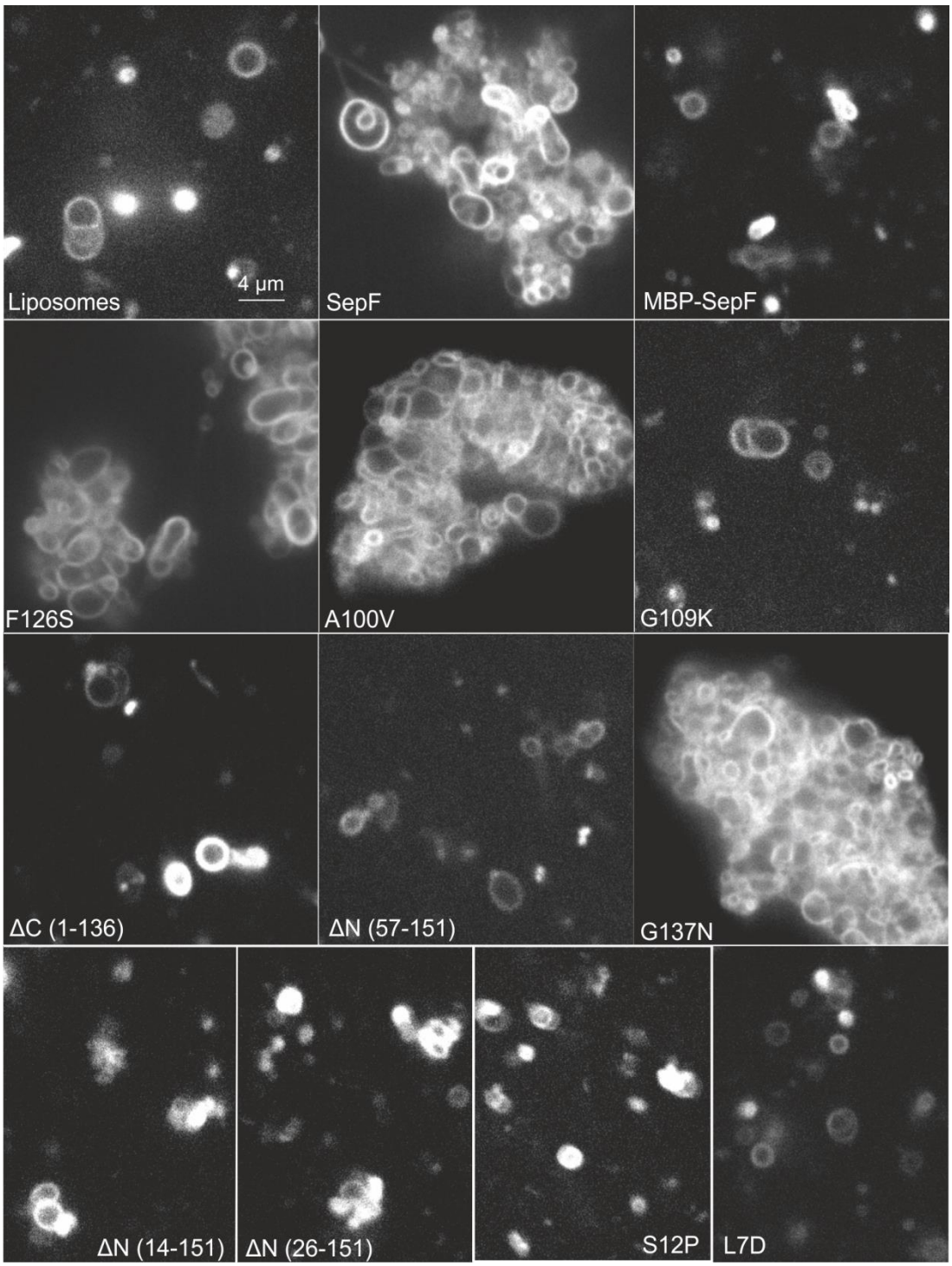

Figure 4.5 SepF and membrane binding mutants of SepF deforms the liposomes. Liposomes were stained with Bodipy FL C16.

4.6. Membrane Interaction is an Essential Characteristic of SepF (Strains used in this section were constructed by Henrik Strahl)

The *in vitro* experiments showed that FtsZ binding is not required for the membrane interaction of SepF while the N-terminus and polymerization of the protein are crucial. The first 12 residues of SepF are shown to be necessary for membrane binding. The next step was to show that the N-terminal end of SepF is able to interact with the cell membrane *in vivo*. For this purpose, *sepF(1-39)-gfp* and *sepF(1-75)-gfp* constructs were placed under control of the P_{xyl} promoter, and integrated at the *amyE* locus. Although SepF (1-25)-GFP showed very weak membrane interaction at septa, SepF (1-13)-GFP readily localized at the cell membrane (Figure 4.6A). It was possible that SepF (1-25)-GFP needed to be polymerized in order to interact with the membrane, so a leucine zipper, c-JunL was inserted between SepF (1-25) and GFP (Szeto et al., 2003). As expected, this construct localized at the cell periphery similar to SepF (1-13)-GFP (Figure 4.6A). As a negative control, SepF (1-13 L7D)-GFP was constructed. Figure 4.6A shows that this mutant is cytoplasmic, further supporting the fact that the amphipathic helix at the N-terminus of SepF is required for membrane interaction.

The next question was whether the membrane binding characteristic of SepF was essential for its function. As mentioned before, the deletion of *ftsA* and *sepF* is lethal and production of SepF from the *amyE* locus rescues the phenotype (Ishikawa et al., 2006). Using this knowledge, we constructed the N-terminal truncations of SepF under control of the P_{xyl} promoter in *amyE* locus. However, attempts to transform these strains with *ftsA* null mutant and *sepF* null mutant DNA were not successful, suggesting that membrane binding is necessary for the function of SepF. According to Ishikawa et al. (2006), overexpression of *sepF* compensates the FtsA mutant phenotype (Ishikawa et al., 2006). Since it was not possible to rescue *ftsA sepF* lethality with overproduction of the N-terminal truncations, they also should not compensate for the cell length phenotype of an *ftsA* null mutant. Figure 4.6B confirms this hypothesis. As can be seen in the figure, overproduction of wild type SepF restores the cell length of the *ftsA* null mutant, but overproduction of SepF (14-151) does not. Replacement studies in which the N-terminal end of SepF was exchanged with the amphipathic helix of MinD showed that overproduction of this chimera restores cell division in an *ftsA* null mutant (Figure 4.6B).

Moreover, the $MinD_{AH}$-SepF (14-151) chimera also compensated the lethality of the *sepF ftsA* double mutant in the presence of xylose (Figure 4.6C).

These experiments suggest that the first 13 residues of SepF are required for the membrane interaction which is essential for the function of SepF.

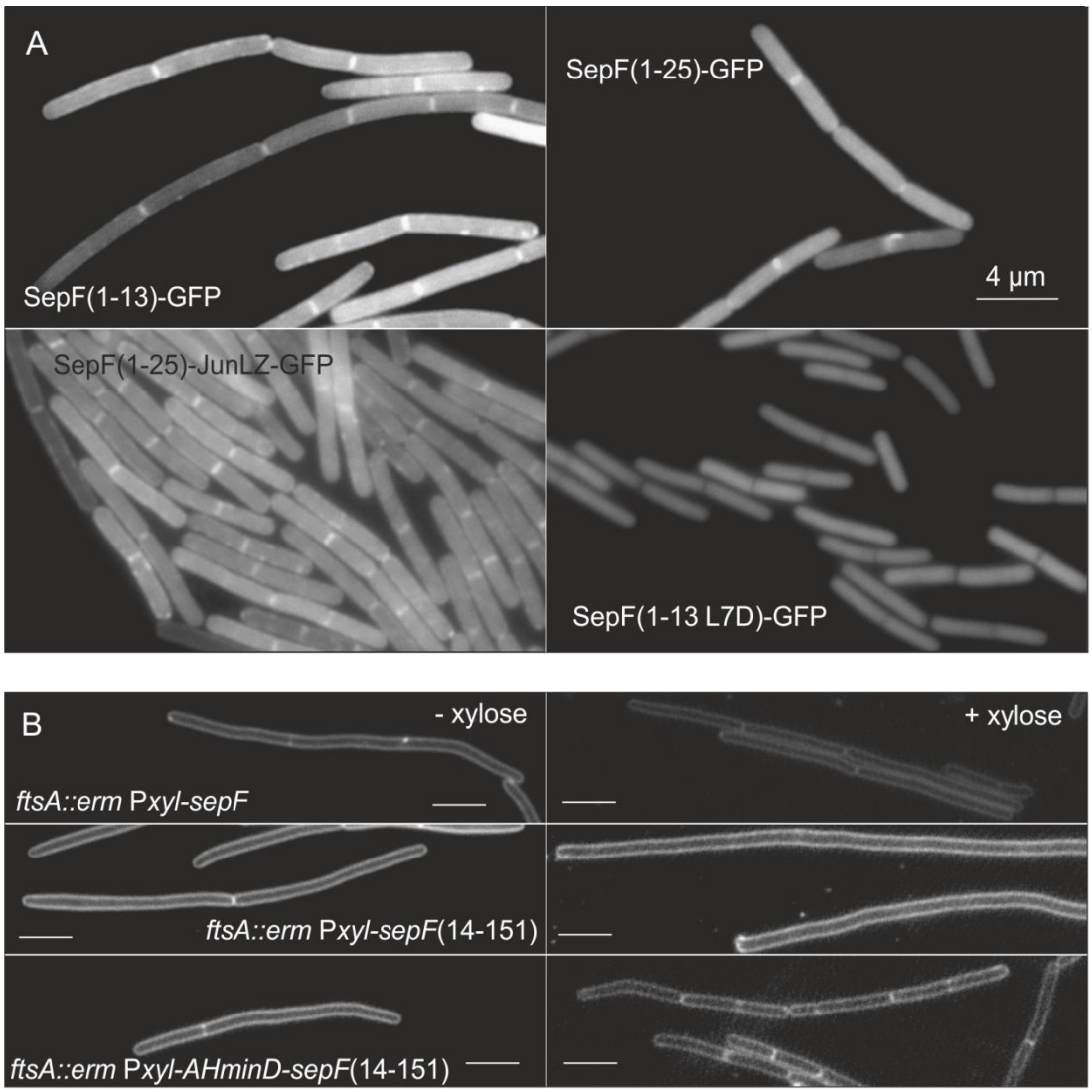

C

sepF::neo, ftsA::erm, P*xyl*-AH*(minD)-sepF*(14-151)

Figure 4.6 The N-terminus of SepF interacts with the membrane. (A) SepF(1-13)-GFP interacts with the membrane unlike SepF(1-13 L7D). SepF(1-25)-GFP interacts with the membrane when JunLZ inserted for polymerization. (B) Deletion of *ftsA* results in filamentous cells which are compensated by overproduction of wild type SepF. Deletion of the N-terminus of SepF results in non-functional protein which is overcome by the replacement with amphipathic helix of MinD. The scale bars show 4 µm (C) AH_{MinD}-SepF(14-151) compensates lethality of *ftsA sepF* double mutant (The strains were constructed by Henrik Strahl).

4.7. SepF is able to Recruit FtsZ to Liposomes

SepF binds FtsZ at the C-terminal domain and interacts with the cell membrane via the N-terminal amphipathic helix. The next question was whether SepF would interact with both at the same time and would tether FtsZ to the cell membrane. Using sucrose gradient centrifugation with FtsZ, SepF and liposomes, it was shown that SepF is indeed able to do this (Figure 4.7A). When loaded at the bottom of the sucrose gradient, FtsZ by itself or together with liposomes stayed at the bottom of the gradient. When incubated with SepF and liposomes, FtsZ was carried to the upper sucrose gradient levels by SepF and liposomes which was not the case for the FtsZ-binding mutant of SepF, F126S (Figure 4.7A). The same set up was repeated in the presence of GTP, because GTP is required for FtsZ polymerization (Mukherjee and Lutkenhaus, 1994). However, no significant change was observed compared to the incubation without GTP (Figure 4.7A). This suggests that GTP, therefore the efficient polymerization of FtsZ, is not required for FtsZ tethering to the membrane by SepF.

High speed centrifugation of FtsZ with SepF and liposomes was also tested to support that SepF tethers FtsZ to the cell membrane. FtsZ pelleted with SepF and liposomes with or without GTP (Figure 4.7B). However, FtsZ alone or with SepF also pelleted after centrifugation. Therefore, no conclusion could be drawn from this data.

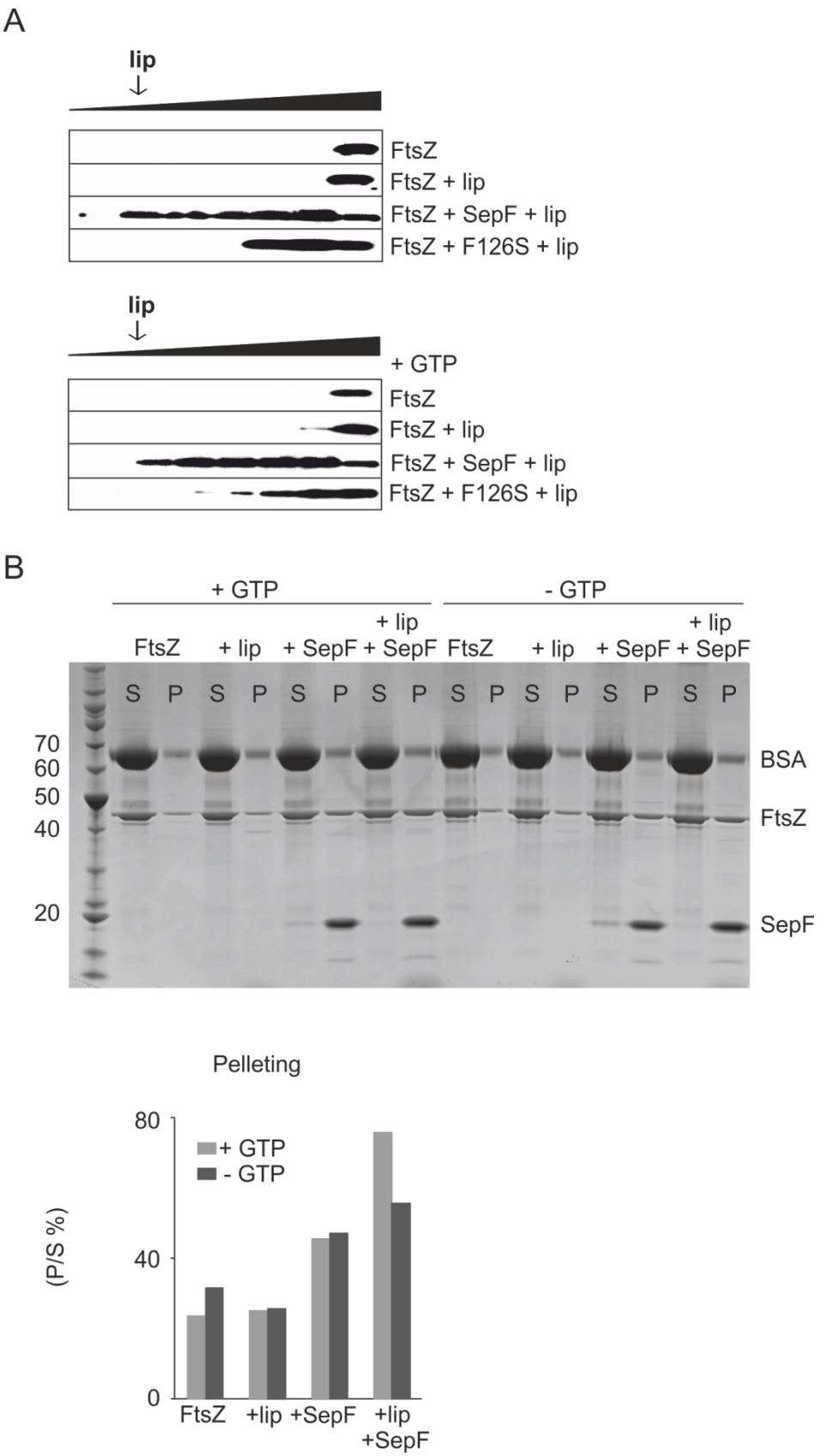

Figure 4.7 SepF tethers FtsZ to the cell membrane. (A) Western blotting of sucrose gradient centrifugation with FtsZ, SepF and liposomes. F126S is the SepF mutant that is deficient in FtsZ binding. (B) Pelleting of FtsZ with SepF and liposomes in the presence and absence of GTP. The gel was stained with Coomassie Blue G. Pelleting efficiencies were calculated by measuring the band intensities of FtsZ in pellet and supernatant.

4.8. Liposomes Bind to the Inside of the SepF ring

As has been shown above and by Gundogdu et al. (2011), SepF forms large rings that are clearly observed by TEM. Therefore, TEM was also used to observe the interaction between liposomes and SepF. Deformation of liposomes caused by SepF is seen in Figure 4.8B. Surprisingly, it was also possible to see SepF rings filled with liposomes (Figure 4.8C). Furthermore, the deformed liposomes visible in Figure 4.8B had a similar diameter as SepF rings. This data suggested that liposomes interact with the inside of the SepF ring.

FtsZ and SepF form large tubules *in vitro*, which can be observed with TEM (Gundogdu et al., 2011). The effect of liposomes on these tubules was examined by incubating FtsZ and SepF with liposomes and GTP. In the absence of liposomes, these tubules are very rare. However, huge structures of tubules were observed with liposomes (Figure 4.8D). Moreover, it was harder to observe liposomes on the grid in the presence of FtsZ and SepF compared to liposomes alone on the grid, supporting the notion that liposomes were inside the SepF rings, and possibly inside the SepF – FtsZ tubules. This also suggested that FtsZ binds to the outside of the rings.

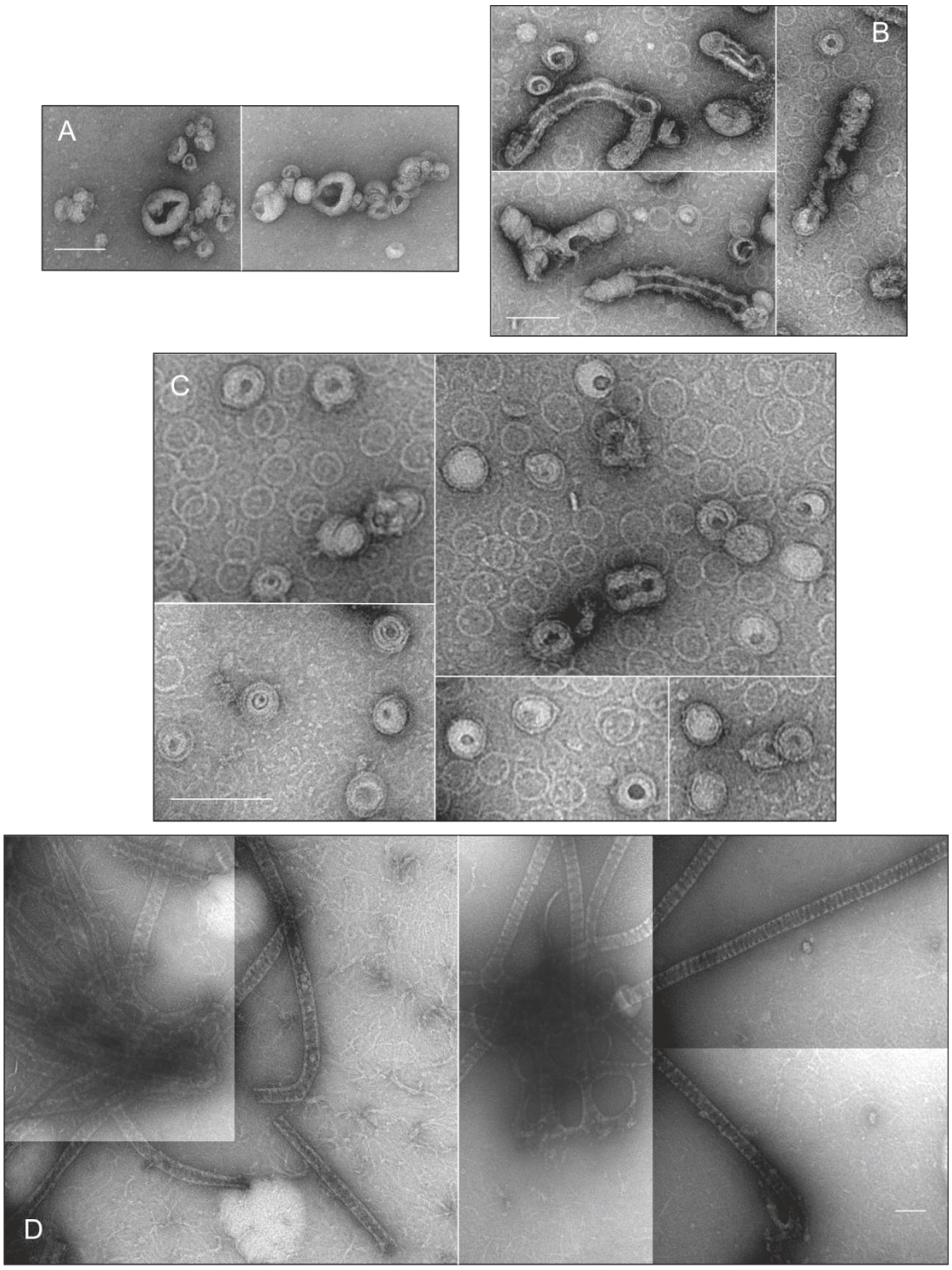

Figure 4.8 Transmission electron microscopy of liposomes (A) with SepF (B and C) and with SepF and FtsZ (D). The scale bars show 100 nm.

4.9. Could Liposomes Stabilize the SepF – FtsZ Tubules?

The large tubular networks of FtsZ and SepF observed in the presence of liposomes (Figure 4.8D) suggested that liposomes would stabilize and stimulate the interaction between SepF and FtsZ. However, it was not possible to quantify this increase with electron microscopy. Therefore, another assay was needed. It was also not possible to use the high speed centrifugation (pelleting) assay for this purpose due to the unspecific pelleting of FtsZ. There are lipids with biotin caps (Avanti) which would bind to magnetic streptavidin beads. Pulling those beads with a magnet should overcome the obstacles of the centrifugation experiments. Using the biotinylated liposomes, the interaction of SepF and FtsZ was studied. Unexpectedly, both SepF (Figure 4.9A) and FtsZ (Figure 4.9B) showed affinity to both biotin and streptavidin beads. Although, several conditions such as high BSA concentrations and salt concentrations were tested, this affinity could not be reduced. Hence, this assay could not be used to quantify the FtsZ – SepF interaction.

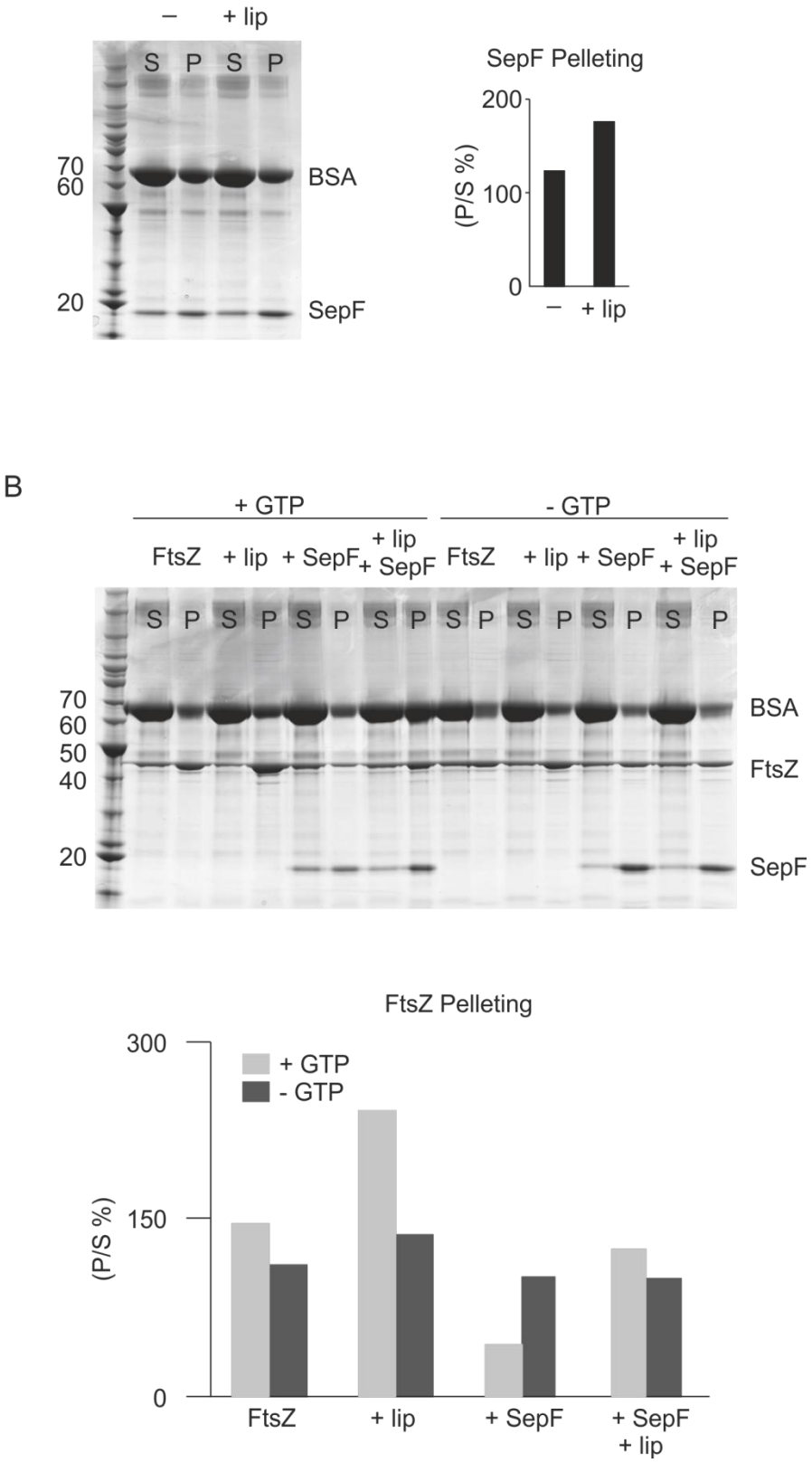

Figure 4.9 Interaction between biotinylated liposomes and SepF (A) and FtsZ and SepF (B). Pelleting was calculated using the band intensities of either SepF or FtsZ in pellet and supernatant. Pelleting term here represents the portion of protein that is pulled down with the streptavidin magnetic beads.

Discussion

This study shows that FtsZ binds to the C-terminal domain of SepF and that the N-terminal domain is not required for FtsZ binding. The FtsZ binding mutants, discovered via Y2H, located at both beta strands and alpha helices in the crystal structure, and did not reveal a clear a pocket-like structure that could accommodate the C-terminus of FtsZ (Figure 4.12).

In this work, several *in vitro* experiments were performed to test the membrane interaction of SepF. Purified SepF protein and SepF mutants were tested for activity with electron microscope. All mutants could form rings except the non-ring forming and non-polymerizing mutants. Also, each liposomes batch was tested with wild type SepF protein to test their behaviour. As mentioned above liposomes and SepF behave different in sucrose gradient assay when they mixed together. It was possible to observe liposomes with naked eye only when SepF was bound to liposomes. After centrifugation almost 20% of SepF was bound to the liposomes (Figure 4.4C). There could be a few reasons for this behaviour. First, interaction between SepF and liposomes may have reached to equilibrium. Second, although SepF forms rings, it is possible that some part of the protein is inactive. Finally, the interaction between SepF and liposomes may not be strong enough to carry all of SepF in the gradient and some of the protein may separate from the liposomes at lower fractions during centrifugation.

The SepF mutants were tested for liposome interaction with sucrose gradient assay and fluorescent microscopy. Some mutants such as ΔC (1-136) and MBP-SepF moved in the sucrose gradient when they were incubated with liposomes (Figure 4.4A). However, the liposomes were not visible after the centrifugation. Also, they could not deform the liposomes (Figure 4.5). Moreover, the mutants A100V and F126S moved in the gradient even without liposomes (Figure 4.4B), but they could deform the liposomes and the liposomes were visible after centrifugation. The results of sucrose gradient, the behaviour of liposomes in the gradient and fluorescent microscopy were used to conclude whether SepF mutants interact with liposomes or not.

SepF(1-13)-GFP and SepF(1-25)-JunLZ-GFP were shown to interact with cell membrane (Figure 4.6A). SepF(1-25)-GFP also show weak interaction with the cell membrane. It is highly likely that the increase of membrane interaction is due to polymerization of SepF(1-25)-JunLZ-GFP. However, it is

also possible that the JunLZ linker increased the distance between SepF(1-25) and GFP which affected the membrane binding of this mutant. In this experiment the expression of these chimera proteins were controlled with Western blotting (personal communication with Henrik Strahl).

In this work, the N-terminal end of SepF was shown to be necessary for membrane interaction using several different assays, both *in vivo* and *in vitro*. It was also shown that polymerization of SepF is important for membrane interaction. On the other hand, FtsZ interaction did not affect binding of SepF to the membrane. Closer analysis of the putative amphipathic helix of SepF showed that it forms a helical structure in the presence of liposomes (personal communication Henrik Strahl). This was detected with CD spectroscopy. The fact that SepF(1-13) formed random coils in the absence of liposomes and α-helices with liposomes confirms that the first 13 residues of SepF form a membrane binding amphipathic helix (Figure 4.10B). Moreover, SepF(1-13) was labelled with a FAM (5 – Carboxyfluorescein) group and mixed with GUVs (Giant Unilamellar Vesicles). Using spinning disk microscopy, localization of FAM-SepF(1-13) was shown to be periphery of liposomes (Figure 4.10C).

SepF was also shown to tether FtsZ to the cell membrane independent of GTP. Other assays such as high speed centrifugation or using biotinylated liposomes were tested to support this role of SepF. However, FtsZ is able to pellet by itself, probably due to polymerization of FtsZ, which resulted in inconclusive results. Moreover, the addition of BSA to the solution may have increased the polymerization of FtsZ due to crowding effect (Rivas et al., 2001, Zhou et al., 2008). Furthermore, we observed that sedimentation of FtsZ was not as efficient as observed in several other studies (Król and Scheffers, 2013). It is possible that the conditions we used in our experiments affected the pelleting, for instance the pH of our buffer (pH 7.5) was higher than the pH of the buffer (pH 6.5) generally used for FtsZ sedimentation assays. In addition to problems we had with pelleting of FtsZ, both SepF and FtsZ had affinity for streptavidin beads used with biotinylated liposomes. Even covering the beads with free biotin after the addition of liposomes did not decrease the nonspecific binding of the proteins.

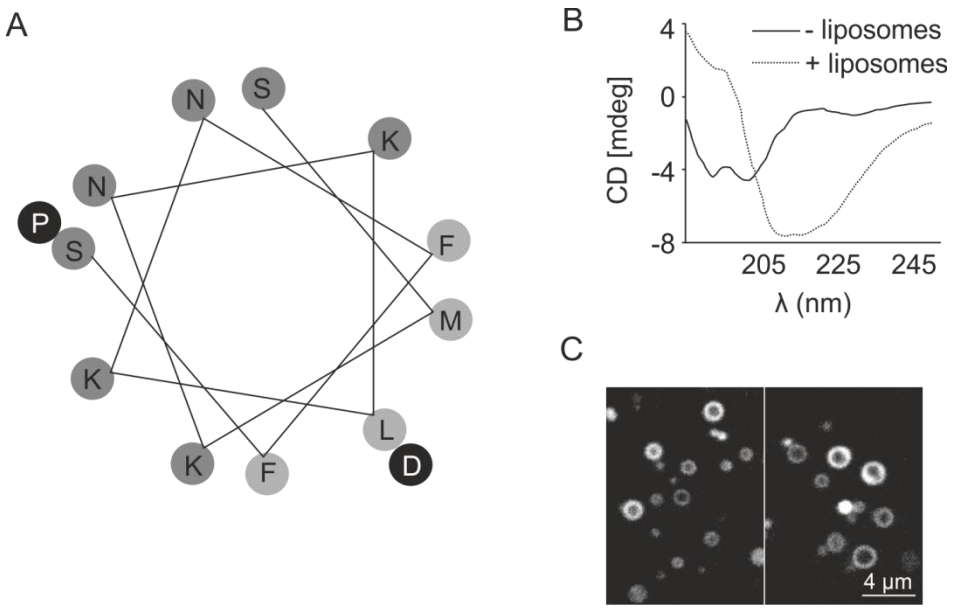

Figure 4.10 The first 12 residues of SepF form an amphipathic helix (by Henrik Strahl). (A) The helical wheel projection of the first 12 residues (SMKNKLKNFFS). Light grey circles show the hydrophobic amino acids. Black circles show the S12P and L7D mutants. (B) CD spectroscopy of SepF (1-13) peptide and liposomes. (C) FAM-SepF (1-13) peptide circles the liposome periphery. Scale bar shows 4 µm (The data was obtained by Henrik Strahl).

Both TEM images and fluorescent microscopy images showed that SepF deformed and clumped liposomes together. This is probably an effect of the amphipathic helix of SepF, since the amphipathic helices of MinD and FtsA were also shown to deform the liposomes (personal communication Henrik Strahl). Although the biological role of this characteristic of amphipathic helices is not understood, it is possible that the deformation of lipid bilayers would facilitate the separation of daughter cells. TEM images of SepF, FtsZ and liposomes suggested that the inside of SepF rings interact with liposomes while outside of SepF rings bind to FtsZ filaments. We attempted to observe this interaction with fluorescence microscopy. However, FtsZ interacted with the fluorescent dyes and we could not use this test to detect FtsZ-SepF-liposome tubules.

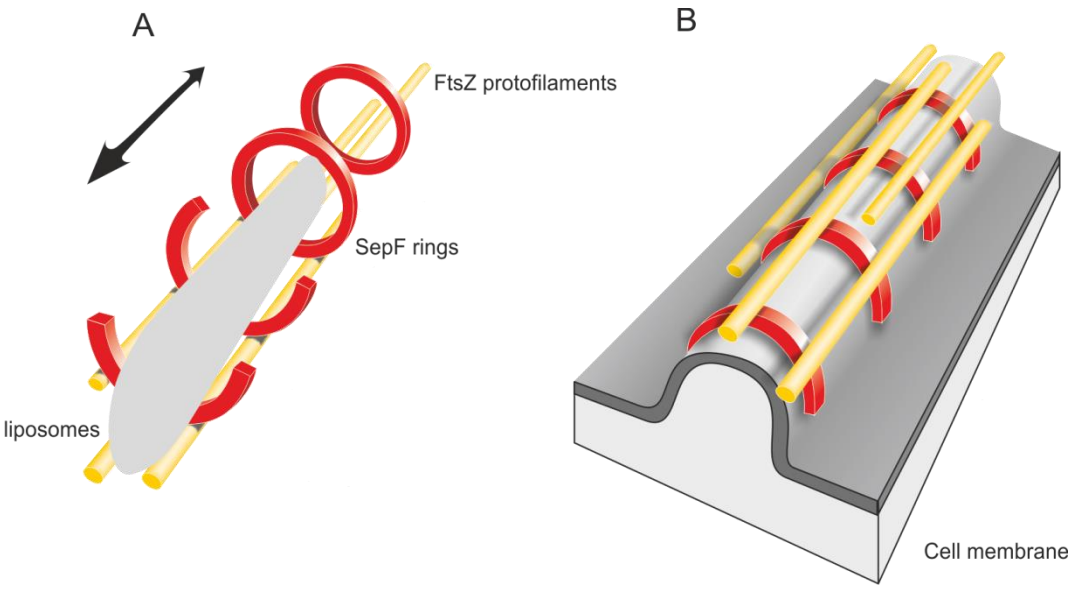

Figure 4.11 The model for the role of SepF *in vitro* (A) and *in vivo* (B)

The results obtained in this study resulted in a model for the role of SepF in cell division (Figure 4.11). In the presence of liposomes and FtsZ, SepF rings are filled with liposomes and covered by FtsZ filaments *in vitro*. This model was modified to elaborate the function of SepF in the cell. In the most likely case, SepF would form arcs instead of rings, so that it could interact with the membrane through the inside of the arc. Then, FtsZ filaments would surround this arc (Figure 4.11B). When mapped on the crystal structure of SepF, the FtsZ binding SepF mutants seemed to be located on the opposite side of the N-terminal domain of SepF (Figure 4.12). Moreover, the diameter of the SepF rings is about 50 nm (Gundogdu et al., 2011) which is only a little bit larger that the septa width in *B. subtilis* (Figure 4.13). Finally, the deletion of *sepF* results in thicker septal (Hamoen et al., 2006). These support the model summarised above.

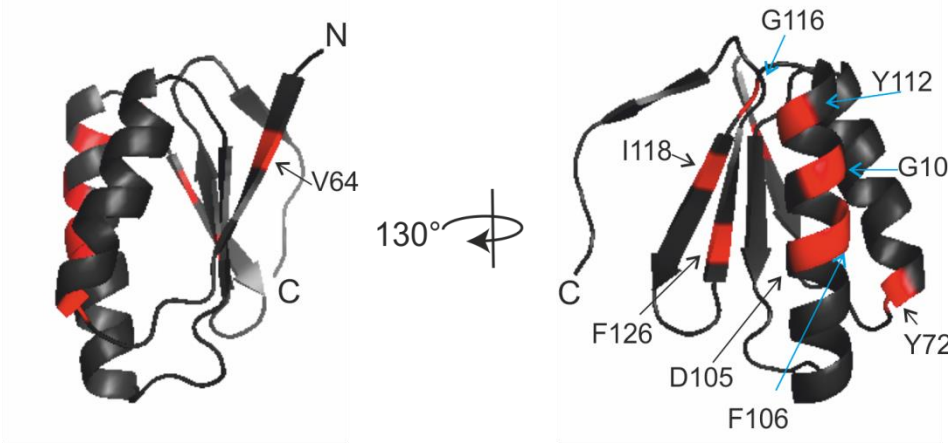

Figure 4.12 The SepF mutants identified at Chapter 4.1 are mapped on the crystal structure of the C-terminal domain of SepF.

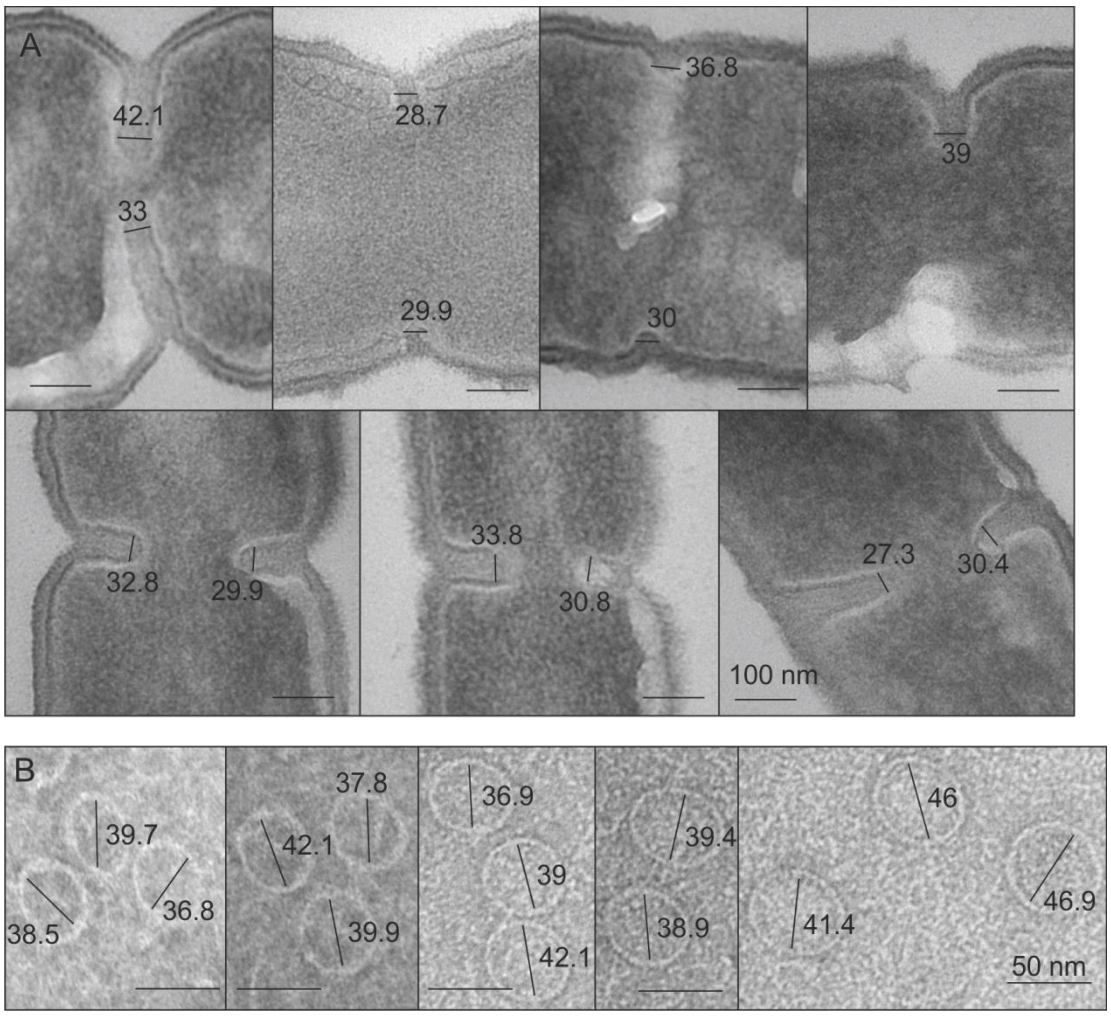

Figure 4.13 The transmission electron microscopy images of *B. subtilis* 168 (A) which has an average width of 32.65±4.3 nm septa and images of SepF rings (B) with an average diameter of 40.4±3.1 nm.

Future Work

In future studies, it would be necessary to locate the FtsZ binding pocket on SepF. The construction of more point mutants and truncations would give information to solve this problem. Moreover, crystallization of SepF with the C-terminal end of FtsZ might reveal the FtsZ binding pocket on SepF. The N-terminal amphipathic helix is required for the function of SepF, since the *sepF* mutants that miss the amphipathic helix did not compensate for the deletion of *ftsA* gene. Our model suggests that SepF arcs interacts with the cell membrane and tethers FtsZ filaments to it. Using the mutants that polymerize but are not able to form rings (Chapter 3, Discussion), this model could be tested. If SepF functions as arcs to control the width of septa, these mutants would result in abnormal septa.

It is suggested that liposomes stabilize and stimulate the SepF – FtsZ tubules. However, the nature of this interaction is not understood. The assays used here did not give quantitative data to speculate on this possibility. It would be important to design another assay that circumvents the nonspecific interactions of FtsZ and SepF that we encountered.

Chapter 5. *Bacillus* Minimal Divisome

In *B. subtilis*, a group of proteins called the divisome complex localizes at the division site. Localization occurs precisely at the middle of the cell and is controlled by several accessory proteins regulating this process either positively or negatively (Figure 5.1) (Adams and Errington, 2009). Although proteins such as FtsZ are essential in *B. subtilis*, there are several non-essential proteins that have a regulatory role or other functions in the divisome complex. In this study, the early non-essential divisome genes (*zapA*, *ezrA*, *sepF*, *ftsA*), and non-essential regulatory genes (*noc*, *minC*, *ugtP*, *minJ*, *clpX*) were removed using a method which resulted in markerless deletions. Our aim was to delete as many of those cell division related genes as possible, so that the minimum number of the proteins would be determined for cell division to occur. Knowledge of the 'minimal divisome' will help to understand what the key processes are in cell division. Here, it is shown that only FtsZ and SepF or only FtsZ, FtsA and EzrA are sufficient to achieve cell division in *B. subtilis*. One of the outcomes of this deletion study is the appearance of suppressor mutations which might reveal unknown division genes.

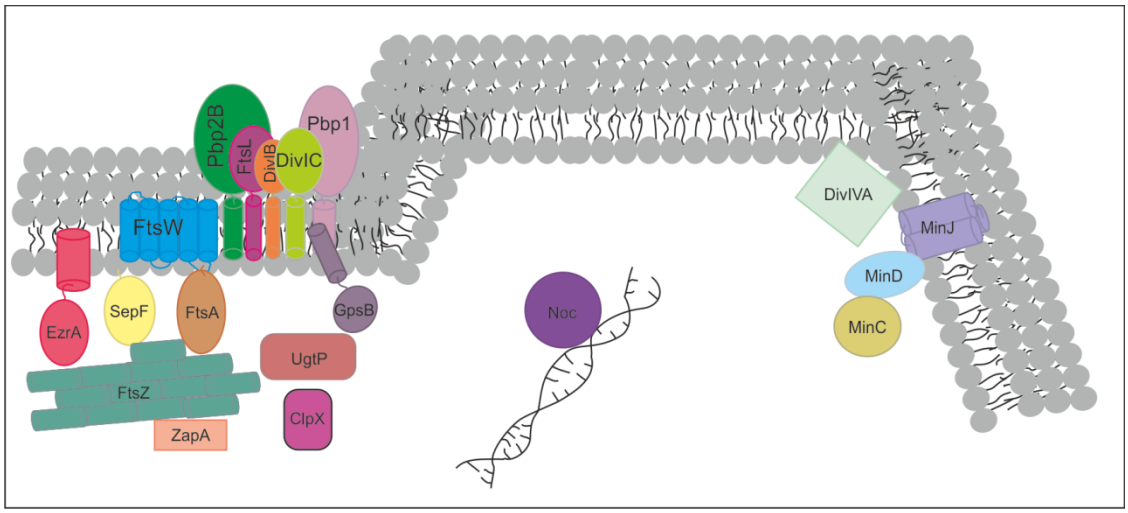

Figure 5.1 An overview of the cell division proteins in *B. subtilis*. Min system prevents cell division at the cell poles, while Noc protects the nucleoid. ZapA, SepF, and FtsA positively regulate Z-ring formation. The latter two and EzrA tether FtsZ to the cell membrane. The late divisome proteins are responsible for cell wall synthesis. ClpX and UgtP regulate FtsZ polymerization.

5.1. Construction of a Minimal Divisome

Morimoto et al. (2011) established a method to construct marker-free gene deletions in *B. subtilis* (Morimoto et al., 2011). This deletion method consists of two steps. The first step results in replacement of the gene of interest by means of homologous recombination with the spectinomycin marker and *mazF* gene under P_{spac} promoter. In the second step, *mazF*, which encodes the *E. coli* toxin MazF, is induced with IPTG (Aizenman et al., 1996). If a cell manages to remove the marker region via intramolecular homologous recombination, the cell would survive in the presence of IPTG, and the gene and the marker would be removed. This project made use of this technique to delete the non-essential Z-ring regulator proteins. However, it was not possible to use the marker-free deletion method for the *ezrA*/*noc* combination. In this case, the *ezrA* gene was deleted using a tetracycline marker.

As described above, the aim of this project was to delete as many of the cell division genes as possible. Studies so far showed that deletion of combinations of several cell division genes, such as *sepF/ezrA*, *zapA/ezrA*, *noc/minC*, *clpX/minC* (in *E. coli*) and *noc/ezrA*, causes synthetic lethality (Hamoen et al., 2006, Wu and Errington, 2004, Gueiros-Filho and Losick, 2002, Camberg et al., 2011). Surprisingly, it was possible to delete more than 8 genes simultaneously (Figure 5.2, Table 5.1). As a result of those deletions, the final strains were called F&A, F and AE mother strains (E, F, and A standing for EzrA, SepF, and FtsA, respectively). All three mother strains, except the AE mother strain, are missing *zapA* (Z), *minC* (C), *ugtP* (U), *minJ* (J), *ezrA* (E), *clpX* (X), and *noc* (N). The *spxA* (S) gene was deleted to ensure that cells maintain genetic competence after the *clpX* deletion (Nakano et al., 2001). The deletion of each gene was checked by PCR primer pairs outside and inside of the gene of interest (Figure 5.3 and Figure 5.4 respectively).

As Table 5.2 shows, both BMD14 and BMD15 are the F&A mother strains. Deletion of *ftsA* from BMD14 resulted in three different F mother strains which are called BMD25, BMD26, and BMD27. These strains were obtained after a search for a strain with all the required deletions using PCR and kept for further analysis. *sepF* and *noc* were deleted in the BMD9 strain using a single crossover deletion for *sepF* via Campbell integration (Vagner et al., 1998), resulting in strains BMD21 and BMD22. However, the *sepF* deletion in these strains was unstable since the mutation was made by Campbell integration

(single crossover). PCR tests showed that those strains still contain part of *sepF* that could support or interfere with division (Figure 5.4). Therefore, chromosomal DNA from a double crossover *sepF* deletion mutant was used. However, the removal of *sepF* from BMD14 restored the *ezrA* deletion in the mother strain. Hamoen et al. (2006) have shown that the *sepF ezrA* double knockout was not viable (Hamoen et al., 2006). Therefore, we accepted BMD28, BMD29 (spec marker) and BMD34 (neo marker) as AE mother strains which miss *sepF*, but contain *ezrA* and *ftsA* genes.

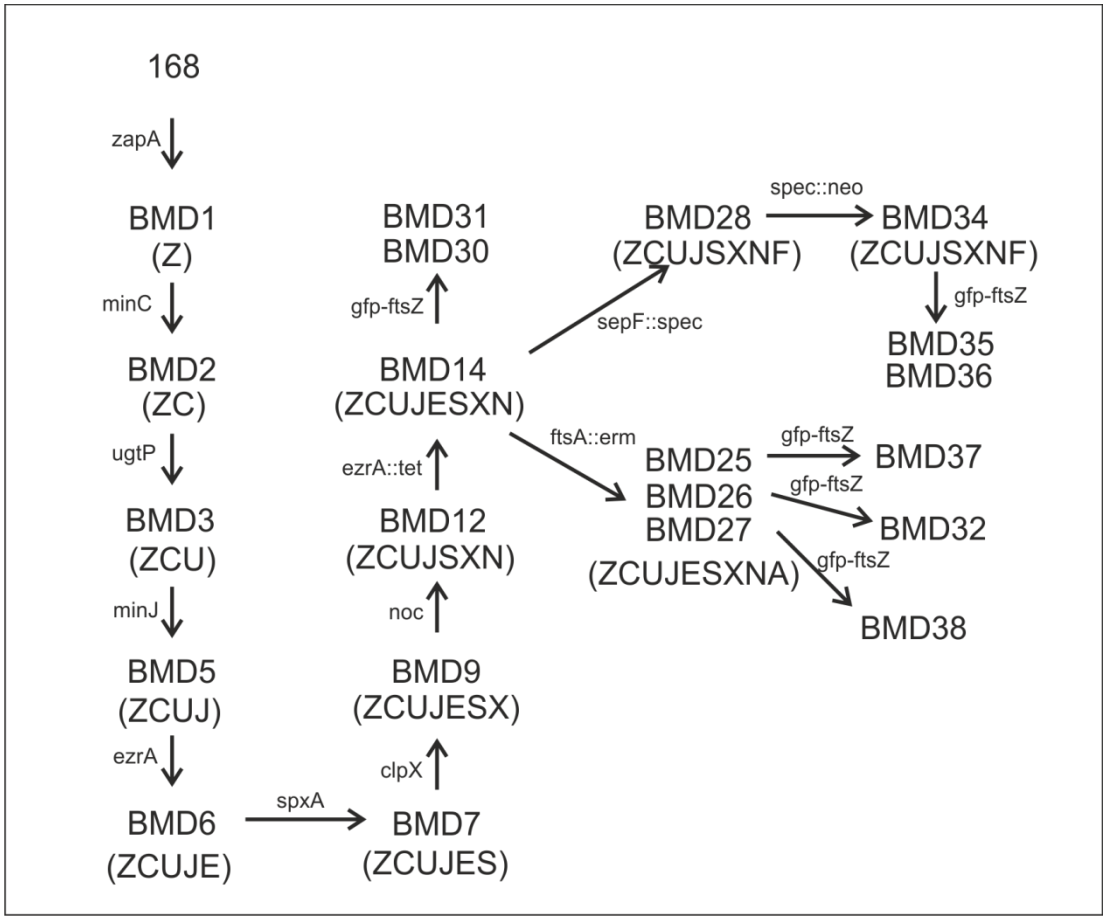

Figure 5.2 The path of the deletions for *Bacillus* Minimal Divisome. More than 8 genes are deleted in the mother strains. These are *zapA* (Z), *minC* (C), *ugtP* (U), *minJ* (J), *ezrA* (E), *spxA* (S), *clpX* (X), *noc* (N), *sepF* (F), and *ftsA* (A). BMD14 is the F&A mother strain which has only *ftsA* and *sepF*. BMD25, 26 and 27 are the F mother strains. BMD34 is the AE mother strain.

Name	Deletions
168	-
BMD1	Δ*zapA*
BMD2	Δ*zapA* Δ*minC*
BMD3	Δ*zapA* Δ*minC* Δ*ugtP*
BMD5	Δ*zapA* Δ*minC* Δ*ugtP* Δ*minJ*
BMD6	Δ*zapA* Δ*minC* Δ*ugtP* Δ*minJ* Δ*ezrA*
BMD7	Δ*zapA* Δ*minC* Δ*ugtP* Δ*minJ* Δ*ezrA* Δ*spxA*
BMD9	Δ*zapA* Δ*minC* Δ*ugtP* Δ*minJ* Δ*ezrA* Δ*spxA* Δ*clpX*
BMD12	Δ*zapA* Δ*minC* Δ*ugtP* Δ*minJ* Δ*spxA* Δ*clpX* Δ*noc*
BMD14	Δ*zapA* Δ*minC* Δ*ugtP* Δ*minJ* Δ*ezrA::tet* Δ*spxA* Δ*clpX* Δ*noc*
BMD25	Δ*zapA* Δ*minC* Δ*ugtP* Δ*minJ* Δ*ezrA::tet* Δ*spxA* Δ*clpX* Δ*noc* Δ*ftsA::erm*
BMD26	Δ*zapA* Δ*minC* Δ*ugtP* Δ*minJ* Δ*ezrA::tet* Δ*spxA* Δ*clpX* Δ*noc* Δ*ftsA::erm*
BMD27	Δ*zapA* Δ*minC* Δ*ugtP* Δ*minJ* Δ*ezrA::tet* Δ*spxA* Δ*clpX* Δ*noc* Δ*ftsA::erm*
BMD34	Δ*zapA* Δ*minC* Δ*ugtP* Δ*minJ* Δ*spxA* Δ*clpX* Δ*noc* Δ*sepF::neo*
BMD33	168 P_{xyl} *gfp-ftsZ*
BMD30	BMD14 P_{xyl} *gfp-ftsZ*
BMD31	BMD14 P_{xyl} *gfp-ftsZ*
BMD35	BMD34 P_{xyl} *gfp-ftsZ*
BMD36	BMD34 P_{xyl} *gfp-ftsZ*
BMD32	BMD26 P_{xyl} *gfp-ftsZ*
BMD37	BMD25 P_{xyl} *gfp-ftsZ*
BMD38	BMD27 P_{xyl} *gfp-ftsZ*

Table 5.1 List of BMD strains used in this work. BMD14 is the F&A mother strain. BMD25, 26 and 27 are the F mother strains. BMD34 is the AE mother strain.

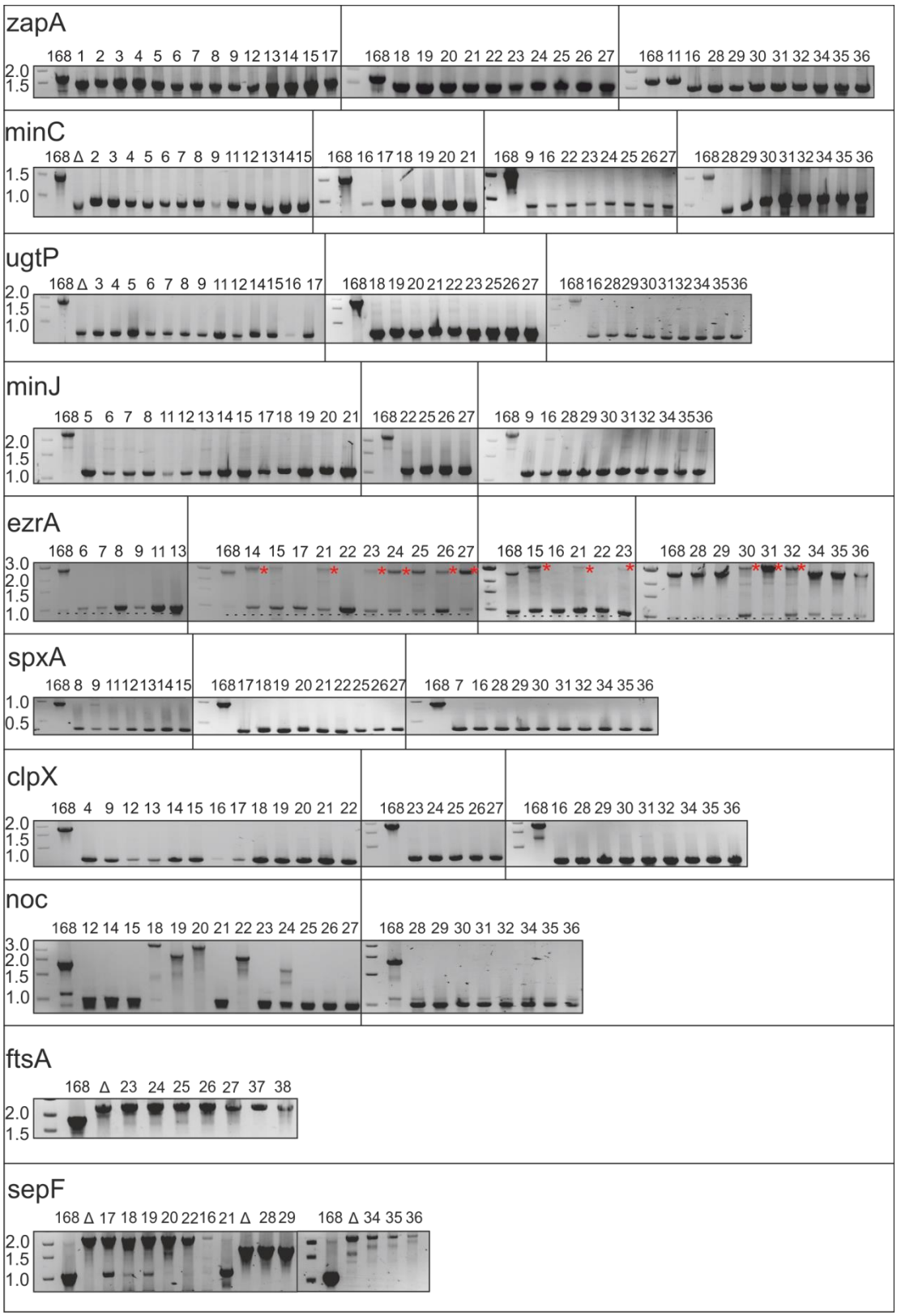

Figure 5.3 Control PCRs using primers from outside of the genes. In case of *ezrA*, *noc*, *sepF* and *ftsA*, the deletions were done using markers. Δ symbol was used to indicate single deletions. 168-lane shows the result of wild type gene. Numbers represent the BMD strains. The dotted lines on the *ezrA* section indicates the unspecific product of PCR, while the red star shows the *ezrA::tet* deletion.

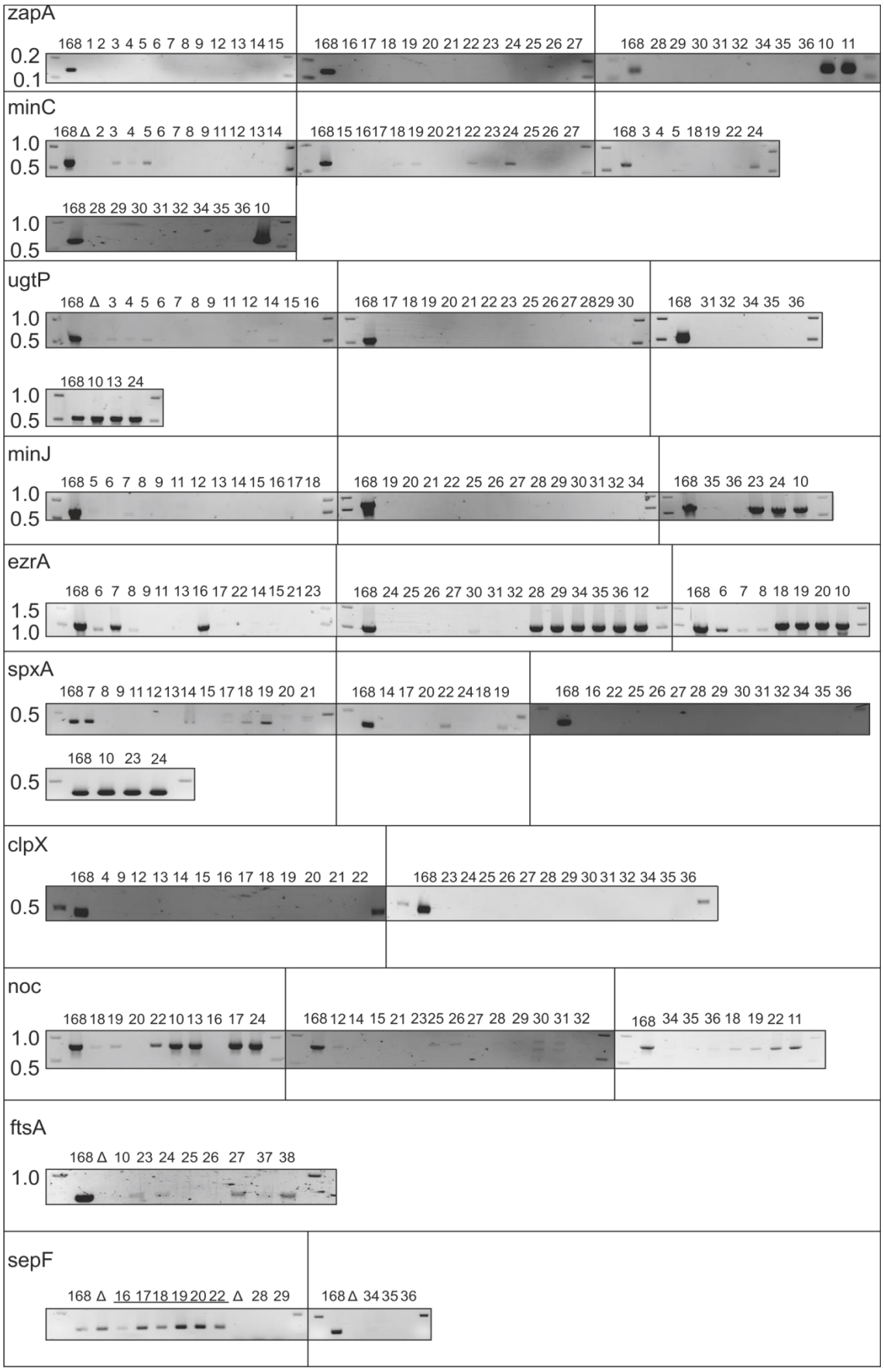

Figure 5.4 Control PCRs with primers from inside of the genes. Δ symbol was used to indicate single deletions. 168-lane shows the result of wild type gene. The strains that contain the unstable *sepF* deletion were underlined in sepF PCR section. Numbers represent the BMD strains.

	zapA	minC	ugtP	minJ	ezrA	spxA	clpX	noc	ftsA	sepF	divIB	gpsB	Pxyl gfp-ftsZ
BMD1													
BMD2													
BMD3													
BMD4													
BMD5													
BMD6													
BMD7													
BMD8													
BMD9													
BMD10													
BMD11													
BMD12													
BMD13													
BMD14					tet								
BMD15					tet								
BMD16										erm			
BMD17										erm			
BMD18								tet		erm			
BMD19								spec		erm			
BMD20								tet		erm			
BMD21					tet					erm			
BMD22								cm		erm			
BMD23					tet				erm				
BMD24					tet				erm				
BMD25					tet				erm				
BMD26					tet				erm				
BMD27					tet				erm				
BMD28										spec			
BMD29										spec			
BMD30					tet								spec
BMD31					tet								spec
BMD32					tet								spec
BMD33													spec
BMD34										neo			
BMD35										neo			spec
BMD36										neo			spec
BMD37					tet				erm				spec
BMD38					tet				erm				spec

Table 5.2 List of strains constructed for *Bacillus* Minimal Divisome project. The dark grey shows marker-free deletions and light grey shows deletions with markers. Tetracycline (tet), neomycin (neo), chloramphenicol (cm), spectinomycin (spec), and erythromycin (erm) markers were used.

In this study, about 40 strains were constructed. However, this work only focuses on the mother strains and their construction. Table 5.3 and Figure 5.2 show the ultimate path to the key minimal divisome mother strains.

	zapA	minC	ugtP	minJ	ezrA	spxA	clpX	noc	ftsA	sepF
168										
BMD1										
BMD2										
BMD3										
BMD5										
BMD6										
BMD7										
BMD9										
BMD12										
BMD14					tet					
BMD25					tet				erm	
BMD26					tet				erm	
BMD27					tet				erm	
BMD34										neo

Table 5.3 The path to the mother strains. The grey areas show the marker-free deletions unless the marker is written. Tetracycline (tet), erythromycin (erm) and neomycin (neo) markers were used. BMD14 is the F&A mother strain. BMD25, 26, and 27 are the F mother strains. BMD34 is the AE mother strain.

5.2. Conformation of the Deletions in F&A and F Mother Strains

Several studies have indicated different synthetic lethal deletion combinations of divisome genes, including *noc/minC*, *zapA/ezrA*, *clpX/minC* (in *E. coli*) and *noc/ezrA* (Wu and Errington, 2004, Gueiros-Filho and Losick, 2002, Camberg et al., 2011, Kawai and Ogasawara, 2006). However, in this study all these combinations turned out to be viable, most likely because of suppression as a result of deletions of other genes. To be absolutely sure that the deleted genes were removed from genomes we also used Southern blotting. In this assay, a specific probe for each gene was selected. Since the *zapA* gene is very small (258 bp), a larger probe was used. Figure 5.5A summarizes Southern blotting results and shows all deletions in the F&A mother (BMD14) and the F mother strains (BMD25, 26 and 27). The last lane in the Figure 5.5A shows the blotting against FtsZ sequence. It was used as a positive control for the test and as an indication for equally loading the lanes. However, for BMD25 and BMD26, FtsZ bands were very weak. Although the gel pictures before the transfer showed comparable amount of DNA (Figure 5.5B), the reason of these weak bands was not understood. Nevertheless, the results obtained with Southern blotting and PCR tests clearly show that the deletion of more than 8 cell division related genes was possible. The F&A mother strain (BMD14) lacks *zapA*, *minC*, *ugtP*, *minJ*, *ezrA*, *spxA*, *clpX*, and *noc*. The F mother strains (BMD25, 26 and 27) lack all these eight genes and *ftsA*. Finally the deletions of AE mother strain (BMD34) consist of *zapA*, *minC*, *ugtP*, *minJ*, *spxA*, *clpX*, and *noc* with *sepF*.

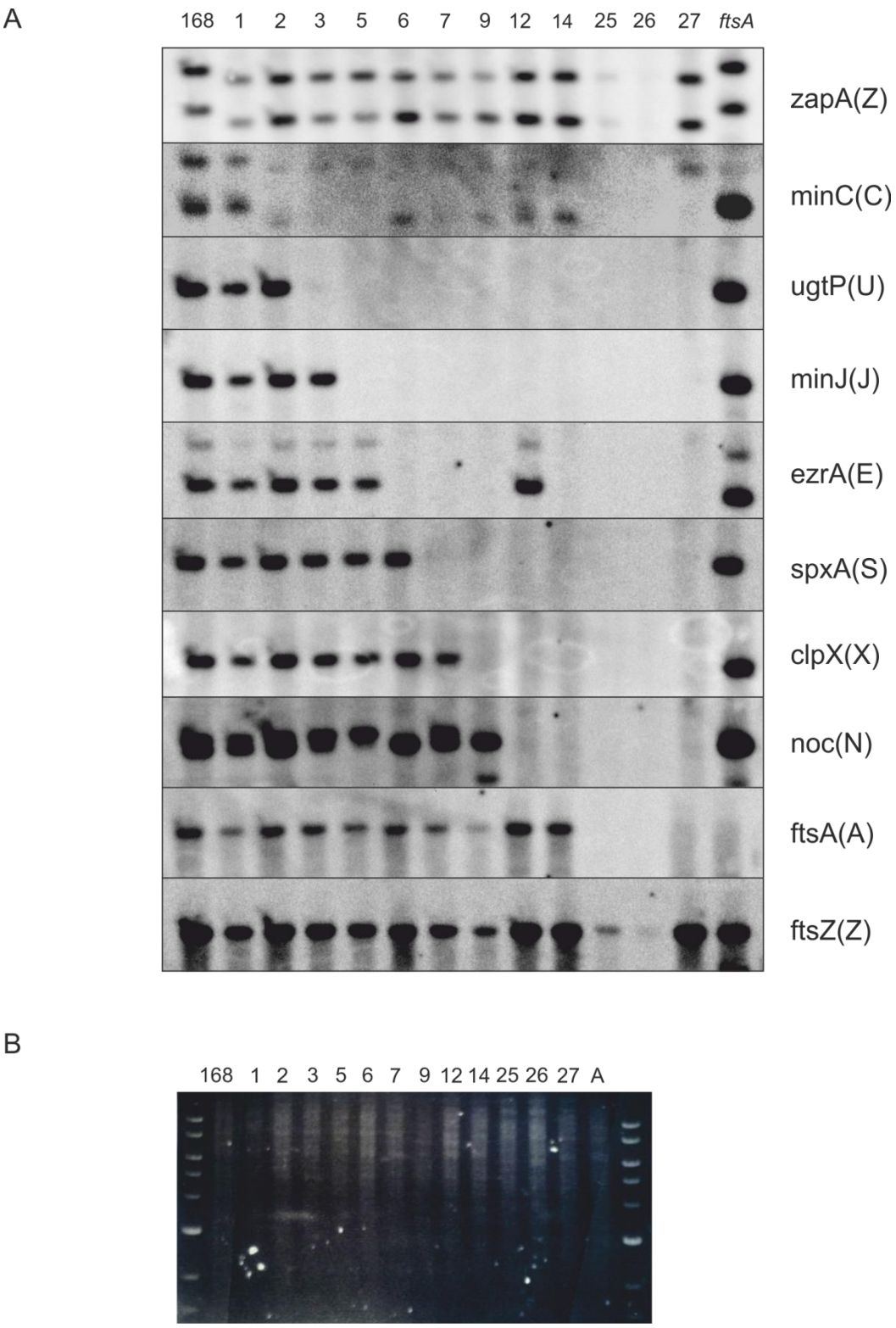

Figure 5.5 Southern blotting of Minimal Divisome strains. If the gene is present it gives a signal in the presence of the probe. In case of *zapA*, the deletions are shown with the size difference. FtsZ was a positive control (A). Agarose gel image before DNA was transferred to the membrane (B).

5.3. Sensitivity to Environmental Conditions

It was rather surprising that we were able to delete so many cell division related genes and still have viable strains. However, the resulting mother strains grew considerably slower than the wild type strain. To determine which deletion step affected viability several growth conditions were tested. A recent study showed that the lipid composition of the cell membrane of *B. subtilis* and other bacteria changes with the media they grow in (Shu et al., 2012). Most of the BMD strains contain the *ugtP* deletion, which would affect the lipid composition of the cell membrane (Jorasch et al., 1998). Therefore, first, the growth on LB and nutrient agar plates were compared (Figure 5.6). Most BMD strains produced larger and smoother colonies on LB agar than nutrient agar. Many of the strains lyse easily and do not sporulate, which is easily observed on plates grown for three days, and therefore lack the dense and brownish appearance of the wild type strain. Interestingly, the *ugtP* deletion was not responsible for the growth difference between nutrient agar and LB plates. On the other hand, the *clpX* deletion alone and the BMD strains without *clpX* gene appear to grow slower than the other strains. It is known that ClpX affects several cellular functions as it is part of the ClpXP chaperone. The F&A mother strain (BMD14) and F mother strains (BMD25, 26 and 27) clearly grow slower compared to the other strains. The AE mother strain (BMD34) did not appear to be as sick as the F&A and F mother strains. Since the strains grow better on LB agar plates, this medium was used for other experiments.

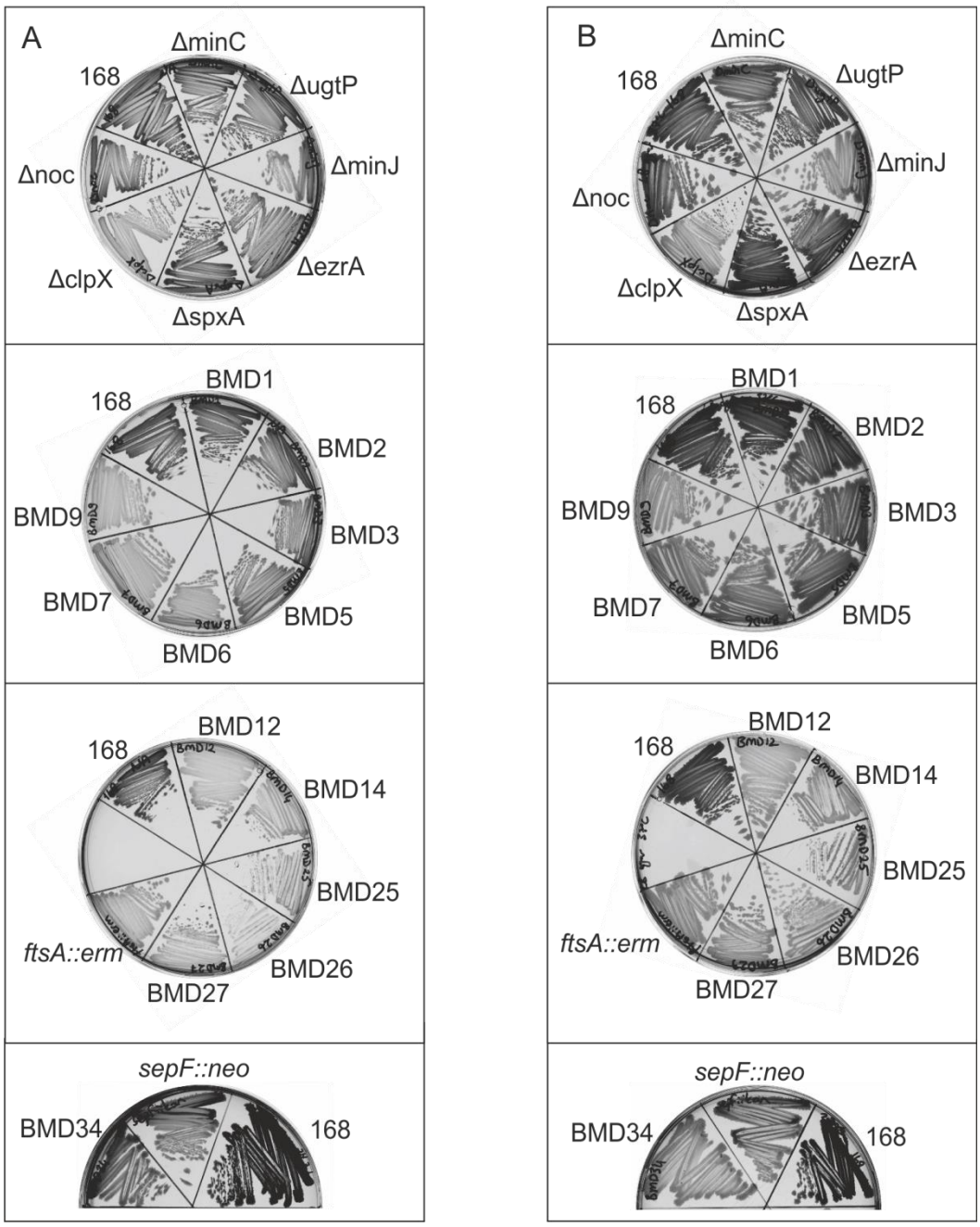

Figure 5.6 Growth of the BMD strains on nutrient agar (A) and LB agar (B)

5.3.1. Effect of temperature, pH and salt concentration

Different growth conditions were tested to examine how sensitive the BMD strains are for environmental stress. Firstly, the effects of low and high growth temperatures were tested by growing the strains at 30°C, 37°C, and 48°C on LB agar (Figure 5.7). Growth of the BMD strains at 48°C decreased as the number of deletions increased. Also, BMD25, BMD26 and BMD27, which are the F mother strains, grew less than other strains at 30°C. Furthermore, the strains that contain the *clpX* deletion grew less than the others at all temperatures tested. Next, the growth was tested with changing acidity of LB agar (Figure 5.8). All the BMD strains grew at neutral pH. When the pH was lowered, BMD14, the F&A mother strain, and BMD27, the F mother strain, formed smaller colonies. If the pH was increased, it was possible to observe that BMD26 grew better than BMD25 and BMD27. Finally, the strains were grown on LB agar without any NaCl and with 0.5 M and 0.75 M NaCl (Figure 5.9). Surprisingly, BMD25 and BMD26 were extremely sick on LB agar without NaCl. These strains needed certain amount of salt to grow. Also, BMD25 was affected at 0.75 M NaCl.

Not surprisingly the F&A and F mother strains were more susceptible environmental stresses. However, the AE mother strain (BMD34) did not show a clear deficiency of growth in any of the conditions tested, except that it grew less at 48°C. Interestingly, the different behaviours of the F mother strains indicated that they might contain different suppressor mutations.

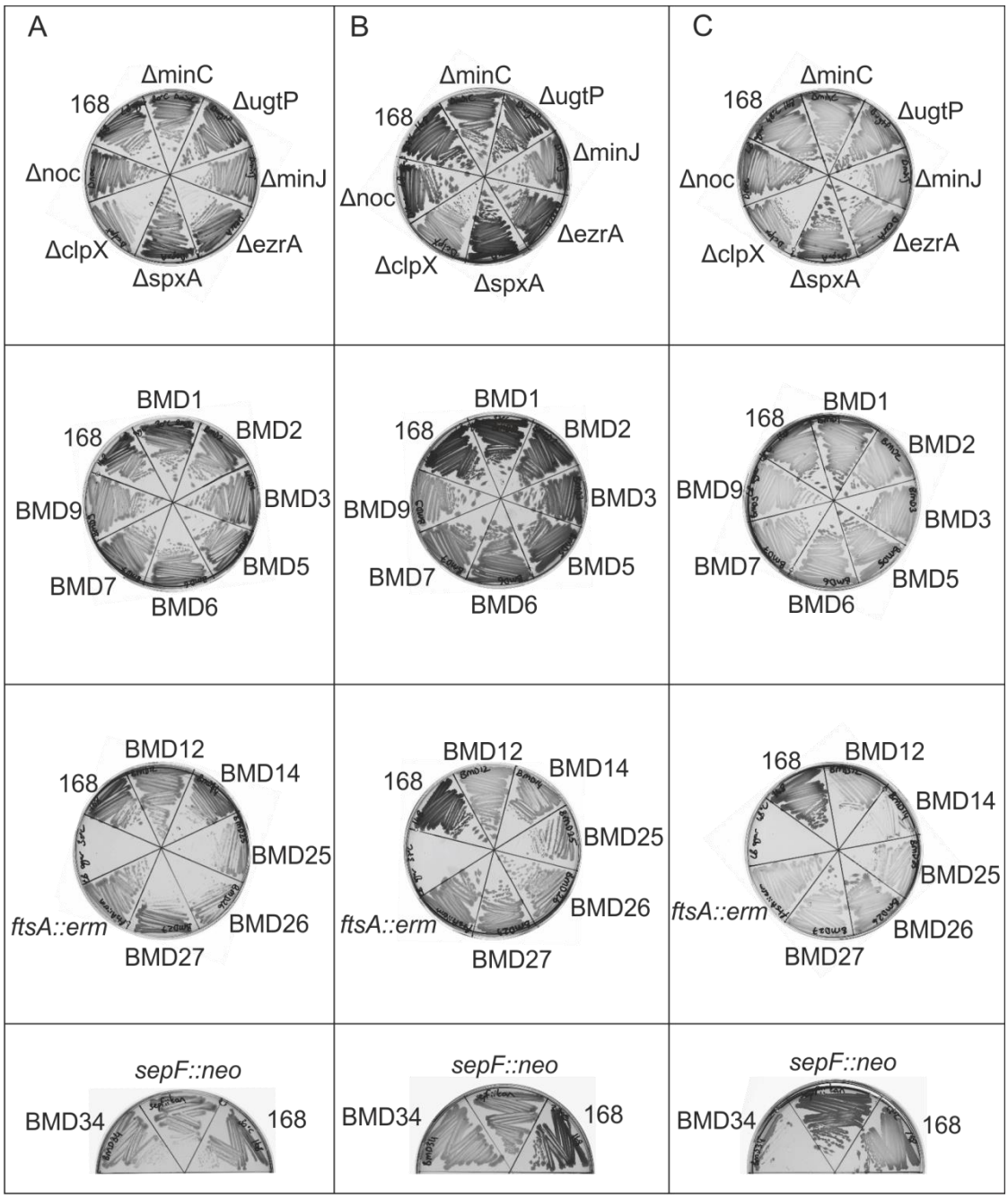

Figure 5.7 Effect of temperature changes on BMD strains (A) 30°C, (B) 37°C, (C) 48°C.

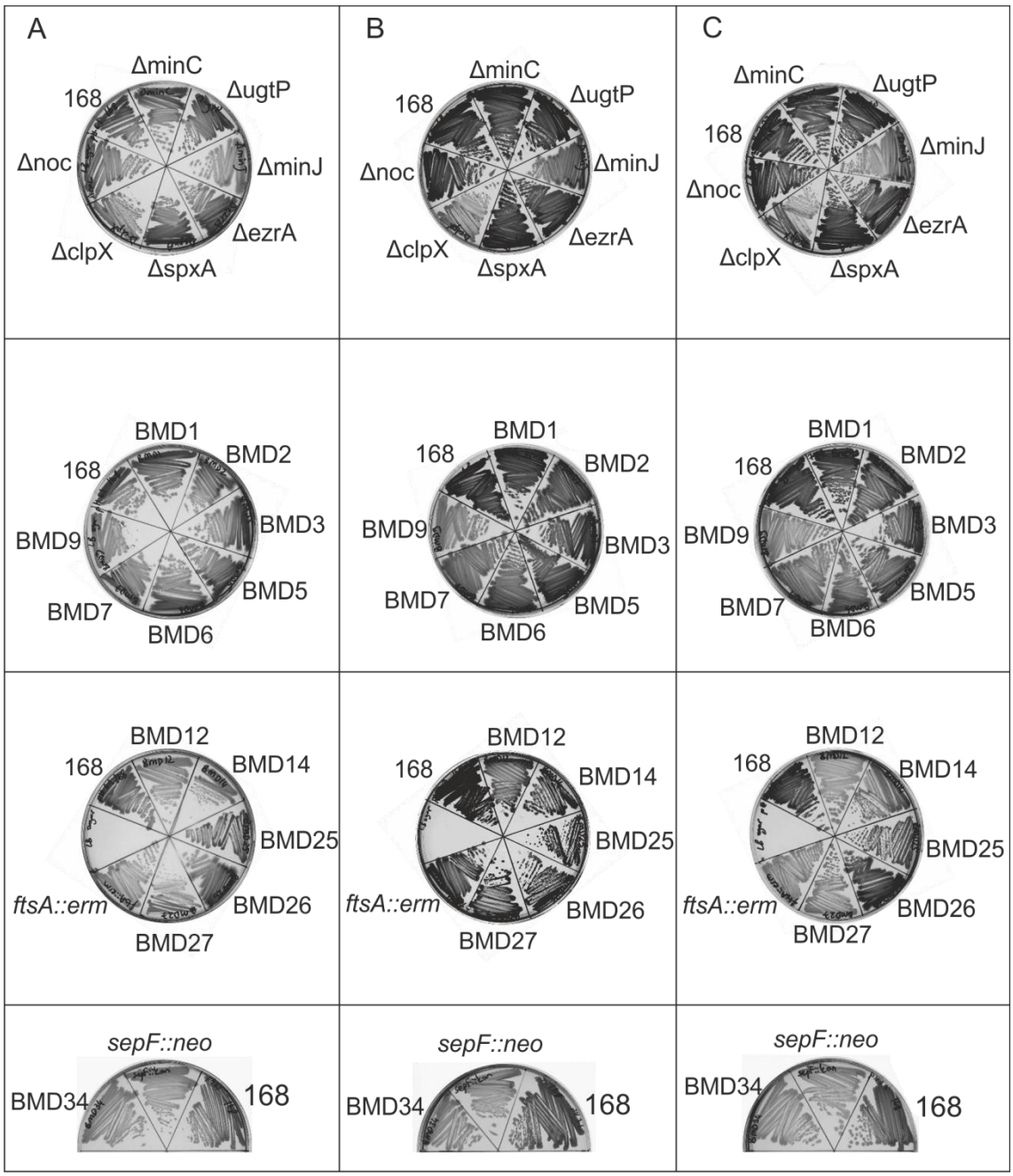

Figure 5.8 Effect of pH changes on BMD strains (A) pH 6.1, (B) pH 7.1, (C) pH 7.7.

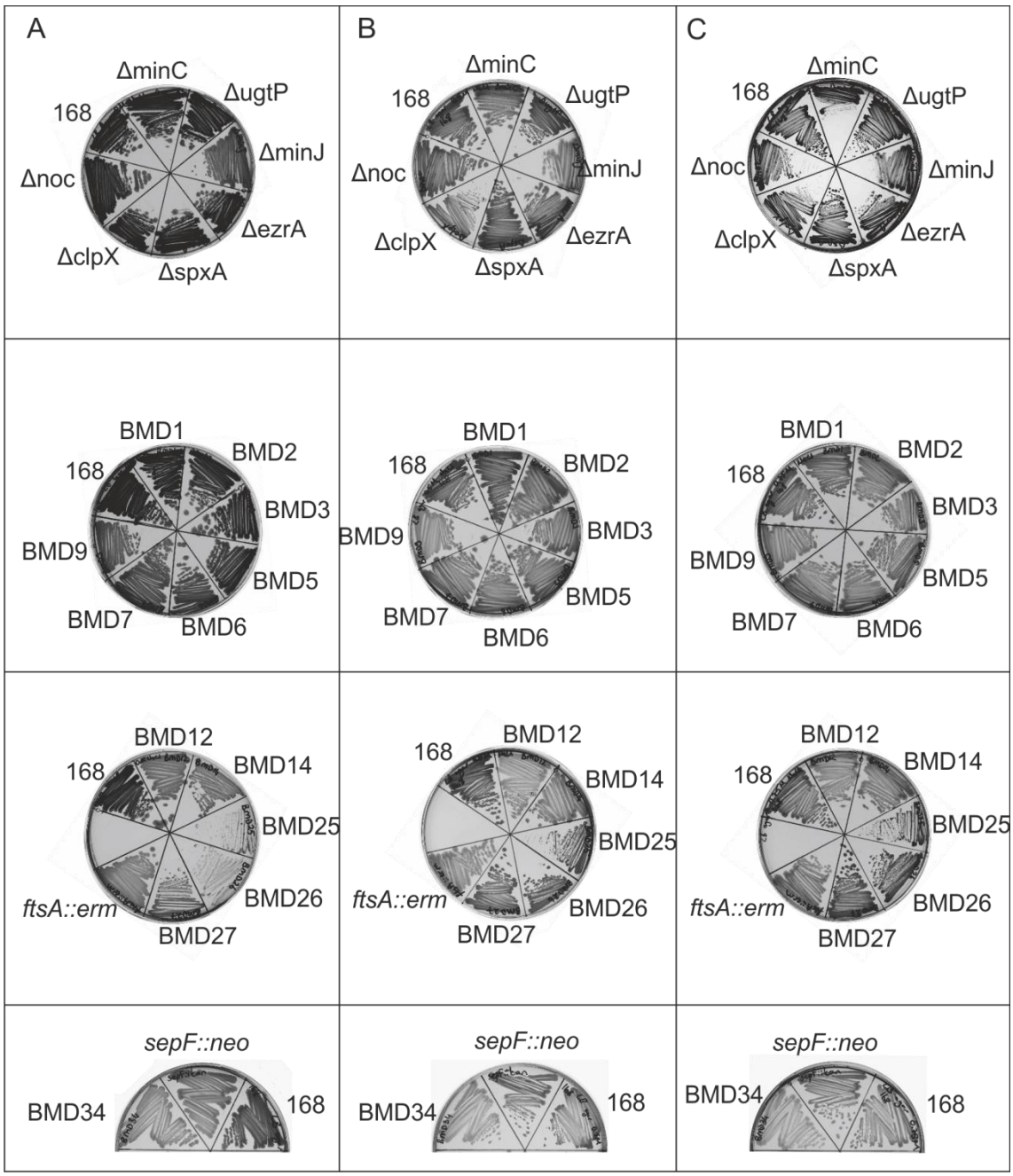

Figure 5.9 Effect of salt changes on BMD strains (A) 0 M, (B) 0.5 M, (C) 0.75 M NaCl

5.3.2. Effect of magnesium, glucose and malate

It is known that the addition of magnesium compensates for the bended and filamentous cell phenotype of *ponA* mutants (Murray et al., 1998). As shown in Figure 5.10A, the addition of Mg^{2+} (10 mM) to the medium did indeed improve growth of the BMD strains (compared to Figure 5.6B). Therefore, magnesium (10 mM) was added to the media to improve the growth of BMD strains during the studies. We noticed that the addition of glucose (0.5%) with magnesium (10 mM) improved growth considerably (Figure 5.10B); therefore glucose (0.5%) was added to the medium. In a recent study, it has been shown that the addition of malate (0.5%) with glucose (0.5%) to the media increased the growth of strains with inactive glycolytic genes (Commichau et al., 2013). To observe whether malate has an effect on the BMD strains, they were grown on plates with magnesium (10 mM) and malate (0.5%) with or without glucose (0.5%). The strains grew slower with only malate (0.5%) and magnesium (10 mM) added (Figure 5.10C). However, adding both malate (0.5%) and glucose (0.5%) together with magnesium (10 mM) had a clear improvement on the growth (Figure 5.10D). These data suggest that BMD strains may have difficulties maintaining balanced glycolytic activities.

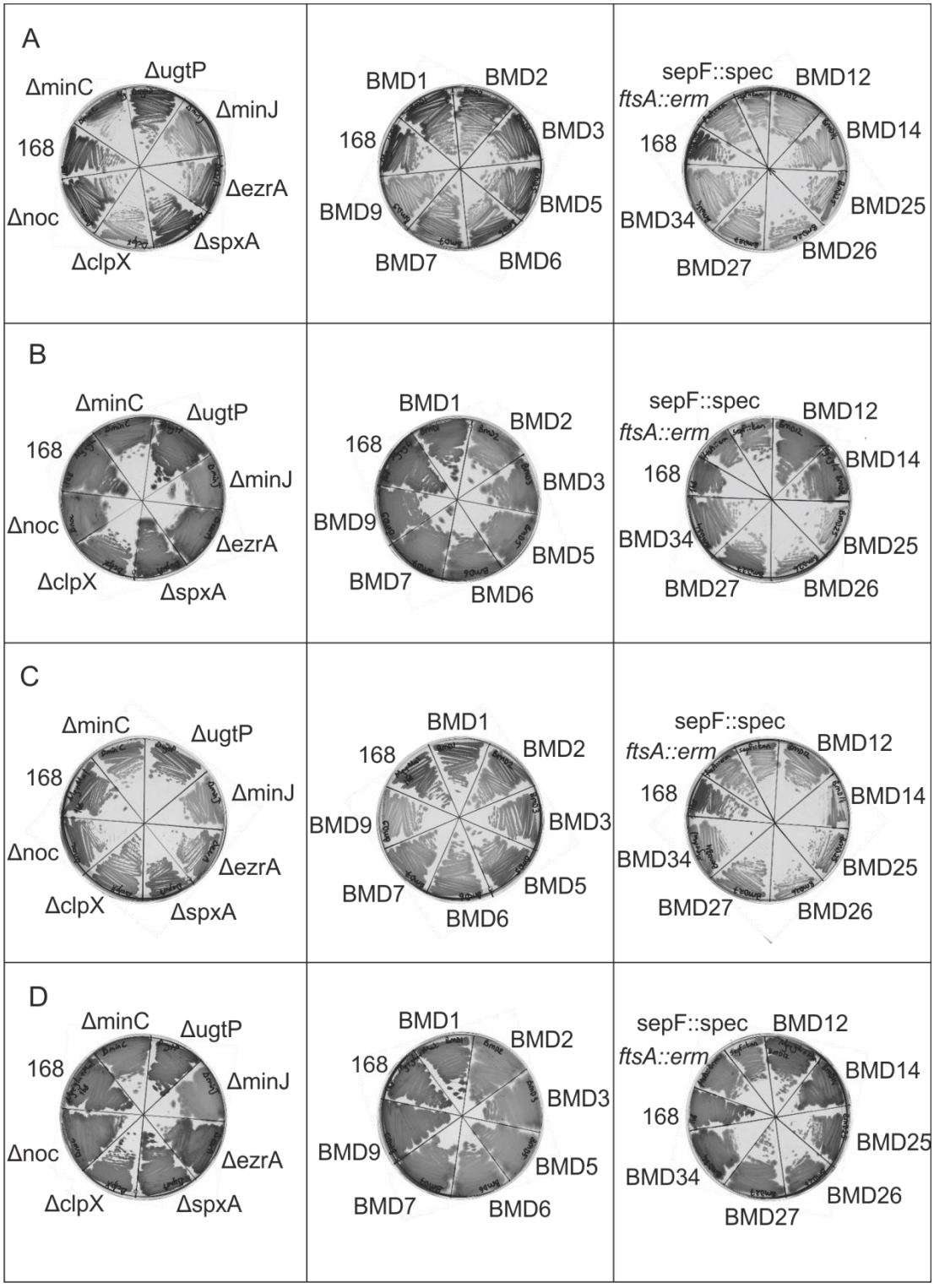

Figure 5.10 Effect of Glucose and Malate on BMDs in the presence of Magnesium. (A) LB agar with Magnesium (10 mM) (B) LB agar with Magnesium (10 mM) and Glucose (0.5%) (C) LB agar with Magnesium (10 mM) and Malate (0.5%) (D) LB agar with Magnesium (10 mM) Glucose (0.5%) and Malate (0.5%).

5.4. Growth Rates in LB with Magnesium (10 mM) and Glucose (1%)

The growth of the Minimal Divisome mutants was also followed in LB with Mg^{2+} (10 mM) and glucose (1%) using a multi-well plate reader (Figure 5.11). The absorbance at 600 nm of each strain was recorded every five minutes over a time period of 20 hours. Figure 5.11 shows the first 8.5 hours of the growth of BMD strains. 168 (wild type), *ftsA::erm* and *sepF::neo* were added for comparison. BMD7, F mother strains (BMD25, 26, and 27) and F&A (BMD14) mother strain together with *ftsA::erm* had very long lag phase. Another difference is that the highest absorbance reached in stationary phase is much lower for these strains.

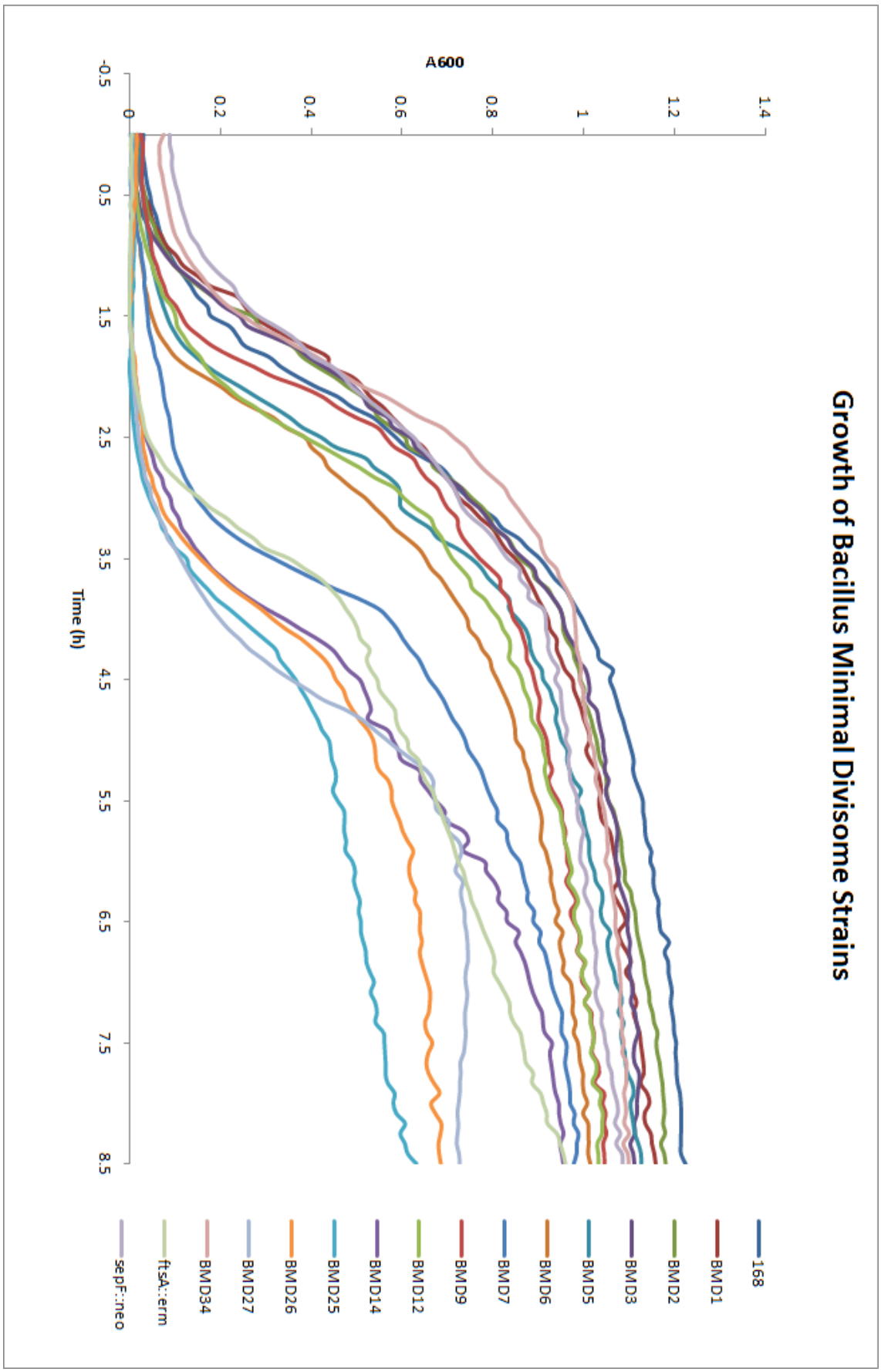

Figure 5.11 Growth of the BMD strains. The growth of 168, BMD12, F&A mother strain (BMD14), F mother strains (BMD25, BMD26, and BMD27), and AE mother strain (BMD34) was compared with the other BMD strains.

Doubling times of absorbance of the BMD strains were calculated during the logarithmic growth phase (Table 5.4 and Figure 5.12). This data shows that deletion of *ugtP* (BMD3) increases the growth rate, while the *minJ* deletion (BMD5) decreases it. The growth of BMD14 strain decreased slightly compared to 168. However, deletion of *ftsA* had a remarkable effect on growth rate, and there was a notable increase in doubling time of the *ftsA::erm* mutant and BMD25. BMD26 and BMD27 also grew much slower than 168, but they were growing faster than BMD25. Again this supports the idea that the F mother strains, BMD25, 26 and 27, contain different suppressor mutations. Doubling time of BMD34 (AE mother strain) was more than BMD14, BMD26, and BMD27, but less than BMD25 which suggests that deletion of *sepF* affects the growth rate almost as much as the *ftsA* deletion. In our hands, *sepF::neo* strain grew much slower than 168 and *ftsA::erm*. However, this was not observed in the previous experiments (personal communication with Leendert Hamoen), so it was not included in the discussion.

Name	Deletions	Doubling Time (min)
168	-	21
BMD1	Z	22
BMD2	ZC	23
BMD3	ZCU	18
BMD5	ZCUJ	28
BMD6	ZCUJE	25
BMD7	ZCUJES	27
BMD9	ZCUJESX	28
BMD12	ZCUJSXN	28
BMD14	ZCUJESXN	27
BMD25	ZCUJESXNA	38
BMD26	ZCUJESXNA	30
BMD27	ZCUJESXNA	30
BMD34	ZCUJSXNF	34
sepF::neo	F	43
ftsA::erm	A	36

Table 5.4 Doubling time of absorbance of the BMD strains in minutes. The deletions are *zapA* (Z), *minC* (C), *ugtP* (U), *minJ* (J), *ezrA* (E), *spxA* (S), *clpX* (X), *noc* (N), *sepF* (F), and *ftsA* (A).

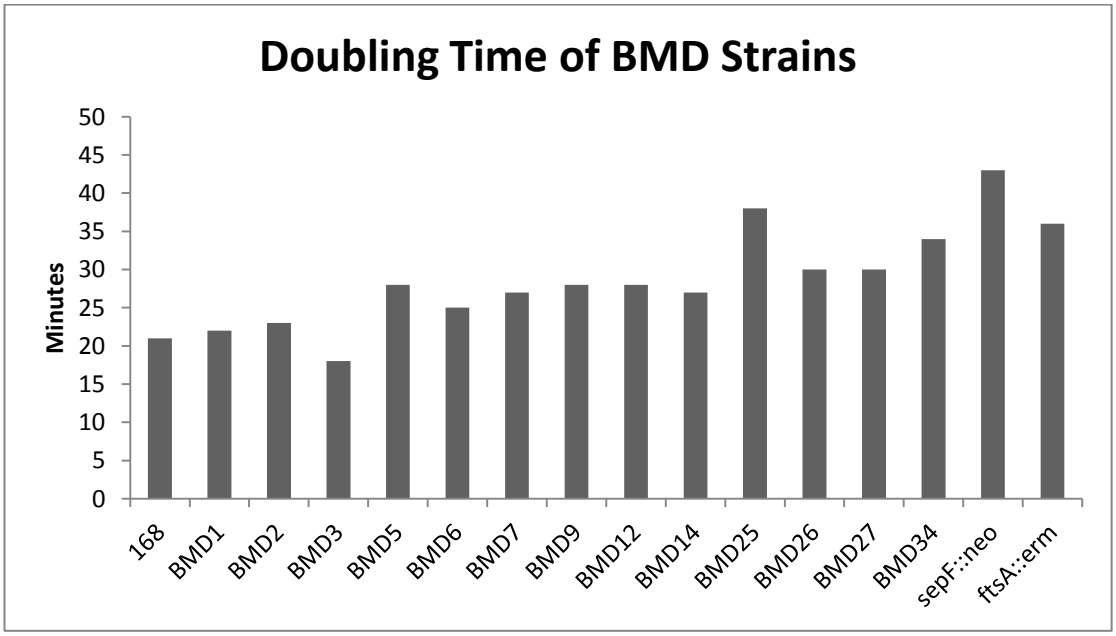

Figure 5.12 Doubling time of absorbance of the BMD strains shown as bar diagram.

5.5. The BMD Strains are Filamentous

The previous section described how the cumulative removal of cell division genes affected growth rates. Table 5.5 and Figure 5.13 show the average cell length of the BMD strains. Cells were grown until mid-exponential phase in LB with glucose (1%) and magnesium (10 mM) and the cell lengths were measured with ImageJ from microscope images. The deletion of subsequent genes appears to increase the average cell length, cumulating in very long cells of the F mother strains (BMD25, BMD26 and BMD27). It seems that deletion of *ftsA* contributes most to the increased filamentation. The average localization of division septa was calculated and presented in Table 5.5 and Figure 5.14 as well. Figure 5.14 shows the distribution of septal localization of several BMD strains. Although the average septal localization data suggests that the BMD strains are able to divide close to the middle of the cell, it is clear that the cell division occurs at random locations in the cells, especially for BMD25, BMD26 and BMD27. Again the *ftsA* deletion seems to be responsible for most of the variation.

	Cell length (μm)			Septal localization		
	Mean	**St. Dev.**	**n**	**Mean**	**St. Dev.**	**n**
168	4.3	1.1	199	0.50	0.03	84
BMD1	3.8	1.0	185	0.50	0.03	102
BMD2	7.1	2.2	161	0.51	0.05	75
BMD3	6.6	2.7	187	0.47	0.13	113
BMD5	6.3	2.5	210	0.48	0.13	85
BMD6	8.5	2.7	190	0.49	0.04	101
BMD7	12.0	4.7	157	0.49	0.07	96
BMD9	8.9	3.4	133	0.49	0.07	69
BMD12	8.4	3.1	151	0.48	0.08	76
BMD14	13.2	6.7	135	0.54	0.16	38
BMD25	20.9	12.9	76	0.43	0.18	13
BMD26	21.8	9.8	77	0.48	0.10	7
BMD27	19.2	7.4	86	0.55	0.19	12
BMD34	10.4	4.2	153	0.50	0.12	52
ftsA::erm	16.4	9.6	46	0.48	0.17	9
sepF::neo	6.0	1.6	147	0.51	0.04	84

Table 5.5 The cell length of the BMD strains and the localization of their septa. The average cell length was shown in μm. The septal localization data assumes that in a cell one pole is 0 and the other pole is 1. Then midcell would be 0.5. The analysis was done in cells that were grown until mid-exponential phase in LB with glucose (1%) and magnesium (10 mM).

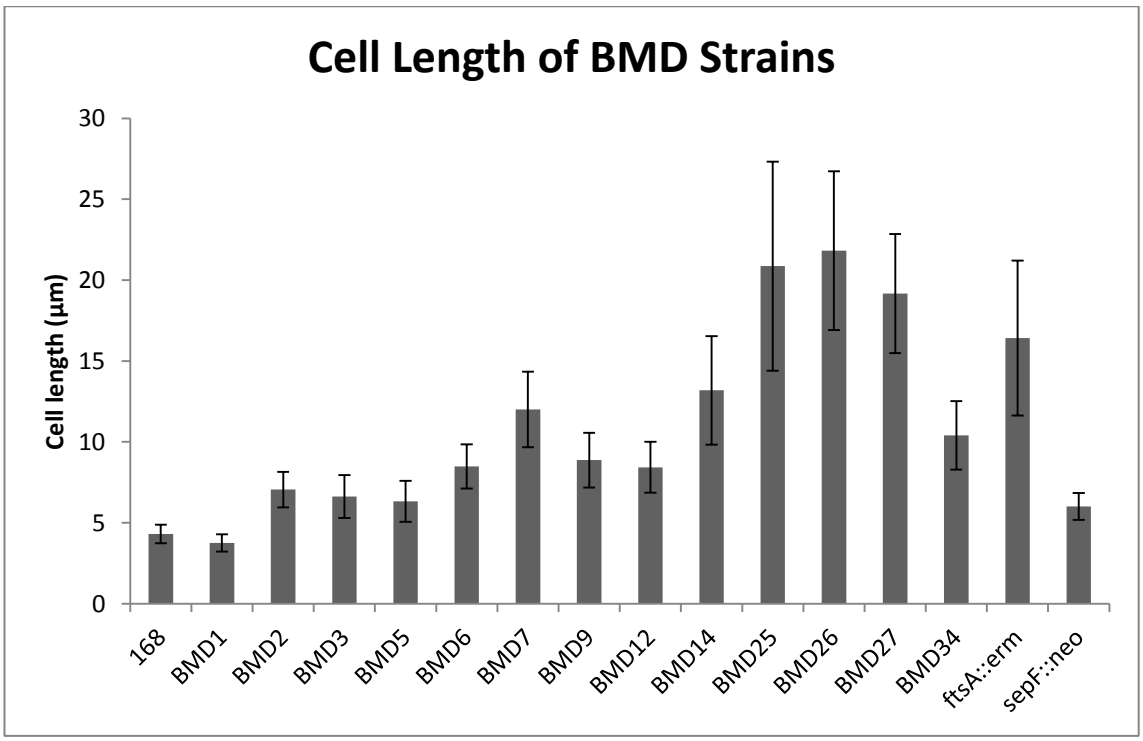

Figure 5.13 Average cell length of the BMD strains. Error bars represent the standard deviation in the cell length.

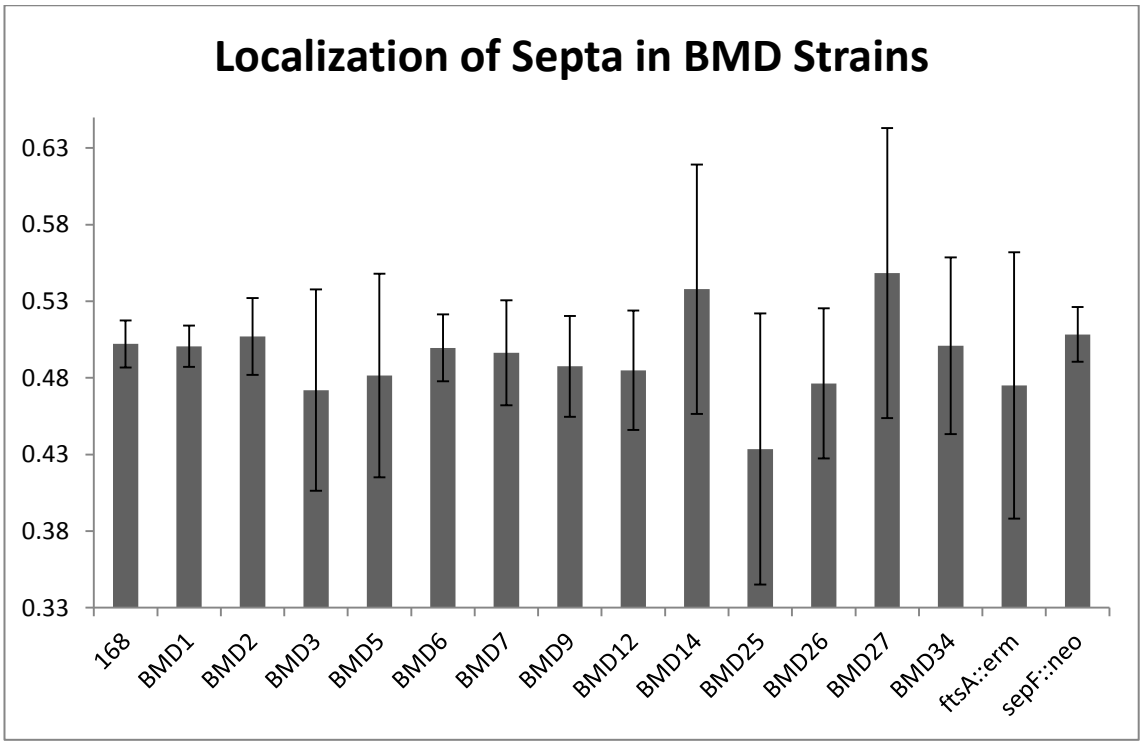

Figure 5.14 Septal localization of the BMD strains. The septal localization data assumes that in a cell one pole is 0 and the other pole is 1. Midcell would be 0.5. Error bars represent the standard deviation in the septal localization of BMD strains.

5.6. Imaging BMD Strains with Fluorescent Microscopy

To examine whether the cell division mutants showed abnormal cell shapes, the strains were grown in LB at 37°C and imaged using fluorescence microscopy (Figure 5.15, Figure 5.16 and Figure 5.17). Deletion of *zapA* (BMD1) did not have a significant effect on cell shape. However, as expected, the removal of *minC* (BMD2) resulted in the formation of minicells. Subsequent deletion of *ugtP* (BMD3) did not have a major effect on cell length. MinJ is a part of the Min system in *B. subtilis*, but has also a role in regulation of divisome disassembly (van Baarle and Bramkamp, 2010). However, subsequent removal of *minJ* (BMD5) did not have an apparent effect on cell shapes. With introduction of an *ezrA* deletion (BMD6), cells seem to increase slightly in size. Moreover, the DNA staining was more diffuse in this strain which could indicate less condensed nucleoid. ClpX is a part of ClpXP chaperone which controls, aside of the Z-ring formation, several other pathways in the cell. One of these pathways is natural genetic competence (Nakano et al., 2000). Deletion of *clpX* will reduce competence, which is required for genetic transformation. This can be bypassed by deletion of *spxA* (Nakano et al., 2001). SpxA is a negative regulator of genetic competence and is cleaved by ClpP proteases (Nakano et al., 2002). Therefore, *spxA* was deleted (BMD7) before the *clpX* deletion was introduced. As shown in Figure 5.15, this deletion caused some elongation, but it also seemed to compensate the increased cell width and the nucleoid morphology observed in BMD6. Subsequent deletion of *clpX* created cells with increased diameter in different sizes (BMD9). This strain also showed a diffuse nucleoid that seems to fill the cell. The combination of *noc* and *ezrA* deletion is synthetic lethal (Wu and Errington, 2004, Kawai and Ogasawara, 2006). In this work, the marker-free deletion method was tried to achieve this combination without any success. The resulting strain lacked *noc*, but had recombined the wild type copy of *ezrA* (BMD12). The width of this strain was narrower than the width of BMD6 or BMD9, but the cells were still longer compared to 168 (Figure 5.16).

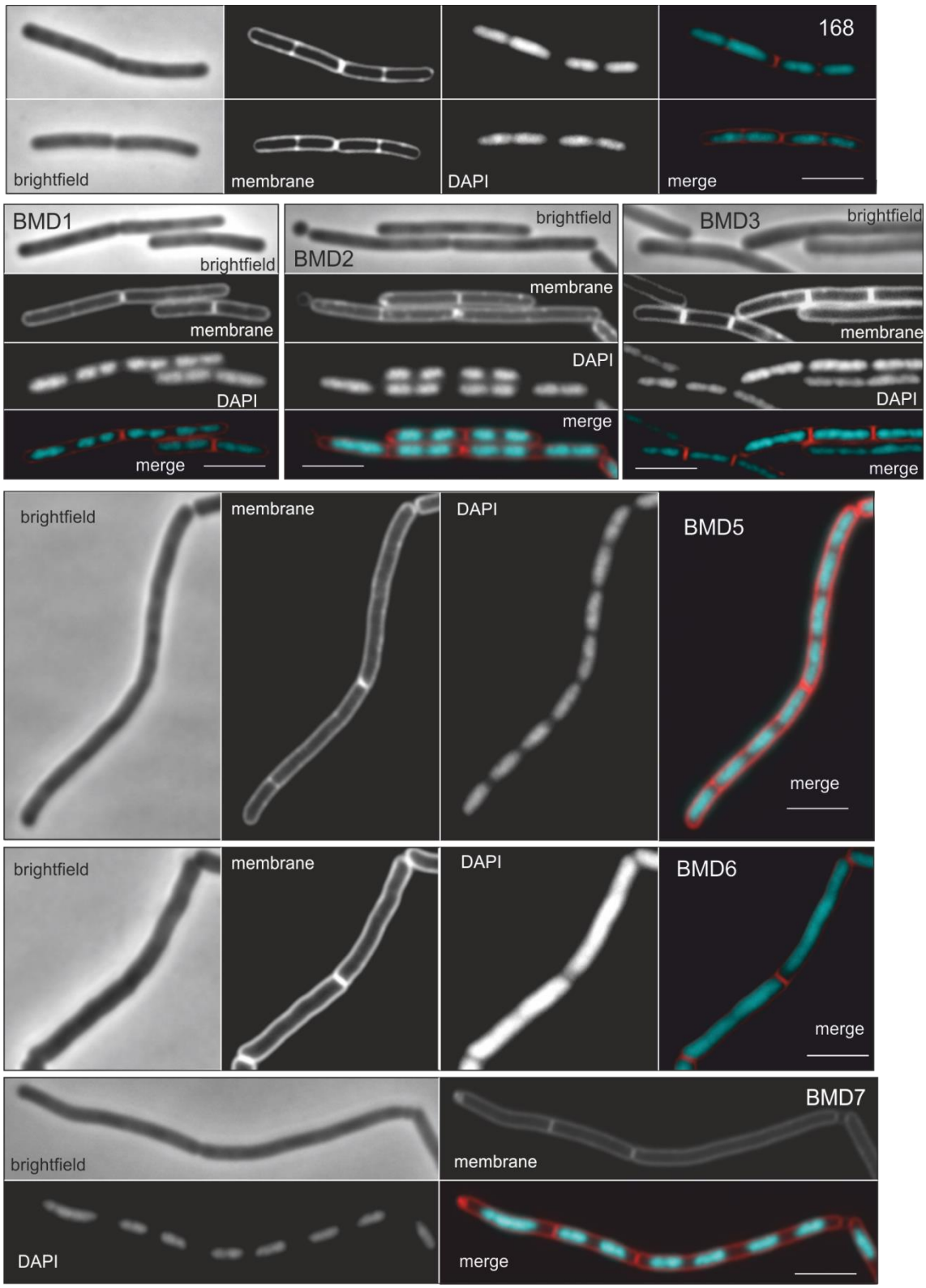

Figure 5.15 Fluorescent microscopy of the BMD strains. Images show the bright field, membrane stain with FM5-95, DNA stain with DAPI and a merge of membrane (red) and DNA (cyan) stain. The scale bars show 4 µm

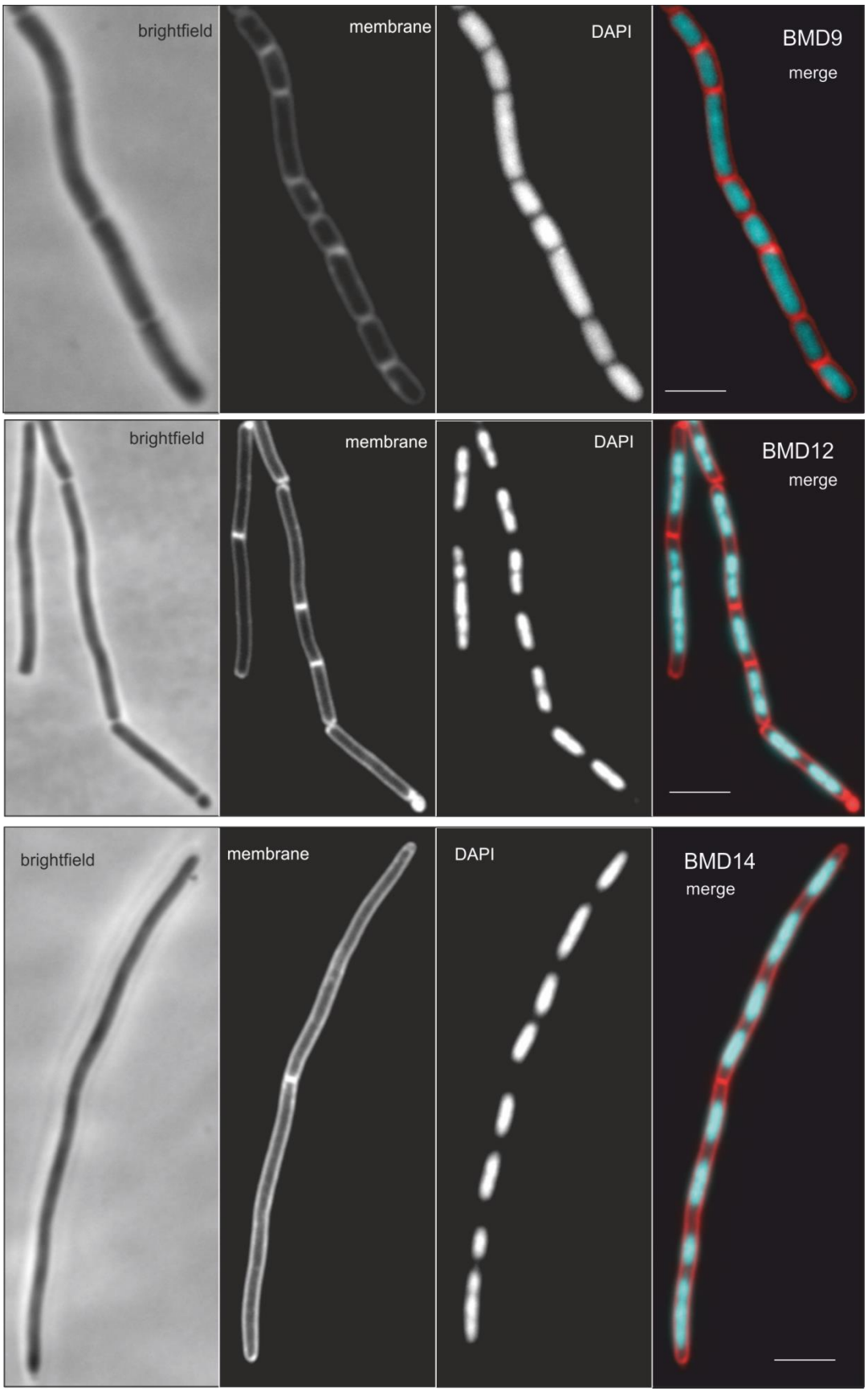

Figure 5.16 Fluorescent microscopy of the BMD strains. Images show the bright field, membrane stain with FM5-95, DNA stain with DAPI and a merge of membrane (red) and DNA (cyan) stain. The scale bars show 4 µm.

In a new attempt to obtain the *noc ezrA* deletion in the BMD strains, the *ezrA::tet* deletion was used. This approach was successful, and the F&A mother strain, BMD14 was constructed containing 8 deletions. As shown in Figure 5.16, BMD14 clearly has a division defect and forms elongated cells.

The deletion of *ftsA* from BMD14 using an *ftsA::erm* construct resulted in three different strains; BMD25, BMD26 and BMD27 which are called the F mother strains. DNA staining of BMD25, BMD26 and BMD27 showed regularly distributed, similarly-sized chromosomes (Figure 5.17). These F mother strains formed septa but even in a lower frequency than F&A mother strain. The cell poles of BMD25, 26, and 27 often showed excess membrane stain (Figure 5.17, white arrows). Structured Illumination Microscopy (SIM) was used to shed some light on these structures. As Figure 5.18 shows, the cell poles contain closely located and very small minicells that result in a strong membrane signal in normal fluorescence light microscopy. This is maybe not surprising since these BMD strains lack many other regulatory cell division proteins. The AE mother strain (BMD34) looked the healthiest of the mother strains constructed in this study.

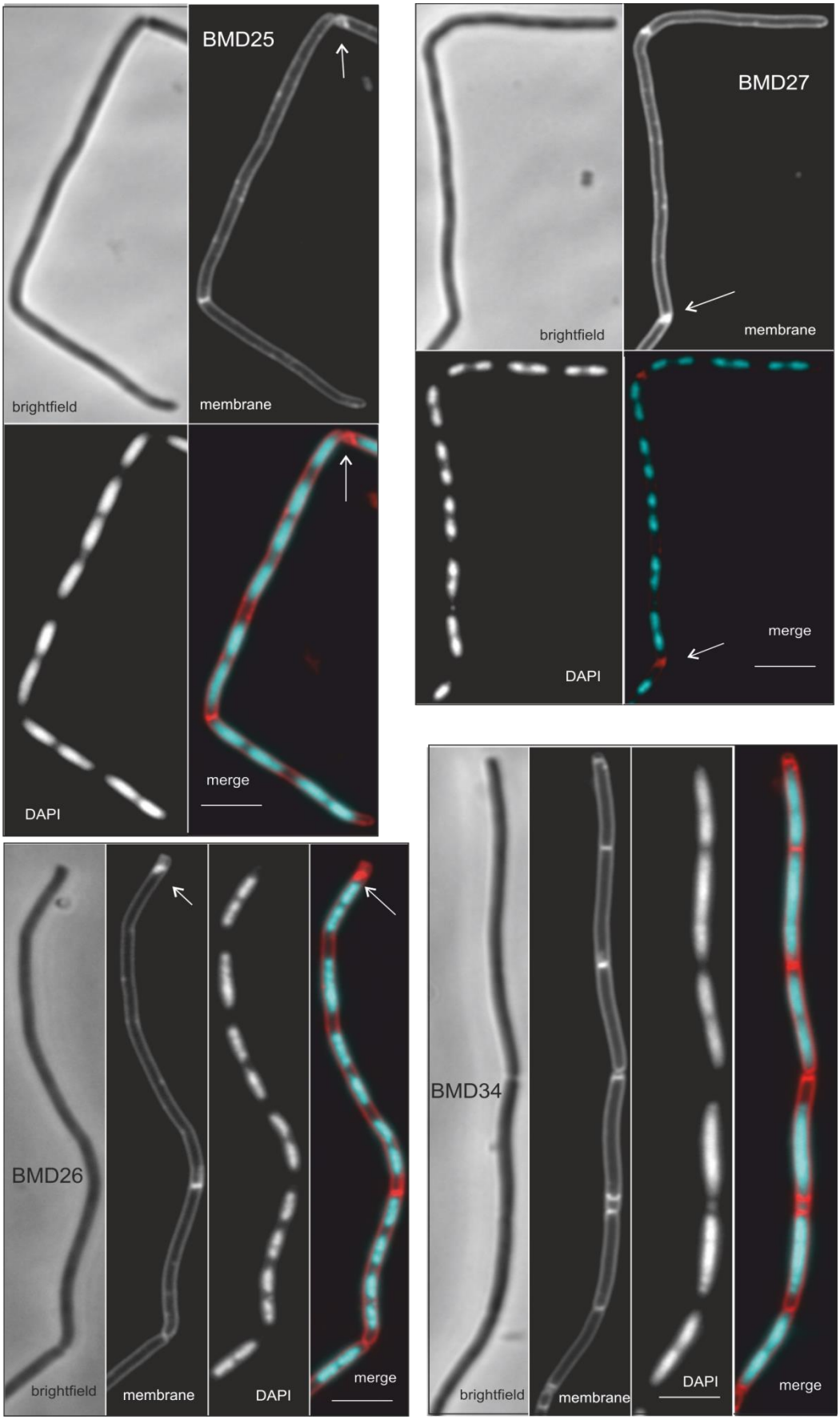

Figure 5.17 Fluorescent microscopy of the BMD strains. Images show the bright field, membrane stain with FM5-95, DNA stain with DAPI and a merge of membrane (red) and DNA (cyan) stain. The white arrows show excess membrane bulbs. The scale bars show 4 µm.

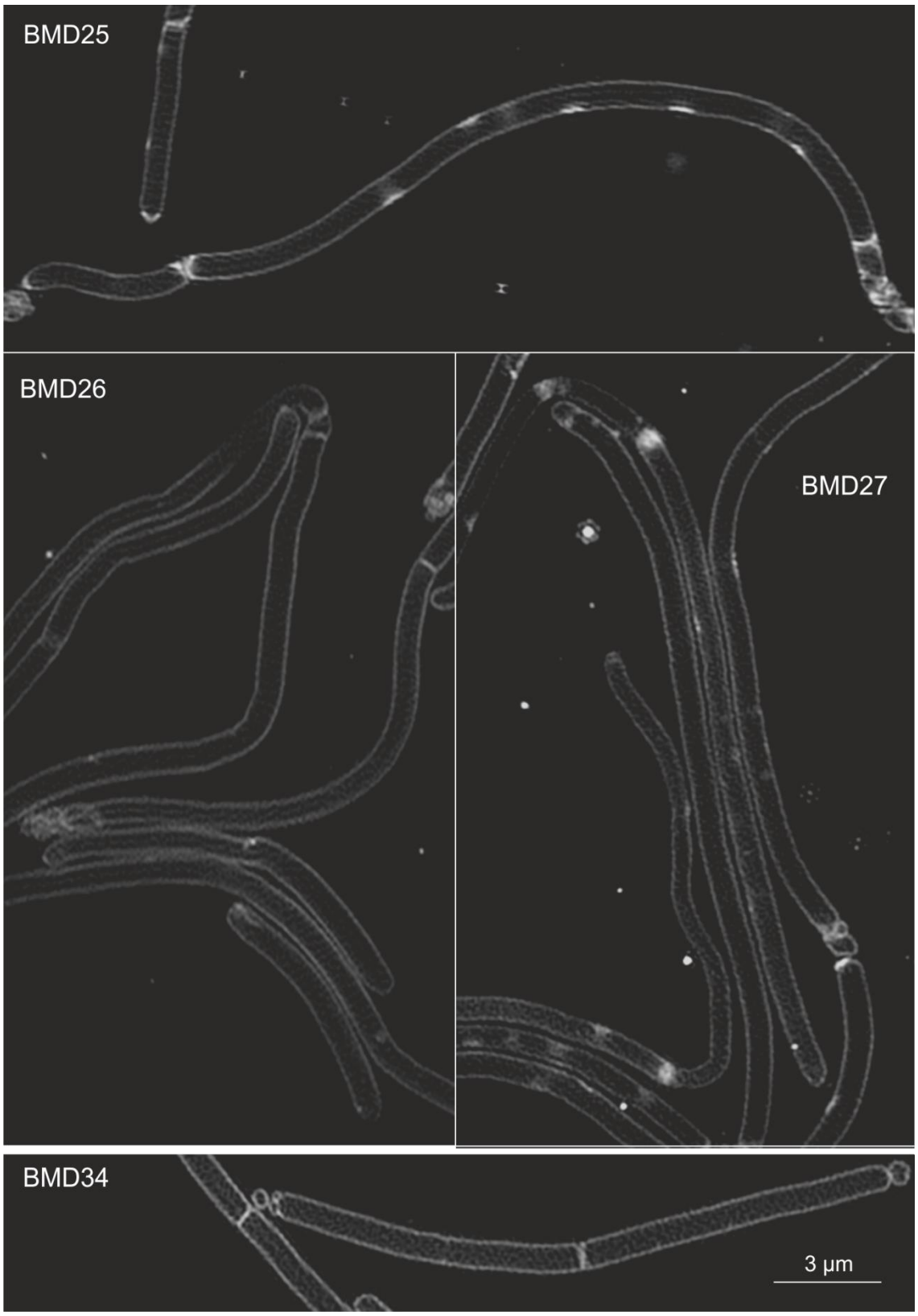

Figure 5.18 Structured Illumination Microscopy (SIM) images of F mother strains (BMD25, 26, 27) and A mother strain (BMD34). Nile red was used to stain the membrane. The scale bar shows 3 µm.

5.7. FtsZ Localization in Mother Strains

Since BMD14, BMD25, 26, and 27, and BMD34 lacked so many FtsZ regulators, we were curious whether FtsZ spirals and/or multiple Z-rings were visible. To examine this, a GFP-FtsZ reporter fusion was introduced. To prevent restoration of cell division genes, the BMD strains (Figure 5.19) were transformed with PCR fragments covering the *amyE::*P_{xyl} *gfp-ftsZ* region from strain 2020 (Laboratory stock). Then, the strains were tested for the deletions with PCR (data not shown). First, wild type strain, 168 was transformed with the PCR product, named BMD33 (168 + GFP-FtsZ), to control whether the transformation is successful (Figure 5.20). Transformation of BMD14 with the PCR product resulted in two strains BMD30 and BMD31. Figure 5.20 shows BMD30 (BMD14 + GFP-FtsZ) strain with GFP-FtsZ located mostly at septa. However, it was possible to observe FtsZ at cell poles (white arrows in BMD30). GFP-FtsZ was mostly cytoplasmic in BMD31 (BMD14 + GFP-FtsZ) with occasional FtsZ bands and helical intermediates (Figure 5.21). Similar to BMD30, some GFP-FtsZ structures were visible at the cell poles (white arrows). Bramkamp et al. (2010) showed that after the cell division completed, FtsA did not dissociate from the new cell poles in *minJ* mutants (van Baarle and Bramkamp, 2010). Since these BMD strains do not contain *minJ*, GFP-FtsZ visible at the cell poles is probably a result of *minJ* deletion.

The AE mother strain, BMD34, was transformed with the PCR product which resulted in two strains, BMD35 and BMD36. Both only showed the Z-rings and no helical GFP-FtsZ pattern (Figure 5.21). Again, GFP-FtsZ did not dissociate completely after septation as indicated by the polar fluorescence GFP spots.

SIM imaging made it possible to observe the localization of GFP-FtsZ with higher resolution, and revealed nascent septa with GFP-FtsZ located at the periphery of constricting membrane. GFP-FtsZ also localizes at the future division site before any constriction of the cell membrane (Figure 5.20).

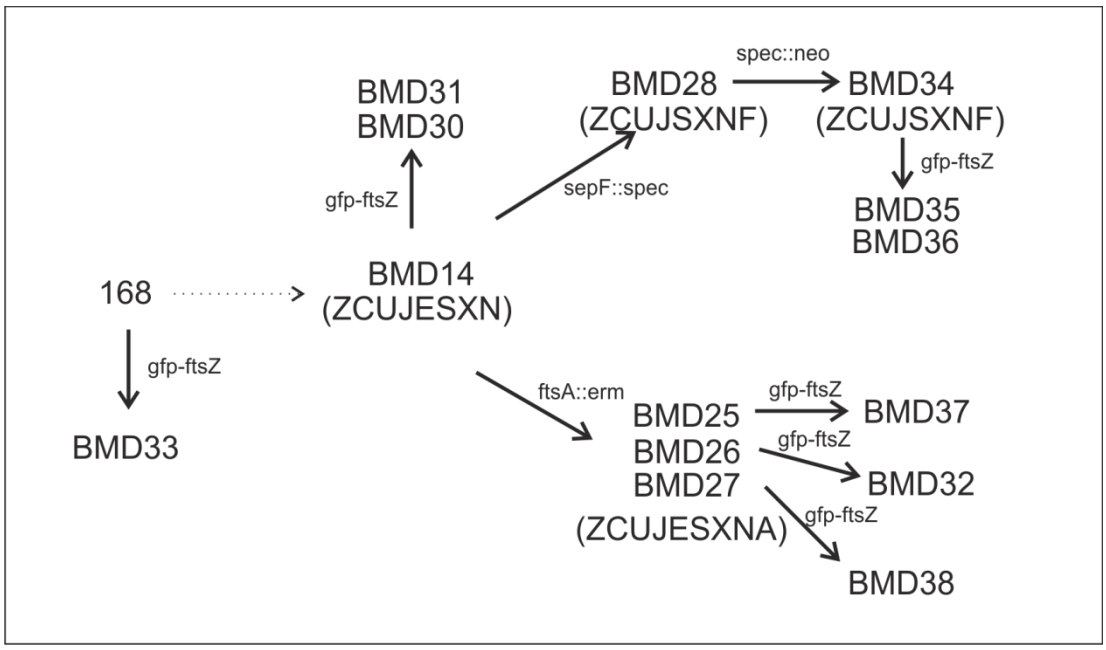

Figure 5.19 Construction of BMD strains with GFP-FtsZ. PCR fragments covering the amyE::Pxyl gfp-ftsZ region from strain 2020 were transformed to 168, BMD14, BMD25, BMD26, BMD27, and BMD34 resulting in strains BMD33, BMD30-31, BMD37, BMD32, BMD38, and BMD35-36, respectively.

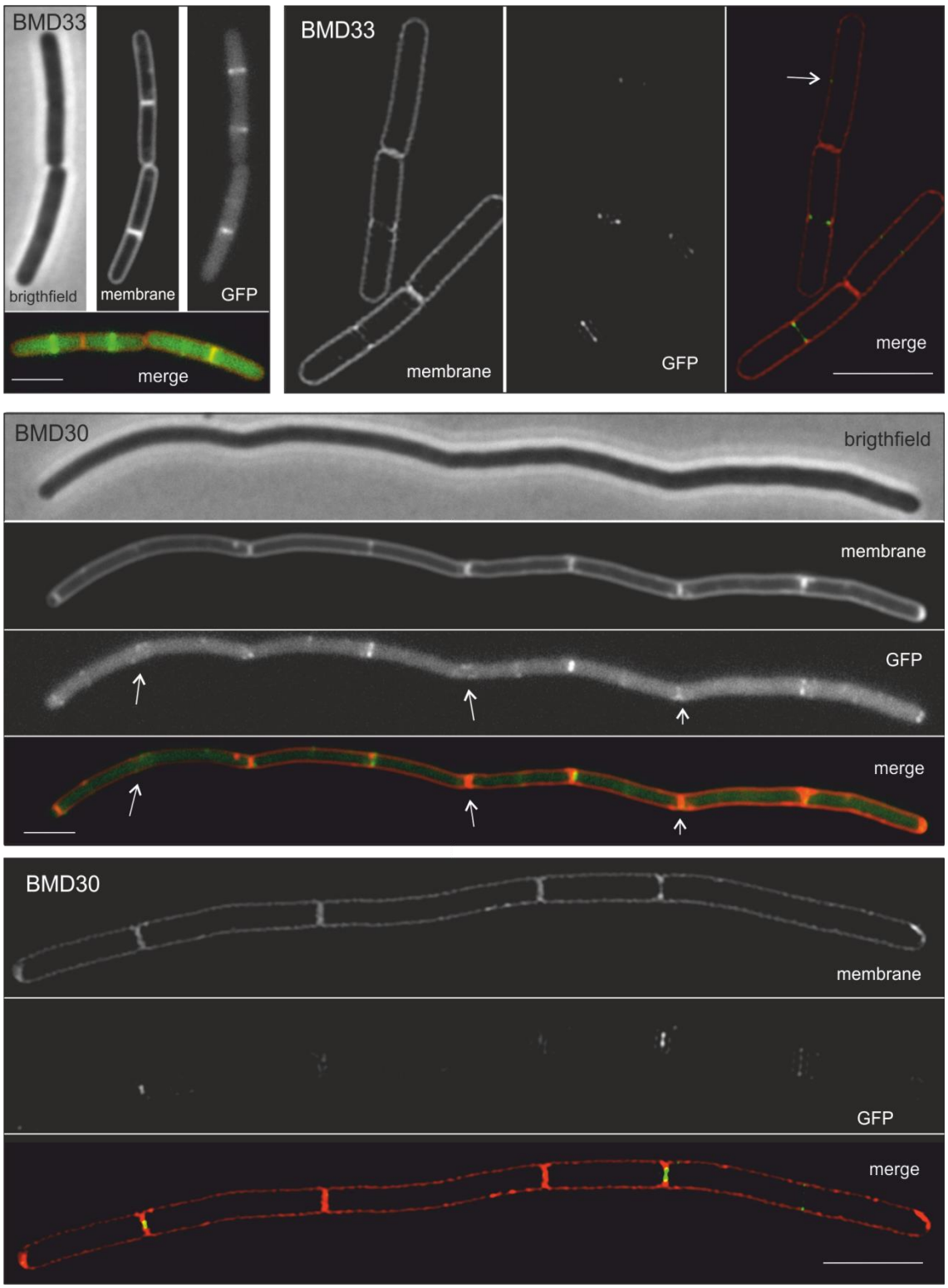

Figure 5.20 Localization of FtsZ in wild type strain (BMD33 (168 + GFP-FtsZ)) and F&A mother strain (BMD30 (BMD14 + GFP-FtsZ)). Xylose (0.25%) induced P_{xyl} *gfp-ftsZ* in *amyE* locus. The membrane was stained with FM5-95. The scale bars show 3 µm for both fluorescent microscope and SIM images. White arrows show abnormal GFP-FtsZ structures for BMD30 and future division site for BMD33.

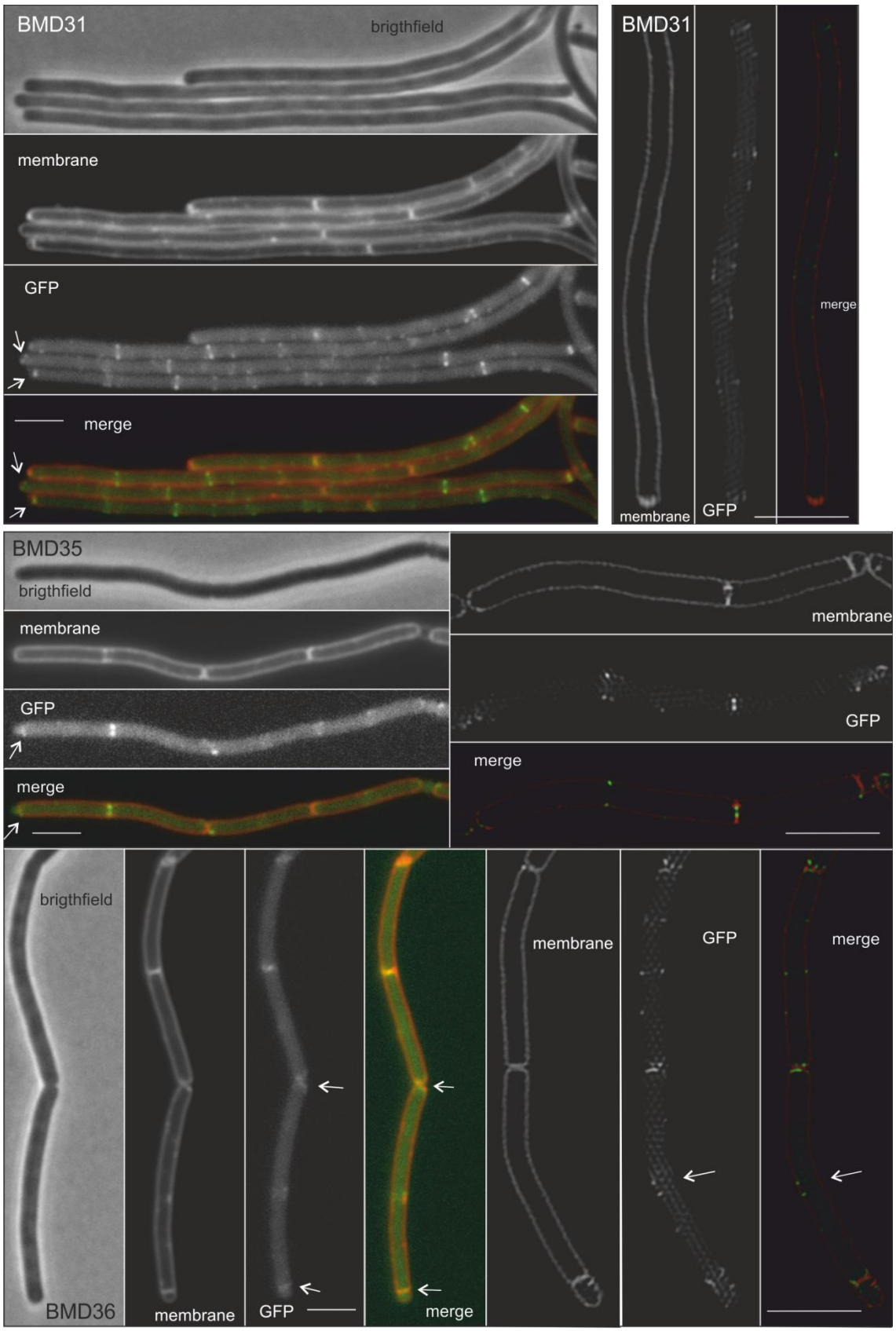

Figure 5.21 Localization of FtsZ in F&A mother strain (BMD31 (BMD14 + GFP-FtsZ)) and AE mother strain (BMD35 (BMD34 + GFP-FtsZ), BMD36 (BMD34 + GFP-FtsZ)). Xylose (0.25%) induced P_{xyl} *gfp-ftsZ* in *amyE* locus. The membrane was stained with FM5-95. The scale bars show 3 µm for both fluorescent microscope and SIM images. White arrows show abnormal GFP-FtsZ structures.

The F mother strains (BMD25, 26, and 27) missed 9 cell division genes including *ftsA*. It was clear that polymerization of FtsZ would be severely affected in these strains, and indeed GFP-FtsZ was mostly cytoplasmic in BMD32 (BMD26 + GFP-FtsZ), BMD37 (BMD25 + GFP-FtsZ), and BMD38 (BMD27 + GFP-FtsZ), as shown in Figure 5.22 and Figure 5.23. In several occasions, GFP-FtsZ formed large structures at the cell poles. Surprisingly, these structures did not superimpose with the cell membrane (white arrows).

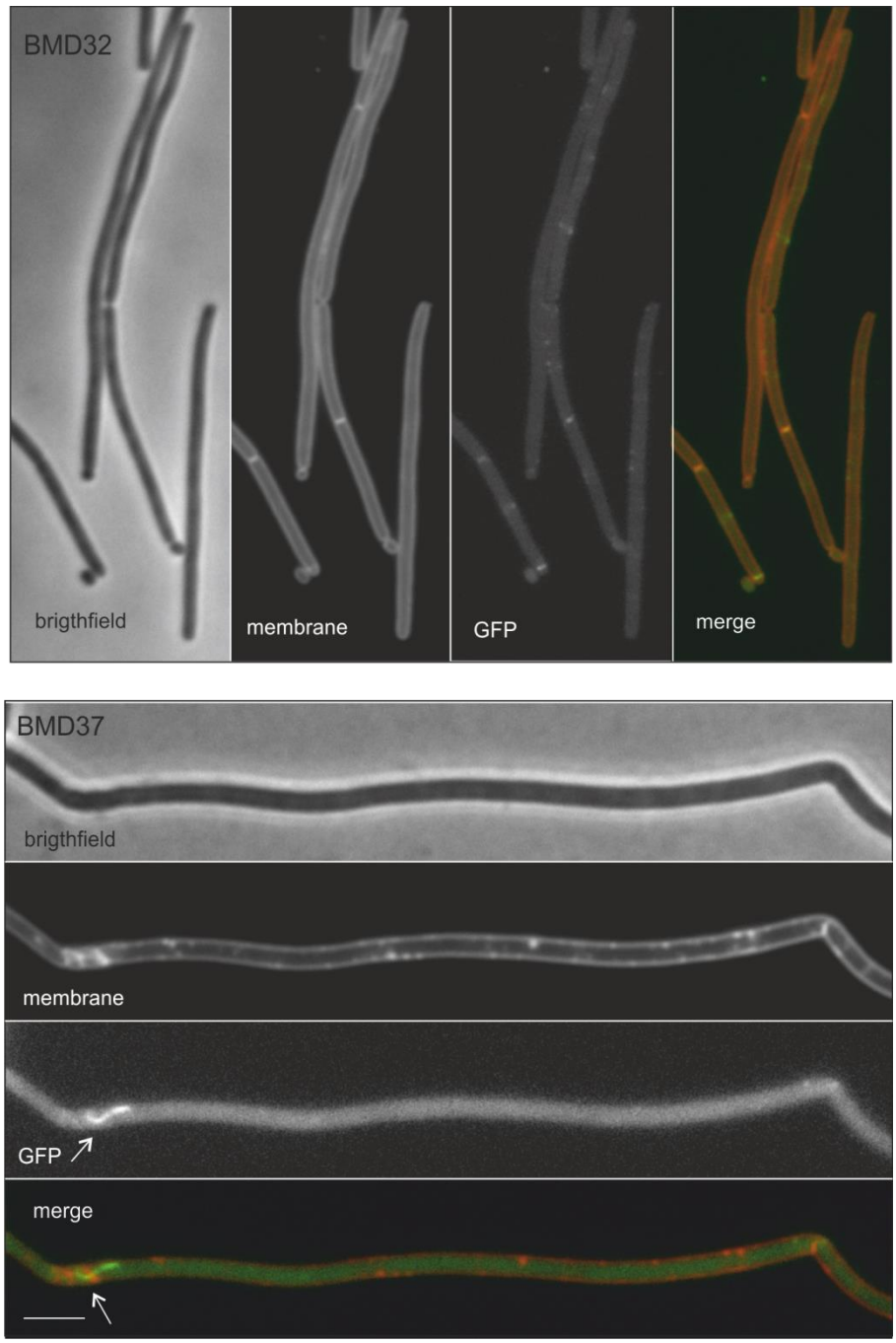

Figure 5.22 Localization of FtsZ in F mother strain (BMD37 (BMD25 + GFP-FtsZ), BMD32 (BMD26 + GFP-FtsZ)). Xylose (0.25%) induced P_{xyl} *gfp-ftsZ* in *amyE* locus. The membrane was stained with FM5-95. The scale bars show 3 µm for both fluorescent microscope images. White arrows show abnormal GFP-FtsZ structures.

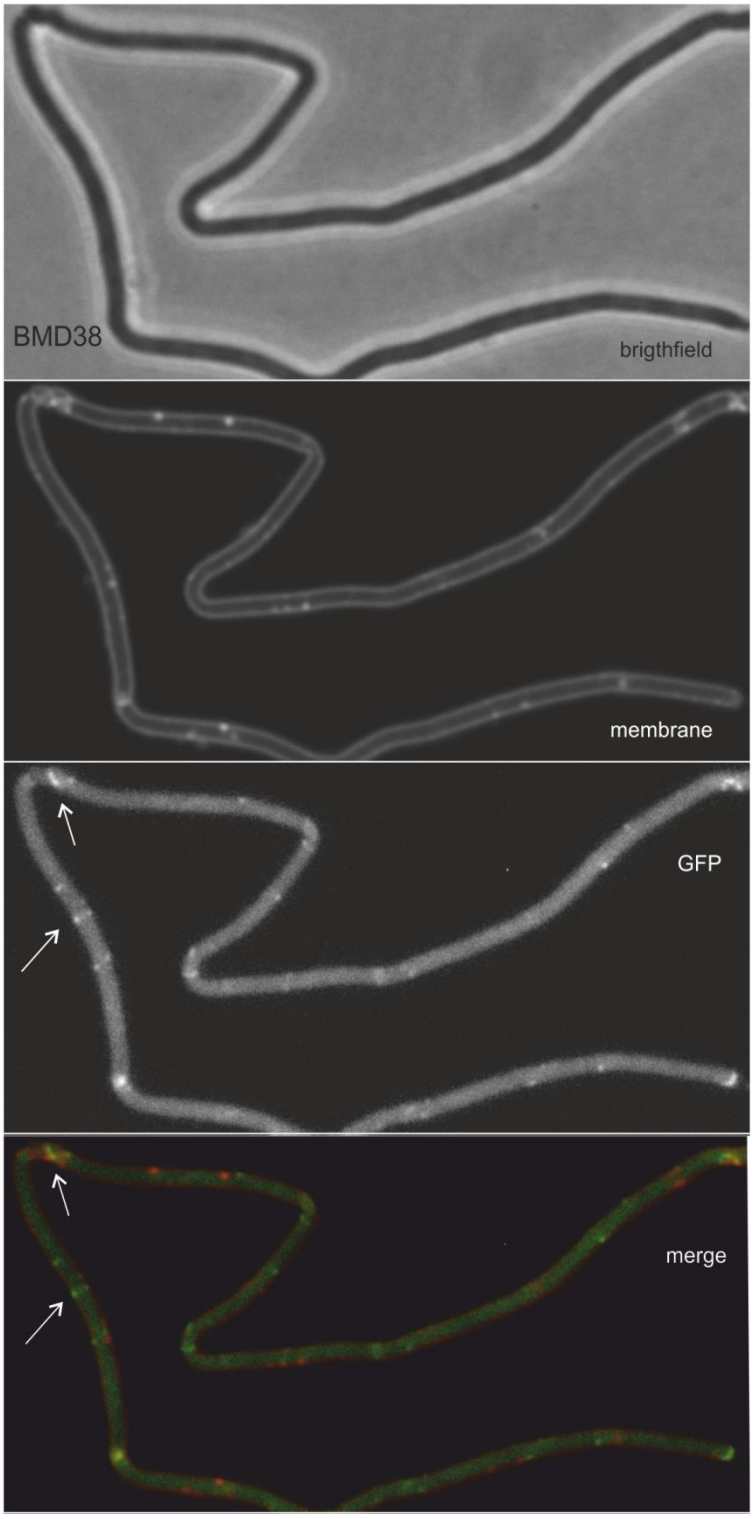

Figure 5.23 Localization of FtsZ in F mother strain (BMD38 (BMD27 + GFP-FtsZ)). Xylose (0.25%) induced P_{xyl} *gfp-ftsZ* in *amyE* locus. The membrane was stained with FM5-95. The scale bars show 3 µm for both fluorescent microscope images. White arrows show abnormal GFP-FtsZ structures.

Discussion

In *B. subtilis*, there are at least 20 proteins that have a role in cell division. Most of these proteins are not essential. However, simultaneous deletion of some of the non-essential proteins have a synthetic lethal effect such as the combinations *noc/ezrA*, *sepF/ezrA, zapA/minC, clpX/minC* (in *E. coli*), *zapA/ezrA* and *ezrA/noc* (Wu and Errington, 2004, Hamoen et al., 2006, Kawai and Ogasawara, 2006, Gueiros-Filho and Losick, 2002, Camberg et al., 2011). Although making such combinations in the Minimal Divisome project presented some difficulties, in the end it was possible to obtain these previously thought lethal combinations. Although it was not possible to delete *sepF* with *ftsA* or *ezrA*, deletion of *zapA*, *minC*, *ezrA, clpX* and *noc* in the same strain was achieved. Presumably, the synthetic lethality effect of several combinations was compensated by other deletions, although it might be that the strain acquired spontaneous mutations that enabled us to obtain the multiple deletion strain. Another reason might be the use of marker-free deletions. In the published synthetic lethal combinations, a small part of the gene might still be expressed that results in inactive proteins which interacts with other proteins such as FtsZ and prevents formation of functional divisome complex.

It was important to confirm the gene deletions in BMD strains, since after each transformation wild type genes might have recombined to BMD strain. Therefore, we first used PCR with primer sets from outside and inside of the gene of interest (Figure 5.3 and 5.4). However, for some genes the outside PCRs showed deletion of the gene while the inside PCRs showed presence of the gene. It was possible that some of the PCRs of the same genes had contamination and showed false positive results. To solve this problem, we performed Southern blotting for the BMD strains we further examined in this study. Southern blots of gene deletions supported the PCR results, so we continued working with the BMD strains.

The BMD strains grew better on LB agar than nutrient agar. Although both media are commonly used for microbial growth, they have different compositions such as difference in yeast and beef extract, peptone and tryptone, and salt concentration. Moreover, the presence of excess NaCl in LB agar might increase the polymerization of FtsZ by decreasing its GTPase activity (Mendieta et al., 2009). These differences are probably the reason of better growth of the BMD strains on LB agar. Several environmental conditions

were tested for growth of the BMD strains. *B. subtilis* can grow at 50°C, but at such high temperatures the final BMD strains BMD14, 25, 26, 27 and 34 grew poorly. The growth of BMD25 and BMD26 (F mother strains) was poor at 30°C, too. The BMD strains grew best at the neutral pH. Surprisingly, BMD26 grew better than BMD25 and BMD27 (F mother strains) under both acidic and basic conditions. Increased salt concentrations did not affect the growth of the BMD strains. On the other hand, BMD25 and BMD26 hardly grew without any NaCl. This suggests that these strains have problem to adjust to osmotic changes. Furthermore, magnesium improved the cell division of the BMD strains. It is known that presence of high salt in the media affects *gpsB* mutants (Claessen et al., 2008) while absence of magnesium in the media results in cell bending and filamentation in cells without PBPs (Murray et al., 1998). It is possible that deletions of cell division genes in the BMD strains affected the functions of these proteins, so that these strains react to the absence or presence of salt and divalent cations.

In a recent study evaluating the essential genes in *B. subtilis*, it was shown that the presence of malate with glucose in the medium improves the growth of strains without glycolytic pathway genes (Commichau et al., 2013). The BMD strains were grown on LB agar with malate and glucose to examine whether these molecules have the same effect on deletion of the divisome genes. The results showed that supplementing the growth media with glucose and malate improved the growth of BMD strains. This might simply mean that the better growth of BMD strains was due to the presence of additional energy source in the media. On the other hand, it was also possible that there is a connection between cell division and the glycolytic pathway. The probable candidates for this connection would be ClpX and UgtP. ClpX is the substrate recognition subunit of chaperone ClpXP which might have an unknown substrate, degradation of which affects the glycolysis pathway, while UgtP is a glucosyltransferase that has a role in production of glycolipids.

The growth rate measurements showed that multiple deletions results in an increased lag time. However, the logarithmic growth rate did not reveal a significant difference between the BMD strains except when the *ftsA* deletion was present, which is known to retard growth in *B. subtilis* (Beall and Lutkenhaus, 1992). The growth rates of the F mother strains differed. BMD25 grew much slower than BMD26 and BMD27. This together with their different

response to temperature and salt concentration suggests that these strains contain different suppressor mutations.

Microscopy studies showed that the BMD strains have problems forming the divisome complex, but they were still able to divide, indicating that the genes *zapA*, *minC*, *ugtP*, *minJ*, *ezrA*, *spxA*, *clpX*, and *noc* are not required for septum formation. Besides inefficient cell division, the BMD strains also showed abnormal nucleoids, indicating the replication of DNA or separation or organization of the chromosomes were not functioning properly. This phenotype has not been described for any of the single mutants. Even the deletion of *noc* did not result in the abnormal nucleoids observed here (Wu and Errington, 2004).

SIM imaging of mother strains showed that in the F mother strains (BMD25, 26 and 27) the number of minicells was highly increased. Moreover, those minicells could not separate from the mother cell resulting in accumulation at the tips of cells. This phenotype was observed only after the deletion of *ftsA* which might somehow prevent completion of cytokinesis. Moreover, localization of GFP-FtsZ in BMD37 (BMD25 + GFP-FtsZ) and BMD38 (BMD27 + GFP-FtsZ) showed that FtsZ did not dissociate from the cell poles which causes the occurrence of subsequent cell division at the cell poles.

In conclusion, the *Bacillus* Minimal Divisome project shows that the presence of FtsZ – SepF, FtsZ – FtsA – EzrA or FtsZ – SepF – FtsA is sufficient for the cell division to occur.

Future Work

This work presented the phenotypic features of the BMD strains. For future work, it will be necessary to sequence the genomes to determine which point mutations the strains have accumulated. Moreover, transcriptome analysis might reveal the connection between the cell division and glycolytic pathway.

While this thesis was being prepared the sequencing of F mother strains BMD25, BMD26, and BMD27 was completed. The comparison of the sequences with the 168 sequence showed that there are single-nucleotide polymorphisms (SNPs) in the *ponA* and *spoVG* genes. As mentioned earlier *ponA* codes for PBP1 gene and deletion of it is compensated by presence of Mg^{2+} in the media (Murray et al., 1998). This would explain why the BMD strains grew better in the presence of magnesium. The SpoVG protein functions in the

Stage V of sporulation in *B. subtilis*. It is suggested that SpoVG interacts with negative regulators of sporulation and ensures that sporulation continues (Matsuno and Sonenshein, 1999). Recently, it was shown that SpoVG homologs from *Borrelia burgdorferi* and *Staphylococcus aureus* interact with the chromosome (Jutras et al., 2013). This suggests that SpoVG might control the chromosome segregation and signal other sporulation proteins to continue. In vegetative cell division, SpoVG might have a similar function as SftA or FtsK which might explain why the F mother strains have SNPs in this gene.

It would be also interesting to see the effect of FtsZ overproduction in the BMD strains. Deletion of *sepF* and *ftsA ezrA* might be attempted while *ftsZ* is overexpressed. Finally, deletion of late divisome proteins might show exciting results.

Chapter 6. Summary & Conclusion

6.1. SepF Orthologs Form Ring-like Structures

Cell division in bacteria occurs at midcell and is executed by proteins that either regulate this event or function in constriction and synthesis of the new cell wall (Adams and Errington, 2009). The focus of this project was SepF which stabilizes and promotes the Z-ring assembly that is necessary to synthesize regular septa (Gundogdu et al., 2011, Hamoen et al., 2006). The first section of this work (Chapter 3) aimed to show that the SepF rings that are observed with electron microscopy are conserved to support the notion that this structure is relevant *in vivo*. When the SepF rings were first observed, it caused a debate in bacterial cell biology field; because, the SepF rings are large enough to be seen with electron microscopy if SepF functions as a ring *in vivo*. However, such structures were not observed with any microscopy studies with *B. subtilis* cells until this date. Therefore, we examined SepF orthologs from several bacteria. Our results showed that most of these SepF orthologs form rings *in vitro*. This shows that SepF ring structure is important for its role in cell division. Moreover, the crystal structure of the C-terminal domain of SepF was solved. The structure showed that SepF exists as dimers in solution and these dimers interact through α-helices to form polymers. However, the structure did not reveal how the polymers form the regular SepF rings. One hypothesis is that the dimers might have a slight angle and polymerization would form the rings. The G137N mutant which is not able to form rings, but polymerizes is mapped to a location where it might change the angle of the dimers. Creating more mutants in this region might give an answer how the SepF rings are formed.

6.2. SepF Tethers FtsZ to the Cell Membrane

SepF interacts with FtsZ through interaction with the C-terminal end of FtsZ (Król et al., 2012, Singh et al., 2008). However, it was not known where FtsZ binds on SepF. In this work, several FtsZ interacting mutants were identified using yeast-two-hybrid assay. These mutants were located at the C-terminal domain of SepF, and most of them were mapped to α-helices (Figure 4.12). These results showed that the C-terminal domain is necessary for polymerization of SepF and interaction between SepF and FtsZ. However, the role of the N-terminal domain was unknown. The *in vitro* and *in vivo* experiments performed showed that the N-terminal end of SepF contains an amphipathic helix. It is also shown that SepF interacts with the cell membrane and tethers FtsZ to it (Figure 6.1).

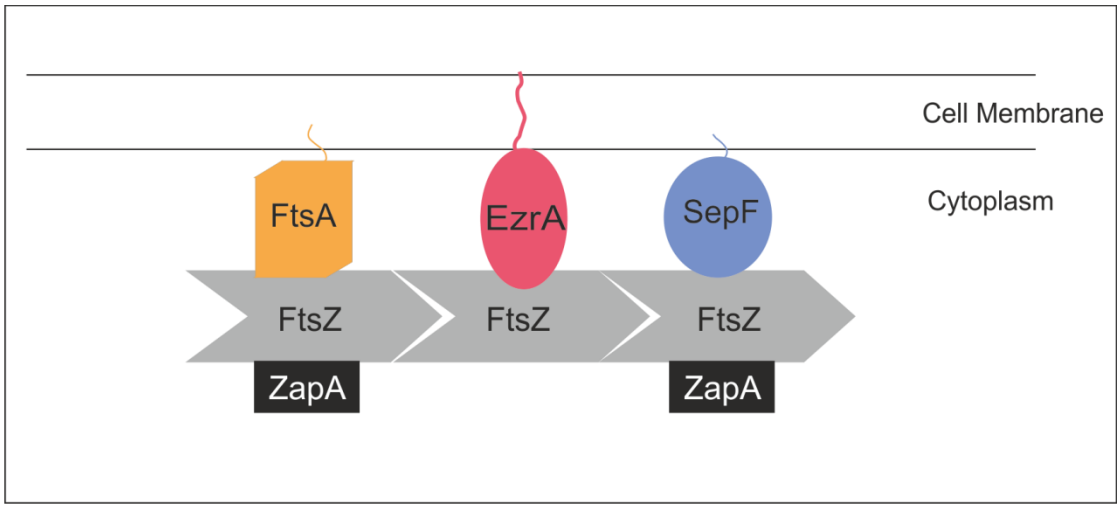

Figure 6.1 Assembly of the Z-ring. SepF and FtsA tether FtsZ to the cell membrane via their amphipathic helix, and EzrA tethers FtsZ to the cell membrane through its transmembrane region while ZapA stabilizes the interaction between FtsZ protofilaments.

The fact that SepF tethers FtsZ to the cell membrane in a similar way as FtsA gives an explanation why FtsA is not essential in *B. subtilis* (Beall and Lutkenhaus, 1992). This also explains how SepF overproduction compensates for *ftsA* deletion and why the *ftsA sepF* double mutant is lethal (Ishikawa et al., 2006).

Interestingly, fluorescent microscopy of liposomes and purified SepF showed that SepF deforms and fuses liposomes (Figure 4.3). The knowledge on SepF obtained so far revealed a model for the role of SepF in cell division

(Figure 4.11). According to this model, SepF forms arcs which surround the newly forming septal membrane. At the same time, the other side of the SepF arcs interacts with FtsZ filaments. Not only SepF forms a membrane anchor for FtsZ, it also limits the width of septa by constraining the FtsZ polymers within a small area; the diameter of the SepF arcs.

6.3. The *Bacillus* Minimal Divisome

The other focus of this work was to construct a strain in which as many non-essential division proteins were removed as possible. Using a novel method, it was possible to have marker-free deletions of 7 genes in a single strain. Additional genes were removed using antibiotic resistant markers. Resulting strains were called F&A, F and AE mother strains (Figure 6.2).

The mother strains showed that cells are able to divide despite missing all known regulatory proteins such as MinC, MinJ, ClpX, UgtP, and Noc. *B. subtilis* only needs SepF and FtsZ or FtsA, EzrA and FtsZ to divide. These proteins form the core divisome complex. It will be interesting to see how many of the late division proteins can be removed.

Some of these deletions have been previously described as being synthetic lethal or synthetic sick. However, we were able to make most combinations; therefore, it is probable that suppressor mutations rescue the cell phenotype. Sequencing of the mother strain genomes will reveal this and might indicate unknown cell division proteins.

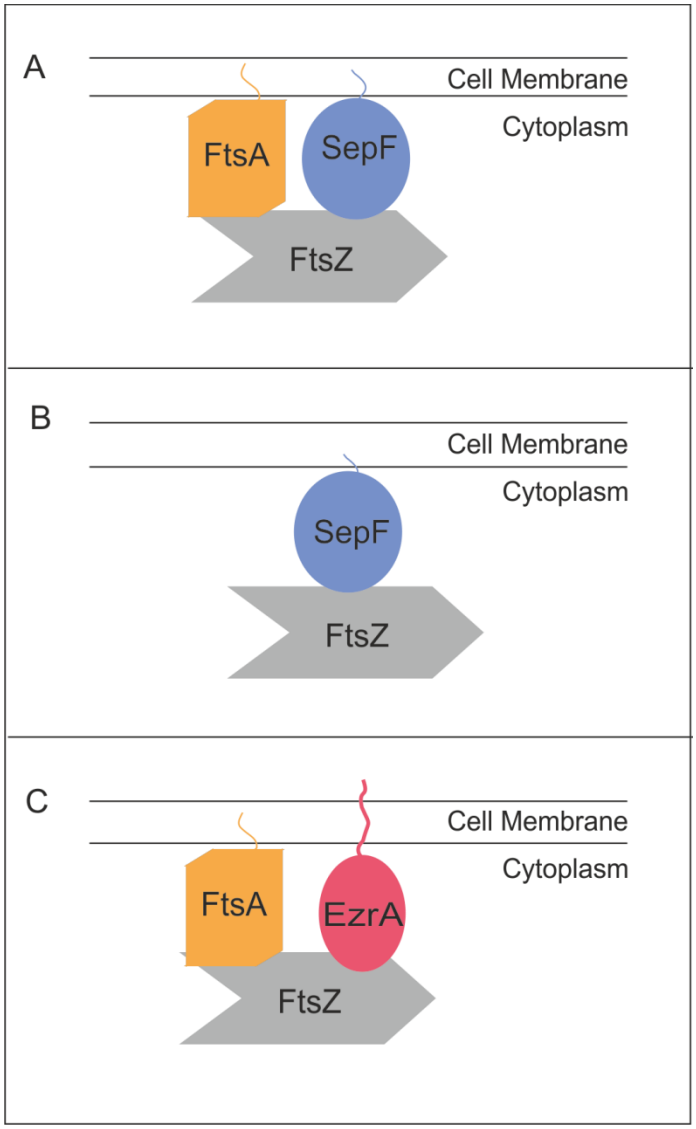

Figure 6.2 The Minimal Divisome mother strains. (A) F&A mother strain contains only SepF and FtsA while misses ZapA, MinC, UgtP, MinJ, EzrA, SpxA, ClpX, and Noc. (B) F mother strain contains only SepF while (C) AE mother strain has EzrA and FtsA.

Chapter 7. Publications

- Van Baarley, S., Celik, I. N., Kaval, K. G., Bramkamp, M., Hamoen, L. W., Halbedel, S. 2013. Protein-protein interaction domains of Bacillus subtilis DivIVA. *Journal of Bacteriology*, 195, 1012-1021.
- Duman, R.*, Ishikawa, S.*, Celik, I.*, Strahl, H., Ogawara, N., Troc, P., Lowe, J., Hamoen, L. W., 2013. Structural and genetic analyses reveal SepF as a new membrane anchor for the Z-ring. *Proceedings of the National Academy of Sciences,* 110(48), 4601-4610 (*these authors contributed equally)

Chapter 8. References

ADAMS, D. W. & ERRINGTON, J. 2009. Bacterial cell division: assembly, maintenance and disassembly of the Z ring. *Nat Rev Micro,* 7**,** 642-653.

ADDINALL, S. G., BI, E. & LUTKENHAUS, J. 1996. FtsZ ring formation in fts mutants. *Journal of Bacteriology,* 178**,** 3877-84.

ADDINALL, S. G., CAO, C. & LUTKENHAUS, J. 1997. FtsN, a late recruit to the septum in Escherichia coli. *Molecular Microbiology,* 25**,** 303-309.

ADDINALL, S. G. & LUTKENHAUS, J. 1996a. FtsA is localized to the septum in an FtsZ-dependent manner. *Journal of Bacteriology,* 178**,** 7167-72.

ADDINALL, S. G. & LUTKENHAUS, J. 1996b. FtsZ-spirals and -arcs determine the shape of the invaginating septa in some mutants of Escherichia coli. *Molecular Microbiology,* 22**,** 231-237.

ADLER H. I., FISHER W. D., COHEN A. & A.A., H. 1967. Miniature Escherichia coli Cells Deficient in DNA. *Proceedings of the National Academy of Sciences,* 57**,** 321-326.

AIZENMAN, E., ENGELBERG-KULKA, H. & GLASER, G. 1996. An Escherichia coli chromosomal "addiction module" regulated by guanosine [corrected] 3',5'-bispyrophosphate: a model for programmed bacterial cell death. *Proceedings of the National Academy of Sciences,* 93**,** 6059-6063.

ALIAS, M., AYUSO-TEJEDOR, S., FERNANDEZ-RECIO, J., CATIVIELA, C. & SANCHO, J. 2010. Helix propensities of conformationally restricted amino acids. Non-natural substitutes for helix breaking proline and helix forming alanine. *Organic & Biomolecular Chemistry,* 8**,** 788-792.

ANAGNOSTOPOULOS, C. & SPIZIZEN, J. 1961. REQUIREMENTS FOR TRANSFORMATION IN BACILLUS SUBTILIS. *Journal of Bacteriology,* 81**,** 741-746.

ANDERSON, D. E., GUEIROS-FILHO, F. J. & ERICKSON, H. P. 2004. Assembly Dynamics of FtsZ Rings in Bacillus subtilis and Escherichia coli and Effects of FtsZ-Regulating Proteins. *Journal of Bacteriology,* 186**,** 5775-5781.

ANDREU, J. M., SCHAFFNER-BARBERO, C., HUECAS, S., ALONSO, D., LOPEZ-RODRIGUEZ, M. L., RUIZ-AVILA, L. B., NÚÑEZ-RAMÍREZ, R., LLORCA, O. & MARTÍN-GALIANO, A. J. 2010. The Antibacterial Cell Division Inhibitor PC190723 Is an FtsZ Polymer-stabilizing Agent That Induces Filament Assembly and Condensation. *Journal of Biological Chemistry,* 285**,** 14239-14246.

BATH, J., WU, L. J., ERRINGTON, J. & WANG, J. C. 2000. Role of Bacillus subtilis SpoIIIE in DNA Transport Across the Mother Cell-Prespore Division Septum. *Science,* 290**,** 995-997.

BEALL, B. & LUTKENHAUS, J. 1992. Impaired cell division and sporulation of a Bacillus subtilis strain with the ftsA gene deleted. *Journal of Bacteriology,* 174**,** 2398-2403.

BEGG, K. J., DEWAR, S. J. & DONACHIE, W. D. 1995. A new Escherichia coli cell division gene, ftsK. *Journal of Bacteriology,* 177**,** 6211-22.

BERNARD, C. S., SADASIVAM, M., SHIOMI, D. & MARGOLIN, W. 2007. An altered FtsA can compensate for the loss of essential cell division protein FtsN in Escherichia coli. *Molecular Microbiology,* 64**,** 1289-1305.

BERNHARDT, T. G. & DE BOER, P. A. J. 2005. SlmA, a Nucleoid-Associated, FtsZ Binding Protein Required for Blocking Septal Ring Assembly over Chromosomes in E. coli. *Molecular cell,* 18**,** 555-564.

BI, E. & LUTKENHAUS, J. 1991. FtsZ ring structure associated with division in Escherichia coli. *Nature,* 354**,** 161-164.
BILLER, S. J. & BURKHOLDER, W. F. 2009. The Bacillus subtilis SftA (YtpS) and SpoIIIE DNA translocases play distinct roles in growing cells to ensure faithful chromosome partitioning. *Molecular Microbiology,* 74**,** 790-809.
BORK, P., SANDER, C. & VALENCIA, A. 1992. An ATPase domain common to prokaryotic cell cycle proteins, sugar kinases, actin, and hsp70 heat shock proteins. *Proceedings of the National Academy of Sciences,* 89**,** 7290-7294.
BOYLE, D. S., KHATTAR, M. M., ADDINALL, S. G., LUTKENHAUS, J. & DONACHIE, W. D. 1997. ftsW is an essential cell-division gene in Escherichia coli. *Molecular Microbiology,* 24**,** 1263-1273.
BRAMHILL, D. & THOMPSON, C. M. 1994. GTP-dependent polymerization of Escherichia coli FtsZ protein to form tubules. *Proceedings of the National Academy of Sciences,* 91**,** 5813-5817.
BRAMKAMP, M., EMMINS, R., WESTON, L., DONOVAN, C., DANIEL, R. A. & ERRINGTON, J. 2008. A novel component of the division-site selection system of Bacillus subtilis and a new mode of action for the division inhibitor MinCD. *Molecular Microbiology,* 70**,** 1556-1569.
BRAMKAMP, M. & VAN BAARLE, S. 2009. Division site selection in rod-shaped bacteria. *Current Opinion in Microbiology,* 12**,** 683-688.
BRAMKAMP, M., WESTON, L., DANIEL, R. A. & ERRINGTON, J. 2006. Regulated intramembrane proteolysis of FtsL protein and the control of cell division in Bacillus subtilis. *Molecular Microbiology,* 62**,** 580-591.
BUDDELMEIJER, N. & BECKWITH, J. 2004. A complex of the Escherichia coli cell division proteins FtsL, FtsB and FtsQ forms independently of its localization to the septal region. *Molecular Microbiology,* 52**,** 1315-1327.
BUDDELMEIJER, N., JUDSON, N., BOYD, D., MEKALANOS, J. J. & BECKWITH, J. 2002. YgbQ, a cell division protein in Escherichia coli and Vibrio cholerae, localizes in codependent fashion with FtsL to the division site. *Proceedings of the National Academy of Sciences,* 99**,** 6316-6321.
BUSKE, P. J. & LEVIN, P. A. 2012. Extreme C Terminus of Bacterial Cytoskeletal Protein FtsZ Plays Fundamental Role in Assembly Independent of Modulatory Proteins. *Journal of Biological Chemistry,* 287**,** 10945-10957.
BUSS, J., COLTHARP, C., HUANG, T., POHLMEYER, C., WANG, S.-C., HATEM, C. & XIAO, J. 2013. In vivo organization of the FtsZ-ring by ZapA and ZapB revealed by quantitative super-resolution microscopy. *Molecular Microbiology,* 89**,** 1099-1120.
CABRÉ, E. J., SÁNCHEZ-GOROSTIAGA, A., CARRARA, P., ROPERO, N., CASANOVA, M., PALACIOS, P., STANO, P., JIMÉNEZ, M., RIVAS, G. & VICENTE, M. 2013. Bacterial Division Proteins FtsZ and ZipA Induce Vesicle Shrinkage and Cell Membrane Invagination. *Journal of Biological Chemistry,* 288**,** 26625-26634.
CAMBERG, J. L., HOSKINS, J. R. & WICKNER, S. 2009. ClpXP protease degrades the cytoskeletal protein, FtsZ, and modulates FtsZ polymer dynamics. *Proceedings of the National Academy of Sciences,* 106**,** 10614-10619.
CAMBERG, J. L., HOSKINS, J. R. & WICKNER, S. 2011. The Interplay of ClpXP with the Cell Division Machinery in Escherichia coli. *Journal of Bacteriology,* 193**,** 1911-1918.

CAPLAN, M. R. & ERICKSON, H. P. 2003. Apparent Cooperative Assembly of the Bacterial Cell Division Protein FtsZ Demonstrated by Isothermal Titration Calorimetry. *Journal of Biological Chemistry,* 278**,** 13784-13788.
CHA, J. H. & STEWART, G. C. 1997. The divIVA minicell locus of Bacillus subtilis. *Journal of Bacteriology,* 179**,** 1671-83.
CHEN, J. C. & BECKWITH, J. 2001. FtsQ, FtsL and FtsI require FtsK, but not FtsN, for co-localization with FtsZ during Escherichia coli cell division. *Molecular Microbiology,* 42**,** 395-413.
CHEN, Y., BJORNSON, K., REDICK, S. D. & ERICKSON, H. P. 2005. A Rapid Fluorescence Assay for FtsZ Assembly Indicates Cooperative Assembly with a Dimer Nucleus. *Biophysical Journal,* 88**,** 505-514.
CHIEN, A.-C., ZAREH, S. K. G., WANG, Y. M. & LEVIN, P. A. 2012. Changes in the oligomerization potential of the division inhibitor UgtP co-ordinate Bacillus subtilis cell size with nutrient availability. *Molecular Microbiology,* 86**,** 594-610.
CHO, H. & BERNHARDT, T. G. 2013. Identification of the SlmA Active Site Responsible for Blocking Bacterial Cytokinetic Ring Assembly over the Chromosome. *PLoS Genet,* 9**,** e1003304.
CHO, H., MCMANUS, H. R., DOVE, S. L. & BERNHARDT, T. G. 2011. Nucleoid occlusion factor SlmA is a DNA-activated FtsZ polymerization antagonist. *Proceedings of the National Academy of Sciences,* 108**,** 3773-3778.
CHUNG, K.-M., HSU, H.-H., GOVINDAN, S. & CHANG, B.-Y. 2004. Transcription Regulation of ezrA and Its Effect on Cell Division of Bacillus subtilis. *Journal of Bacteriology,* 186**,** 5926-5932.
CHUNG, K.-M., HSU, H.-H., YEH, H.-Y. & CHANG, B.-Y. 2007. Mechanism of Regulation of Prokaryotic Tubulin-like GTPase FtsZ by Membrane Protein EzrA. *Journal of Biological Chemistry,* 282**,** 14891-14897.
CLAESSEN, D., EMMINS, R., HAMOEN, L. W., DANIEL, R. A., ERRINGTON, J. & EDWARDS, D. H. 2008. Control of the cell elongation–division cycle by shuttling of PBP1 protein in Bacillus subtilis. *Molecular Microbiology,* 68**,** 1029-1046.
COMMICHAU, F. M., PIETACK, N. & STULKE, J. 2013. Essential genes in Bacillus subtilis: a re-evaluation after ten years. *Molecular BioSystems*.
CONSIDINE, K. M., SLEATOR, R. D., KELLY, A. L., FITZGERALD, G. F. & HILL, C. 2011. Identification and characterization of an essential gene in Listeria monocytogenes using an inducible gene expression system. *Bioengineered,* 2**,** 150-159.
CORBIN, B. D., GEISSLER, B., SADASIVAM, M. & MARGOLIN, W. 2004. Z-Ring-Independent Interaction between a Subdomain of FtsA and Late Septation Proteins as Revealed by a Polar Recruitment Assay. *Journal of Bacteriology,* 186**,** 7736-7744.
DAI, K. & LUTKENHAUS, J. 1992. The proper ratio of FtsZ to FtsA is required for cell division to occur in Escherichia coli. *Journal of Bacteriology,* 174**,** 6145-6151.
DAI, K., XU, Y. & LUTKENHAUS, J. 1993. Cloning and characterization of ftsN, an essential cell division gene in Escherichia coli isolated as a multicopy suppressor of ftsA12(Ts). *Journal of Bacteriology,* 175**,** 3790-3797.
DAI, K., XU, Y. & LUTKENHAUS, J. 1996. Topological characterization of the essential Escherichia coli cell division protein FtsN. *Journal of Bacteriology,* 178**,** 1328-34.

DAJKOVIC, A., LAN, G., SUN, S. X., WIRTZ, D. & LUTKENHAUS, J. 2008. MinC Spatially Controls Bacterial Cytokinesis by Antagonizing the Scaffolding Function of FtsZ. *Current Biology,* 18**,** 235-244.

DANIEL, R. A. & ERRINGTON, J. 2000. Intrinsic instability of the essential cell division protein FtsL of Bacillus subtilis and a role for DivIB protein in FtsL turnover. *Molecular Microbiology,* 36**,** 278-289.

DANIEL, R. A., HARRY, E. J., KATIS, V. L., WAKE, R. G. & ERRINGTON, J. 1998. Characterization of the essential cell division gene ftsL (yllD) of Bacillus subtilis and its role in the assembly of the division apparatus. *Molecular Microbiology,* 29**,** 593-604.

DANIEL, R. A., NOIROT-GROS, M.-F., NOIROT, P. & ERRINGTON, J. 2006. Multiple Interactions between the Transmembrane Division Proteins of Bacillus subtilis and the Role of FtsL Instability in Divisome Assembly. *Journal of Bacteriology,* 188**,** 7396-7404.

DE BOER, P., CROSSLEY, R. & ROTHFIELD, L. 1992a. The essential bacterial cell-division protein FtsZ is a GTPase. *Nature,* 359**,** 254-256.

DE BOER, P. A., CROSSLEY, R. E. & ROTHFIELD, L. I. 1992b. Roles of MinC and MinD in the site-specific septation block mediated by the MinCDE system of Escherichia coli. *Journal of Bacteriology,* 174**,** 63-70.

DE BOER, P. A. J., CROSSLEY, R. E., HAND, A. R. & ROTHFIELD, L. I. 1991. THE MIND PROTEIN IS A MEMBRANE ATPASE REQUIRED FOR THE CORRECT PLACEMENT OF THE ESCHERICHIA-COLI DIVISION SITE. *Embo Journal,* 10**,** 4371-4380.

DE BOER, P. A. J., CROSSLEY, R. E. & ROTHFIELD, L. I. 1989. A division inhibitor and a topological specificity factor coded for by the minicell locus determine proper placement of the division septum in E. coli. *Cell,* 56**,** 641-649.

DE LEEUW, E., GRAHAM, B., PHILLIPS, G. J., TEN HAGEN-JONGMAN, C. M., OUDEGA, B. & LUIRINK, J. 1999. Molecular characterization of Escherichia coli FtsE and FtsX. *Molecular Microbiology,* 31**,** 983-993.

DEMPWOLFF, F., WISCHHUSEN, H. M., SPECHT, M. & GRAUMANN, P. L. 2012. The deletion of bacterial dynamin and flotillin genes results in pleitrophic effects on cell division, cell growth and in cell shape maintenance. *BMC Microbiology,* 12**,** 1-12.

DEN BLAAUWEN, T., BUDDELMEIJER, N., AARSMAN, M. E. G., HAMEETE, C. M. & NANNINGA, N. 1999. Timing of FtsZ Assembly in Escherichia coli. *Journal of Bacteriology,* 181**,** 5167-5175.

DIN, N., QUARDOKUS, E. M., SACKETT, M. J. & BRUN, Y. V. 1998. Dominant C-terminal deletions of FtsZ that affect its ability to localize in Caulobacter and its interaction with FtsA. *Molecular Microbiology,* 27**,** 1051-1063.

DOMÍNGUEZ-CUEVAS, P., PORCELLI, I., DANIEL, R. A. & ERRINGTON, J. 2013. Differentiated roles for MreB-actin isologues and autolytic enzymes in Bacillus subtilis morphogenesis. *Molecular Microbiology,* 89**,** 1084-1098.

DORAZI, R. & DEWAR, S. J. 2000. Membrane topology of the N-terminus of the Escherichia coli FtsK division protein. *FEBS Letters,* 478**,** 13-18.

DRAPER, G. C., MCLENNAN, N., BEGG, K., MASTERS, M. & DONACHIE, W. D. 1998. Only the N-Terminal Domain of FtsK Functions in Cell Division. *Journal of Bacteriology,* 180**,** 4621-4627.

DURAND-HEREDIA, J., RIVKIN, E., FAN, G., MORALES, J. & JANAKIRAMAN, A. 2012. Identification of ZapD as a Cell Division Factor That Promotes

the Assembly of FtsZ in Escherichia coli. *Journal of Bacteriology,* 194**,** 3189-3198.
DURAND-HEREDIA, J. M., YU, H. H., DE CARLO, S., LESSER, C. F. & JANAKIRAMAN, A. 2011. Identification and Characterization of ZapC, a Stabilizer of the FtsZ Ring in Escherichia coli. *Journal of Bacteriology,* 193**,** 1405-1413.
EBERSBACH, G., GALLI, E., MØLLER-JENSEN, J., LÖWE, J. & GERDES, K. 2008. Novel coiled-coil cell division factor ZapB stimulates Z ring assembly and cell division. *Molecular Microbiology,* 68**,** 720-735.
EDWARDS, D. H. & ERRINGTON, J. 1997. The Bacillus subtilis DivIVA protein targets to the division septum and controls the site specificity of cell division. *Molecular Microbiology,* 24**,** 905-915.
EGAN, A. J. F. & VOLLMER, W. 2013. The physiology of bacterial cell division. *Annals of the New York Academy of Sciences,* 1277**,** 8-28.
ERICKSON, H. P. 2001. The FtsZ protofilament and attachment of ZipA—structural constraints on the FtsZ power stroke. *Current Opinion in Cell Biology,* 13**,** 55-60.
ERICKSON, H. P., TAYLOR, D. W., TAYLOR, K. A. & BRAMHILL, D. 1996. Bacterial cell division protein FtsZ assembles into protofilament sheets and minirings, structural homologs of tubulin polymers. *Proceedings of the National Academy of Sciences,* 93**,** 519-523.
ERRINGTON, J., DANIEL, R. A. & SCHEFFERS, D.-J. 2003. Cytokinesis in Bacteria. *Microbiology and Molecular Biology Reviews,* 67**,** 52-65.
ERRINGTON, J. & JONES, D. 1987. Cloning in Bacillus subtilis by Transfection with Bacteriophage Vector ϕ105J27: Isolation and Preliminary Characterization of Transducing Phages for 23 Sporulation Loci. *Journal of General Microbiology,* 133**,** 493-502.
ESPELI, O., BORNE, R., DUPAIGNE, P., THIEL, A., GIGANT, E., MERCIER, R. & BOCCARD, F. 2012. A MatP-divisome interaction coordinates chromosome segregation with cell division in E. coli. *EMBO J,* 31**,** 3198-3211.
FADDA, D., PISCHEDDA, C., CALDARA, F., WHALEN, M. B., ANDERLUZZI, D., DOMENICI, E. & MASSIDDA, O. 2003. Characterization of divIVA and Other Genes Located in the Chromosomal Region Downstream of the dcw Cluster in Streptococcus pneumoniae. *Journal of Bacteriology,* 185**,** 6209-6214.
FEUCHT, A., LUCET, I., YUDKIN, M. D. & ERRINGTON, J. 2001. Cytological and biochemical characterization of the FtsA cell division protein of Bacillus subtilis. *Molecular Microbiology,* 40**,** 115-125.
FU, X., SHIH, Y.-L., ZHANG, Y. & ROTHFIELD, L. I. 2001. The MinE ring required for proper placement of the division site is a mobile structure that changes its cellular location during the Escherichia coli division cycle. *Proceedings of the National Academy of Sciences,* 98**,** 980-985.
GALLI, E. & GERDES, K. 2010. Spatial resolution of two bacterial cell division proteins: ZapA recruits ZapB to the inner face of the Z-ring. *Molecular Microbiology,* 76**,** 1514-1526.
GALLI, E. & GERDES, K. 2012. FtsZ-ZapA-ZapB Interactome of Escherichia coli. *Journal of Bacteriology,* 194**,** 292-302.
GAMBA, P., VEENING, J.-W., SAUNDERS, N. J., HAMOEN, L. W. & DANIEL, R. A. 2009. Two-Step Assembly Dynamics of the Bacillus subtilis Divisome. *Journal of Bacteriology,* 191**,** 4186-4194.

GARTI-LEVI, S., HAZAN, R., KAIN, J., FUJITA, M. & BEN-YEHUDA, S. 2008. The FtsEX ABC transporter directs cellular differentiation in Bacillus subtilis. *Molecular Microbiology,* 69**,** 1018-1028.
GAYDA, R. C., HENK, M. C. & LEONG, D. 1992. C-shaped cells caused by expression of an ftsA mutation in Escherichia coli. *Journal of Bacteriology,* 174**,** 5362-5370.
GEISSLER, B., ELRAHEB, D. & MARGOLIN, W. 2003. A gain-of-function mutation in ftsA bypasses the requirement for the essential cell division gene zipA in Escherichia coli. *Proceedings of the National Academy of Sciences,* 100**,** 4197-4202.
GEISSLER, B. & MARGOLIN, W. 2005. Evidence for functional overlap among multiple bacterial cell division proteins: compensating for the loss of FtsK. *Molecular Microbiology,* 58**,** 596-612.
GEISSLER, B., SHIOMI, D. & MARGOLIN, W. 2007. The ftsA* gain-of-function allele of Escherichia coli and its effects on the stability and dynamics of the Z ring. *Microbiology,* 153**,** 814-825.
GÉRARD, P., VERNET, T. & ZAPUN, A. 2002. Membrane Topology of the Streptococcus pneumoniae FtsW Division Protein. *Journal of Bacteriology,* 184**,** 1925-1931.
GERDING, M. A., LIU, B., BENDEZÚ, F. O., HALE, C. A., BERNHARDT, T. G. & DE BOER, P. A. J. 2009. Self-Enhanced Accumulation of FtsN at Division Sites and Roles for Other Proteins with a SPOR Domain (DamX, DedD, and RlpA) in Escherichia coli Cell Constriction. *Journal of Bacteriology,* 191**,** 7383-7401.
GILL, D., HATFULL, G. & SALMOND, G. C. 1986. A new cell division operon inEscherichia coli. *Molecular and General Genetics MGG,* 205**,** 134-145.
GOEHRING, N. W., PETROVSKA, I., BOYD, D. & BECKWITH, J. 2007a. Mutants, Suppressors, and Wrinkled Colonies: Mutant Alleles of the Cell Division Gene ftsQ Point to Functional Domains in FtsQ and a Role for Domain 1C of FtsA in Divisome Assembly. *Journal of Bacteriology,* 189**,** 633-645.
GOEHRING, N. W., ROBICHON, C. & BECKWITH, J. 2007b. Role for the Nonessential N Terminus of FtsN in Divisome Assembly. *Journal of Bacteriology,* 189**,** 646-649.
GOFFIN, C. & GHUYSEN, J.-M. 1998. Multimodular Penicillin-Binding Proteins: An Enigmatic Family of Orthologs and Paralogs. *Microbiology and Molecular Biology Reviews,* 62**,** 1079-1093.
GONZÁLEZ, J. M., VÉLEZ, M., JIMÉNEZ, M., ALFONSO, C., SCHUCK, P., MINGORANCE, J., VICENTE, M., MINTON, A. P. & RIVAS, G. 2005. Cooperative behavior of Escherichia coli cell-division protein FtsZ assembly involves the preferential cyclization of long single-stranded fibrils. *Proceedings of the National Academy of Sciences of the United States of America,* 102**,** 1895-1900.
GOUJON, M., MCWILLIAM, H., LI, W., VALENTIN, F., SQUIZZATO, S., PAERN, J. & LOPEZ, R. 2010. A new bioinformatics analysis tools framework at EMBL–EBI. *Nucleic Acids Research,* 38**,** W695-W699.
GUEIROS-FILHO, F. J. & LOSICK, R. 2002. A widely conserved bacterial cell division protein that promotes assembly of the tubulin-like protein FtsZ. *Genes & Development,* 16**,** 2544-2556.
GUNDOGDU, M. E., KAWAI, Y., PAVLENDOVA, N., OGASAWARA, N., ERRINGTON, J., SCHEFFERS, D.-J. & HAMOEN, L. W. 2011. Large

ring polymers align FtsZ polymers for normal septum formation. *EMBO J,* 30**,** 617-626.
GUZMAN LM, BARONDESS JJ & J, B. 1992. FtsL, an essential cytoplasmic membrane protein involved in cell division in Escherichia coli. *Journal of Bacteriology,* 174**,** 7716-7728.
HAEUSSER, D. P., GARZA, A. C., BUSCHER, A. Z. & LEVIN, P. A. 2007. The Division Inhibitor EzrA Contains a Seven-Residue Patch Required for Maintaining the Dynamic Nature of the Medial FtsZ Ring. *Journal of Bacteriology,* 189**,** 9001-9010.
HAEUSSER, D. P., LEE, A. H., WEART, R. B. & LEVIN, P. A. 2009. ClpX Inhibits FtsZ Assembly in a Manner That Does Not Require Its ATP Hydrolysis-Dependent Chaperone Activity. *Journal of Bacteriology,* 191**,** 1986-1991.
HAEUSSER, DANIEL P. & MARGOLIN, W. 2011. Prokaryotic Cytokinesis: Little Rings Bring Big Cylindrical Things. *Current Biology,* 21**,** R221-R223.
HAEUSSER, D. P., SCHWARTZ, R. L., SMITH, A. M., OATES, M. E. & LEVIN, P. A. 2004. EzrA prevents aberrant cell division by modulating assembly of the cytoskeletal protein FtsZ. *Molecular Microbiology,* 52**,** 801-814.
HALE, C. A. & DE BOER, P. A. J. 1997. Direct Binding of FtsZ to ZipA, an Essential Component of the Septal Ring Structure That Mediates Cell Division in E. coli. *Cell,* 88**,** 175-185.
HALE, C. A. & DE BOER, P. A. J. 1999. Recruitment of ZipA to the Septal Ring ofEscherichia coli Is Dependent on FtsZ and Independent of FtsA. *Journal of Bacteriology,* 181**,** 167-176.
HALE, C. A. & DE BOER, P. A. J. 2002. ZipA Is Required for Recruitment of FtsK, FtsQ, FtsL, and FtsN to the Septal Ring in Escherichia coli. *Journal of Bacteriology,* 184**,** 2552-2556.
HALE, C. A., MEINHARDT, H. & DE BOER, P. A. J. 2001. Dynamic localization cycle of the cell division regulator MinE in Escherichia coli. *EMBO J,* 20**,** 1563-1572.
HALE, C. A., RHEE, A. C. & DE BOER, P. A. J. 2000. ZipA-Induced Bundling of FtsZ Polymers Mediated by an Interaction between C-Terminal Domains. *Journal of Bacteriology,* 182**,** 5153-5166.
HALE, C. A., SHIOMI, D., LIU, B., BERNHARDT, T. G., MARGOLIN, W., NIKI, H. & DE BOER, P. A. J. 2011. Identification of Escherichia coli ZapC (YcbW) as a Component of the Division Apparatus That Binds and Bundles FtsZ Polymers. *Journal of Bacteriology,* 193**,** 1393-1404.
HAMOEN, L. W., MEILE, J.-C., DE JONG, W., NOIROT, P. & ERRINGTON, J. 2006. SepF, a novel FtsZ-interacting protein required for a late step in cell division. *Molecular Microbiology,* 59**,** 989-999.
HAMOEN, L. W., SMITS, W. K., JONG, A. D., HOLSAPPEL, S. & KUIPERS, O. P. 2002. Improving the predictive value of the competence transcription factor (ComK) binding site in Bacillus subtilis using a genomic approach. *Nucleic Acids Research,* 30**,** 5517-5528.
HANEY, S. A., GLASFELD, E., HALE, C., KEENEY, D., HE, Z. & DE BOER, P. 2001. Genetic Analysis of the Escherichia coli FtsZ·ZipA Interaction in the Yeast Two-hybrid System: CHARACTERIZATION OF FtsZ RESIDUES ESSENTIAL FOR THE INTERACTIONS WITH ZipA AND WITH FtsA. *Journal of Biological Chemistry,* 276**,** 11980-11987.
HARRY, E. J., PARTRIDGE, S. R., WEISS, A. S. & WAKE, R. G. 1994. Conservation of the 168 divIB gene in Bacillus subtilis W23 and B.

licheniformis, and evidence for homology to ftsQ of Escherichia coli. *Gene,* 147**,** 85-89.
HARRY, E. J. & WAKE, R. G. 1989. Cloning and expression of a Bacillus subtilis division initiation gene for which a homolog has not been identified in another organism. *Journal of Bacteriology,* 171**,** 6835-6839.
HARRY, E. J. & WAKE, R. G. 1997. The membrane-bound cell division protein DivIB is localized to the division site in Bacillus subtilis. *Molecular Microbiology,* 25**,** 275-283.
HAYDON, D. J., STOKES, N. R., URE, R., GALBRAITH, G., BENNETT, J. M., BROWN, D. R., BAKER, P. J., BARYNIN, V. V., RICE, D. W., SEDELNIKOVA, S. E., HEAL, J. R., SHERIDAN, J. M., AIWALE, S. T., CHAUHAN, P. K., SRIVASTAVA, A., TANEJA, A., COLLINS, I., ERRINGTON, J. & CZAPLEWSKI, L. G. 2008. An Inhibitor of FtsZ with Potent and Selective Anti-Staphylococcal Activity. *Science,* 321**,** 1673-1675.
HEITKAMP, T., KALINOWSKI, R., BÖTTCHER, B., BÖRSCH, M., ALTENDORF, K. & GREIE, J.-C. 2008. K+-Translocating KdpFABC P-Type ATPase from Escherichia coli Acts as a Functional and Structural Dimer†. *Biochemistry,* 47**,** 3564-3575.
HENRIQUES, A. O., DE LENCASTRE, H. & PIGGOT, P. J. 1992. A Bacillus subtilis morphogene cluster that includes spoVE is homologous to the mra region of Escherichia coli. *Biochimie,* 74**,** 735-748.
HÖLTJE, J.-V. 1998. Growth of the Stress-Bearing and Shape-Maintaining Murein Sacculus of Escherichia coli. *Microbiology and Molecular Biology Reviews,* 62**,** 181-203.
HU, Z. & LUTKENHAUS, J. 2000. Analysis of MinC Reveals Two Independent Domains Involved in Interaction with MinD and FtsZ. *Journal of Bacteriology,* 182**,** 3965-3971.
HU, Z. & LUTKENHAUS, J. 2001. Topological Regulation of Cell Division in E. coli: Spatiotemporal Oscillation of MinD Requires Stimulation of Its ATPase by MinE and Phospholipid. *Molecular Cell,* 7**,** 1337-1343.
HU, Z. & LUTKENHAUS, J. 2003. A conserved sequence at the C-terminus of MinD is required for binding to the membrane and targeting MinC to the septum. *Molecular Microbiology,* 47**,** 345-355.
HU, Z., MUKHERJEE, A., PICHOFF, S. & LUTKENHAUS, J. 1999. The MinC component of the division site selection system in Escherichia coli interacts with FtsZ to prevent polymerization. *Proceedings of the National Academy of Sciences,* 96**,** 14819-14824.
IKEDA, M., SATO, T., WACHI, M., JUNG, H. K., ISHINO, F., KOBAYASHI, Y. & MATSUHASHI, M. 1989. Structural similarity among Escherichia coli FtsW and RodA proteins and Bacillus subtilis SpoVE protein, which function in cell division, cell elongation, and spore formation, respectively. *Journal of Bacteriology,* 171**,** 6375-6378.
ISHIKAWA, S., KAWAI, Y., HIRAMATSU, K., KUWANO, M. & OGASAWARA, N. 2006. A new FtsZ-interacting protein, YlmF, complements the activity of FtsA during progression of cell division in Bacillus subtilis. *Molecular Microbiology,* 60**,** 1364-1380.
JENSEN, S. O., THOMPSON, L. S. & HARRY, E. J. 2005. Cell Division in Bacillus subtilis: FtsZ and FtsA Association Is Z-Ring Independent, and FtsA Is Required for Efficient Midcell Z-Ring Assembly. *Journal of Bacteriology,* 187**,** 6536-6544.

JONES, D. T. 1999. Protein secondary structure prediction based on position-specific scoring matrices. *Journal of Molecular Biology,* 292**,** 195-202.
JORASCH, P., WOLTER, F. P., ZÄHRINGER, U. & HEINZ, E. 1998. A UDP glucosyltransferase from Bacillus subtilis successively transfers up to four glucose residues to 1,2-diacylglycerol: expression of ypfP in Escherichia coli and structural analysis of its reaction products. *Molecular Microbiology,* 29**,** 419-430.
JORGE, A. M., HOICZYK, E., GOMES, J. P. & PINHO, M. G. 2011. EzrA Contributes to the Regulation of Cell Size in <italic>Staphylococcus aureus</italic>. *PLoS ONE,* 6**,** e27542.
JUTRAS, B. L., CHENAIL, A. M., ROWLAND, C. L., CARROLL, D., MILLER, M. C., BYKOWSKI, T. & STEVENSON, B. 2013. Eubacterial SpoVG Homologs Constitute a New Family of Site-Specific DNA-Binding Proteins. *PLoS ONE,* 8**,** e66683.
KAIMER, C., GONZÁLEZ-PASTOR, J. E. & GRAUMANN, P. L. 2009. SpoIIIE and a novel type of DNA translocase, SftA, couple chromosome segregation with cell division in Bacillus subtilis. *Molecular Microbiology,* 74**,** 810-825.
KATIS, V. L., HARRY, E. J. & WAKE, R. G. 1997. The Bacillus subtilis division protein DivIC is a highly abundant membrane-bound protein that localizes to the division site. *Molecular Microbiology,* 26**,** 1047-1055.
KATIS, V. L. & WAKE, R. G. 1999. Membrane-Bound Division Proteins DivIB and DivIC ofBacillus subtilis Function Solely through Their External Domains in both Vegetative and Sporulation Division. *Journal of Bacteriology,* 181**,** 2710-2718.
KATIS, V. L., WAKE, R. G. & HARRY, E. J. 2000. Septal Localization of the Membrane-Bound Division Proteins ofBacillus subtilis DivIB and DivIC Is Codependent Only at High Temperatures and Requires FtsZ. *Journal of Bacteriology,* 182**,** 3607-3611.
KAWAI, Y., DANIEL, R. A. & ERRINGTON, J. 2009. Regulation of cell wall morphogenesis in Bacillus subtilis by recruitment of PBP1 to the MreB helix. *Molecular Microbiology,* 71**,** 1131-1144.
KAWAI, Y. & OGASAWARA, N. 2006. Bacillus subtilis EzrA and FtsL synergistically regulate FtsZ ring dynamics during cell division. *Microbiology,* 152**,** 1129-1141.
KRÓL, E. & SCHEFFERS, D.-J. 2013. FtsZ Polymerization Assays: Simple Protocols and Considerations. e50844.
KRÓL, E., VAN KESSEL, S. P., VAN BEZOUWEN, L. S., KUMAR, N., BOEKEMA, E. J. & SCHEFFERS, D.-J. 2012. <italic>Bacillus subtilis</italic> SepF Binds to the C-Terminus of FtsZ. *PLoS ONE,* 7**,** e43293.
KUNST, F., OGASAWARA, N., MOSZER, I., ALBERTINI, A. M., ALLONI, G., AZEVEDO, V., BERTERO, M. G., BESSIERES, P., BOLOTIN, A., BORCHERT, S., BORRISS, R., BOURSIER, L., BRANS, A., BRAUN, M., BRIGNELL, S. C., BRON, S., BROUILLET, S., BRUSCHI, C. V., CALDWELL, B., CAPUANO, V., CARTER, N. M., CHOI, S. K., CODANI, J. J., CONNERTON, I. F., CUMMINGS, N. J., DANIEL, R. A., DENIZOT, F., DEVINE, K. M., DUSTERHOFT, A., EHRLICH, S. D., EMMERSON, P. T., ENTIAN, K. D., ERRINGTON, J., FABRET, C., FERRARI, E., FOULGER, D., FRITZ, C., FUJITA, M., FUJITA, Y., FUMA, S., GALIZZI, A., GALLERON, N., GHIM, S. Y., GLASER, P., GOFFEAU, A., GOLIGHTLY, E. J., GRANDI, G., GUISEPPI, G., GUY, B. J., HAGA, K.,

HAIECH, J., HARWOOD, C. R., HENAUT, A., HILBERT, H., HOLSAPPEL, S., HOSONO, S., HULLO, M. F., ITAYA, M., JONES, L., JORIS, B., KARAMATA, D., KASAHARA, Y., KLAERR-BLANCHARD, M., KLEIN, C., KOBAYASHI, Y., KOETTER, P., KONINGSTEIN, G., KROGH, S., KUMANO, M., KURITA, K., LAPIDUS, A., LARDINOIS, S., LAUBER, J., LAZAREVIC, V., LEE, S. M., LEVINE, A., LIU, H., MASUDA, S., MAUEL, C., MEDIGUE, C., MEDINA, N., MELLADO, R. P., MIZUNO, M., MOESTL, D., NAKAI, S., NOBACK, M., NOONE, D., O'REILLY, M., OGAWA, K., OGIWARA, A., OUDEGA, B., PARK, S. H., PARRO, V., POHL, T. M., PORTETELLE, D., PORWOLLIK, S., PRESCOTT, A. M., PRESECAN, E., PUJIC, P., PURNELLE, B., et al. 1997. The complete genome sequence of the Gram-positive bacterium Bacillus subtilis. *Nature,* 390**,** 249-256.

LARA, B. & AYALA, J. A. 2002. Topological characterization of the essential Escherichia coli cell division protein FtsW. *FEMS Microbiology Letters,* 216**,** 23-32.

LENARCIC, R., HALBEDEL, S., VISSER, L., SHAW, M., WU, L. J., ERRINGTON, J., MARENDUZZO, D. & HAMOEN, L. W. 2009. Localisation of DivIVA by targeting to negatively curved membranes. *EMBO J,* 28**,** 2272-2282.

LEVIN P. A., MARGOLIS P.S., SETLOW P., LOSICK R. & D., S. 1992. Identification of Bacillus subtilis genes for septum placement and shape determination. *Journal of Bacteriology,* 174**,** 6717-6728.

LEVIN, P. A., KURTSER, I. G. & GROSSMAN, A. D. 1999. Identification and characterization of a negative regulator of FtsZ ring formation in Bacillus subtilis. *Proceedings of the National Academy of Sciences,* 96**,** 9642-9647.

LEVIN, P. A. & LOSICK, R. 1994. Characterization of a cell division gene from Bacillus subtilis that is required for vegetative and sporulation septum formation. *Journal of Bacteriology,* 176**,** 1451-1459.

LEVIN, P. A., SCHWARTZ, R. L. & GROSSMAN, A. D. 2001. Polymer Stability Plays an Important Role in the Positional Regulation of FtsZ. *Journal of Bacteriology,* 183**,** 5449-5452.

LI, Z., TRIMBLE, M. J., BRUN, Y. V. & JENSEN, G. J. 2007. The structure of FtsZ filaments in vivo suggests a force-generating role in cell division. *EMBO J,* 26**,** 4694-4708.

LIU, G., DRAPER, G. C. & DONACHIE, W. D. 1998. FtsK is a bifunctional protein involved in cell division and chromosome localization in Escherichia coli. *Molecular Microbiology,* 29**,** 893-903.

LIU, Z., MUKHERJEE, A. & LUTKENHAUS, J. 1999. Recruitment of ZipA to the division site by interaction with FtsZ. *Molecular Microbiology,* 31**,** 1853-1861.

LOOSE, M., FISCHER-FRIEDRICH, E., HEROLD, C., KRUSE, K. & SCHWILLE, P. 2011. Min protein patterns emerge from rapid rebinding and membrane interaction of MinE. *Nat Struct Mol Biol,* 18**,** 577-583.

LÓPEZ-MONTERO, I., LÓPEZ-NAVAJAS, P., MINGORANCE, J., VÉLEZ, M., VICENTE, M. & MONROY, F. 2013. Membrane reconstitution of FtsZ–ZipA complex inside giant spherical vesicles made of E. coli lipids: Large membrane dilation and analysis of membrane plasticity. *Biochimica et Biophysica Acta (BBA) - Biomembranes,* 1828**,** 687-698.

LOW, H. H., MONCRIEFFE, M. C. & LÖWE, J. 2004. The Crystal Structure of ZapA and its Modulation of FtsZ Polymerisation. *Journal of Molecular Biology,* 341**,** 839-852.
LÖWE, J. 1998. Crystal Structure Determination of FtsZ fromMethanococcus jannaschii. *Journal of Structural Biology,* 124**,** 235-243.
LU, C., REEDY, M. & ERICKSON, H. P. 2000. Straight and Curved Conformations of FtsZ Are Regulated by GTP Hydrolysis. *Journal of Bacteriology,* 182**,** 164-170.
LUTKENHAUS, J. 2009. FtsN—Trigger for Septation. *Journal of Bacteriology,* 191**,** 7381-7382.
MA, X., EHRHARDT, D. W. & MARGOLIN, W. 1996. Colocalization of cell division proteins FtsZ and FtsA to cytoskeletal structures in living Escherichia coli cells by using green fluorescent protein. *Proceedings of the National Academy of Sciences,* 93**,** 12998-13003.
MA, X. & MARGOLIN, W. 1999. Genetic and Functional Analyses of the Conserved C-Terminal Core Domain of Escherichia coli FtsZ. *Journal of Bacteriology,* 181**,** 7531-7544.
MARBOUTY, M., SAGUEZ, C., CASSIER-CHAUVAT, C. & CHAUVAT, F. 2009. Characterization of the FtsZ-Interacting Septal Proteins SepF and Ftn6 in the Spherical-Celled Cyanobacterium Synechocystis Strain PCC 6803. *Journal of Bacteriology,* 191**,** 6178-6185.
MARGOLIN, W. 2005. FtsZ and the division of prokaryotic cells and organelles. *Nat Rev Mol Cell Biol,* 6**,** 862-871.
MARSTON, A. L., THOMAIDES, H. B., EDWARDS, D. H., SHARPE, M. E. & ERRINGTON, J. 1998. Polar localization of the MinD protein of Bacillus subtilis and its role in selection of the mid-cell division site. *Genes & Development,* 12**,** 3419-3430.
MASSON, S., KERN, T., LE GOUËLLEC, A., GIUSTINI, C., SIMORRE, J.-P., CALLOW, P., VERNET, T., GABEL, F. & ZAPUN, A. 2009. Central Domain of DivIB Caps the C-terminal Regions of the FtsL/DivIC Coiled-coil Rod. *Journal of Biological Chemistry,* 284**,** 27687-27700.
MATSUHASHI, M. 1994. *Utilization of lipid-linked precursors and the formation of peptidoglycan in the process of cell growth and division: membrane enzymes involved in the final steps of peptidoglycan synthesis and the mechanism of their regulation,* Amsterdam, Elsevier Science BV.
MATSUNO, K. & SONENSHEIN, A. L. 1999. Role of SpoVG in Asymmetric Septation inBacillus subtilis. *Journal of Bacteriology,* 181**,** 3392-3401.
MEISNER, J., MONTERO LLOPIS, P., SHAM, L.-T., GARNER, E., BERNHARDT, T. G. & RUDNER, D. Z. 2013. FtsEX is required for CwlO peptidoglycan hydrolase activity during cell wall elongation in Bacillus subtilis. *Molecular Microbiology,* 89**,** 1069-1083.
MENDIETA, J., RICO, A. I., LÓPEZ-VIÑAS, E., VICENTE, M., MINGORANCE, J. & GÓMEZ-PUERTAS, P. 2009. Structural and Functional Model for Ionic (K+/Na+) and pH Dependence of GTPase Activity and Polymerization of FtsZ, the Prokaryotic Ortholog of Tubulin. *Journal of Molecular Biology,* 390**,** 17-25.
MINGORANCE, J., TADROS, M., VICENTE, M., GONZÁLEZ, J. M., RIVAS, G. & VÉLEZ, M. 2005. Visualization of Single Escherichia coli FtsZ Filament Dynamics with Atomic Force Microscopy. *Journal of Biological Chemistry,* 280**,** 20909-20914.

MIYAGISHIMA, S.-Y., WOLK, C. P. & OSTERYOUNG, K. W. 2005. Identification of cyanobacterial cell division genes by comparative and mutational analyses. *Molecular Microbiology,* 56**,** 126-143.
MOHAMMADI, T., PLOEGER, G. E. J., VERHEUL, J., COMVALIUS, A. D., MARTOS, A., ALFONSO, C., VAN MARLE, J., RIVAS, G. N. & DEN BLAAUWEN, T. 2009. The GTPase Activity of Escherichia coli FtsZ Determines the Magnitude of the FtsZ Polymer Bundling by ZapA in Vitro. *Biochemistry,* 48**,** 11056-11066.
MOHAMMADI, T., VAN DAM, V., SIJBRANDI, R., VERNET, T., ZAPUN, A., BOUHSS, A., DIEPEVEEN-DE BRUIN, M., NGUYEN-DISTECHE, M., DE KRUIJFF, B. & BREUKINK, E. 2011. Identification of FtsW as a transporter of lipid-linked cell wall precursors across the membrane. *EMBO J,* 30**,** 1425-1432.
MONAHAN, L. G., ROBINSON, A. & HARRY, E. J. 2009. Lateral FtsZ association and the assembly of the cytokinetic Z ring in bacteria. *Molecular Microbiology,* 74**,** 1004-1017.
MORIMOTO, T., ARA, K., OZAKI, K. & OGASAWARA, N. 2011. A Simple Method for Introducing Marker-Free Deletions in the Bacillus subtilis Genome. *In:* WILLIAMS, J. A. (ed.) *Strain Engineering.* Humana Press.
MOSYAK, L., ZHANG, Y., GLASFELD, E., HANEY, S., STAHL, M., SEEHRA, J. & SOMERS, W. S. 2000. The bacterial cell-division protein ZipA and its interaction with an FtsZ fragment revealed by X-ray crystallography. *EMBO J,* 19**,** 3179-3191.
MOY, F. J., GLASFELD, E., MOSYAK, L. & POWERS, R. 2000. Solution Structure of ZipA, a Crucial Component of Escherichia coli Cell Division†. *Biochemistry,* 39**,** 9146-9156.
MUKHERJEE, A., DAI, K. & LUTKENHAUS, J. 1993. Escherichia coli cell division protein FtsZ is a guanine nucleotide binding protein. *Proceedings of the National Academy of Sciences,* 90**,** 1053-1057.
MUKHERJEE, A. & LUTKENHAUS, J. 1994. Guanine nucleotide-dependent assembly of FtsZ into filaments. *Journal of Bacteriology,* 176**,** 2754-2758.
MUKHERJEE, A. & LUTKENHAUS, J. 1998. Dynamic assembly of FtsZ regulated by GTP hydrolysis. *EMBO J,* 17**,** 462-469.
MURRAY, T., POPHAM, D. L. & SETLOW, P. 1998. Bacillus subtilis Cells Lacking Penicillin-Binding Protein 1 Require Increased Levels of Divalent Cations for Growth. *Journal of Bacteriology,* 180**,** 4555-4563.
NAKANO, M. M., HAJARIZADEH, F., ZHU, Y. & ZUBER, P. 2001. Loss-of-function mutations in yjbD result in ClpX- and ClpP-independent competence development of Bacillus subtilis. *Molecular Microbiology,* 42**,** 383-394.
NAKANO, M. M., NAKANO, S. & ZUBER, P. 2002. Spx (YjbD), a negative effector of competence in Bacillus subtilis, enhances ClpC–MecA–ComK interaction. *Molecular Microbiology,* 44**,** 1341-1349.
NAKANO, M. M., ZHU, Y., LIU, J., REYES, D. Y., YOSHIKAWA, H. & ZUBER, P. 2000. Mutations conferring amino acid residue substitutions in the carboxy-terminal domain of RNA polymerase α can suppress clpX and clpP with respect to developmentally regulated transcription in Bacillus subtilis. *Molecular Microbiology,* 37**,** 869-884.
NISHIBORI, A., KUSAKA, J., HARA, H., UMEDA, M. & MATSUMOTO, K. 2005. Phosphatidylethanolamine Domains and Localization of Phospholipid Synthases in Bacillus subtilis Membranes. *Journal of Bacteriology,* 187**,** 2163-2174.

NOIRCLERC-SAVOYE, M., LE GOUËLLEC, A., MORLOT, C., DIDEBERG, O., VERNET, T. & ZAPUN, A. 2005. In vitro reconstitution of a trimeric complex of DivIB, DivIC and FtsL, and their transient co-localization at the division site in Streptococcus pneumoniae. *Molecular Microbiology,* 55**,** 413-424.

OLIVA, M. A., HUECAS, S., PALACIOS, J. M., MARTÍN-BENITO, J., VALPUESTA, J. M. & ANDREU, J. M. 2003. Assembly of Archaeal Cell Division Protein FtsZ and a GTPase-inactive Mutant into Double-stranded Filaments. *Journal of Biological Chemistry,* 278**,** 33562-33570.

OLIVA, M. A., TRAMBAIOLO, D. & LÖWE, J. 2007. Structural Insights into the Conformational Variability of FtsZ. *Journal of Molecular Biology,* 373**,** 1229-1242.

OSAWA, M., ANDERSON, D. E. & ERICKSON, H. P. 2008. Reconstitution of Contractile FtsZ Rings in Liposomes. *Science,* 320**,** 792-794.

OSAWA, M. & ERICKSON, H. P. 2011. Inside-out Z rings – constriction with and without GTP hydrolysis. *Molecular Microbiology,* 81**,** 571-579.

OSAWA, M. & ERICKSON, H. P. 2013. Liposome division by a simple bacterial division machinery. *Proceedings of the National Academy of Sciences,* 110**,** 11000-11004.

PACHECO‐GÓMEZ, R., CHENG, X., HICKS, M. R., SMITH, C. J. I., ROPER, D. I., ADDINALL, S., RODGER, A. & DAFFORN, T. R. 2013. Tetramerization of ZapA is required for FtsZ bundling. *Biochemical Journal,* 449**,** 795-802.

PARK, K.-T., WU, W., BATTAILE, KEVIN P., LOVELL, S., HOLYOAK, T. & LUTKENHAUS, J. 2011. The Min Oscillator Uses MinD-Dependent Conformational Changes in MinE to Spatially Regulate Cytokinesis. *Cell,* 146**,** 396-407.

PASTORET, S., FRAIPONT, C., DEN BLAAUWEN, T., WOLF, B., AARSMAN, M. E. G., PIETTE, A., THOMAS, A., BRASSEUR, R. & NGUYEN-DISTÈCHE, M. 2004. Functional Analysis of the Cell Division Protein FtsW of Escherichia coli. *Journal of Bacteriology,* 186**,** 8370-8379.

PATRICK, J. E. & KEARNS, D. B. 2008. MinJ (YvjD) is a topological determinant of cell division in Bacillus subtilis. *Molecular Microbiology,* 70**,** 1166-1179.

PAZOS, M., NATALE, P. & VICENTE, M. 2013. A Specific Role for the ZipA Protein in Cell Division: STABILIZATION OF THE FtsZ PROTEIN. *Journal of Biological Chemistry,* 288**,** 3219-3226.

PETERS, P. C., MIGOCKI, M. D., THONI, C. & HARRY, E. J. 2007. A new assembly pathway for the cytokinetic Z ring from a dynamic helical structure in vegetatively growing cells of Bacillus subtilis. *Molecular Microbiology,* 64**,** 487-499.

PICHOFF, S. & LUTKENHAUS, J. 2002. Unique and overlapping roles for ZipA and FtsA in septal ring assembly in Escherichia coli. *EMBO J,* 21**,** 685-693.

PICHOFF, S. & LUTKENHAUS, J. 2005. Tethering the Z ring to the membrane through a conserved membrane targeting sequence in FtsA. *Molecular Microbiology,* 55**,** 1722-1734.

PICHOFF, S. & LUTKENHAUS, J. 2007. Identification of a region of FtsA required for interaction with FtsZ. *Molecular Microbiology,* 64**,** 1129-1138.

PICHOFF, S., SHEN, B., SULLIVAN, B. & LUTKENHAUS, J. 2012. FtsA mutants impaired for self-interaction bypass ZipA suggesting a model in

which FtsA's self-interaction competes with its ability to recruit downstream division proteins. *Molecular Microbiology,* 83**,** 151-167.
POPHAM, D. L. & SETLOW, P. 1995. Cloning, nucleotide sequence, and mutagenesis of the Bacillus subtilis ponA operon, which codes for penicillin-binding protein (PBP) 1 and a PBP-related factor. *Journal of Bacteriology,* 177**,** 326-35.
POPP, D., IWASA, M., NARITA, A., ERICKSON, H. P. & MAÉDA, Y. 2009. FtsZ condensates: An in vitro electron microscopy study. *Biopolymers,* 91**,** 340-350.
PRICE, K. D., ROELS, S. & LOSICK, R. 1997. A Bacillus subtilis gene encoding a protein similar to nucleotide sugar transferases influences cell shape and viability. *Journal of Bacteriology,* 179**,** 4959-61.
RAYCHAUDHURI, D. 1999. ZipA is a MAP-Tau homolog and is essential for structural integrity of the cytokinetic FtsZ ring during bacterial cell division. *EMBO J,* 18**,** 2372-2383.
RAYCHAUDHURI, D. & PARK, J. T. 1992. Escherichia coli cell-division gene ftsZ encodes a novel GTP-binding protein. *Nature,* 359**,** 251-254.
REDDY, M. 2007. Role of FtsEX in Cell Division of Escherichia coli: Viability of ftsEX Mutants Is Dependent on Functional SufI or High Osmotic Strength. *Journal of Bacteriology,* 189**,** 98-108.
RICO, A. I., GARCÍA-OVALLE, M., MINGORANCE, J. & VICENTE, M. 2004. Role of two essential domains of Escherichia coli FtsA in localization and progression of the division ring. *Molecular Microbiology,* 53**,** 1359-1371.
RICO, A. I., GARCÍA-OVALLE, M., PALACIOS, P., CASANOVA, M. & VICENTE, M. 2010. Role of Escherichia coli FtsN protein in the assembly and stability of the cell division ring. *Molecular Microbiology,* 76**,** 760-771.
RIVAS, G., FERNÁNDEZ, J. A. & MINTON, A. P. 2001. Direct observation of the enhancement of noncooperative protein self-assembly by macromolecular crowding: Indefinite linear self-association of bacterial cell division protein FtsZ. *Proceedings of the National Academy of Sciences,* 98**,** 3150-3155.
ROBICHON, C., KING, G. F., GOEHRING, N. W. & BECKWITH, J. 2008. Artificial Septal Targeting of Bacillus subtilis Cell Division Proteins in Escherichia coli: an Interspecies Approach to the Study of Protein-Protein Interactions in Multiprotein Complexes. *Journal of Bacteriology,* 190**,** 6048-6059.
ROBSON, S., GORBATYUK, V., MACIEJEWSKI, M. & KING, G. 2005. Letter to the Editor: Backbone and side-chain 1H, 15N, and 13C assignments for the β domain of the bacterial cell division protein DivIB. *Journal of Biomolecular NMR,* 31**,** 261-262.
ROBSON, S. & KING, G. 2005. Backbone and Side-Chain 1H, 15N and 13C Assignments for the cis Conformer of the β Domain of the Bacterial Cell Division Protein DivIB. *Journal of Biomolecular NMR,* 33**,** 135-135.
ROBSON, S. A. & KING, G. F. 2006. Domain architecture and structure of the bacterial cell division protein DivIB. *Proceedings of the National Academy of Sciences,* 103**,** 6700-6705.
ROBSON, S. A., MICHIE, K. A., MACKAY, J. P., HARRY, E. & KING, G. F. 2002. The Bacillus subtilis cell division proteins FtsL and DivIC are intrinsically unstable and do not interact with one another in the absence of other septasomal components. *Molecular Microbiology,* 44**,** 663-674.
RODRIGUES, C. D. A. & HARRY, E. J. 2012. The Min System and Nucleoid Occlusion Are Not Required for Identifying the Division Site in

<italic>Bacillus subtilis</italic> but Ensure Its Efficient Utilization. *PLoS Genet,* 8**,** e1002561.

ROMBERG, L. & MITCHISON, T. J. 2003. Rate-Limiting Guanosine 5'-Triphosphate Hydrolysis during Nucleotide Turnover by FtsZ, a Prokaryotic Tubulin Homologue Involved in Bacterial Cell Division†. *Biochemistry,* 43**,** 282-288.

ROMBERG, L., SIMON, M. & ERICKSON, H. P. 2001. Polymerization of FtsZ, a Bacterial Homolog of Tubulin: IS ASSEMBLY COOPERATIVE? *Journal of Biological Chemistry,* 276**,** 11743-11753.

ROTHFIELD, L., JUSTICE, S. & GARCÍA-LARA, J. 1999. BACTERIAL CELL DIVISION. *Annual Review of Genetics,* 33**,** 423-448.

ROWLAND, S. L., KATIS, V. L., PARTRIDGE, S. R. & WAKE, R. G. 1997. DivIB, FtsZ and cell division in Bacillus subtilis. *Molecular Microbiology,* 23**,** 295-302.

RUEDA, S., VICENTE, M. & MINGORANCE, J. 2003. Concentration and Assembly of the Division Ring Proteins FtsZ, FtsA, and ZipA during the Escherichia coli Cell Cycle. *Journal of Bacteriology,* 185**,** 3344-3351.

SANCHEZ, M., VALENCIA, A., FERRANDIZ, M., SANDER, C. & VICENTE, M. 1994. Correlation between the structure and biochemical activities of FtsA, as essential cell division protein of the actin family. *EMBO J,* 13**,** 4919-4925.

SAPAY, N., GUERMEUR, Y. & DELEAGE, G. 2006. Prediction of amphipathic in-plane membrane anchors in monotopic proteins using a SVM classifier. *BMC Bioinformatics,* 7**,** 255.

SCHEFFERS, D.-J. 2008. The effect of MinC on FtsZ polymerization is pH dependent and can be counteracted by ZapA. *FEBS Letters,* 582**,** 2601-2608.

SCHEFFERS, D.-J., DE WIT, J. G., DEN BLAAUWEN, T. & DRIESSEN, A. J. M. 2001. GTP Hydrolysis of Cell Division Protein FtsZ: Evidence that the Active Site Is Formed by the Association of Monomers†. *Biochemistry,* 41**,** 521-529.

SCHEFFERS, D.-J. & ERRINGTON, J. 2004. PBP1 Is a Component of the Bacillus subtilis Cell Division Machinery. *Journal of Bacteriology,* 186**,** 5153-5156.

SCHEFFERS, D.-J., JONES, L. J. F. & ERRINGTON, J. 2004. Several distinct localization patterns for penicillin-binding proteins in Bacillus subtilis. *Molecular Microbiology,* 51**,** 749-764.

SCHMIDT, K. L., PETERSON, N. D., KUSTUSCH, R. J., WISSEL, M. C., GRAHAM, B., PHILLIPS, G. J. & WEISS, D. S. 2004. A Predicted ABC Transporter, FtsEX, Is Needed for Cell Division in Escherichia coli. *Journal of Bacteriology,* 186**,** 785-793.

SHEN, B. & LUTKENHAUS, J. 2009. The conserved C-terminal tail of FtsZ is required for the septal localization and division inhibitory activity of MinCC/MinD. *Molecular Microbiology,* 72**,** 410-424.

SHIOMI, D. & MARGOLIN, W. 2007a. The C-Terminal Domain of MinC Inhibits Assembly of the Z Ring in Escherichia coli. *Journal of Bacteriology,* 189**,** 236-243.

SHIOMI, D. & MARGOLIN, W. 2007b. Dimerization or oligomerization of the actin-like FtsA protein enhances the integrity of the cytokinetic Z ring. *Molecular Microbiology,* 66**,** 1396-1415.

SHIOMI, D. & MARGOLIN, W. 2008. Compensation for the loss of the conserved membrane targeting sequence of FtsA provides new insights into its function. *Molecular Microbiology,* 67**,** 558-569.
SHU, X., LI, Y., LIANG, M., YANG, B., LIU, C., WANG, Y. & SHU, J. 2012. Rapid lipid profiling of bacteria by online MALDI-TOF mass spectrometry. *International Journal of Mass Spectrometry,* 321–322**,** 71-76.
SIEVERS, F., WILM, A., DINEEN, D., GIBSON, T. J., KARPLUS, K., LI, W., LOPEZ, R., MCWILLIAM, H., REMMERT, M., SODING, J., THOMPSON, J. D. & HIGGINS, D. G. 2011. Fast, scalable generation of high-quality protein multiple sequence alignments using Clustal Omega. *Mol Syst Biol,* 7.
SIEVERS, J. & ERRINGTON, J. 2000a. Analysis of the Essential Cell Division Gene ftsL ofBacillus subtilis by Mutagenesis and Heterologous Complementation. *Journal of Bacteriology,* 182**,** 5572-5579.
SIEVERS, J. & ERRINGTON, J. 2000b. The Bacillus subtilis cell division protein FtsL localizes to sites of septation and interacts with DivIC. *Molecular Microbiology,* 36**,** 846-855.
SINGH, J. K., MAKDE, R. D., KUMAR, V. & PANDA, D. 2007. A Membrane Protein, EzrA, Regulates Assembly Dynamics of FtsZ by Interacting with the C-Terminal Tail of FtsZ†. *Biochemistry,* 46**,** 11013-11022.
SINGH, J. K., MAKDE, R. D., KUMAR, V. & PANDA, D. 2008. SepF Increases the Assembly and Bundling of FtsZ Polymers and Stabilizes FtsZ Protofilaments by Binding along Its Length. *Journal of Biological Chemistry,* 283**,** 31116-31124.
SRINIVASAN, R., MISHRA, M., WU, L., YIN, Z. & BALASUBRAMANIAN, M. K. 2008. The bacterial cell division protein FtsZ assembles into cytoplasmic rings in fission yeast. *Genes & Development,* 22**,** 1741-1746.
STEELE, V. R., BOTTOMLEY, A. L., GARCIA-LARA, J., KASTURIARACHCHI, J. & FOSTER, S. J. 2011. Multiple essential roles for EzrA in cell division of Staphylococcus aureus. *Molecular Microbiology,* 80**,** 542-555.
STEINER, W., LIU, G., DONACHIE, W. D. & KUEMPEL, P. 1999. The cytoplasmic domain of FtsK protein is required for resolution of chromosome dimers. *Molecular Microbiology,* 31**,** 579-583.
STORTS, D. R., APARICIO, O. M., SCHOEMAKER, J. M. & MARKOVITZ, A. 1989. Overproduction and identification of the ftsQ gene product, an essential cell division protein in Escherichia coli K-12. *Journal of Bacteriology,* 171**,** 4290-4297.
SUGIMOTO, S., YAMANAKA, K., NISHIKORI, S., MIYAGI, A., ANDO, T. & OGURA, T. 2010. AAA+ Chaperone ClpX Regulates Dynamics of Prokaryotic Cytoskeletal Protein FtsZ. *Journal of Biological Chemistry,* 285**,** 6648-6657.
SYSTEM, T. P. M. G. *In:* SCHRODINGER, L. (ed.) 1.2r3pre ed.
SZETO, T. H., ROWLAND, S. L., HABRUKOWICH, C. L. & KING, G. F. 2003. The MinD Membrane Targeting Sequence Is a Transplantable Lipid-binding Helix. *Journal of Biological Chemistry,* 278**,** 40050-40056.
SZWEDZIAK, P., WANG, Q., FREUND, S. M. V. & LOWE, J. 2012. FtsA forms actin-like protofilaments. *EMBO J,* 31**,** 2249-2260.
TADROS, M., GONZÁLEZ, J. M., RIVAS, G., VICENTE, M. & MINGORANCE, J. 2006. Activation of the Escherichia coli cell division protein FtsZ by a low-affinity interaction with monovalent cations. *FEBS Letters,* 580**,** 4941-4946.

TAVARES, J. R., DE SOUZA, R. F., MEIRA, G. L. S. & GUEIROS-FILHO, F. J. 2008. Cytological Characterization of YpsB, a Novel Component of the Bacillus subtilis Divisome. *Journal of Bacteriology,* 190**,** 7096-7107.

THANEDAR, S. & MARGOLIN, W. 2004. FtsZ Exhibits Rapid Movement and Oscillation Waves in Helix-like Patterns in Escherichia coli. *Current Biology,* 14**,** 1167-1173.

TONTHAT, N. K., AROLD, S. T., PICKERING, B. F., VAN DYKE, M. W., LIANG, S., LU, Y., BEURIA, T. K., MARGOLIN, W. & SCHUMACHER, M. A. 2011. Molecular mechanism by which the nucleoid occlusion factor, SlmA, keeps cytokinesis in check. *EMBO J,* 30**,** 154-164.

TRIP, E. N., VEENING, J.-W., STEWART, E. J., ERRINGTON, J. & SCHEFFERS, D.-J. 2013. Balanced transcription of cell division genes in Bacillus subtilis as revealed by single cell analysis. *Environmental Microbiology***,** n/a-n/a.

URSINUS, A., VAN DEN ENT, F., BRECHTEL, S., DE PEDRO, M., HÖLTJE, J.-V., LÖWE, J. & VOLLMER, W. 2004. Murein (Peptidoglycan) Binding Property of the Essential Cell Division Protein FtsN from Escherichia coli. *Journal of Bacteriology,* 186**,** 6728-6737.

VAGNER, V., DERVYN, E. & EHRLICH, S. D. 1998. A vector for systematic gene inactivation in Bacillus subtilis. *Microbiology,* 144**,** 3097-3104.

VAN BAARLE, S. & BRAMKAMP, M. 2010. The MinCDJ System in <italic>Bacillus subtilis</italic> Prevents Minicell Formation by Promoting Divisome Disassembly. *PLoS ONE,* 5**,** e9850.

VAN DEN ENT, F., AMOS, L. A. & LOWE, J. 2001. Prokaryotic origin of the actin cytoskeleton. *Nature,* 413**,** 39-44.

VAN DEN ENT, F. & LOWE, J. 2000. Crystal structure of the cell division protein FtsA from Thermotoga maritima. *EMBO J,* 19**,** 5300-5307.

VARLEY, A. W. & STEWART, G. C. 1992. The divIVB region of the Bacillus subtilis chromosome encodes homologs of Escherichia coli septum placement (minCD) and cell shape (mreBCD) determinants. *Journal of Bacteriology,* 174**,** 6729-6742.

WADENPOHL, I. & BRAMKAMP, M. 2010. DivIC Stabilizes FtsL against RasP Cleavage. *Journal of Bacteriology,* 192**,** 5260-5263.

WADSWORTH, K. D., ROWLAND, S. L., HARRY, E. J. & KING, G. F. 2008. The divisomal protein DivIB contains multiple epitopes that mediate its recruitment to incipient division sites. *Molecular Microbiology,* 67**,** 1143-1155.

WANG, L., KHATTAR, M. K., DONACHIE, W. D. & LUTKENHAUS, J. 1998. FtsI and FtsW Are Localized to the Septum inEscherichia coli. *Journal of Bacteriology,* 180**,** 2810-2816.

WANG, L. & LUTKENHAUS, J. 1998. FtsK is an essential cell division protein that is localized to the septum and induced as part of the SOS response. *Molecular Microbiology,* 29**,** 731-740.

WANG, X. & LUTKENHAUS, J. 1993. The FtsZ protein of Bacillus subtilis is localized at the division site and has GTPase activity that is dependent upon FtsZ concentration. *Molecular Microbiology,* 9**,** 435-442.

WEART, R. B., LEE, A. H., CHIEN, A.-C., HAEUSSER, D. P., HILL, N. S. & LEVIN, P. A. 2007. A Metabolic Sensor Governing Cell Size in Bacteria. *Cell,* 130**,** 335-347.

WEART, R. B. & LEVIN, P. A. 2003. Growth Rate-Dependent Regulation of Medial FtsZ Ring Formation. *Journal of Bacteriology,* 185**,** 2826-2834.

WEART, R. B., NAKANO, S., LANE, B. E., ZUBER, P. & LEVIN, P. A. 2005. The ClpX chaperone modulates assembly of the tubulin-like protein FtsZ. *Molecular Microbiology,* 57**,** 238-249.

WU, L. & ERRINGTON, J. 1994. Bacillus subtilis spoIIIE protein required for DNA segregation during asymmetric cell division. *Science,* 264**,** 572-575.

WU, L. J. & ERRINGTON, J. 1997. Septal localization of the SpoIIIE chromosome partitioning protein in Bacillus subtilis. *EMBO J,* 16**,** 2161-2169.

WU, L. J. & ERRINGTON, J. 2004. Coordination of Cell Division and Chromosome Segregation by a Nucleoid Occlusion Protein in Bacillus subtilis. *Cell,* 117**,** 915-925.

WU, L. J. & ERRINGTON, J. 2012. Nucleoid occlusion and bacterial cell division. *Nat Rev Micro,* 10**,** 8-12.

WU, L. J., ISHIKAWA, S., KAWAI, Y., OSHIMA, T., OGASAWARA, N. & ERRINGTON, J. 2009. Noc protein binds to specific DNA sequences to coordinate cell division with chromosome segregation. *EMBO J,* 28**,** 1940-1952.

WU, L. J., LEWIS, P. J., ALLMANSBERGER, R., HAUSER, P. M. & ERRINGTON, J. 1995. A conjugation-like mechanism for prespore chromosome partitioning during sporulation in Bacillus subtilis. *Genes & Development,* 9**,** 1316-1326.

YAN, K., PEARCE, K. H. & PAYNE, D. J. 2000. A Conserved Residue at the Extreme C-Terminus of FtsZ Is Critical for the FtsA-FtsZ Interaction in Staphylococcus aureus. *Biochemical and Biophysical Research Communications,* 270**,** 387-392.

YANG, D. C., PETERS, N. T., PARZYCH, K. R., UEHARA, T., MARKOVSKI, M. & BERNHARDT, T. G. 2011. An ATP-binding cassette transporter-like complex governs cell-wall hydrolysis at the bacterial cytokinetic ring. *Proceedings of the National Academy of Sciences,* 108**,** E1052–E1060.

YANG, J.-C., VAN DEN ENT, F., NEUHAUS, D., BREVIER, J. & LÖWE, J. 2004. Solution structure and domain architecture of the divisome protein FtsN. *Molecular Microbiology,* 52**,** 651-660.

YANOURI, A., DANIEL, R. A., ERRINGTON, J. & BUCHANAN, C. E. 1993. Cloning and sequencing of the cell division gene pbpB, which encodes penicillin-binding protein 2B in Bacillus subtilis. *Journal of Bacteriology,* 175**,** 7604-7616.

YIM, L., VANDENBUSSCHE, G., MINGORANCE, J., RUEDA, S., CASANOVA, M., RUYSSCHAERT, J.-M. & VICENTE, M. 2000. Role of the Carboxy Terminus of Escherichia coli FtsA in Self-Interaction and Cell Division. *Journal of Bacteriology,* 182**,** 6366-6373.

YOUNG, F. E. & SPIZIZEN, J. 1961. PHYSIOLOGICAL AND GENETIC FACTORS AFFECTING TRANSFORMATION OF BACILLUS SUBTILIS. *Journal of Bacteriology,* 81**,** 823-829.

YU, X.-C. & MARGOLIN, W. 1997. Ca2+-mediated GTP-dependent dynamic assembly of bacterial cell division protein FtsZ into asters and polymer networks in vitro. *EMBO J,* 16**,** 5455-5463.

YU, X.-C., TRAN, A. H., SUN, Q. & MARGOLIN, W. 1998a. Localization of Cell Division Protein FtsK to theEscherichia coli Septum and Identification of a Potential N-Terminal Targeting Domain. *Journal of Bacteriology,* 180**,** 1296-1304.

YU, X.-C., WEIHE, E. K. & MARGOLIN, W. 1998b. Role of the C Terminus of FtsK in Escherichia coli Chromosome Segregation. *Journal of Bacteriology,* 180**,** 6424-6428.
ZHOU, H.-X., RIVAS, G. & MINTON, A. P. 2008. Macromolecular Crowding and Confinement: Biochemical, Biophysical, and Potential Physiological Consequences*. *Annual Review of Biophysics,* 37**,** 375-397.